2014

P2X7 receptor-induced CD23 shedding from B cells

Aleta Pupovac
University of Wollongong, ap251@uow.edu.au

P2X7 receptor-induced CD23 shedding from B cells

A thesis submitted in fulfilment of the requirements for the award of the degree

Doctor of Philosophy

from

UNIVERSITY OF WOLLONGONG

by

Aleta Pupovac

Bachelor of Biotechnology (Adv) (Hons)

Illawarra Health and Medical Research Institute

School of Biological Sciences

2014

THESIS CERTIFICATION

I, Aleta Pupovac, declare that this thesis, submitted in fulfilment of the requirements for the award of Doctor of Philosophy, in the Department of Biological Sciences, University of Wollongong, is wholly my own work unless otherwise referenced or acknowledged. The document has not been submitted for qualifications at any other academic institution.

Aleta Pupovac

2014

ACKNOWLEDGEMENTS

I would like to thank my supervisor, Ron Sluyter, for providing me with the skills and patience to tackle science confidently in the future. Your knowledge, guidance and support were essential in the completion of this project, and have moulded me into the scientist that I always hoped to be. I will be forever grateful that you gave me the opportunity to be a part of your lab, and for your excellent supervision. A student cannot ask for a better supervisor.

Also thanks to my co-supervisor Marie Ranson, for providing helpful advice over the years.

To all the past and current members of the Sluyter lab, I enjoyed working with all of you. In particular, Pan, Safina, Mar and Rach, I thank you for your support and entertainment on most days in and out of the lab, but more so during the challenging times thrown at me by science over the years. Also a big thankyou to Vanessa Sluyter for providing assistance and order in the lab, your level of organisation is something I hope to achieve one day. I also want to thank people from neighbouring labs (past and present), including Simon, Blake, James, Carola, Bec, Corky, Di, Raf and Dave for laughs, inspiration, scientific/life advice and support. Meeting all of you was an unexpected (even delightful) highlight of my PhD experience.

Finally, I want to thank my family and friends, including those mentioned already and those outside of research, for your love and support. Without you I wouldn't have had the motivation or strength to achieve what I have and no words can express my gratitude to you.

TABLE OF CONTENTS

LIST OF FIGURES

LIST OF TABLES

LIST OF ABBREVIATIONS

7AAD	7-aminoactinomycin D
Aβ	Amyloid-β peptide
Ab	Antibody
ADAM	A disintegrin and metalloprotease
ADP	Adenosine 5'-diphosphate
APC	Allophycocyanin
APP	Amyloid precursor protein
AREG	Amphiregulin
ART	ADP-ribosyltransferase
aSmase	Acid sphingomyelinase
ATP	Adenosine 5'-triphosphate
ATPγS	Adenosine 5'-O-(3-thio) triphosphate
BAPTA-AM	1,2-bis(o-aminophenoxy)ethane-N,N,N',N'-tetraacetic acid
BBG	Brilliant blue G
bp	Base pairs
BSA	Bovine serum albumin
BTC	Betacellulin
BzATP	2'(3')-*O*-(4-benzoylbenzoyl)adenosine-5'-triphosphate
$CaCl_2$	Calcium chloride
cDNA	Complementary DNA
CHO	Chinese hamster ovary
Choline Cl	Choline chloride
CLL	Chronic lymphocytic leukaemia
CTF	Carboxyl-terminal fragment
DCF	Dichlorofluorescein

DMSO	Dimethyl sulphoxide
DPI	Diphenyleneiodonium
DUOX	Dual oxidase
EC_{50}	Half maximal effective concentration
E-cadherin	Epithelial cadherin
EGF	Epidermal growth factor
EGFR	Epidermal growth factor receptor
EGTA	Ethylene glycol tetraacetic acid
ELISA	Enzyme-linked immunosorbent assay
ERK	Extracellular regulated kinase
ERM	Ezrin radixin moesin
FITC	Fluorescein isothiocyanate
FSC	Forward scatter
GSK-3	Glycogen synthase kinase-3
H_2DCFDA	Dichlorodihydrofluorescein diacetate
H_2O_2	Hydrogen peroxide
HBE	Human bronchial epithelial
HB-EGF	Heparin-binding EGF-like growth factor
HEK	Human embryonic kidney
HEPES	4-(2-hydroxyethyl)-1-piperazineethanesulfonic acid
IC_{50}	Half maximal inhibitory concentration
ICAM	Intercellular adhesion molecule
Ig	Immunoglobulin
IL	Interleukin
IL-6R	Interleukin-6 receptor
JNK	c-Jun N-terminal kinase
KCl	Potassium chloride

LPS	Lipopolysaccharide
mAb	Monoclonal antibody
MAPK	Mitogen-activated protein kinase
mEF	Murine embryonic fibroblasts
MEK	Mitogen/extracellular regulated kinase
MEL	Murine erythroleukaemia cells
MFI	Mean fluorescence intensity
$MgCl_2$	Magnesium chloride
MHC	Major histocompatibility complex
MMP	Matrix metalloprotease
mRNA	Messenger RNA
NaCl	Sodium chloride
NAD	Nicotinamide adenine dinucleotide
NADPH	Nicotinamide adenine dinucleotide phosphate
NCAM	Neural cell adhesion molecule
NFAT	Nuclear factor of activated T cells
NH_4Cl	Ammonium chloride
oATP	periodate-oxidised adenosine 5'-triphosphate
PBMCs	Peripheral blood mononuclear cells
PBS	Phosphate-buffered saline
PCR	Polymerase chain reaction
PE	Phycoerythrin
PI3K	Phosphatidyl-inositol-3-kinase
PKC	Protein kinase C
PLA2	Phospholipase A2
PLC	Phospholipase C
PLD	Phospholipase D

PMA	Phorbol-12-myristate-13-acetate
PPADs	Pyridoxal phosphate-6-azophenyl-2-4-disulphonic acid
PS	Phosphatidylserine
ROS	Reactive oxygen species
RT-PCR	Reverse transcriptase-polymerase chain reaction
sAPP	Soluble amyloid precursor protein
SD	Standard deviation
siRNA	Short interfering RNA
SNP	Single nucleotide polymorphism
SSC	Side scatter
TGF	Transforming growth factor
THCE	SV-40 immortalised human corneal epithelial cells
TIM	T cell immunoglobulin and mucin
TLR	Toll-like receptor
TNF	Tumor necrosis factor
TNFR	Tumor necrosis factor receptor
UDP	Uridine 5'-diphosphate
UTP	Uridine 5'-triphosphate
v/v	Volume/volume
w/v	Weight/volume

CHAPTER PUBLICATIONS

This thesis includes data that has been published in the following journal articles:

Chapter 3:

Farrell, A. W., Gadeock S., **Pupovac, A**., Wang, B., Jalilian, I., Ranson, M. and Sluyter R (2010). "P2X7 receptor activation induces cell death and CD23 shedding in human RPMI 8226 multiple myeloma cells". *Biochimica et Biophysica Acta* **1800(11)**: 1173-1182.

Gadeock, S., **Pupovac, A.**, Sluyter, V., Spildrejorde, M. and Sluyter R (2012). "P2X7 receptor activation mediates organic cation uptake into human myeloid leukaemic KG-1 cells". *Purinergic Signalling* **8(4)**: 669-676.

Chapter 4:

Pupovac, A., Stokes, L. and Sluyter, R (2013). "CAY10593 inhibits the human P2X7 receptor independently of phospholipase D1 stimulation". *Purinergic Signalling* **(9)4**: 609-619.

Chapter 6:

Pupovac, A., Foster, C. M. and Sluyter, R (2013). "Human P2X7 receptor activation induces the rapid shedding of CXCL16". *Biochemical and Biophysical Research Communications* **432(4)**: 626-631.

Chapter 7:

Pupovac, A., Geraghty, N. J., Watson, D. and Sluyter, R (2014). "Activation of the P2X7 receptor induces the rapid shedding of CD23 from human and murine B cells". *Immunology and Cell Biology* doi: 10.1038/icb.2014.69.

ADDITIONAL PUBLICATION

Tran, J. N., **Pupovac, A**., Taylor, R. M., Wiley, J. S., Byrne, S. N. and Sluyter, R. (2009). "Murine epidermal Langerhans cells and keratinocytes express functional P2X7 receptors". *Experimental Dermatology* **19(8)**: e151-e157

LIST OF CONFERENCE PRESENTATIONS

Pupovac, A., Wang, B. Foster, C. M. and Sluyter R. "P2X7 receptor activation induces ADAM10-mediated shedding of CD23 and CXCL16". Poster presentation. Annual Meeting of the Australian Society for Immunology, Wellington, New Zealand, December 2013

Pupovac, A., Wang, B. Foster, C. M. and Sluyter R. "Human P2X7 receptor activation induces ADAM10-mediated shedding of CD23 and CXCL16". *Journal of Immunology*, (Meeting Abstract Supplement 112.2). Poster presentation. Annual Meeting of the American Association of Immunology, Honolulu, U.S.A, May 2013

Pupovac, A., Foster, C. M. and Sluyter, R. "P2X7 activation induces the shedding of CD23 and CXCL16". Oral presentation. Gage Ion Channels and Transporters Conference, Canberra, April 2013

Pupovac, A. "P2X7 activation induces the shedding of CD23 and CXCL16". Oral presentation. Postgraduate Conference, School of Biological Sciences, Kioloa, Australia, November 2012

Pupovac, A. "The role of P2X7 and CD23 in rheumatoid arthritis". Oral presentation. Postgraduate Conference, School of Biological Sciences, Kangaroo Valley, Australia, November 2011

Pupovac, A. "The P2X7 receptor and the release of soluble CD23". Oral presentation. Postgraduate Conference, School of Biological Sciences, Kangaroo Valley, Australia, November 2010

Pupovac, A., Farrell, A. W., Wang, B., Gadeock, S., Jalilian, I., Ranson, M. and Sluyter, R. "P2X7 receptor activation induces CD23 shedding from human RPMI 8226 B cells via activation of a metalloprotease". Oral presentation, NSW/ACT Branch Meeting of the Australasian Society of Immunology, Bowral Australia, September 2010

ABSTRACT

The P2X7 receptor is a ligand-gated cation channel, which is expressed on a variety of cell types, including human B cells. P2X7 activation induces a variety of downstream events, including the shedding of the immunoglobulin E receptor, CD23. Cell surface CD23 and soluble CD23 are important in the regulation of immunoglobulin E. Furthermore, soluble CD23 functions as a proinflammatory mediator. Thus it is important to elucidate the mechanisms involved in CD23 shedding. A disintegrin and metalloprotease (ADAM) 10 constitutively sheds CD23 from the surface of cells but whether P2X7 activates ADAM10, or other signalling processes to mediate CD23 shedding are unknown. Our laboratory has shown that P2X7 is expressed on human RPMI 8226 multiple myeloma B cells and that P2X7 activation on these cells induces the shedding of CD23. The primary aims of this thesis were: to confirm the presence of and to further characterise P2X7 in RPMI 8226 cells; to examine the signalling pathways involved in P2X7-induced CD23 shedding using this cell line as a model; to determine, using RPMI 8226 cells, whether ADAM10 is involved in P2X7-induced CD23 shedding; and finally to determine whether P2X7 activation induces CD23 shedding from primary human and murine B cells.

Messenger RNA (mRNA) expression of molecules was detected by reverse transcriptase-polymerase chain reaction. P2X7, CD23 and CXCL16 expression was detected by immunolabelling and measured by flow cytometry. Nucleotide-induced ethidium^{+} uptake (pore formation) was measured by flow cytometry or spectrofluorometry. Soluble CD23 and CXCL16 were measured by enzyme-linked immunosorbent assay. ATP-induced currents were measured by electrophysiology.

RPMI 8226 cells were shown to express mRNA for P2X7 and other P2X subtypes (P2X1, P2X4 and P2X5). Functional P2X7 was present on RPMI 8226 cells, and the new generation P2X7 antagonist AZ10606120, near-completely impaired both P2X7-induced pore formation and CD23 shedding in these cells. This data confirmed that the RPMI 8226 cell line is an adequate model to investigate the molecules and processes involved in P2X7-induced CD23 shedding.

Several signalling pathways involved in other P2X7-induced responses including reactive oxygen species formation, as well as changes in intracellular cation concentrations, were not involved in P2X7-induced CD23 shedding from RPMI 8226 cells. However, the phospholipase (PLD)1 antagonist, CAY10593 (VU0155069) impaired P2X7-induced CD23 shedding from RPMI 8226 cells. CAY10593 also impaired pore formation in RPMI 8226 cells, P2X7-transfected human embryonic kidney 293 cells and peripheral blood mononuclear cells. CAY10593 impaired P2X7-induced pore formation in RPMI 8226 cells more potently than the PLD2 antagonist CAY10594 and the non-specific PLD antagonist halopemide. CAY10593 also inhibited P2X7-mediated inward currents. Notably, PLD1 was absent in RPMI 8226 cells. This data indicates that CAY10593 impairs human P2X7 independently of PLD1 stimulation and highlights the importance of ensuring that compounds used in signalling studies downstream of P2X7 activation do not affect the receptor itself.

RPMI 8226 cells were shown to express mRNA for ADAM10. The ADAM10 antagonist, GI254023X significantly impaired P2X7-induced CD23 shedding from RPMI 8226 cells. ATP treatment of RPMI 8226 cells induced the rapid shedding of another ADAM10 substrate, CXCL16. The P2X7 antagonists, AZ10606120 and KN-62 near completely impaired ATP-induced CXCL16 shedding from RPMI 8226 cells and treatment of these cells with GI254023X significantly impaired P2X7-induced CXCL16

shedding. This data indicates that human P2X7 activation induces the rapid shedding of CD23 and CXCL16, and that these processes are mediated by ADAM10.

ATP treatment of primary human and murine B cells also induced the rapid shedding of CD23. Treatment of cells with AZ10606120, near-completely impaired ATP-induced CD23 shedding from both human and murine B cells. ATP-induced CD23 shedding was also impaired in B cells from P2X7 knockout mice. GI254023X impaired P2X7-induced CD23 shedding from both human and murine B cells. This data indicates that P2X7 activation induces the rapid shedding of CD23 from primary human and murine B cells, and that this process is also mediated by ADAM10.

Overall, this study shows, for the first time that ADAM10 mediates P2X7-induced CD23 and CXCL16 shedding from RPMI 8226 cells, as well as CD23 shedding from primary human and murine B cells. Moreover, this study excludes a potential role for various signalling molecules, including reactive oxygen species formation and the flux of various cations in P2X7-induced CD23 shedding. Finally, this study shows that the PLD1 antagonist, CAY10593, impairs P2X7 independently of PLD1.

CHAPTER 1

Introduction

1.1 CD23

1.1.1 Structure and features

CD23 is a 45 kDa, type II transmembrane glycoprotein that is composed of 321 amino acids (Ludin et al. 1987, Suter et al. 1987). The glycoprotein consists of a large, C-type lectin head domain that participates in immunoglobulin (Ig)E binding, followed by a stalk region, which is important in CD23 oligomerisation, and a short N-terminal cytoplasmic domain (Rosenwasser and Meng 2005, Acharya et al. 2010) (Figure 1.1).

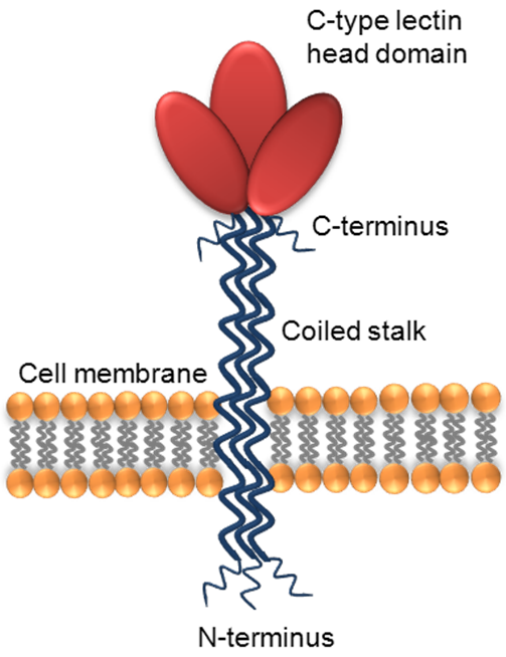

Figure 1.1: The structure of membrane-bound CD23. Each CD23 molecule consists of a C-type lectin head that binds immunoglobulin IgE and a coiled stalk region that participates in CD23 oligomerisation to form trimeric CD23 at the cell surface. Adapted from Gould and Sutton 2008.

CD23 is often referred to as the low affinity IgE receptor (FcεRII) as it binds its main ligand, IgE at a lower affinity compared to the high affinity IgE receptor (FcεRI) (Rosenwasser and Meng 2005, Acharya et al. 2010). Two isoforms of CD23 have been identified, CD23a and CD23b; these differ between species (human and murine), and in tissue specific gene expression and regulation (Yokota et al. 1988). CD23a is expressed constitutively in primary B cells and B cell lines (Yokota et al. 1988), whereas CD23b is induced in various cell types and may be upregulated during viral infection (Wang et al. 1991), and following stimulation by interleukin (IL)-4 (Defrance et al. 1987, Vercelli et al. 1988, Yokota et al. 1988) and engagement of the co-stimulatory molecule CD40 on B cells (Gordon et al. 1991). These isoforms share a common C-terminal region, but contain 6-7 differing amino acids in their N-terminal cytoplasmic domains in both humans and mice, and are associated with different signalling pathways and downstream effects in cells (Rosenwasser and Meng 2005, Acharya et al. 2010).

1.1.2 Distribution

CD23 is expressed on many cell types including B cells (Kikutani et al. 1989), T cells (Armitage et al. 1989), monocytes and macrophages (Vercelli et al. 1988), neutrophils (Yamaoka et al. 1996), eosinophils (Chihara et al. 1992), platelets (Klouche et al. 1997), epidermal Langerhans cells (Bieber et al. 1989), follicular dendritic cells (Rieber et al. 1993), keratinocytes (Becherel et al. 1997), intestinal epithelial cells (Yu et al. 2003), bone marrow stromal cells (Fourcade et al. 1992) and airway smooth muscle cells (Hakonarson et al. 1999).

1.1.3 Roles of membrane CD23

Membrane CD23 exists at the cell surface as a trimer (Kilmon et al. 2004) (Figure 1.1). Its primary role as a membrane-bound receptor is negative feedback regulation of IgE production (Yu et al. 1994, Cooper et al. 2012). In allergy, negative regulation of IgE synthesis occurs by co-ligation of allergen-IgE complexes with IgE and CD23 on the cell membrane (see review by Gould and Sutton 2008 for further detail). Membrane CD23 is also mitogenic for normal B cells and B cell lines, which suggests CD23 may be involved in autocrine control of B cell growth (Cairns and Gordon 1990).

Although IgE is the main ligand of membrane CD23, other ligands can also bind CD23, including the complement receptor type 2 (CD21), major histocompatibility complex (MHC) class II molecules and integrins. As membrane receptors, CD23 and CD21 interact to function as adhesion molecules in homotypic aggregation of human B cells (Bjorck et al. 1993). In contrast to this, homotyptic aggregation of murine B cells is independent of CD23 (Davey et al. 1995). Soluble CD21 also induces activation and differentiation of human monocytes by binding membrane CD23 (Fremeaux-Bacchi et al. 1998a). Furthermore, MHC II molecules can interact with the stalk region of CD23 (Kijimoto-Ochiai and Noguchi 2000), indicating CD23 functions as a co-stimulatory adhesion molecule in antigen presentation by B cells (Flores-Romo et al. 1990). Recombinant full-length CD23 incorporated into liposomes (Lecoanet-Henchoz et al. 1995) and a mouse CD23 fusion protein, ZZ-CD23 (Lecoanet-Henchoz et al. 1997) interact with integrins αMβ2 (CD11b) and αXβ2 (CD11c) on human monocytes, integrin-transfected COS-7 fibroblast-like cells (Lecoanet-Henchoz et al. 1995), murine peritoneal macrophages and RAW264.7 macrophage cells (Lecoanet-Henchoz et al.

1997). This interaction is thought to regulate monocyte/macrophage activation (Lecoanet-Henchoz et al. 1995, Lecoanet-Henchoz et al. 1997). Interactions of the above ligands with soluble CD23 are also discussed in section 1.1.4.3.

1.1.4 Generation and roles of soluble CD23

1.1.4.1 Shedding of membrane CD23

Membrane CD23 is sensitive to proteolytic shedding that is mediated by membrane metalloproteases of the a disintegrin and metalloprotease (ADAM) family (Weskamp et al. 2006, Lemieux et al. 2007). After proteolytic cleavage, membrane CD23 may be released from the cell as soluble CD23 into molecules of varying sizes including 37, 33, 25 (Letellier et al. 1990) and 16 kDa (Grenier-Brossette et al. 1992). ADAM10 is thought to be the main metalloprotease responsible for constitutive CD23 shedding (Weskamp et al. 2006, Lemieux et al. 2007) (Figure 1.2). Furthermore, murine B cells lacking ADAM10 expression, display defective release of CD23 and a significant reduction in soluble CD23 generation. This confirms ADAM10 is required for constitutive CD23 cleavage *in vivo* (Gibb et al. 2010). It is thought that ADAM-mediated cleavage occurs predominantly at the cell surface however, it has also been shown that internalisation of membrane CD23 results in ADAM10-mediated incorporation into exosomes, with cleavage occurring inside the exosome prior to release of soluble CD23 from cells (Mathews et al. 2010). ADAM10 is also involved in inducible CD23 shedding, including phorbol-12-myristate-13-acetate (PMA)-,

Ca^{2+}/ionomycin- (Weskamp et al. 2006, Le Gall et al. 2009) and lysophosphatidic acid- (Lemieux et al. 2007) induced CD23 shedding.

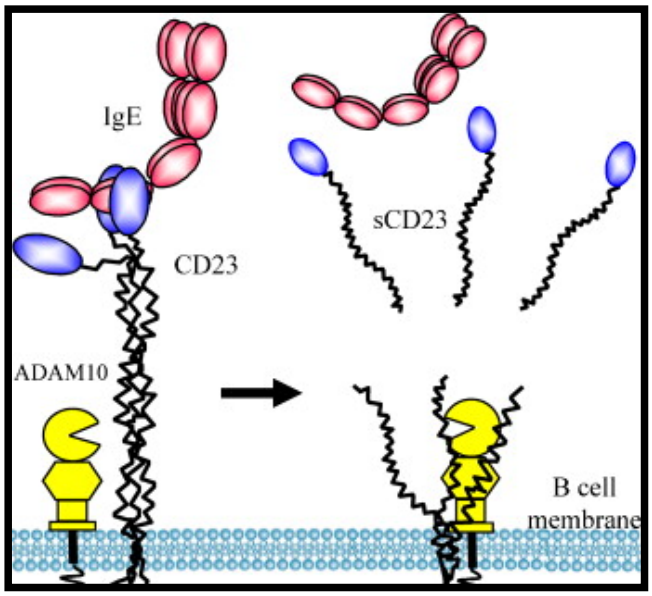

Figure 1.2: Shedding of CD23. In the absence of IgE, ADAM10 cleaves CD23 and releases soluble CD23 from the B cell membrane. From Gibb et al. 2010. **Abbreviations:** IgE, Immunoglobulin E; sCD23, soluble CD23; ADAM10, a metalloprotease and disintegrin 10.

Several other ADAM members have been implicated in the release of CD23 from cells. ADAM8, 15, and 28 have been associated with constitutive shedding of CD23 in CD23-transfected, and ADAM and CD23 co-transfected human embryonic kidney (HEK) 293 cells (Fourie et al. 2003). However, the involvement of these ADAMs has been disputed with loss-of-function studies with ADAM-deficient cells, and gain-of-function studies with overexpressed ADAMs failing to demonstrate involvement of ADAM15 and ADAM28 (Weskamp et al. 2006). Furthermore, mice lacking ADAM8 fail to show impaired CD23 shedding (Weskamp et al. 2006). ADAM33 has also been implicated in CD23 shedding (Rosenwasser and Meng 2005),

however the specific ADAM10 inhibitor GI254023X, impairs CD23 shedding in primary B cells at a concentration that does not inhibit ADAM33 (Weskamp et al. 2006). Despite this, ADAM33 may play a minor role in this process in the absence of ADAM10 (Weskamp et al. 2006). Matrix metalloprotease (MMP) 9, which is not an ADAM family member, mediates Toll-like receptor-4-induced CD23 shedding in human and murine lymphocytes (Jackson et al. 2009). However, the rate of shedding by this mechanism is slower (Jackson et al. 2009) than that of other inducers of CD23 shedding (Weskamp et al. 2006, Lemieux et al. 2007, Le Gall et al. 2009).

1.1.4.2 Roles of soluble CD23 and IgE

Soluble CD23 binds IgE, acts as positive regulator of IgE synthesis and controls IgE homeostasis (Cooper et al. 2012, Padro et al. 2013). In the soluble form, CD23 also interacts with other ligands to induce biological effects, for example, soluble CD21 and CD23 can form complexes, which inhibit soluble CD23-induced IgE synthesis in B cells (Fremeaux-Bacchi et al. 1998b). The role of soluble CD23 and IgE production are beyond the scope of this thesis but readers are referred to Gould and Sutton, (2008) for a more extensive review.

1.1.4.3 Roles of soluble CD23 as a cytokine

Soluble CD23 has pleiotropic, cytokine-like effects on monocytes, B cells and T cells (summarised in Table 1.1). Soluble CD23 is an important regulator of monocytes, for example recombinant soluble CD23 promotes the proliferation of myeloid precursors in the presence of IL-1α (Mossalayi et al. 1990a) and interacts with integrins CD11b and

CD11c, triggering an increase in nitric oxide and hydrogen peroxide, and the production of proinflammatory cytokines including IL-1β, IL-6 and tumor necrosis factor (TNF)-α (Lecoanet-Henchoz et al. 1995). The ligation of CD11b and CD11c by soluble CD23 also induces secretion of IL-8, macrophage inflammatory protein-1α and macrophage inflammatory protein-1β from monocytes (Rezzonico et al. 2001). Secretion of macrophage inflammatory proteins from monocytes may play an important role in the recruitment of other cells that participate in the inflammatory response (Rezzonico et al. 2001).

Table 1.1: Biological effects of soluble CD23 on immune cells.

Cell Type	Biological Effect	Reference
Monocytes	Promotes differentiation of myeloid cell precursors in the presence of IL-1α	(Mossalayi et al. 1990a)
	Drives cytokine release from monocytes	(Hermann et al. 1999) (Lecoanet-Henchoz et al. 1995) (Rezzonico et al. 2001) (Armant et al. 1995)
B cells	Attenuates apoptosis of B cell precursors	(White et al. 1997)
	Sustains growth of B cell precursors	(Borland et al. 2007)
	Promotes differentiation of germinal centre centroblasts into plasma cells in the presence of IL-1α	(Liu et al. 1991)
T cells	Promotes differentiation in the presence of IL-1α	(Mossalayi et al. 1990b) (Bertho et al. 1991)

Abbreviations: IL, interleukin.

Soluble CD23 also induces human monocytes to stimulate resting T cells, therefore soluble CD23, when produced locally at a site of an immune response, may trigger an inflammatory response via cytokine release and further amplify it via the stimulation of non-antigen-specific T cells (Armant et al. 1995). Monocytes activated by soluble CD23 also express increased levels of molecules involved in B cell and T cell adhesion, including the Toll-like receptor associated molecule CD14, the cell adhesion molecule CD54, and the co-stimulatory molecules CD40, and CD80 (Armant et al. 1995).

Soluble CD23 promotes the survival of B cells (Liu et al. 1991, White et al. 1997) and sustains the growth of human B cell precursors via interaction with the αVβ5 integrin (Borland et al. 2007). The αVβ3 integrin or more commonly termed, vitronectin receptor, and its associated protein CD47, may also function as a receptor for soluble CD23 (Hermann et al. 1999). This interaction mediates proinflammatory cytokine synthesis and may contribute to inflammatory processes involved in chronic disorders such as rheumatoid arthritis (Hermann et al. 1999). In the presence of IL-1α, soluble CD23 also promotes the differentiation of B cells (Liu et al. 1991) and T cells (Mossalayi et al. 1990b, Bertho et al. 1991).

1.1.5 Soluble CD23 in disease

It is well-established that soluble CD23 plays a pivotal role in allergy and allergic reactions (Gould and Sutton 2008). However, soluble CD23 also plays a role in a variety of other diseases including autoimmune and inflammatory disorders. Elevated soluble CD23 has been detected in the serum and saliva of patients with primary

Sjogren's syndrome (Bansal et al. 1992, Takei et al. 1995) and in the serum of patients with systemic lupus erythematosus (Bansal et al. 1992). The elevated level of soluble CD23 in saliva has also been correlated with active sialectasis in Sjogren's syndrome (Takei et al. 1995) indicating soluble CD23 contributes to the pathology of this disease. Soluble CD23 is elevated in patients with adult rheumatoid arthritis, which correlates with disease status (Bansal et al. 1994) and in juvenile chronic arthritis (Massa et al. 1998). However, it remains unclear how soluble CD23 contributes to pathology of these diseases. Elevated soluble CD23 has also been detected in patients with B cell-derived chronic lymphocytic leukaemia (CLL) (Sarfati et al. 1988) and is used to predict time to treatment in CLL patients (Meuleman et al. 2008). In this regard, soluble CD23 is a surrogate marker for total CLL cell numbers.

1.2 CXCL16

1.2.1 Structure and features

Chemokines are cytokines that can induce chemotaxis of cells, and may be loosely categorised as bearing homeostatic or inflammatory functions (Le et al. 2004). Homeostatic chemokines are constitutively expressed and are involved in lymphocyte and dendritic cell trafficking, as well as tissue organogenesis (Le et al. 2004). Inflammatory chemokines are upregulated by proinflammatory stimuli and participate in the innate and adaptive immune responses (Le et al. 2004). Many chemokines are further classified on the basis of the arrangement of cysteine residues in their N-terminal region, yielding the CXC, CC, C or CX3C classes of chemokines (Le et al. 2004). The

four different chemokine classes usually attract different types of leukocytes; CC chemokines attract mononuclear cells, eosinophils and basophils. Glu-Leu-Arg motif (ELR)-positive CXC chemokines attract neutrophils, while ELR motif-negative CXC chemokines attract lymphocytes. C chemokines attract T cells and CX3C chemokines attract T cells, natural killer cells and monocytes (Le et al. 2004). Most chemokines are in soluble forms, however some, namely CXCL16 and CX3CL1 (fractalkine) are associated with glucosaminoglycan moieties on the cell surface and can be released by metalloprotease cleavage (see section 1.2.4).

CXCL16 is a ligand for the CXC-chemokine receptor CXCR6 (Bonzo) (Matloubian et al. 2000) and has functional characteristics of CXC chemokines (Wilbanks et al. 2001). The molecule is expressed on the cell membrane as a multidomain molecule (Matloubian et al. 2000). CXCL16 is much like the CX3CL1 chemokine in structure (White and Greaves 2012), consisting of a chemokine domain, a glycosylated mucin-like stalk, single transmembrane helix and a short cytoplasmic tail (Bazan et al. 1997, Wilbanks et al. 2001) (Figure 1.3). The amino acid sequence suggests a molecular weight of approximately 24 kDa for membrane CXCL16, however glycosylation of the mucin stalk gives the full-length protein a molecular weight of 60 kDa (Matloubian et al. 2000).

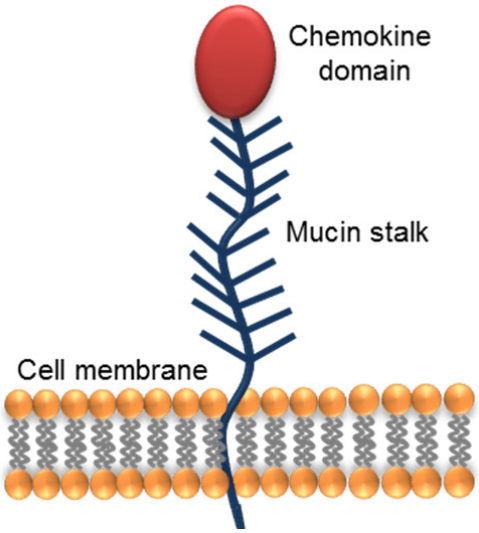

Figure 1.3: The structure of membrane-bound CXCL16. CXCL16 consists of a chemokine domain, a mucin-like stalk and a short cytoplasmic tail. Adapted from White and Greaves 2012.

1.2.2 Distribution of CXCL16

CXCL16 is expressed on the surface of antigen presenting cells including subsets of B cells, and monocytes and macrophages (Wilbanks et al. 2001). CXCL16 is also expressed on dendritic cells (Tabata et al. 2005), aortic smooth muscle cells (Chandrasekar et al. 2004), astrocytes, microglia, and neurons (Rosito et al. 2012). After cytokine stimulation, CXCL16 may be expressed on several other cell types. Interferon-γ and TNF-α induce CXCL16 expression on endothelial cells, smooth muscle cells, fibroblasts (Abel et al. 2004), astroglia and glioma cells (Ludwig et al. 2005b). IL-8 also induces CXCL16 expression on aortic smooth muscle cells (Chandrasekar et al. 2005).

1.2.3 Roles of membrane CXCL16

Membrane CXCL16 predominantly functions as an adhesion receptor for cells expressing CXCR6 (Shimaoka et al. 2004). Treatment with the broad spectrum metalloprotease inhibitor, GM6001 enhances the adhesion of CXCL16-transfected COS-7 fibroblast-like cells to CXCR6-expressing T cells by increasing cell surface expression of CXCL16, and decreasing soluble CXCL16 (Shimaoka et al. 2004) (see also section 1.2.4.1). Besides possessing adhesion activity, membrane CXCL16 functions as a scavenger receptor that binds phosphatidylserine (PS) and oxidised low density lipoprotein (Shimaoka et al. 2000). Membrane CXCL16 also mediates cell adhesion and phagocytosis of bacteria, and therefore may facilitate the uptake of various pathogens during infection (Shimaoka et al. 2003, Gursel et al. 2006).

1.2.4 Generation and roles of soluble CXCL16

1.2.4.1 Shedding of membrane CXCL16

Metalloprotease cleavage of CXCL16 results in a soluble 35 kDa molecule (Matloubian et al. 2000). Similar to soluble CD23, soluble CXCL16 is generated after proteolytic cleavage of the membrane protein (Abel et al. 2004, Gough et al. 2004, Ludwig et al. 2005a, Hundhausen et al. 2007). Experiments using the ADAM10 inhibitor GI254023X and the combined ADAM10/ADAM17 inhibitor GW280264X, (Abel et al. 2004), short interfering RNA (siRNA) knockdown of ADAM10 and overexpression of ADAM10 in cells (Gough et al. 2004) show ADAM10 is primarily responsible for the generation of soluble CXCL16 and the regulation of cell surface CXCL16. In contrast, siRNA

knockdown of ADAM17 in human mesangial cells impairs CXCL16 shedding and has implicated ADAM17 in the constitutive shedding of CXCL16 (Schramme et al. 2008). Thus while ADAM10 is the principal constitutive CXCL16 sheddase, it is possible that ADAM17 may function as the main sheddase in certain conditions or cell types.

Using metalloprotease inhibitors, it has been shown that PMA-induced CXCL16 shedding is attributed to ADAM17 rather than ADAM10 (Abel et al. 2004, Ludwig et al. 2005a, Hundhausen et al. 2007). However, siRNA knockdown of ADAM10 or ADAM17 in human mesangial cells, impairs cytokine-induced shedding of CXCL16, implying a role for both ADAM10 and ADAM17 in this process (Schramme et al. 2008). In contrast, Ca^{2+}/ionomycin-induced shedding of CXCL16 is attributed to ADAM10 rather than ADAM17 (Hundhausen et al. 2007). Thus, like constitutive CXCL16 shedding, the ADAM responsible for inducible CXCL16 shedding may be dependent on the conditions or cell types involved. Further studies are needed to deduce the mechanism by which these ADAMs cleave CXCL16.

1.2.4.2 Roles of soluble CXCL16

A major role for soluble CXCL16 is the induction of chemotaxis of cells. Recombinant soluble CXCL16 binds CXCR6-transfected L1-2 lymphoma B cells and induces Ca^{2+} flux and chemotaxis of these cells (Wilbanks et al. 2001). Soluble CXCL16 also induces strong chemotactic responses in activated $CD4^+$ and $CD8^+$ T cells (Matloubian et al. 2000). Besides chemotactic activity, recombinant human soluble CXCL16 also acts as an angiogenic factor by inducing the proliferation, migration and tube formation

of human umbilical vein endothelial cells (Zhuge et al. 2005). More recently, it has been shown that recombinant soluble CXCL16 protects hippocampal neurons from excitotoxic cell death and protects from oxygen glucose deprivation damage (Rosito et al. 2012).

1.2.5 Soluble CXCL16 and disease

Like soluble CD23, soluble CXCL16 has also been implicated in several inflammatory and autoimmune diseases, as well as acute coronary syndromes and cancer. Amounts of CXCL16 in serum and cerebrospinal fluid are increased in patients with systemic lupus erythematosus, multiple sclerosis and meningitis (le Blanc et al. 2006). CXCL16 is also elevated in serum of patients with inflammatory bowel disease (Lehrke et al. 2008, Diegelmann et al. 2010), and in the synovial fluid of rheumatoid arthritis patients (van der Voort et al. 2005). Moreover, serum concentrations of CXCL16 reflect disease activity, and may be a novel biomarker and potential predictor of multiple sclerosis (Holmoy et al. 2013), colorectal cancer (Matsushita et al. 2012), atherosclerosis (Lehrke et al. 2007), acute coronary syndromes (Sun et al. 2008, Jansson et al. 2009) and renal injury in type 2 diabetes mellitus (Zhao et al. 2014).

1.3 Purinergic signalling and purinergic receptors

1.3.1 Introduction

Purinergic transmitters and receptors have become an increasingly important focus in physiology and pathophysiology since the elucidation of the role played by extracellular adenosine 5'-triphosphate (ATP) in neurotransmission and neuromodulation (Burnstock 2007). Currently, it is well-known that extracellular nucleotides activate a network of purinergic signalling cascades involving membrane receptors and ectoenzymes (Burnstock 2007, Yegutkin 2008). ATP and other nucleotides such as adenosine, adenosine 5'-diphosphate (ADP), uridine 5'-triphosphate (UTP) and uridine 5'-diphosphate (UDP)-glucose can be released into the extracellular environment by a variety of conditions (Lazarowski et al. 2003). ATP can be released as a neurotransmitter, autocrine and paracrine signalling molecule in excitatory tissues, during infection, inflammation and other pathological conditions (Lazarowski et al. 2003). Once in the extracellular fluid, nucleosides and nucleotides activate two types of purinergic receptors, termed P1 and P2 receptors respectively. P1 and P2 receptors are characterised based on molecular structure, function and pharmacological profile. The P1 receptor group comprises A_1, A_{2A}, A_{2B} and A_3 adenosine receptors; these receptors are G protein-coupled and are predominantly selective for adenosine (Ralevic and Burnstock 1998). The P2 receptor group is sub-divided into P2X and P2Y receptors based on whether they are ligand-gated (P2X) or G protein-coupled (P2Y) and are predominantly selective for ATP, although ADP, UTP and UDP-glucose also activate some P2Y receptors (Khakh and North 2006) (Figure 1.4). P2X and P2Y activation induces downstream signalling that affects many cellular processes. Although the

downstream functions of each P2 receptor remains to be fully elucidated, it is widely accepted that purinergic signalling is involved in a large array of physiological responses including neurotransmission, coagulation, inflammation, proliferation, differentiation and cell death, and tissue regeneration (Burnstock 2007).

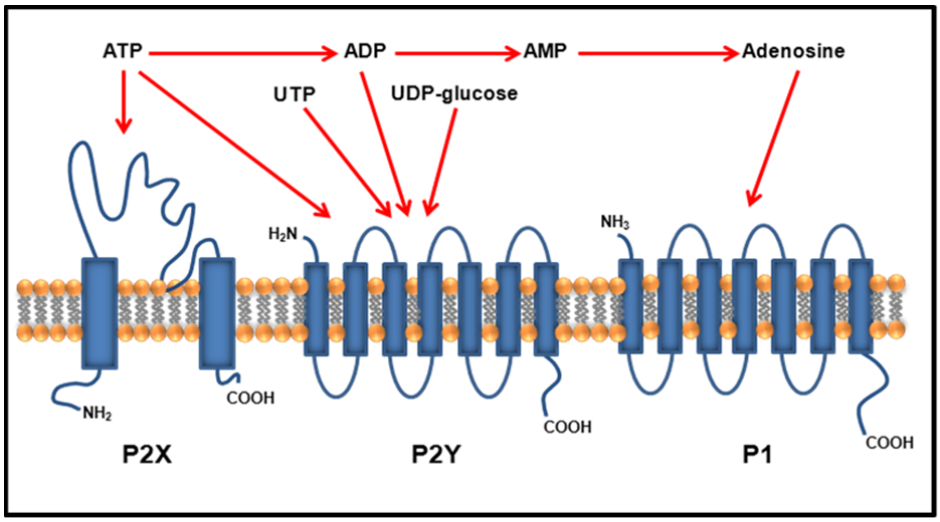

Figure 1.4: **Extracellular nucleosides and nucleotides activate P1 and P2 purinergic receptors.** Adenosine activates P1 receptors and ATP activates P2X receptors, while several nucleotides including ATP, ADP, UTP and UDP-glucose activate P2Y receptors. Adapted from Khakh and North 2006. **Abbreviations:** ATP, adenosine 5'-triphosphate; ADP, adenosine 5'-diphosphate; UTP, uridine 5'-triphosphate; UDP, uridine 5'-diphosphate; AMP, adenosine monophosphate

1.3.2 P2Y receptors

P2Y receptors, like other G protein-coupled receptors, contain an intracellular C-terminus, an extracellular N-terminus and seven transmembrane (TM1-7) α-helical domains that form the ligand-binding site (Jacobson et al. 2012). P2Y receptors possess a high level of sequence homology between transmembrane regions TM3, TM6 and TM7, and structurally diverse intracellular loops and C-termini which influence the

degree of G protein coupling (Jacobson et al. 2012). Currently eight P2Y receptor subtypes (P2Y1, 2, 4, 6, 11-14) have been cloned, and these receptors may be sub-divided based on coupling to specific G proteins (Jacobson and Boeynaems 2010). P2Y1, 2, 4, 6, and 11 couple to $G_{q,}$ to activate phospholipase C (PLC) β via adenylyl cyclase, whereas P2Y12, 13, and 14 couple to G_i, to inhibit adenylyl cyclase. P2Y11 is unique amongst the P2Y receptors in its ability to couple to both G_q and G_s (Jacobson and Boeynaems 2010). P2Y receptors mediate a variety of downstream signalling events including the stimulation of phospholipases A, C and D, mitogen-activated protein kinase (MAPK), Rho-kinase and protein tyrosine kinase. The pharmacological properties and tissue distribution varies between P2Y receptors (Burnstock and Knight 2004). Recently, the crystal structures of P2Y12 complexed with its agonist, 2-methylthio-adenosine-5'-diphosphate (Zhang et al. 2014a) and antagonist, AZD1283 (Zhang et al. 2014b) have been reported. These structural studies will provide insight into the pharmacology of agonists and antagonists for P2Y12 and other P2Y receptors, and further the development of drug candidates for P2Y receptors.

1.3.3 P2X receptors

P2X receptors are non-selective, ligand-gated cation channels, which upon activation allow an influx of Ca^{2+} and Na^{+}, and an efflux of K^{+} along an electrochemical gradient (Jarvis and Khakh 2009). These receptors are unique structurally compared to other ligand-gated channels such as the nicotinic acetylcholine and glutamate receptors (Kaczmarek-Hajek et al. 2012). P2X receptors are trimers of subunits, each with two transmembrane domains (TM1 and TM2), intracellular N- and C-termini and a large extracellular loop per subunit (Kaczmarek-Hajek et al. 2012). Seven P2X receptors

(P2X1-7) have been cloned and characterised, these possess a broad tissue distribution and differing pharmacological properties (Burnstock and Knight 2004).

P2X structural and functional properties have predominantly been determined by cDNA cloning however, the crystal structure of the zebrafish P2X4 receptor (Kawate et al. 2009) has provided a three dimensional resource available for further structural and functional studies of P2X receptors (Figure 1.5). The P2X4 crystal structure has enabled analysis and interpretation of previous structural and functional work, and will also allow for studies using homology models of other P2X receptor subtypes from different species (Young 2010). This advancement will contribute to further the understanding of ligand binding, the structure of the open, closed and dilated channel, as well as ion permeation, which are all important in structure-based drug design (Browne et al. 2010, Jiang et al. 2013). The further elucidation of structure and function of P2X receptors may be useful for new therapeutics for neuropathic pain and inflammation (Browne et al. 2010, Jiang et al. 2013).

1.4 The P2X7 receptor

1.4.1 Structure and function

The human, mouse, rat, dog and rhesus macaque monkey P2X7 protein subunit consists of 595 amino acids (Surprenant et al. 1996, Rassendren et al. 1997, Chessell et al. 1998b, Roman et al. 2009, Bradley et al. 2011b), while guinea-pig P2X7 consists of 594 amino acids (Fonfria et al. 2008). This introduction however, will predominantly focus

on human and murine P2X7, the two species studied in this thesis. Computer modelling suggests that P2X7 has a structure similar to that of other P2X receptors (Figure 1.5)

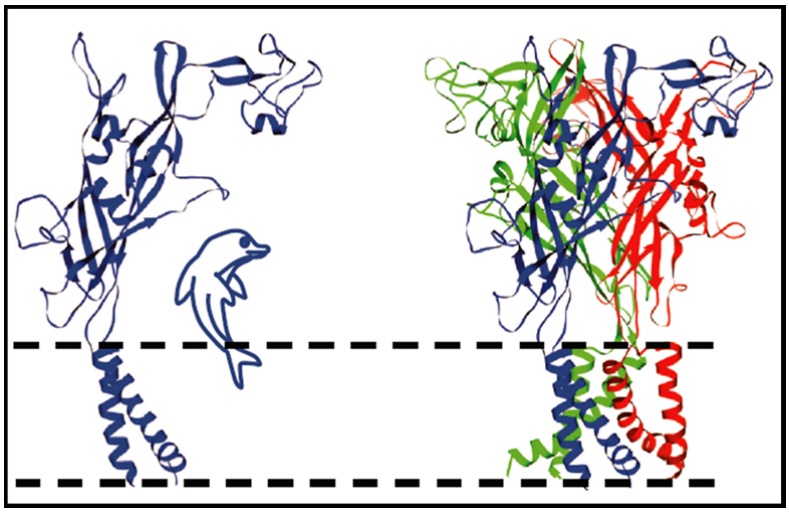

Figure 1.5: The structure of P2X receptors. A P2X7 subunit, shaped similarly to a dolphin (left), and the chalice shaped trimeric receptor (right), is shown parallel to the cell membrane. Each subunit is depicted in a different colour and represents the general structure of P2X receptors. The structure of P2X7 is shown based on the crystal structure of zebrafish P2X4. From Jiang 2012.

(Jiang 2012, Jiang et al. 2013). ATP activation of P2X7 induces the immediate opening of a non-selective cation channel, which allows an influx of Ca^{2+} and Na^{+}, and an efflux of K^{+} across the cell membrane (Surprenant et al. 1996, Rassendren et al. 1997, Chessell et al. 1998b). P2X7 is viewed historically as biologically unique in its ability to induce pore formation upon prolonged (>30s) ATP activation (Burnstock 2007). However, it is now known that activation of other P2X receptors including P2X2 (Virginio et al. 1999, Chaumont and Khakh 2008), P2X4 (Seil et al. 2010) and P2X2/5 (Compan et al. 2012)

can also induce permeabilisation of cells. P2X7 activation allows the uptake of organic cations including N-methyl-D-glucamine^{+}, ethidium^{+} and YO-PRO-1^{2+} (Jiang et al. 2005, Cankurtaran-Sayar et al. 2009), and organic anions including Lucifer yellow and calcein (Cankurtaran-Sayar et al. 2009). After P2X7 activation, organic cations and anions are thought to enter the cell via different permeation pathways (Cankurtaran-Sayar et al. 2009).

Originally, it was thought that the P2X7 channel dilated to a pore over prolonged agonist application (North 2002). Later, it was shown that activated P2X7 interacts with the hemichannel pannexin-1, which functions as the P2X7-induced pore (Pelegrin and Surprenant 2006, Locovei et al. 2007). More recently however, studies have shown that pannexin-1 is not the main pore pathway induced after P2X7 activation. Macrophages from pannexin-1 knockout mice display ATP-induced YO-PRO-1^{2+} uptake (Qu et al. 2011) and siRNA knockdown of pannexin-1 does not affect P2X7 responses, including dye uptake in murine macrophages (Alberto et al. 2013). In support of this, it has been shown that large organic dyes permeate the P2X7 receptor ion channel itself (Browne et al. 2013).

1.4.2 Polymorphic and splice variants

1.4.2.1 Single nucleotide polymorphisms

The human *P2RX7* gene is highly polymorphic and contains over 1500 single nucleotide polymorphisms (SNPs). The majority of these are intronic and

approximately 150 are non-synonymous (Sluyter and Stokes 2011). There are 20 characterised SNPs that alter P2X7 function, including the loss-of-function SNPs V76A, R117W, G150R, E186K, L191P, R276H, R307Q, T357S, E496A and I568N (Wiley et al. 2003, Gu et al. 2004, Roger et al. 2010, Stokes et al. 2010), and the gain-of-function SNPs H155Y, H270R, and A348T (Cabrini et al. 2005, Roger et al. 2010, Stokes et al. 2010). The R307Q loss-of-function SNP was originally thought to reduce P2X7 function by abolishing binding of ATP to P2X7 (Gu et al. 2004), however, as Arg307 is involved in hydrogen bonding and salt bridge interactions, it has been suggested that the R307Q SNP leads to a loss of these interactions (Jiang et al. 2013). The I568N SNP prevents normal cell trafficking of P2X7, and thus cell surface expression and function (Wiley et al. 2003). It remains to be determined how other loss-of-function SNPs cause a loss of function effect. The gain-of-function SNP H155Y affects P2X7 cell surface expression (Bradley et al. 2011a), while other gain-of-function SNP effects remain to be determined. The Q460R SNP has minimal effect on P2X7 function itself, but is co-inherited with other gain-of-function SNPs in a haplotype termed P2X7-4 (Stokes et al. 2010).

The murine *P2XR7* gene has more than 1700 SNPs and similar to the human gene, are mainly intronic. There are 10 reported non-synonomous SNPs only of which the naturally occurring P451L has been characterised (Bartlett et al. 2014). This SNP was originally identified in C57BL/6 mice (Adriouch et al. 2002). T cells from these mice have lower sensitivity to ATP (Adriouch et al. 2002) and display significantly impaired P2X7-induced cell death (Le Stunff et al. 2004) compared to T cells from wild-type 451P BALB/c mice. Furthermore, astrocytes from C57BL/6 mice have reduced P2X7 mediated pannexin-1 currents, ATP release and intracellular Ca^{2+} spread compared to

astrocytes from BALB/c mice, which are wild-type at position 451 (Suadicani et al. 2009). The P451L SNP is also present in other mouse strains including the C57BL/10, DBA/1 and DBA/2 strains (Adriouch et al. 2002). Other SNPs that have been identified include the L11F, T221A and T283M SNPs in P2X7 cloned from the NTW8 murine microglia cell line. Of these, only the T283M SNP exhibited low P2X7 function (Young et al. 2006).

1.4.2.2 Splice variants

Human P2X7 has nine naturally occurring splice variants termed P2X7B-P2X7J. The full-length 595 amino acid protein is termed P2XA (Cheewatrakoolpong et al. 2005, Feng et al. 2006). Truncated variants P2X7B, C, E, and G have short C-termini, while P2X7C-F are missing exons which code for the extracellular domain. P2X7G and H have additional exons in the extracellular domain (Cheewatrakoolpong et al. 2005). P2X7I leads to a null allele (Skarratt et al. 2005) and P2X7J is also a truncated variant, which lacks exons from the extracellular loop to the C-terminus (Feng et al. 2006). P2X7B can form functional channels but not pores and potentiates P2X7A-mediated effects including dye uptake. P2X7B coexpression with P2XA, results in heteromeric receptors that induce signalling pathways to stimulate cell growth (Adinolfi et al. 2010). P2X7J cannot form pores but oligomerises with P2X7A, to prevent its trafficking to the cell surface resulting in reduced P2X7 function (Feng et al. 2006).

In mice, three naturally occurring P2X7 splice variants have been identified, termed P2X7K (Nicke et al. 2009), P2X713B and P2X713C (Masin et al. 2012). P2X7K has an

alternate N-terminus and first transmembrane domain (Nicke et al. 2009). It is functional with 8-fold higher sensitivity to the P2X7 agonist 2'(3')-*O*-(4-benzoylbenzoyl)adenosine-5'-triphosphate (BzATP) (see section 1.4.3), slower deactivation kinetics and increased tendency to form pores compared to P2X7A (Nicke et al. 2009). P2X713B and P2X13C are C-terminal truncated variants with alternative exons 13. When these variants are expressed in HEK 293 cells, they show low channel function, cell expression and absent pore formation (Masin et al. 2012). P2X713B is inefficiently trafficked and coassembles with P2X7A to inhibit P2X7 function (Masin et al. 2012). P2X7K also escapes deletion in the GlaxoSmithKline P2X7 knockout mice (Nicke et al. 2009) generated by Chessell and colleagues (Chessell et al. 2005), while P2X13B and C escape deletion in the Pfizer P2X7 knockout mice (Masin et al. 2012) generated by Solle and colleagues (Solle et al. 2001). Despite the discovery of human and murine P2X7 SNPs and variants, the functional significance of these is poorly understood.

1.4.3 Pharmacology

Human and murine P2X7 were first cloned from cDNA obtained from human monocytes (Rassendren et al. 1997) and the NTW8 murine microglia cell line (Chessell et al. 1998b) respectively. ATP is the natural ligand of P2X7, and requires higher concentrations (half maximal effective concentration (EC_{50}) of more than 100 μM) for activation compared to other P2X receptors (North 2002). How such high concentrations of extracellular ATP are achieved *in vivo* is often questioned. However, comparison of P2X7-deficient mice and wild-type controls in a number of disease models has highlighted a role for P2X7 and indirectly demonstrated that sufficient

concentrations of extracellular ATP can be obtained *in vivo* under some conditions (Labasi et al. 2002, Ke et al. 2003, Chessell et al. 2005, Beaucage et al. 2014). The agonist order of potency for human P2X7 is BzATP >> ATP > 2-methylthio-adenosine-5'-triphosphate > adenosine 5'-O-(3-thio) triphosphate (ATPγS) >> ADP (Donnelly-Roberts et al. 2009). This order is similar for murine P2X7 however, 2-methylthio-adenosine-5'-triphosphate and ATPγS are ineffective activators of this receptor (Donnelly-Roberts et al. 2009). As BzATP is the most potent P2X7 agonist, it is often confused as a selective agonist of P2X7. However, it is well known that BzATP can activate other P2 receptors including P2X1 (Bianchi et al. 1999), P2X2 (Lynch et al. 1999), P2X3 (Bianchi et al. 1999), P2Y2 (Wildman et al. 2003) and P2Y11 (Communi et al. 1999).

An ATP-independent pathway can also activate murine P2X7. ADP-ribosyltransferase (ART) 2 in murine T cells, transfers an ADP-ribose group from nicotinamide adenine dinucleotide (NAD) to activate P2X7 (Seman et al. 2003). Similar to ATP-induced P2X7 activation, NAD-induced P2X7 activation causes Ca^{2+} flux, pore formation, PS exposure, L-selectin (CD62L) shedding and apoptosis (Seman et al. 2003). As shown by P2X7-induced PS exposure, lower concentrations of NAD are required to activate P2X7 compared to ATP (EC_{50} of 2 uM vs 100 uM) (Seman et al. 2003). NAD-induced activation of P2X7 does not occur in humans due to the inactivation of the *ART2* gene (Haag et al. 1994).

A number of P2X7 antagonists have been identified, these include the first generation antagonists suramin, brilliant blue G (BBG), pyridoxal phosphate-6-azophenyl-2-4-

disulphonic acid (PPADs), periodate-oxidised ATP (oATP) and KN-62. Of these, BBG remains the most commonly used, particularly in *in vivo* studies (Bartlett et al. 2014). BBG is generally considered a specific antagonist, especially at murine P2X7 (Jiang et al. 2000). However, BBG, as well as suramin, both block pannexin-1 (Qiu and Dahl 2009). Suramin and PPADs are also well-known broad spectrum P2 receptor antagonists (Kaczmarek-Hajek et al. 2012). Likewise oATP has been shown to inhibit other P2X receptors (Evans et al. 1995) and KN-62 inhibits calmodulin-dependent protein kinase, when used at concentrations 10-fold higher than that for P2X7 (Di Virgilio 2003).

In more recent years, specific second generation antagonists of P2X7 have been generated. These include A-438079, A839977, AZ10606120, AZ11645373 and A740003 (Bartlett et al. 2014). Many studies tend to use new generation antagonists for *in vitro* assays but continue to utilise first generation antagonists for *in vivo* studies (Bartlett et al. 2014). Extracellular cations such as Na^{+}, Ca^{2+} and Mg^{2+} are also known to inhibit P2X7 function by binding to an unidentified inhibitory site or by reducing the availability of the ATP^{4-} species required for P2X7 activation (Wiley et al. 1992, Michel et al. 1999). Therefore, these cations are often excluded from incubation media during *in vitro* investigations to increase P2X7 function and aid measurements of receptor function (Virginio et al. 1997).

1.4.4 Distribution

P2X7 is expressed on a variety of cell lineages including hematopoietic cells, osteoblasts, fibroblasts, endothelial cells, epithelial cells, and cells from the central and peripheral nervous systems (Lenertz et al. 2011, Wiley et al. 2011). P2X7 was originally thought to be expressed only on hematopoietic cells, and therefore its presence is well established on these cell types (Wiley et al. 2011). Several studies show the presence of P2X7 on human primary B cells (Gu et al. 2000, Gu et al. 2001) as well as malignant B cells from patients with CLL (Wiley et al. 1992, Gu et al. 2000, Shemon et al. 2008). While many studies show P2X7 expression on human B cells, a few studies show the presence of P2X7 on murine B cells. In fact, some early studies suggest that P2X7 is not expressed on murine B cells (Chused et al. 1996, Tsukimoto et al. 2006). In contrast, others have shown that P2X7 activation induces the shedding of the TNF receptor, CD27 from murine B cells (Moon et al. 2006). Therefore, it remains to be established if murine B cells express functional P2X7.

1.4.5 Downstream events

P2X7 activation elicits a variety of downstream events including IL-1 cytokine family member secretion, cell death and proliferation, transcription factor activation, reactive oxygen species (ROS) formation and various membrane-related events.

1.4.5.1 IL-1 cytokine family member secretion

P2X7 induces the secretion of cytokines belonging to the IL-1 family including IL-1β (Ferrari et al. 1997a, Mehta et al. 2001, Brough et al. 2003, Pelegrin and Surprenant 2007), IL-18 (Mehta et al. 2001), IL-1α (Brough et al. 2003), IL-36α (Martin et al. 2009) and the IL-1 receptor antagonist (Wilson et al. 2004). P2X7-induced IL-1β secretion is the most studied and relies on NLRP3 inflammasome activation and K^+ efflux (Perregaux and Gabel 1994, Andrei et al. 2004, Munoz-Planillo et al. 2013). Other signalling molecules involved in P2X7-induced IL-1β secretion include Rho-kinases and caspases (Verhoef et al. 2003), as well as phospholipases A and C (Andrei et al. 2004). Recently, prostaglandin release has been shown in conjunction with IL-1β release following P2X7 activation in macrophages (Barbera-Cremades et al. 2012). P2X7-induced prostaglandin release involves activation of MAPKs including c-Jun N-terminal kinase (JNK) and extracellular regulated kinases (ERK), as well as activation of the enzyme cyclooxygenase-2 (Barbera-Cremades et al. 2012).

1.4.5.2 Cell death and proliferation

Classically, P2X7 activation is known to induce cell death by apoptosis, which involves the activation of caspase-1, -3 and -8 (Ferrari et al. 1999) or JNK (Humphreys et al. 2000). Paradoxically, P2X7 is also involved in cell proliferation. In T cells, P2X7 activates the nuclear factor of activated T cells (NFAT) transcription factor to induce T cell proliferation by secretion of the growth factor, IL-2 (Yip et al. 2009). P2X7-induced cell proliferation has also been shown in microglia, however the downstream effectors remain to be determined (Bianco et al. 2006, Monif et al. 2009). The P2X7 splice variant, P2X7B, is thought to primarily promote cell proliferation,

while P2X7A is considered the 'death receptor' (Adinolfi et al. 2010). P2X7 activation also promotes survival and neuroprotection in neurons, which involves glycogen synthase kinase-3 (GSK-3) (Ortega et al. 2009) and phosphatidyl-inositol-3-kinase (PI3K) (Ortega et al. 2010).

1.4.5.3 Transcription factor activation

Several studies suggest that P2X7 activation influences gene expression due to the regulation of several gene transcription factors. In addition to NFAT in T cells (Yip et al. 2009), these include nuclear factor-κB in microglia (Ferrari et al. 1997b) and osteoclasts (Korcok et al. 2004), cyclic adenosine monophosphate response element binding protein activation (Gavala et al. 2008), FBJ murine osteosarcoma viral oncogene homolog B/activation protein-1 in monocytes and osteoblasts (Gavala et al. 2010), and early growth response protein-1 in P2X7-transfected HEK 293 cells (Stefano et al. 2007).

1.4.5.4 ROS formation

It is well established that P2X7 activation plays a role in the generation of ROS. P2X7 activation induces ROS generation via nicotinamide adenine dinucleotide phosphate (NADPH) oxidase in macrophages (Lenertz et al. 2009), microglia (Bartlett et al. 2013), submandibular glands (Seil et al. 2008) and erythroid cells (Wang and Sluyter 2013). MAPK, ERK1/2 and protein kinase C (PKC) activation are involved in P2X7-induced ROS production (Seil et al. 2008, Lenertz et al. 2009).

1.4.5.5 Membrane-related events

P2X7 is involved in the regulation of phagocytosis. Transfection of P2X7 into non-phagocytic HEK 293 cells allows these cells to phagocytose latex beads or bacteria (Gu et al. 2010, Wiley and Gu 2012). This process requires that P2X7 be complexed with the non-muscle myosin IIA and does not require activation by ATP (Gu et al. 2010, Wiley and Gu 2012). P2X7 activation induces the killing of *mycobacterium tuberculosis* in macrophages, and requires the signalling molecule phospholipase D (PLD) (Kusner and Adams 2000). P2X7 activation also induces lysosome secretion of cathepsins B, K, L and S, which are released by Ca^{2+}-dependent exocytosis from monocytes and macrophages (Lopez-Castejon et al. 2010). Furthermore, P2X7 activation induces membrane blebbing, which involves MAPKs (Pfeiffer et al. 2004) and Rho-kinases (Verhoef et al. 2003), and elicits other cell-membrane-related events including microparticle release (Qu and Dubyak 2009) and the shedding of cell surface molecules (see section 1.5).

1.4.6 Disease

P2X7 is implicated in a number of inflammatory and immune diseases including rheumatoid arthritis (Portales-Cervantes et al. 2010), Sjogren's syndrome (Lester et al. 2013), graft-versus-host disease (Wilhelm et al. 2010), multiple sclerosis (Yiangou et al. 2006), glomerulonephritis (Taylor et al. 2009b) and inflammatory pain (Chessell et al. 2005). Several studies report that P2X7 also plays a role in neurodegenerative diseases including Alzheimer's disease (Diaz-Hernandez et al. 2012), Huntington's disease (Diaz-Hernandez et al. 2009) and amyotrophic lateral sclerosis (Yiangou et al. 2006). P2X7 also plays a role in cancer (Adinolfi et al. 2012) and infectious diseases (Miller et

al. 2011a, Miller et al. 2011b). Furthermore, *P2RX7* SNPs have been associated with disorders. The Q460R SNP is associated with bipolar affective disorder (Barden et al. 2006), major depressive disorder (Lucae et al. 2006) and Sjogren's syndrome (Lester et al. 2013). The R307Q SNP is associated with low lumbar spine bone mineral density (Gartland et al. 2012), while the A348T SNP is associated with a lower vertebral fracture incidence in women ten years after menopause (Jorgensen et al. 2012). The A348T SNP is also increased in frequency in Arabic rheumatoid arthritis patients (Al-Shukaili et al. 2011) and depressive disorder patients (Lucae et al. 2006).

1.5 Nucleotide-induced shedding of cell surface molecules

1.5.1 Introduction

Ectodomain shedding is a vital post-translational modification which downregulates cell surface expression of molecules and causes their release in a soluble form (Hayashida et al. 2010). The soluble form may retain its original activity and induce functional responses in an autocrine or paracrine manner (Hayashida et al. 2010). Ectodomain shedding is exhibited by a diverse range of molecules including cytokines, growth factors and cell adhesion molecules, and can be stimulated by a variety of mechanisms (see Hayashida et al. 2010 for further review). Nucleotide or P2 receptor-induced shedding is also exhibited by a variety of molecules including CD23 and CD62L (Figure 1.6) and will be discussed in further detail below.

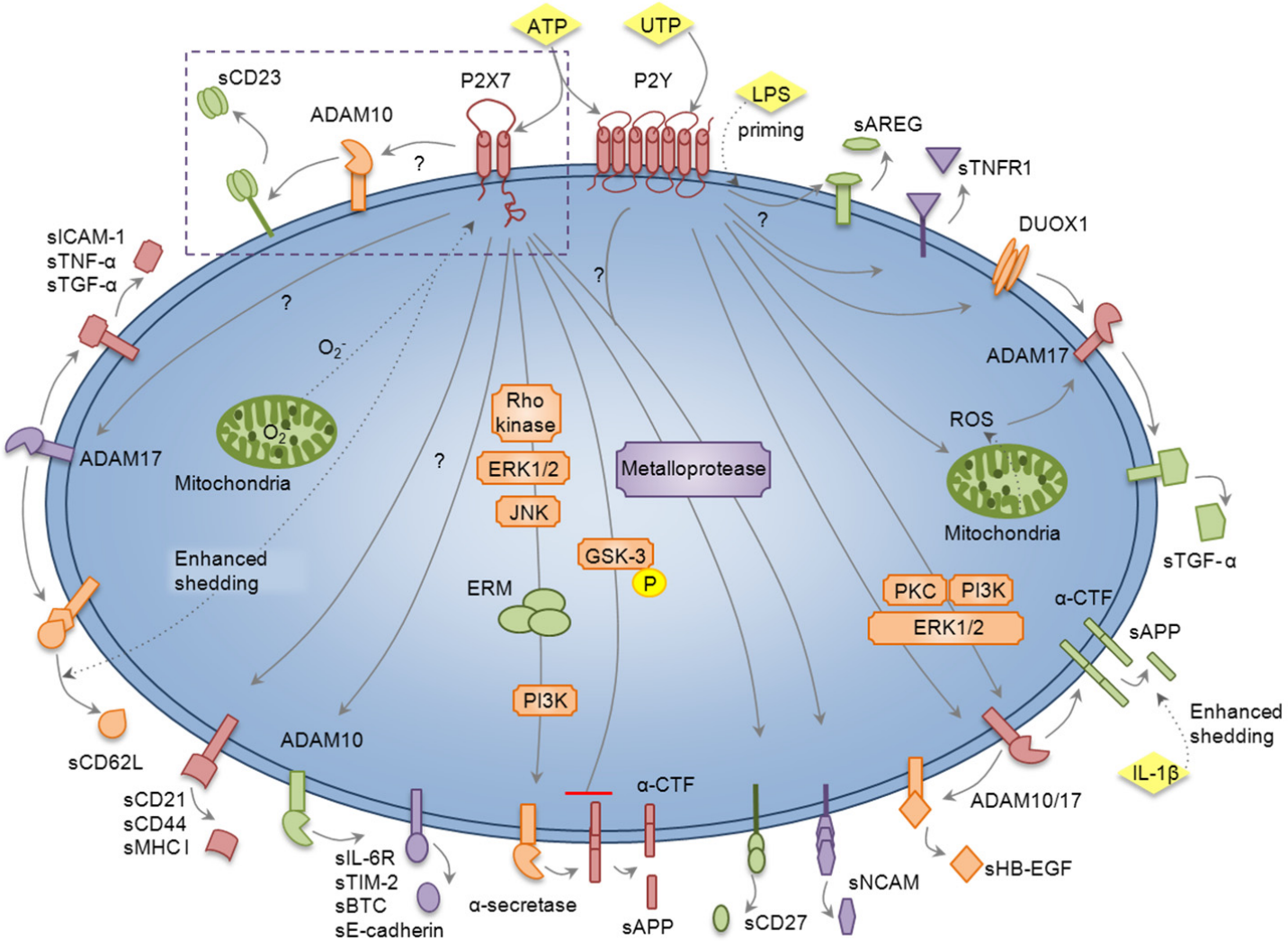
ATP
UTP
sCD23
P2X7
P2Y
LPS
priming
ADAM10
?
sAREG
sTNFR1
DUOX1
sICAM-1
sTNF-α
sTGF-α
?
?
?
O_2^-
ADAM17
ADAM17
Rho kinase
ROS
O_2
Mitochondria
ERK1/2
Metalloprotease
?
JNK
Mitochondria
sTGF-α
GSK-3
P
Enhanced shedding
ERM
PKC
PI3K
ERK1/2
α-CTF
sAPP
PI3K
Enhanced shedding
sCD62L
ADAM10
IL-1β
α-CTF
sCD21
sCD44
sMHC I
ADAM10/17
sIL-6R
sTIM-2
sBTC
sE-cadherin
α-secretase
sAPP
sCD27
sNCAM
sHB-EGF

Figure 1.6 Nucleotide-induced shedding of cell surface molecules. The nucleotides ATP and UTP activate P2X and P2Y receptors to induce the shedding of cell surface molecules. ADAM10 is involved in nucleotide or P2X7-induced shedding of CD23, IL-6R, TIM-2, BTC, and E-cadherin. Whether P2X7 activates ADAM10 to induce the shedding of CD23 and other molecules remains unknown. ADAM17 is involved in P2X7-induced shedding of CD62L, ICAM-1, TNF-α and TGF-α. P2X7 activation also induces the shedding of CD21, CD44, MHC I, CD27 and possibly NCAM. The involvement of other intracellular signalling molecules in the shedding of the above molecules remains unclear. P2X7 activation also induces APP processing via an intracellular signalling cascade involving Rho-kinase, ERK1/2, JNK, ERM and PI3K. However, an opposing role for P2X7 in APP processing is also suggested, whereby APP processing is inhibited by GSK-3 after P2X7 activation. P2Y receptors are involved in the activation of mitochondrial ROS and DUOX-1, which activate ADAM17 to shed TGF-α. Furthermore P2Y receptor activation is linked to the stimulation of ADAM10 and ADAM17, and several downstream molecules, including PKC, PI3K and ERK1/2 which participate in HB-EGF and APP processing. P2Y receptor activation also induces AREG and TNFR1 shedding, however the mechanisms remain undetermined. The focus of the current research is highlighted by the dashed box. **Abbreviations:** ADAM, a disintegrin and metalloprotease; APP, amyloid precursor protein; AREG, amphiregulin; ATP, adenosine 5'-triphosphate; CD21, complement receptor 2; CD23, IgE receptor; CD27, tumor necrosis factor receptor; CD44, hyaluronic acid receptor; CD62L, L-selectin; CTF, carboxyl-terminal fragment; DUOX, dual oxidase; E-cadherin, epithelial cadherin; ERK, extracellular signal-regulated kinase; ERM, ezrin radixin moesin; GSK, glycogen synthase kinase; HB-EGF, heparin-binding-epidermal growth factor; ICAM, intercellular adhesion molecule; IL, interleukin; IL-6R, interleukin-6 receptor, JNK, c-Jun N-terminal kinase; LPS, lipopolysaccharide; MHC, major histocompatibility complex; NCAM, neural cell adhesion molecule; PI3K, phosphatidylinositide 3-kinase; PKC, protein kinase C; ROS, reactive oxygen species; TIM, T cell immunoglobulin and mucin; TGF, transforming growth factor; TNF, tumor necrosis factor; TNFR, tumor necrosis factor receptor; UTP, uridine 5'-triphosphate.

Using protease inhibitors (Table 1.2), studies have shown a role for sheddases in nucleotide-induced ectodomain shedding of molecules. Although, these inhibitors have been useful in implicating a role for metalloproteases in this process, there is still a lack of specific metalloprotease inhibitors available. GI254023X (Table 1.2) is a specific ADAM10 inhibitor (Ludwig et al. 2005a), however it can also impair other ADAMs at concentrations above 5 μM (Weskamp et al. 2006). Future development of more specific metalloprotease antagonists will be beneficial to the study of mechanisms involved in nucleotide-induced shedding.

1.5.2 CD23

As noted in section 1.1, CD23 is involved in the regulation of IgE levels (Gould and Sutton 2008) and functions as an adhesion molecule. Moreover, in the soluble form, CD23 also exerts cytokine-like activities (Acharya et al. 2010). ATP and BzATP-induced CD23 shedding was first shown to occur from CLL lymphocytes (Gu et al. 1998). The P2X7 antagonists, KN-62 and oxATP impair nucleotide-induced CD23 shedding from CLL cells, thus confirming a role for P2X7 in CD23 shedding (Gu et al. 1998). Since then, P2X7-induced CD23 shedding has been described for human monocyte-derived dendritic cells (Sluyter and Wiley 2002), monocyte-derived Langerhans cells (Georgiou et al. 2005) and RPMI 8226 multiple myeloma B cells (Farrell 2008). Dendritic cells and Langerhans cells, from subjects who were homozygous for the loss-of-function polymorphism E496A, exhibited attenuated ATP-induced CD23 shedding (Sluyter and Wiley 2002, Georgiou et al. 2005) further supporting a role for P2X7 in this process. Furthermore, BzATP induces CD23 shedding from CD23-transfected Chinese hamster ovary (CHO) cells (Le Gall et al.

2009) and downregulates CD23 surface expression on murine B cells (Le Gall et al. 2010).

Table 1.2: Protease inhibitors used in studies of nucleotide-induced ectodomain shedding.

Compound	Specificity	Reference
BB-2516	Broad spectrum metalloprotease inhibitor	(Wada et al. 2003)
BB-3103	Broad spectrum metalloprotease inhibitor	(Mirastschijski et al. 2002)
BB-94	Broad spectrum metalloprotease inhibitor	(Davies et al. 1993)
E64	Non-selective cysteine protease inhibitor	(Susa et al. 2004)
Decanoyl-RVKR-CMK	Non-selective convertase inhibitor	(Denault et al. 1995)
GI254023X	ADAM10 inhibitor	(Ludwig et al. 2005a)
GM6001	Broad spectrum metalloprotease inhibitor	(Grobelny et al. 1992)
GW280264X	ADAM10/ADAM17 inhibitor	(Ludwig et al. 2005a)
MG132	Proteasome inhibitor	(Palombella et al. 1994)
Phenanthroline	Broad spectrum metalloprotease inhibitor	(Sellers and Woessner 1980)
TAPI-1	Broad spectrum metalloprotease inhibitor	(Mullberg et al. 1995)
TAPI-2	Broad spectrum metalloprotease inhibitor	(Arribas et al. 1996)
Ro 31-9790	Broad spectrum metalloprotease inhibitor	(Steinmann-Niggli et al. 1997)

Abbreviations: ADAM, a disintegrin and metalloprotease

While several studies show CD23 shedding is induced following P2X7 activation, a lack of knowledge exists on the signalling pathways involved in this process. PMA induces CD62L, but not CD23 shedding, and the hydroxamic acid-based protease inhibitor of zinc-dependent MMPs, Ro 31-9790, inhibits P2X7-induced CD23 shedding more potently than CD62L shedding (Gu et al. 1998). Therefore, it is thought that P2X7-induced CD23 and CD62L shedding are regulated by different metalloproteases (Gu et al. 1998). Furthermore, using BB-94, preliminary data from our laboratory implies a role for metalloproteases in ATP-induced CD23 shedding from RPMI 8226 cells (Wang and Sluyter, *personal communication*). A role for ADAM10 in ATP- or BzATP-induced CD23 shedding has been shown using the inhibitory prodomain construct of ADAM10, A10-(23-213) (Lemieux et al. 2007) and in CD23-transfected CHO cells and murine B cells using GI254023X (Le Gall et al. 2009, Le Gall et al. 2010). However, a direct role for P2X7 in ADAM10-mediated CD23 shedding was not established in any of these studies.

1.5.3 CD62L

CD62L is a cell-adhesion molecule that consists of an extracellular, N-terminal lectin domain, an epidermal growth factor (EGF) domain, two consensus repeat domains, a transmembrane domain and a cytoplasmic tail (Smalley and Ley 2005). CD62L is involved in constitutive trafficking of lymphocytes through lymphoid organs, and rolling of leukocytes on inflamed vascular endothelium (Smalley and Ley 2005). Like CD23, ATP was first shown to induce CD62L shedding from the cell surface of CLL lymphocytes (Jamieson et al. 1996). The nucleotides adenosine, ADP and UTP do not affect CD62L shedding, while oxATP inhibits both ATP and BzATP-induced CD62L

shedding from these cells (Jamieson et al. 1996). Furthermore, KN-62 also inhibits ATP-induced CD62L shedding from CLL lymphocytes, confirming a role for P2X7 in this process (Gargett and Wiley 1997, Gu et al. 1998). Finally, BzATP-induced CD62L shedding is drastically impaired in CLL cells expressing non-functional P2X7 (Gu et al. 2000).

Following the studies above, it was shown P2X7-induced CD62L shedding occurs from human B cells and T cells (Sengstake et al. 2006) and subsets of these cells, including $CD4^+$ and $CD8^+$ T cells (Elliott and Higgins 2004, Aswad and Dennert 2006, Sengstake et al. 2006, Sluyter and Wiley 2014), and $CD27^-$ and $CD27^+$ B cells (Sengstake et al. 2006). In murine T cells, NAD is able to induce CD62L shedding via the activation of ART2 and P2X7 (see section 1.4.3) (Seman et al. 2003, Krebs et al. 2005). Furthermore, ATP-induced CD62L shedding is almost absent from monocytes and lymphocytes obtained from subjects containing the E496A loss-of-function polymorphism (Sluyter et al. 2004, Sluyter and Wiley 2014), and from Pfizer P2X7 knockout mice (Labasi et al. 2002). In contrast, BzATP-induced CD62L shedding is more rapid in T cells from GlaxoSmithKline P2X7 knockout mice (Taylor et al. 2009a), presumably due to the presence of the escape variant P2X7K (Nicke et al. 2009, Schwarz et al. 2012).

A role for P2X7-induced CD62L shedding was implicated in T cell transendothelial migration to the heart in a murine model of Duchenne muscular dystrophy (Cascabulho et al. 2012). This study showed that BBG treatment of *mdx/mdx* mice allowed the transendothelial migration of T cells to the heart by allowing sustained CD62L expression (Cascabulho et al. 2012). This suggests that impaired P2X7-induced CD62L

shedding may contribute to the pathology of Duchenne muscular dystrophy (Cascabulho et al. 2012). In contrast to this study, Chen and colleagues showed that oxATP does not affect the loss of CD62L during CLL lymphocyte transmigration (Chen et al. 1999) suggesting P2X7 does not play a role in this process. This difference may be due to different experimental conditions and may be dependent on cell types and species involved. Overall, the above studies confirm a major role for P2X7 in CD62L shedding from B and T cells, and monocytes.

Although a clear mechanism has not been attributed to P2X7-induced CD62L shedding, metalloproteases were first implicated when it was shown that Ro 31-9790 inhibits CD62L shedding (Gu et al. 1998). Now, ADAM17 is thought to be the principal sheddase of CD62L in nucleotide-induced shedding from murine B cells and T cells (Le Gall et al. 2009, Le Gall et al. 2010). However, in the absence of ADAM17, ADAM10 is able to shed CD62L after ATP treatment of these cells (Le Gall et al. 2009, Le Gall et al. 2010). BzATP-stimulated CD62L shedding induced by ADAM17 is significantly more rapid than shedding induced by ADAM10, corroborating a role for ADAM17 as the principal sheddase (Le Gall et al. 2010).

The 4,4'-diisothiocyanatosilbene-2,2'-disulphonic acid, an inhibitor of PS translocation, has implicated a role for non-apoptotic PS exposure in P2X7-induced CD62L shedding from murine $CD4^{+}CD45RB^{lo}$ T cells, a population of live cells with constitutive PS exposure (Elliott et al. 2005). However, the precise mechanism remains undefined. Other studies have shown that P2X7-induced CD62L shedding does not involve PKC (Jamieson et al. 1996), PI3K or ERK1/2 (Foster et al. 2013). In contrast, Foster and

colleagues show that rottlerin, an inhibitor of PKC, increases ATP-induced CD62L loss from human $CD4^+$ T cells (Foster et al. 2013). Furthermore, P2X7-mediated loss of CD62L from human $CD4^+$ T cells is enhanced by diphenyleneiodonium, which can uncouple complex I of the mitochondrial respiratory chain to cause ROS formation (Foster et al. 2013). P2X7-mediated loss is also enhanced by rotenone and antimycin A, which uncouple complex I and III, respectively (Foster et al. 2013). While Foster and colleagues did not directly show that this process involves ADAM17, ROS is able to activate ADAM17 via oxidation of cysteine motifs, which are critical for CD62L cleavage (Wang et al 2009). Furthermore, ROS production is involved in PMA-induced ectodomain shedding of tumor necrosis factor receptor (TNFR) 2 (Zhang et al. 2001) and ATP-induced shedding of transforming growth factor (TGF)-α (Myers et al. 2009) (see section 1.5.9.2). Therefore, ROS may play a role in P2X7-induced activation of ADAM17 (Foster et al. 2013).

1.5.4 CD21

Two main complement receptors have been described, complement receptor 1 (CD35) and complement receptor 2 (CD21). In humans, different genes code these receptors, whereas in mice they are alternative splice products of the same gene (Chen et al. 2000). CD21 consists of tandem repeat motifs called short consensus repeats, which contain the binding site for complement fragments. CD21 is predominantly expressed on follicular dendritic cells and B cells, and binds complements iC3b, C3dg, C3d and C4d (Chen et al. 2000). BzATP-induces CD21 shedding from human B cells, which is inhibited in the presence of oxATP and KN-62, confirming a role for P2X7 in CD21 shedding (Sengstake et al. 2006). The mechanism by which this process occurs remains

elusive, and to date, Sengstake and colleagues are the only group to show P2X7-inducible release of CD21 (Sengstake et al. 2006). Constitutive CD21 shedding is known to be a redox-regulated process, and can be induced by oxidising agent pervanadate (Aichem et al. 2006). PKC, serine proteases and metalloproteases are involved in this redox-regulated process (Aichem et al. 2006). CD21 shedding can also be induced by ROS scavengers, such as N-acetylcysteine and glutathione, which can be impaired by metalloprotease inhibitors (Aichem et al. 2006). It would be of interest to determine whether P2X7-induced ROS formation and ADAM activation affect CD21 shedding.

1.5.5 CD44

CD44 is a type I transmembrane glycoprotein which consists of a short cytoplasmic tail, a transmembrane domain, a glycosylated variable region and hyaluronic acid binding domains (Petrey and de la Motte 2014). CD44 is expressed on several cell types including leukocytes, neutrophils, macrophages, fibroblasts, epithelial and endothelial cells (Petrey and de la Motte 2014). CD44 plays roles in tumour metastasis, lymphocyte adhesion, T cell signalling, angiogenesis and inflammation (Petrey and de la Motte 2014). ATP induces CD44 shedding from murine P388D1 lymphoid neoplasm cells (Lin et al. 2012). KN-62 and P2X7 short hairpin RNA inhibited ATP-induced cell surface loss, as well as release of soluble CD44, which confirms a role for P2X7 in the process. In contrast, ATP is unable to alter the expression of CD44 in CLL cells (Gu et al. 1998). Therefore, P2X7-induced CD44 shedding may be cell or species specific. While the mechanism involved in P2X7-induced CD44 shedding remains undefined, ADAM10 (Anderegg et al. 2009), ADAM17 (Takamune et al. 2007), MMP 9 (Chetty et

al. 2012) and MMP 14 (Kajita et al. 2001) are involved in constitutive CD44 shedding and thus may play a role in nucleotide-induced CD44 shedding.

1.5.6 Epithelial-cadherin

Epithelial cadherin (E-cadherin) is a member of the classical cadherin family. It contains a single pass transmembrane glycoprotein with five extracellular repeats that bind E-cadherin molecules on opposing cells (Canel et al. 2013). E-cadherin mediates cell-cell adhesion in epithelial tissues and loss of this molecule promotes epithelial tumour metastasis (Canel et al. 2013). Melittin, the major component of bee venom induces ADAM-dependent E-cadherin shedding from human HaCaT keratinocytes (Sommer et al. 2012). Melittin also induces ATP release, ERK phosphorylation and EGF receptor activation in these cells (Sommer et al. 2012). The P2 receptor antagonists PPADS, Evans Blue and suramin suppress melittin-mediated ADAM activation suggesting a contribution of P2 receptor activation to melittin-induced shedding (Sommer et al. 2012). Furthermore, P2X7-transfected but not mock transfected HEK 293 cells show increased melittin-induced phosphorylation of ERK, which can be abrogated by apyrase, thus confirming a role for the ATP-P2X7 axis in this process (Sommer et al. 2012). Melittin-induced E-cadherin shedding is inhibited by broad spectrum metalloprotease inhibitor BB-2516, GI254023X and GW280264X (Sommer et al. 2012). While P2X7 may play a role in this process, further evidence is needed to establish a role for P2X7 or another P2 receptor in ADAM10-dependent E-cadherin shedding in HaCaT keratinocytes.

1.5.7 Ig superfamily members

Nucleotides induce the loss of several molecules of the Ig superfamily including the MHC class I, the IL-6 receptor (IL-6R), T cell immunoglobulin and mucin (TIM)-2, neural cell adhesion molecule (NCAM) and the intercellular adhesion molecule (ICAM)-1.

1.5.7.1 MHC molecules

MHC molecules are involved in initiating antigen-specific T cell immune responses (Germain 1994). Typically, MHC class I presents intracellular antigen to $CD8^+$ T cells, while MHC class II presents extracellular antigen to $CD4^+$ T cells (Germain 2002, Pearce et al. 2004). MHC class I is composed of a single transmembrane heavy chain ($\alpha1\alpha2$ and $\alpha3$ domains) paired with β_2 microglobulin (Maenaka and Jones 1999), and is highly expressed on hematopoietic cells (Germain 1994). BzATP induces MHC class I cell surface loss from lymphocytes obtained from NOD.E and C57BL/10 mice, but whether this loss is due to shedding or internalisation remains unclear (Elliott and Higgins 2004).

ATP also induces a loss of MHC class I from the cell surface of murine bone marrow-derived macrophages. This effect is absent in macrophages from Pfizer P2X7 knockout mice (Baroja-Mazo et al. 2013). Furthermore, ADP and adenosine do not seem to play a role in this loss. Both A-438079 and A74003 impaired ATP-induced MHC I loss from these cells (Baroja-Mazo et al. 2013), confirming a role for P2X7. Similar to BzATP-induced MHC class I loss from lymphocytes (Elliott and Higgins 2004), it

remains unclear whether ATP-induced loss of MHC class I is due to shedding or internalisation (Baroja-Mazo et al. 2013). The protease inhibitor E64, proteasome inhibitor MG132, GM6001, and zinc chelator TPEN do not impair ATP-induced loss of MHC I from the cell surface of these cells (Baroja-Mazo et al. 2013) suggesting a protease does not play a role in this process.

Establishing a mechanism for P2X7 in BzATP- and ATP-induced MHC class I loss may be of interest particularly as P2X7 plays a role in biological processes involving other human leukocyte antigen molecules. P2X7-induced microvesicle and exosome release of MHC II has been shown to occur from macrophages (Qu and Dubyak 2009), while ATP does not induce a loss of this molecule from the surface of CLL cells (Gu et al. 1998). Conversely, P2X7 plays a role in inhibiting soluble human leukocyte antigen-G release from lipopolysaccharide (LPS)-activated peripheral blood mononuclear cells (PBMCs) (Rizzo et al. 2009), suggesting a complex role for P2X7 in the release of human leukocyte antigen molecules from cells.

1.5.7.2 IL-6R

IL-6 is a cytokine involved in homeostasis as well as immune responses, and is thus secreted by both immune and non-immune cells (Chalaris et al. 2011). It induces the proliferation and differentiation of T cells, macrophages and neutrophils, and can induce fever in the presence of TNF-α and IL-1 (Chalaris et al. 2011). The IL-6R mediates the biological activities of IL-6. The IL-6 and IL-6R complex is composed of a type I transmembrane glycoprotein and a type I transmembrane signal transducer protein

(glycoprotein130) (Chalaris et al. 2011). This complex binds to two molecules of glycoprotein130 to induce downstream signalling involving the janus kinase-signal transducer and activator of transcription, ERK and PI3K signalling pathways (Chalaris et al. 2011). Furthermore, soluble IL-6R released by shedding, also binds IL-6 to activate cells that do not express this receptor (Chalaris et al. 2011).

BzATP induces IL-6R shedding from wild-type murine splenic cells, but not from cells obtained from Pfizer P2X7 knockout mice (Garbers et al. 2011). The serum level of the IL-6R from these knockout mice is also reduced significantly compared to wild-type mice, suggesting a role for P2X7 in IL-6R shedding. KN-62 inhibits both the BzATP-induced cell surface loss of the IL-6R, as well as soluble IL-6R generation, confirming a role for P2X7 in IL-6R shedding. GI254023X and GW280264X inhibit BzATP-induced IL-6R shedding in P2X7 and IL-6R co-transfected NIH3T3 mouse embryonic fibroblasts, and HEK 293 cells (Garbers et al. 2011) suggesting ADAM10 is involved in this process. Furthermore, the ADAM10 prodomain, A10-(23-213) inhibits BzATP-induced IL-6R shedding from wild-type murine T cells, and in T cells from mice with dramatically reduced ADAM17 expression. Therefore, ADAM10 plays a predominant role in P2X7-induced IL-6R shedding (Garbers et al. 2011). It remains unclear how P2X7 activates ADAM10 to induce IL-6R shedding.

1.5.7.3 TIM-2

The TIM family consists of eight murine members (TIM1-8) and three human members (TIM-1, TIM-3 and TIM-4) (Freeman et al. 2010). TIM molecules are type I cell

surface glycoproteins, with an N-terminal linked immunoglobulin-like domain, a mucin domain and a cytoplasmic region containing tyrosine phosphorylation motifs (Freeman et al. 2010). TIM-2 is expressed on rodent Th2 cells and splenic B cells (Freeman et al. 2010). TIM-2 functions as a negative regulator of T cell activation and binds H-ferritin, which leads to endocytosis of extracellular H-ferritin (Freeman et al. 2010). BzATP induces TIM-2 shedding from murine splenic B cells, and P2X7 and TIM-2 co-transfected HEK 293 cells (Dewitz et al. 2014). Both GI254023X and GW280264X inhibit BzATP-induced TIM-2 shedding, confirming a role for ADAM10 in this process (Dewitz et al. 2014), however a direct role for P2X7 remains to be established.

1.5.7.4 NCAM

NCAMs consist of three major isoforms including NCAM120, NCAM140 and NCAM180, which differ in intracellular length (Dallerac et al. 2013). NCAM extracellular domains contain five Ig motifs and two fibronectin type III domains. These molecules are involved in cell migration, cell survival, axon guidance and synaptic targeting (Dallerac et al. 2013). ATP induces NCAM shedding from embryonic rat hippocampal neurons, and the shedding of each of the three major isoforms from NCAM-transfected L929 murine fibroblasts (Hubschmann et al. 2005). ATP at a concentration of 2.5 mM is needed to induce significant shedding of NCAM180 (Hubschmann et al. 2005), indicating a possible role for P2X7 in ATP-induced NCAM shedding. The broad spectrum metalloprotease inhibitors, BB-3103 and GM6001, inhibit ATP-induced NCAM shedding from NCAM180-transfected L929 cells. GM6001 also inhibits ATP-induced shedding of the major NCAM isoforms from NCAM-transfected L929 cells (Hubschmann et al. 2005), confirming a role for

metalloproteases in the process. Lysosomal, proteasomal, calpain, PI3K and PKC inhibitors had no effect on ATP-induced NCAM shedding (Hubschmann et al. 2005). Furthermore, the extracellular ATP binding site of NCAM is not required for ATP-induced NCAM shedding, which further supports a role for a P2 receptor in this process (Hubschmann et al. 2005). Given the high concentration of ATP required to induce NCAM shedding, it is feasible that P2X7 may play a role in ATP-induced NCAM shedding.

1.5.7.5 ICAM-1

ICAMs are transmembrane glycoproteins, and ligands for β2 integrins on leukocytes. There are five ICAMs identified (ICAM-1-5), of which ICAM-1 is most studied (Hua 2013). ICAM-1 is involved in inflammatory cell trafficking, leukocyte effector functions, adhesion of antigen presenting cells to T cells and signal transduction pathways (Hua 2013). BzATP stimulates ICAM-1 shedding from ICAM-1 and P2X7 co-transfected murine embryonic fibroblasts (mEFs) (Le Gall et al. 2009). GI254023X inhibits BzATP-induced shedding in ADAM17-knockout mEF cells, which express endogenous ADAM10, but not in ADAM10-knockout mEF cells, which express ADAM17. Furthermore, BzATP does not induce ICAM-1 shedding in ADAM10/17 double knockout cells (Le Gall et al. 2009). BB-2516, but not GI254023X, impairs BzATP-induced ICAM-1 shedding in CHO cells, which express endogenous P2X7 and both ADAMs (Le Gall et al. 2009). Overall, the data suggests that BzATP-induced ICAM-1 shedding predominantly involves ADAM17. However, in the absence of ADAM17, ADAM10 can also cleave ICAM-1 (Le Gall et al. 2009). Further studies are

needed to corroborate a direct role for P2X7 in this process, given that CHO cells also express P2Y receptors (Myers et al. 2009).

1.5.8 TNF-α and TNFRs

TNF-α is a proinflammatory cytokine that plays a critical role in immunity and chronic inflammatory disease. The precursor form, transmembrane TNF-α binds TNF-α receptors and induces cell signalling (Horiuchi et al. 2010). ADAM17 cleaves transmembrane TNF-α to the soluble form, which mediates its biological activities through TNFRs 1 and 2 (Horiuchi et al. 2010). The TNFR family, induce a variety of biological activities including promotion of cell survival, cell differentiation and death (So et al. 2006). These receptors are active in trimeric form on the cell surface and in the soluble form after extracellular cleavage (So et al. 2006). This family of receptors can be divided into two groups based on binding properties and amino acid sequences of the cytoplasmic domains (So et al. 2006). These include TNFRs that contain a death domain, such as TNFR1, which interacts with death domain proteins and leads to apoptosis, while those that do not contain death domains associate with TNF receptor-associated factors and lead to induction of proinflammatory activities (So et al. 2006). Members of this family, including CD27, support activation, differentiation and survival of B cells, T cells and dendritic cells (So et al. 2006). CD27 is a type I transmembrane glycoprotein which is expressed on T cells (Camerini et al. 1991) and B cells (Maurer et al. 1990). CD27 is involved in T cell activation (Agematsu et al. 1994) and B cell-B cell interactions (Maurer et al. 1990).

1.5.8.1 TNF-α

BzATP induces the shedding of TNF-α from TNF-α and P2X7 co-transfected mEFs (Le Gall et al. 2009). GI254023X impairs BzATP-induced shedding of TNF-α only in ADAM17-knockdown mEF cells, which express ADAM10, but not in ADAM10-knockdown mEF cells, which express ADAM17 (Le Gall et al. 2009). In CHO cells, which endogenously express P2X7 and the ADAM proteases, GI254023X does not impair BzATP-induced shedding, suggesting that ADAM10 contributes to the shedding only in the absence of ADAM17 (Le Gall et al. 2009). The contribution of P2X7 in this process remains to be established.

1.5.8.2 TNFR1

Recently, it was shown that the P2Y2 and P2Y4 agonist, UTP, induces the shedding of soluble TNFR1 from human corneal epithelial cells (Sakimoto et al. 2014). Furthermore, the eye drop diquafosol sodium, a P2Y2 agonist, increases soluble TNFR1 in tear fluids of patients with short break-up time dry eye (Sakimoto et al. 2014). A role for downstream signalling molecules in UTP-induced TNFR1 shedding remains to be determined. Rowlands and colleagues show that soluble TNF-α induces mitochondrial Ca^{2+} oscillations while concomitantly, P2Y2 potentiates and prolongs these Ca^{2+} oscillations, which lead to ROS-dependent activation of ADAM17. Subsequently, ADAM17 cleaves TNFR1 (Rowlands et al. 2011). Thus, it would be of interest to determine the mechanism involved in direct nucleotide-induced TNFR1 shedding and whether ADAM17 and mitochondrial Ca^{2+} oscillations are involved in this process.

1.5.8.3 CD27

ATP induces a loss of surface CD27 from murine B and T cells (Moon et al. 2006). Surface plasmon resonance shows that supernatants from ATP-treated splenocytes display significant binding to immobilised anti-CD27 antibody (Moon et al. 2006) indicating ATP-induced loss of CD27 is due to shedding. BzATP induces CD27 shedding more potently than ATP, and ATP induced CD27 shedding is impaired by KN-62 confirming a role for P2X7 (Moon et al. 2006). Several antagonists targeting signalling molecules including tyrosine kinases, PI3K, MEK-1 and p38 MAPK could not impair P2X7-induced CD27 shedding. GM6001, almost completely impaired P2X7-induced CD27 shedding suggesting a role for metalloproteases in this process (Moon et al. 2006). However, the specific metalloproteases involved remain to be determined.

1.5.9 Epidermal growth factor receptor ligands

Epidermal growth factor receptor (EGFR) activation involves the binding of growth factor ligands EGF, heparin-binding EGF-like growth factor (HB-EGF), TGF-α, amphiregulin, betacellulin, epiregulin and epigen (Schneider and Wolf 2008). The EGFR ligands are type I transmembrane proteins that contain an N-terminal extension, EGF module, a short juxtamembrane stalk, transmembrane domain and C-terminal cytoplasmic tail (Schneider and Wolf 2008). Ectodomain shedding of these ligands generates the soluble version, which binds and activates the EGFR (Schneider and Wolf 2008). EGFR ligands are involved in the modulation of cell proliferation, apoptosis and migration in a variety of cancers and other diseases (Schneider and Wolf 2008). These

ligands also play important roles in processes such as wound healing, tumorigenesis and bone formation (Schneider and Wolf 2008).

1.5.9.1 HB-EGF

The first indication of nucleotide-induced HB-EGF release was indirectly shown using a neutralising antibody against HB-EGF, which inhibited ATP-induced mitogenic effects in guinea pig Muller glial cells (Milenkovic et al. 2003). It was postulated that ATP-induced P2Y receptor activation leads to the release of HB-EGF from the cell, which mediates transactivation of the EGF receptor (Milenkovic et al. 2003). Later, direct evidence of nucleotide-induced HB-EGF shedding was shown using ATPγS-treated HB-EGF-transfected SV-40 immortalised human corneal epithelial cells (THCE) (Yin et al. 2007, Yin and Yu 2009). Wounding, which increases ATP in the culture medium, as well as ADP, also induced HB-EGF shedding from THCE cells (Yin et al. 2007, Yin and Yu 2009). The P2Y receptor inhibitor, reactive blue 2 inhibited ATPγS-induced HB-EGF shedding confirming a role for a P2Y receptor in this process (Yin et al. 2007). GM6001, GW280264X (Yin et al. 2007) and GI254023X (Yin and Yu 2009) inhibited HB-EGF shedding from these cells. Furthermore, the MEK and ERK1/2 inhibitors, PD98059 and U0126 respectively, also inhibited ATPγS- and wound-induced HB-EGF shedding. Overall, these studies suggest that ADAM10, ADAM17, MEK and ERK1/2 are involved in ATP-induced HB-EGF shedding from THCE cells and that this process may be relevant during wound healing. ATPγS is known to activate P2Y2 and partially P2Y4 (Ralevic and Burnstock 1998). It also partially activates all P2X receptors except murine P2X7 (Kaczmarek-Hajek et al.

2012). Therefore further pharmacological characterisation is required to determine which P2 receptor is involved in HB-EGF shedding.

1.5.9.2 TGF-α

Several studies show that nucleotide treatment of cells induces TGF-α release. BzATP induces the shedding of TGF-α from TGF-α-transfected CHO cells (Le Gall et al. 2009), and from TGF-α and P2X7 co-transfected mEFs (Le Gall et al. 2010). TGF-α shedding from CHO cells is impaired by BB-2516 but not GI254023X, suggesting a role for ADAM17 in the process (Le Gall et al. 2009). P2X7 seems to be involved in TGF-α shedding, however further confirmation is required as P2Y receptors have also been implicated in TGF-α shedding. Myers and colleagues have shown that both ATP and UTP induce TGF-α shedding from TGF-α-transfected CHO cells (Myers et al. 2009). Based on UTP-induced shedding and P2Y2 mRNA expression in these cells, the authors suggest a role for P2Y2 (Myers et al. 2009). The broad spectrum metalloprotease inhibitor, TAPI-2 inhibits ATP-induced TGF-α shedding from CHO cells, but, ATP does not induce TGF-α shedding from M2 CHO cells, which are deficient in ADAM17 (Myers et al. 2009). ATP, ATPγS and UTP also induce the release of endogenous TGF-α from EC-4 murine fibroblasts. ATP-induced TGF-α shedding only occurs in EC-4 fibroblasts that express ADAM17 compared to complimentary EC-2 fibroblasts, which are deficient in ADAM17 (Myers et al. 2009). Therefore, ADAM17 is involved in nucleotide-induced TGF-α shedding.

Ca^{2+} chelators, BAPTA-AM and EGTA suppress ATP-induced shedding of TGF-α from CHO cells, indicating this process is regulated by both intracellular and extracellular calcium (Myers et al. 2009). The ROS scavenger N-acetylcysteine, near completely inhibits ATP-induced TGF-α shedding, while the mitochondrial complex I inhibitor, rotenone impairs the majority of ATP-stimulated TGF-α shedding. Together, the mitochondrial complex III inhibitor myxothiazol and rotenone inhibit ATP-induced TGF-α shedding as effectively as N-acetylcysteine (Myers et al. 2009). Therefore, mitochondrial ROS play major roles in nucleotide-induced TGF-α shedding (Myers et al. 2009). However, as indicated elsewhere (section 1.5.3) rotenone can also induce mitochondrial ROS formation, thus the role of ROS in ATP-induced shedding of molecules require further investigation.

ATP also induces endogenous TGF-α shedding from the human bronchial epithelial (HBE) 1 cell line, which is impaired by siRNA directed against the NADPH oxidase homolog, dual oxidase 1 (Boots et al. 2009). Silencing of dual oxidase 1 impairs ADAM17 activity, indicating a role for both molecules in ATP-induced TGF-α shedding (Boots et al. 2009). Suramin inhibition of ATP-induced ADAM17 activation implicates P2Y receptor activity in TGF-α shedding from these cells. (Boots et al. 2009). Melittin, which induces ATP secretion, also induces TGF-α shedding from HaCaT keratinocytes, also suggesting a role for P2 receptors in this process (Sommer et al. 2012). The ERK1/2 inhibitor, U0126 also impaired ATP-induced ADAM17 activity in HBE1 cells (Boots et al. 2009) suggesting that ERK1/2 is involved in ATP-induced stimulation of ADAM17. Collectively, the above studies suggest a role for both P2Y2 and P2X7 receptor activation in nucleotide-induced TGF-α shedding, but more evidence is required to show a specific role for each receptor in this process.

1.5.9.3 Amphiregulin

ATP and ATPγS induce amphiregulin shedding from human monocyte-derived dendritic cells, which is enhanced in the presence of LPS (Bles et al. 2010). However, ATP and ATPγS do not induce amphiregulin shedding from murine bone marrow derived dendritic cells unless cells are pre-stimulated with LPS (Bles et al. 2010). UTP also induces amphiregulin shedding from murine bone marrow-derived dendritic cells in the presence of LPS (Bles et al. 2010) suggesting a role for P2Y2 in this process. Moreover, suramin inhibits nucleotide-induced amphiregulin shedding from human monocyte-derived dendritic cells (Bles et al. 2010) consistent with a role for P2Y receptors in the process. However, further pharmacological evidence is required to confirm a role for P2Y receptors in nucleotide-induced amphiregulin shedding.

1.5.9.4 Betacellulin

P2X7 is implicated in the shedding of betacellulin (Le Gall et al. 2009, Le Gall et al. 2010). BzATP induces betacellulin shedding from betacellulin-transfected CHO cells, and betacellulin and P2X7 co-transfected mEFs (Le Gall et al. 2009). BzATP-induced betacellulin shedding is impaired by BB-2516, GI254023X and dominant negative ADAM10, which lacks the metalloprotease domain (Le Gall et al. 2009). When P2X7 is co-expressed with betacellulin in ADAM17-knockdown mEFs, which express endogenous ADAM10, GI254023X impairs BzATP-induced betacellulin shedding. However, in ADAM10-knockdown mEFs, which express endogenous ADAM17, BzATP does not induce betacellulin shedding (Le Gall et al. 2009). Collectively this suggests ADAM10 is the dominant metalloprotease involved in BzATP-induced betacellulin shedding.

Given that multiple P2 receptors are implicated in EGFR ligand shedding, it will be of value to determine the specific mechanisms and conditions required for each receptor in these processes.

1.5.10 Amyloid precursor protein

Amyloid-β peptide (Aβ) accumulation is a major pathological hallmark of Alzheimer's disease (Haass et al. 2012). Amyloid precursor protein (APP) is a type I membrane protein with an intracellular C-terminus and an extracellular N-terminus (Haass et al. 2012). APP can be cleaved by two alternate proteolytic pathways, termed the amyloidogenic and anti-amyloidogenic pathways (Figure 1.7). In the amyloidogenic pathway, APP is cleaved by the β-secretase and then the γ-secretase to generate Aβ. (Haass et al. 2012). Specifically, the β-secretase first cleaves the APP ectodomain to generate the soluble fragment, soluble amyloid precursor protein β (sAPPβ) and the β-carboxyl-terminal fragment (β-CTF) in the transmembrane domain. β-CTF itself is then subsequently cleaved by γ-secretase to generate Aβ, which is found in extracellular fluids (Haass et al. 2012). In contrast, the anti-amyloidogenic pathway involves α-secretase activity, which cleaves APP in the middle of the Aβ domain and results in the secretion of soluble amyloid precursor protein α (sAPPα) and the generation of membrane α-carboxyl-terminal fragment (α-CTF). α-CTF is then cleaved by γ-secretase to generate the truncated Aβ peptide termed p3 (Haass et al. 2012). Several ADAM metalloproteases including ADAM9, ADAM10, ADAM17 and ADAM19 can function as α-secretases. It is thought these pathways compete with each other, as enhancing α-secretase activity in animal models of Alzheimer's disease lowers Aβ generation (Haass et al. 2012).

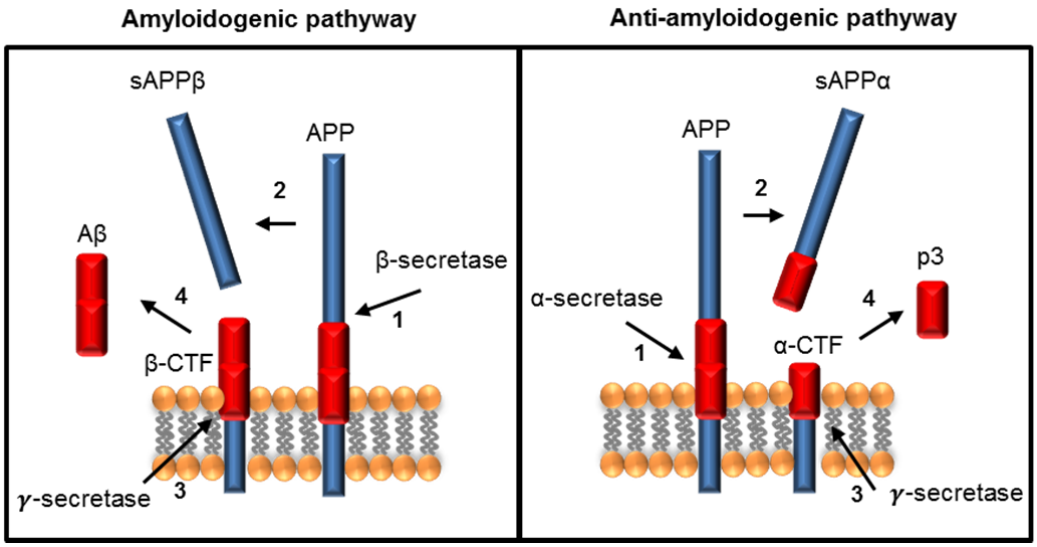

Figure 1.7: APP processing pathways. The amyloidogenic pathway (left) is (1) initiated with the cleavage of APP by β-secretase (2) to generate sAPPβ and β-CTF. (3) β-CTF is subsequently cleaved by γ-secretase (4) to generate Aβ. The anti-amyloidogenic pathway (right) is (1) initiated with the cleavage of APP by α-secretase (2) to generate sAPPα and α-CTF. (3) α-CTF is subsequently cleaved by γ-secretase (4) to generate truncated Aβ peptide termed p3 (adapted from Haas et al. 2012). **Abbreviations:** APP, amyloid precursor protein; sAPPβ, soluble amyloid precursor protein β; β-CTF, β-carboxyl-terminal fragment; sAPPα, soluble amyloid precursor protein α; α-CTF, α-carboxyl-terminal fragment

Both P2Y2 and P2X7 activation are involved in the release of sAPPα from cells. P2Y2 was first implicated in this process using P2Y2-transfected human 1321N1 astrocytoma cells (Camden et al. 2005). UTP-induced shedding of sAPPα from 1321N1 cells is dependent on the presence of extracellular Ca^{2+}, and partially on ERK1/2 (Camden et al. 2005). The metalloprotease inhibitors phenanthroline and TAPI-2, as well as the pro-protein convertase inhibitor, decanoyl-RVKR-CMK ketone, inhibit UTP-induced sAPPα shedding (Camden et al. 2005), implying a role for metalloproteases in the process. siRNA silencing of ADAM10 and ADAM17 reduced UTP-induced sAPPα

shedding, and when silenced simultaneously, near completely suppressed shedding (Camden et al. 2005). This indicates that both ADAM10 and ADAM17 are involved in P2Y2-induced sAPPα shedding.

UTP-induced sAPPα shedding is enhanced after pre-treatment with IL-1β in rat primary cortical neurons, which endogenously express P2Y2 (Kong et al. 2009). In agreement with Camden and colleagues, TAPI-2 near-completely inhibits, while U0126 partially inhibits UTP-induced sAPPα shedding. Conflicting with Camden and colleagues, who found that UTP-induced sAPPα shedding is independent of PKC activation (Camden et al. 2005), Kong and colleagues found that the PKC inhibitor, GF109203, partially inhibits UTP-induced sAPPα shedding (Kong et al. 2009). The PI3K inhibitor, LY294002 also significantly inhibits UTP-induced sAPPα shedding (Kong et al. 2009). These studies indicate that ADAM10/17 and PI3K regulate P2Y2-induced sAPPα shedding, which is enhanced in the presence of IL-1β, and involves both PKC and ERK1/2 (Camden et al. 2005, Kong et al. 2009). However, these studies do not show direct activation of P2Y2 and therefore cannot discount the effect of other P2 receptors. In particular, P2Y4 which is also activated by UTP and may be involved in UTP-induced APP processing from primary rat cortical astrocytes (Tran 2011).

ATP and BzATP also induce the shedding of sAPPα from human APP-transfected murine Neuro2a neuroblastoma cells (Delarasse et al. 2011). P2X7 antagonists, A-438079 and BBG, as well as P2X7 siRNA inhibit BzATP-induced shedding of sAPPα from these cells. BzATP also induces sAPPα shedding from SK-N-BE human neuroblastoma cells which express endogenous P2X7 and APP (Delarasse et al. 2011).

The P2X7 antagonists, oATP and A-438079 also impair BzATP-induced sAPPα shedding from these cells (Delarasse et al. 2011). Collectively, this data suggests that P2X7 activation induces sAPPα release from neuroblastoma cells. Furthermore, BzATP fails to induce sAPPα shedding from astrocytes and neural progenitor cells from Pfizer P2X7 knockout mice (Delarasse et al. 2011), confirming a role for P2X7 in this process. TAPI-2 and GM6001 inhibit BzATP-induced sAPPα shedding from Neuro2a cells establishing a role for metalloproteases. However, siRNA silencing of ADAM 9, 10 and 17 does not inhibit P2X7-induced shedding of sAPPα from these cells (Delarasse et al. 2011), suggesting the involvement of an alternate α-secretase in P2X7-induced shedding. Furthermore, U0126 and the JNK inhibitor, SP600125, as well as siRNA against intracellular signalling complex, ezrin radixin and moesin (ERM) impair P2X7-induced sAPPα shedding from APP-transfected Neuro2a cells (Delarasse et al. 2011, Darmellah et al. 2012). The Rho-kinase inhibitor, fasudil, and the PI3K inhibitors, LY294002 and wortmannin also impair P2X7-induced sAPPα shedding from these cells (Darmellah et al. 2012). The PI3K inhibitors do not impair ERM phosphorylation, suggesting PI3K is activated downstream of the ERM (Darmellah et al. 2012). Overall, P2X7-induced shedding of sAPPα from neural cells depends on Rho kinase, MAP kinase, ERM phosphorylation, PI3K and involves metalloprotease action.

In contrast to the above data, Diaz-Hernandez and colleagues show an opposing role for P2X7 in APP processing. P2X7 antagonists, BBG and A-438079 inhibit GSK-3 by increasing ser9/ser21 phosphorylation, which subsequently increases the α-secretase product, α-CTF in Neuro2a cells (Diaz-Hernandez et al. 2012). Whereas, BzATP treatment of Neuro2a cells decreases α-CTF and activates GSK-3 by decreasing ser9/ser21 phosphorylation. This α-CTF product decreases when Neuro2a cells are

treated with broad spectrum metalloprotease inhibitor TAPI-1 (Diaz-Hernandez et al. 2012). Similar effects were also observed in P2X7-transfected HEK 293 cells (Diaz-Hernandez et al. 2012). Furthermore, *in vivo* antagonism of P2X7 by BBG in a murine model of early onset familial Alzheimer's disease inhibits GSK-3 and the development of Aβ plaques via regulation of α-secretase activity (Diaz-Hernandez et al. 2012). This work is corroborated by Leon-Otegui and colleagues who also show BzATP decreases α-CTF in Neuro2a cells and BBG reverts this inhibition, thus proposing a role for P2X7 in the inhibition of α-secretase activity (Leon-Otegui et al. 2011). Diaz-Hernandez and colleagues critique the use of higher BzATP concentrations by Delarasse and colleagues, and suggest a role for P2Y2 in their system. Indeed, Leon-Otegui and colleagues show that BzATP used at a concentration above 100 μM increases α-CTF and thus α-secretase activity via P2Y2 (Leon-Otegui et al. 2011). It is unclear which P2X7 mechanism prevails in APP processing and thus further studies are warranted. Interestingly, it has been shown that Aβ can promote the caspase-mediated cleavage of P2X4 (Varma et al. 2009), suggesting a complex role for P2 receptors in the amyloidogenic and anti-amyloidogenic pathways.

1.6 Summary and aims of current research

Nucleotide induced P2 receptors activate several signalling pathways which result in the shedding of membrane molecules (Figure 1.6). P2X7 is involved in the shedding of several different membrane molecules including CD23. P2X7 and soluble CD23 play a key role in inflammatory and immune diseases, but how both molecules contribute to these diseases has not been determined. Moreover, the role of P2X7 in ATP-induced CD23 shedding is limited to malignant B cells and dendritic cells derived in culture,

thus whether this process occurs in primary B cells remains unknown. Furthermore, the mechanism by which P2X7 induces CD23 shedding from cells, particularly B cells remains elusive. Currently, it is known that the ADAM10 metalloprotease constitutively sheds CD23 from the cell surface, but whether P2X7 activates ADAM10 and/or other downstream signalling molecules to induce the shedding of CD23 has not been elucidated. Therefore the aims of the current research are to:

1. Confirm the presence of and to further characterise P2X7 on RPMI 8226 multiple myeloma B cells;
2. Examine the signalling pathways involved in P2X7-induced CD23 shedding using RPMI 8226 cells as a model;
3. Examine whether ROS are involved in P2X7-induced CD23 shedding from RPMI 8226 cells;
4. Determine, using RPMI 8226 cells, whether ADAM10 is involved in P2X7-induced CD23 shedding and;
5. Determine whether P2X7 activation induces CD23 shedding from primary human and murine B cells.

Elucidating the mechanisms involved in P2X7-induced CD23 shedding and identifying the cell types associated with this process may reveal potential novel therapeutic targets for autoimmune and inflammatory disorders.

CHAPTER 2

Materials and methods

2.1 Reagents

RPMI-1640 medium (containing 10 mM 4-(2-hydroxyethyl)-1-piperazineethanesulfonic acid (HEPES)), L-glutamine, GlutaMAX, DMEM:F12 medium (containing 10 mM HEPES) penicillin/streptomycin, probenecid, G418, dichlorodihydrofluorescein diacetate (H_2DCFDA), mitoSOX™ Red and YO-PRO-1 iodide solution were from Life Technologies (Grand Island, NY). Foetal bovine serum was from either Lonza (Basal, Switzerland) or Bovogen Biologicals (East Keilor, Australia). Agarose and HyperLadder^{TM} I molecular weight markers were from Bioline (Alexandria, Australia). Adenosine 5'-triphosphate (ATP), 2'(3')-O-(4-benzoylbenzoyl)adenosine-5'-triphosphate, adenosine 5'-diphosphate, uridine 5'-triphosphate, paraformaldehyde, colchicine, *N*-methyl-D-glucamine, 1,2-bis(o-aminophenoxy)ethane-N,N,N',N'-tetraacetic acid (BAPTA-AM), imipramine, poly-D-lysine, hydrogen peroxide, rotenone, high grade bovine serum albumin (BSA), 2,2′-azino-bis(3-ethylbenzothiazoline-6-sulfonic acid and red blood cell lysis buffer were from Sigma-Aldrich (St. Louis, MO). Sodium chloride (NaCl), potassium chloride (KCl), D-glucose, HEPES, calcium chloride ($CaCl_2$), sucrose, BSA, ethylene glycol tetraacetic acid (EGTA), dimethyl sulphoxide, Tween-20 and ethidium bromide were from Amresco (Solon, OH). Magnesium chloride ($MgCl_2$) was from Chem-Supply (Gillman, Australia). AZ10606120, AZ11645373, A-438079, SB216763 and BB-94 were from Tocris Bioscience (Ellisville, MO). Choline chloride (choline Cl) and ammonium chloride were from Univar (Downers Grove, IL). Rottlerin, SB202190, SB203580, U0126 and SP600125 were from Merck Chemicals (Darmstadt, Germany). AG-126, GF109203X, D609, Fasudil, Y-27632, AACOCF3 and 7-aminoactinomycin D (7AAD) were from Enzo Life Sciences (Plymouth Meeting, PA). LY294002 and GM6001 were from Calbiochem (Darmstadt, Germany). GI254023X was kindly provided by

GlaxoSmithKline (Stevenage, United Kingdom). KN-62 was from Alexis Biochemicals (Lausen, Switzerland). CAY10593 (VU0155069), CAY10594, halopemide and diphenyleneiodonium were from Cayman Chemical Company (Ann Arbor, MI). Ficoll Paque™ PLUS was from GE Healthcare Bio-Sciences AB (Uppsala, Sweden).

2.2 Antibodies

Purified anti-human P2X7 monoclonal antibody (mAb) (clone L4) and isotype control (clone WMD7) conjugated to Alexa Fluor® 647 (Life Technologies) was kindly provided by Dr. Ronald Sluyter (University of Wollongong, Wollongong, Australia). Phycoerythrin (PE) and allophycocyanin (APC)-conjugated murine anti-human CD23 (clone EBVCS2) and isotype control (clone P3.6.2.8.1) mAbs, APC-conjugated murine anti-human CD19 (clone HIB19), fluorescein isothiocyanate (FITC)-conjugated rat anti-murine CD23 (clone B3B4), FITC-conjugated isotype control (clone eBR2a), APC-conjugated rat anti-murine CD19 (clone eBio1D3) and PE-conjugated murine anti-human Toll-like receptor 9 (TLR-9) (clone eB72-1665) mAbs were from eBioscience (San Diego, CA). Rabbit anti-human CXCL16 and control IgG antibodies (Ab) were from Peprotech (Rocky Hill, NJ), and FITC-conjugated sheep anti-rabbit Ab was from Silenus Laboratories (Hawthorn, Australia).

2.3 Cells

2.3.1 Cell lines

Human RPMI 8226 multiple myeloma B cells and human A431 skin epithelial carcinoma cells (European Collection of Cell Cultures, Porton Down, UK) were maintained in complete RPMI-1640 medium (RPMI-1640 medium containing 10% (v/v) foetal bovine serum and 2 mM GlutaMAX or L-glutamine) at 37ºC and 95% air/5% CO_2. Murine erythroleukaemia cells (MEL) cells were kindly provided by Dr. Sally Eaton (University of Sydney, Sydney, Australia) and maintained as above. Human embryonic kidney (HEK) 293 cells (American Type Culture Collection, Rockville, MD) stably expressing human P2X7 were maintained by Dr. Leanne Stokes (University of Sydney, Penrith, Australia), in complete DMEM:F12 medium (DMEM:F12 medium containing 10% foetal bovine serum, 100 U/ml penicillin, 100 μg/ml streptomycin, 2 mM L-glutamine and 800 μg/ml G418). Cell lines were routinely checked for mycoplasma using the MycoAlert™ Mycoplasma Detection Kit (Lonza) and were consistently negative for mycoplasma.

2.3.2 Human peripheral blood mononuclear cells

All experiments involving human blood were approved by the University of Wollongong Human Ethics Committee. Human peripheral blood was collected into VACUETTE® lithium heparin tubes (Greiner Bio-One, Frickenhausen, Germany) and diluted with an equal volume of incomplete RPMI 1640 medium or phosphate-buffered saline (PBS). Peripheral blood mononuclear cells (PBMCs) were separated by density

gradient centrifugation over Ficoll-Paque^{TM} PLUS (560 x *g* for 30 min) and washed once in incomplete RPMI 1640 medium or twice in NaCl medium (145 mM NaCl, 5 mM KCl, 5 mM D-glucose, 10 mM HEPES, pH 7.4) (450 x *g* for 10 min).

2.3.3 Murine splenic cells

All experiments involving mice were approved by the University of Wollongong Animal Ethics Committee. C57BL/6 and DBA/1 mice were from Animal Resources Centre (Perth, Australia) or Australian BioResources (Moss Vale, Australia). P2X7 knockout mice (Solle et al. 2001) backcrossed onto a C57BL/6 background (Tran et al. 2010), were bred at the Centenary Institute (Sydney, Australia) by Dr. Bernadette Saunders or the University of Wollongong (Wollongong, Australia) by Vanessa Sluyter. Mice were euthanised by CO_2 and spleens collected in ice-cold PBS. Spleens were teased apart using a needle and forceps in ice-cold PBS, and cells were filtered through a 70 μm nylon cell strainer (BD, San Jose, CA). Splenic cells were then washed in ice-cold PBS (400 x *g* for 5 min) and the pellet resuspended in red blood cell lysis buffer. Red blood cells were lysed for 3 min at room temperature with agitation and the remaining leukocytes were washed once with ice-cold DMEM/F12 medium. Cells were then washed twice in NaCl medium.

2.4 Detection of specific messenger RNA expression by reverse transcriptase-polymerase chain reaction

Total RNA was isolated from cells using the RNeasy Mini Kit (Qiagen, Hilden, Germany) according to the manufacturer's instructions. Primers to P2X1-6 (Wareham et al. 2009), phospholipase D (PLD)1 (designed using OligoPerfect^{TM} Designer, Life Technologies) PLD2 (Scott et al. 2009) (Table 2.1) and a disintegrin and metalloprotease (ADAM) 10 (Verrier et al. 2004) were obtained from GeneWorks (Hindmarsh, Australia). Primers to P2X7 (Skarratt et al. 2005) (Table 2.1) were obtained from Sigma-Genosys (Castle Hill, Australia).

Table 2.1: Primer pairs used to detect mRNA of P2X receptors, PLD isoforms and ADAM10.

Molecule	Forward (5'-3')	Reverse (5'-3')
P2X1	CGTCATCGGGTGGGTGTTTCTCTA	AGGGCGCGGGATGTCGTCA
P2X2	GGGCCCCGAGAGCTCCATCATC	GCAGGCAGGTCCAGGTCACAGTCC
P2X3	ACTGGCCGCTGCGTGAACTACA	CACGTCGAAGCGGATGCCAAAAG
P2X4	CGGCACCCACAGCAACGGAGTCT	TGTATCGAGGCGGCGGAAGGAGTA
P2X5	GGCCCCAAGAACCACTACTGC	CCTCGGCCTCCTGGGAACTGTCT
P2X6	AGCCCCTACTGTCCCGTGTTCC	GCCTTGGCCTCCTCATACTTTGTC
P2X7	GGATGGTGAACCAGCAGCTA	AAGCCACTGTACTGCCCTTC
PLD1	TCATGTGTCATCCACCGTCT	GGCGTGGAGTACCTGTCAAT
PLD2	GGCGATGAGATTGTGGACA	CTGGAAGAAGTCATCACAGA
ADAM10	GCAGAATCATGATGACTACTGTTTG	TATAGCCACAATCACATTCTTCACC

Abbreviations: ADAM10, A disintegrin and metalloprotease 10; mRNA, messenger RNA; PLD, Phospholipase D

Reverse transcriptase-polymerase chain reaction (RT-PCR) amplification of P2X receptor mRNA was performed using Superscript™ III One-Step RT-PCR System Platinum *Taq* DNA polymerase (Life Technologies) according to the manufacturer's instructions using a Mastercycler Pro S (Eppendorf, North Ryde, Australia). Polymerase chain reaction (PCR) cycling conditions for P2X1-7 were 54°C for 30 min, 95°C for 2 min, 30 cycles of 95°C for 15 s, 58°C (P2X1 primer pair), 59°C (P2X2 primer pair), 58°C (P2X3 primer pair), 58°C (P2X4 primer pair), 55°C (P2X5 primer pair), 58°C (P2X6 primer pair) or 55°C (P2X7 primer pair) for 30 s, and 72°C for 1 min, followed by a final step of 72°C for 5 min. RT-PCR amplification of PLD1, PLD2 and ADAM10 was performed using the MyTaq One-Step RT-PCR Kit (Bioline) according to the manufacturer's instructions. PCR cycling conditions for PLD were 45°C for 20 min, 94°C for 2 min, 30 cycles of 94°C for 30 s, 54°C (PLD1 primer pair) or 57°C (PLD2 primer pair) for 1 min, and 72°C for 1 min, and a final step of 72°C for 5 min. PCR cycling conditions for ADAM10 were 45°C for 20 min, 30 cycles of 94°C for 10 s, 49°C for 1 min 30 s and 72°C for 1 min, and a final step of 72°C for 10 min. Amplicons were separated on a 2% (w/v) agarose gel by electrophoresis using the Mini-Sub™ Cell GT System tank (BioRad, Hercules, CA). Amplicons were visualised using ethidium bromide and the Gel Logic 2200 Pro Imaging System (Carestream Health, Rochester, NY). Amplicon size was determined using the HyperLadder™ I molecular weight markers.

2.5 P2X receptor sequencing

Total RNA was isolated as in Section 2.4. RT-PCR was performed using the Superscript™ III One-Step RT-PCR System Platinum *Taq* DNA polymerase for P2X5

or the MyTaq One-Step RT-PCR Kit for P2X7 according to the manufacturer's instructions. Primer pairs used for P2X5 complementary DNA (cDNA) are shown in Table 2.1. Primer pairs (GeneWorks) specific for four overlapping regions of full-length P2X7 cDNA including parts of the untranslated 5′ and 3′ ends are shown in Table 2.2. The PCR cycling conditions for P2X5 were as in Section 2.4. The PCR cycling conditions for P2X7 were 45 °C for 20 min, 95 °C for 1 min, 40 cycles of 95 °C for 10 s, 63 °C (primer pair 1), 59 °C (primer pair 2), 62 °C (primer pair 3) or 61 °C (primer pair 4) for 10 s, and 72 °C for 30 s, and a final step of 72 °C for 5 min. Amplicons were ran on 2% (w/v) agarose gels and visualised by ethidium bromide staining (as above, Section 2.4), and then excised and purified using the Wizard SV Gel and PCR Clean-Up System (Promega, Madison, WI) according to the manufacturer's instructions. Purified amplicons were sequenced using the above primers with the BigDye Terminator v3.1 Cycle Sequencing Kit (Applied Biosystems, Carlsbad, CA) and an Applied Biosystems 3130xl Genetic Analyzer by Margaret Phillips (University of Wollongong). PCR cycling conditions for sequencing were 95 °C for 2 min, and then 25 cycles of 96 °C for 30 s, 55 °C for 15 s and 60 °C for 4 min. Results were analysed using Clustal W (Larkin et al. 2007) for P2X5 and Geneious (Biomatters, Auckland, New Zealand) for P2X7.

Table 2.2: Primer pairs used to sequence full-length P2X7 cDNA.

Primer pairs	Forward (5'-3')	Reverse (5'-3')
1	TGGCCCTGTCAGGAAGAGTA	CACCAGGCAGAGACTTCACA
2	TTGTAAAAAGGGATGGATGGA	AAATATGGGAGCGACAGCAG
3	TACATCGGCTCAACCCTCTC	GAACAGCTCTGAGGTGGTGA
4	GTCTGGTGCCAGTGTGGAA	ACTCCCGACCTCAGGTGAT

2.6 Detection of P2X7 expression by flow cytometry

Cell surface and total P2X7 expression was examined in fresh cells, or fixed and permeabilised cells, by immunofluorescent labelling and flow cytometry. For the detection of cell-surface P2X7, fresh RPMI 8226 cells (1 x 10^6 cells/ml) were washed once in PBS. For the detection of total P2X7 (cell surface and intracellular), RPMI 8226 cells were fixed and permeabilised using the Intracellular Fixation and Permeabilisation Buffer Set (eBioscience) according to manufacturer's instructions. Briefly, RPMI 8226 cells were fixed with 0.2% (w/v) paraformaldehyde in PBS for 20 min and centrifuged (400 x g for 5 min). Fixed cells were permeabilised with 0.1% (w/v) saponin in PBS. Fresh, or fixed and permeabilised cells were then incubated with Alexa-Fluor® 647-conjugated anti-P2X7 or isotype control mAb for 20 min at room temperature; 7AAD was included with fresh cells to exclude dead cells. The mean fluorescence intensity (MFI) of P2X7 expression was determined using a LSR II flow cytometer (BD) (using band-pass filters of 660/20 for Alexa-Fluor® 647 and 695/40 for 7AAD). Analysis was performed using FlowJo software (Tree Star, Ashland, OR).

2.7 Measurement of P2X7-induced pore formation by flow cytometry

2.7.1 Cell lines and human PBMCs

P2X7-mediated pore formation was assessed using a fixed-time assay as described (Constantinescu et al. 2010). Cell lines or human PBMCs suspended in NaCl medium (1 x 10^6 cells/ml) were incubated with 25 μM ethidium$^+$ in the absence or presence of

ATP (as indicated) at 37 °C. In some experiments, cells were resuspended in either NaCl medium containing 1.5 mM $CaCl_2$ and 1 mM $MgCl_2$, sucrose medium (280 mM sucrose, 5 mM KCl, 10 mM *N*-methyl-D-glucamine, 5 mM D-glucose, 10 mM HEPES, pH 7.4), KCl medium (150 mM KCl, 5 mM D-glucose, 10 mM HEPES, pH 7.4), or choline Cl medium (150 mM choline Cl, 5 mM KCl, 5 mM D-glucose, 10 mM HEPES, pH 7.4) and incubated with 25 μM ethidium$^+$ in the absence or presence of ATP (as indicated) for 5 min at 37 °C. In other experiments, cells in NaCl medium were preincubated in the absence or presence of antagonist (as indicated), and then with 25 μM ethidium$^+$ in the absence or presence of ATP (as indicated) for 5 min at 37°C. All ATP incubations were stopped by addition of an equal volume of ice-cold $MgCl_2$ medium (NaCl medium containing 20 mM $MgCl_2$) and centrifugation (300 x *g* for 5 min). Cells were washed once with NaCl medium. PBMCs were then incubated with APC-conjugated anti-human CD19 mAb for 20 min at 4°C and washed once with NaCl medium. The MFI of ethidium$^+$ uptake was determined using flow cytometry (using a 575/26 nm band-pass filter for ethidium$^+$ or 660/20 nm for APC) and FlowJo software. For PBMCs, lymphocytes and monocytes were gated by forward and side scatter, and B cells and T cells on $CD19^+$ and $CD19^-$ lymphocytes, respectively.

2.7.2 Murine cells

P2X7-induced pore formation into murine splenic cells was assessed by flow cytometric measurements of ATP-induced YO-PRO-1^{2+} uptake as described (Jalilian et al. 2012). Splenic cells suspended in NaCl medium (1 x 10^6 cells/ml) were preincubated in the absence or presence of 10 μM AZ10606120 (as indicated), and then with 1 μM YO-PRO-1^{2+} in the absence or presence of ATP (as indicated) for 15 min at 37°C.

Incubations were stopped by addition of an equal volume of ice-cold $MgCl_2$ medium and centrifugation (350 x *g* for 3 min). Cells were washed once with NaCl medium. Cells were labelled with APC-conjugated anti-murine CD19 mAb and 7AAD for 20 min at 4°C and washed once with NaCl medium. The MFI of YO-PRO-1^{2+} uptake into $CD19^{+}$ cells was determined using flow cytometry (using band-pass filters of 515/20 nm for YO-PRO-1^{2+}, 660/20 nm for APC and 695/40 for 7AAD) and FlowJo software.

2.8 Measurement of P2X7-induced CD23 and CXCL16 loss by flow cytometry

2.8.1 RPMI 8226 cells

Nucleotide-induced CD23 and CXCL16 loss from RPMI 8226 cells was assessed by flow cytometric measurements of cell surface CD23 or CXCL16 expression as described (Farrell 2008). RPMI 8226 cells in NaCl medium (1 x 10^6 cells/ml) were incubated in the absence or presence of nucleotide (as indicated) at 37ºC. In some experiments, cells suspended in NaCl medium were preincubated in the absence or presence of antagonist (as indicated), and then in the absence or presence of 1 mM ATP at 37ºC. In other experiments, cells were suspended in either choline Cl medium, KCl medium or NaCl medium containing either 0.1 mM EGTA or 50 μM BAPTA-AM for 5 min, and then in the absence or presence of 1 mM ATP for 7 min at 37ºC. All nucleotide incubations were stopped by addition of an equal volume of ice-cold $MgCl_2$ medium and centrifugation (300 x *g* for 5 min). Cells were washed once with NaCl medium and incubated with PE- or APC-conjugated anti-human CD23 or isotype

control mAb for 30 min at room temperature. Alternatively, cells were washed once with NaCl medium and incubated with anti-CXCL16 or IgG control Ab for 30 min at room temperature, washed twice and incubated with a FITC-conjugated anti-rabbit IgG Ab for 30 min at room temperature. The MFI of cell surface CD23 or CXCL16 expression was measured using flow cytometry (using band-pass filters of 515/20 nm for FITC, 575/26 nm for PE and 660/20 nm for APC) and FlowJo software.

2.8.2 PBMCs and splenic cells

Nucleotide-induced shedding of CD23 from PBMCs or splenic cells was assessed in a similar manner to that for RPMI 8226 cells (Section 2.8.1). Briefly, cells suspended in NaCl medium (1 x 10^6 cells/ml), were incubated in the absence or presence of nucleotide (as indicated) for up to 30 min at 37ºC. In some experiments, cells in NaCl medium were pre-incubated at 37°C for 15 min in the absence or presence of antagonist, and then in the absence or presence of 1 mM ATP (as indicated). Incubations with nucleotide were stopped by addition of an equal volume of ice-cold $MgCl_2$ medium and centrifugation (350 x *g* for 3 min). Cells were then washed once with NaCl medium and incubated with species-specific fluorochrome-conjugated anti-CD23 (or isotype control) mAb, anti-CD19 mAb and 7AAD for 30 min at 4ºC. The MFI of cell-surface CD23 expression on viable $CD19^+7AAD^-$ cells was determined using flow cytometry (using band-pass filters of 515/20 nm for FITC or 575/26 for PE, 660/20 nm for APC and 695/40 nm for 7AAD) and FlowJo software.

2.9 Detection of TLR-9 and CD23 by flow cytometry

Cell surface and total TLR-9 and CD23 expression in RPMI 8226 and splenic cells was measured as previously described (Schmid et al. 1991). Splenic cells were washed once with NaCl medium (1 x 10^6 cells/ml) and labelled with APC-conjugated anti-murine CD19 or, isotype control mAb, and 7AAD for 30 min at 4ºC. Cells were then fixed by suspension in ice-cold 0.25% (w/v) paraformaldehyde in PBS for 1 hour at 4°C. RPMI 8226 cells or splenic cells were then either washed once (RPMI 8226 cells: 300 x *g* for 5 min or splenic cells: 350 x *g* for 3 min) in cold PBS (fixed) or in 0.2% (v/v) Tween-20 in PBS (fixed and permeabilised) and labelled with PE-conjugated anti human-TLR-9 or isotype control mAb, or FITC-conjugated anti-murine CD23 or isotype control mAb, respectively, for 30 min at 4°C. The MFI of cell surface and total (cell surface and intracellular) TLR-9 or CD23 expression on RPMI 8226 cells or $CD19^+$ splenic cells respectively, was determined using flow cytometry (using band-pass filters 515/20 nm for FITC, 575/26 for PE, 660/20 nm for APC and 695/40 nm for 7AAD) and FlowJo software.

2.10 Measurement of soluble CD23 and CXCL16 by enzyme-linked immunosorbent assay

2.10.1 Soluble CD23

RPMI 8226 cells, PBMCs or splenic cells suspended in NaCl medium containing 0.1% (w/v) BSA (RPMI 8226 cells: as indicated, PBMCs and splenic cells: 5 x 10^6 cells/ml)

were incubated in the absence or presence of 1 mM ATP for 20 min at 37°C. Incubations were stopped by centrifugation (11,000 x *g* for 10 s). Cell-free supernatants were stored at -80°C until required. Soluble CD23 was quantified using the Human CD23/FcεRII Quantikine enzyme-linked immunosorbent assay (ELISA) Kit or the Mouse CD23/FcεRII DuoSet ELISA Development Kit (both R&D Systems, Minneapolis, MN), according to the manufacturer's instructions.

2.10.2 Soluble CXCL16

RPMI 8226 cells suspended in NaCl medium containing 0.1% BSA (w/v) (1×10^7 cells/ml) were incubated in the absence or presence of 1 mM ATP for 10 min at 37°C. Incubations were stopped by centrifugation (11,000 x *g* for 10 s). Cell-free supernatants were stored at -80 °C until required. Soluble CXCL16 was quantified using the Human CXCL16 Mini ELISA Development Kit (Peprotech) according to the manufacturer's instructions. High grade BSA was used to prepare assay diluent and blocking buffer, and 2,2′-azino-bis(3-ethylbenzothiazoline-6-sulfonic acid was used as a substrate.

2.11 Measurement of P2X7 channel activity by electrophysiology

P2X7 channel activity in P2X7-transfected HEK 293 cells was kindly assessed by Dr. Leanne Stokes using electrophysiological measurements of ATP-induced currents as described (Stokes et al. 2010). Briefly, whole-cell patch-clamp recordings were performed at room temperature using an EPC10 amplifier and Patchmaster acquisition

software (HEKA, Lambrecht, Germany). ATP and CAY10593 were delivered using the RSC-160 fast-flow system (Bio-Logic Science Instruments, Claix, France). Membrane potential was clamped at -60 mV in all experiments. External solution was 145 mM NaCl, 5 mM KCl, 2 mM $CaCl_2$, 1 mM $MgCl_2$, 13 mM D-glucose, 10 mM HEPES, and internal solution was 145 mM NaCl, 10 mM HEPES, 10 mM EGTA. Both solutions were adjusted to pH 7.3 with 5 M NaOH and were 300-310 mOsm/L.

2.12 Measurement of P2X7-induced pore formation using a fluorescent plate reader

Ethidium$^+$ uptake assays on human P2X7-transfected HEK 293 cells were kindly performed by Dr. Leanne Stokes using a fluorescent plate reader (Optima FLUOSTAR, BMG Labtech, Offenburg, Germany). Cells (5 x 10^4 cells/well) were incubated overnight in a 96-well poly-D-lysine coated plate. Ethidium$^+$ (25 μM) was added in low divalent solution (145 mM NaCl, 5 mM KCl, 0.2 mM $CaCl_2$, 13 mM D-glucose, 10 mM HEPES, pH 7.3). Cells were preincubated with CAY10593 for 15 min at 37°C before measurements started. ATP was injected after 40 second measurements commenced. Fluorescence was measured using a 485 nm excitation filter and a 520 nm emission filter block. Gain was set at the beginning of the experiment to 30% required value and fluorescence measurements were taken every 10 s.

2.13 Measurement of reactive oxygen species formation

Reactive oxygen species (ROS) formation was measured as previously described (Foster et al. 2013, Wang and Sluyter 2013). RPMI 8226 cells in NaCl medium

(1 x 10^6 cells/ml) were loaded with the broad spectrum ROS indicator, 5 μM H_2DCFDA, for 5 min or with the mitochondrial superoxide indicator, 2.5 μM mitoSOX™ Red for 30 min at 37 °C. Cells were centrifuged (300 x *g* for 5 min) and washed once with NaCl medium. H_2DCFDA or mitoSOX™ Red-loaded cells in NaCl medium were incubated in the absence or presence of 1 mM ATP or ROS-inducing compounds (as indicated) at 37°C. Incubations were stopped by addition of an equal volume of ice-cold $MgCl_2$ medium and centrifugation (300 x *g* for 5 min). Cells were then were washed once with NaCl medium. The MFI of dichlorofluorescein fluorescence (ROS formation) or mitoSOX Red (superoxide generation) was measured using flow cytometry (using bandpass filters of 515/20 nm for dichlorofluorescein and 575/26 nm for mitoSOX™ Red) and FlowJo software.

2.14 Presentation of data and statistics

Data is presented as mean ± standard deviation. Differences between multiple groups was analysed by the one-way analysis of variance using Tukey's multiple comparison test. Differences between two groups was analysed by an unpaired Student's t-test, except for human PBMC ELISA data for which a paired Student's t-test was used. Statistical analyses were performed using GraphPad Prism 5 (Windows version 5.01; GraphPad Software, San Diego, CA) with $P < 0.05$ considered significant.

CHAPTER 3

Characterisation of the P2X7 receptor in human multiple myeloma RPMI 8226 B cells

3.1 Introduction

The P2X7 receptor is a trimeric ligand-gated cation channel belonging to the family of P2X receptors (Jiang 2012). Activation of P2X7 by adenosine 5'-triphosphate (ATP) causes a flux of Ca^{2+}, Na^{+} and K^{+}, as well as the uptake of organic cations including the fluorescent dye, ethidium^{+} (Jiang et al. 2005, Cankurtaran-Sayar et al. 2009). The relative function of P2X7 is also increased in the absence of extracellular Ca^{2+}, Mg^{2+} and Na^{+} ions (Jarvis and Khakh 2009). P2X7 is present on haemopoietic cells, including human primary B cells and malignant B cells from patients with chronic lymphocytic leukaemia (CLL) (Gu et al. 2000). P2X7 is also expressed on the human acute monocytic leukaemic cell line, THP-1 but these cells require treatment with inflammatory mediators to induce P2X7 expression (Humphreys and Dubyak 1998) before use. Examples of other human cell lines which express P2X7 are limited. Therefore, there is a lack of suitable human models to study P2X7 that is constitutively expressed on human cell lines. Preliminary data from our laboratory indicates that the human multiple myeloma B cell line, RPMI 8226 expresses functional P2X7 (Farrell 2008, Pupovac 2009). This same cell line also expresses the low affinity IgE receptor, CD23 (Genty et al. 2004). Other preliminary data from our laboratory indicates that P2X7 activation induces rapid CD23 shedding from RPMI 8226 cells (Farrell 2008). Collectively, this suggests that RPMI 8226 cells may serve as a model cell line to study the mechanisms involved in P2X7-induced CD23 shedding. Therefore, this chapter aims to confirm the presence of and to further characterise P2X7 in RPMI 8226 cells.

3.2 Results

3.2.1 RPMI 8226 cells express P2X1, P2X4, P2X5 and P2X7 messenger RNA

To confirm the presence of P2X7 in RPMI 8226 cells and to examine the presence of other P2X subtypes, RNA was isolated from these cells and analysed by reverse transcriptase-polymerase chain reaction (RT-PCR). RT-PCR revealed strong expression of P2X7, as well as P2X4 and P2X5 (Figure 3.1). Weak expression of P2X1 was also observed but was not readily apparent when captured as an electronic image (Figure 3.1). The respective amplicons corresponded to the predicted sizes of P2X1 (400 base pairs (bp)), P2X4 (433 bp) and P2X7 (544 bp). In contrast the amplicon for P2X5 was 501 bp, approximately 71 bp larger than the predicted size (430 bp). Sequence analysis of the P2X5 amplicon revealed an extra 66 bp (Figure 3.2). This insert is located between exon 9 and exon 10 of the *P2RX5* gene (Figure 3.2). P2X2, P2X3 and P2X6 were absent from RPMI 8226 cells (Figure 3.1).

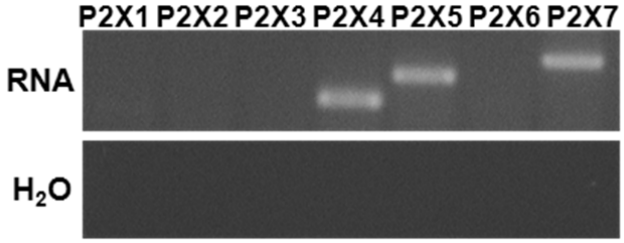

Figure 3.1: RPMI 8226 cells express P2X1, P2X4, P2X5 and P2X7 messenger RNA. RNA was isolated from RPMI 8226 cells and analysed by RT-PCR using primers to P2X1-7. RNA substituted with H_2O was used as a negative control. PCR products were visualised using ethidium bromide. Representative result of three experiments is shown.

Figure 3.2: P2X5 complementary DNA (cDNA) from RPMI 8226 cells contains a 66 nucleotide bp insert. RNA was isolated from RPMI 8226 cells and RT-PCR performed using primers to P2X5. The amplicon was excised from a 2% agarose gel after electrophoresis separation then purified and sequenced. Representative sequence from three separate sequencing reactions is shown.

3.2.2 RPMI 8226 cells express cell surface but not intracellular P2X7

Previous data from our group demonstrates surface expression of P2X7 on RPMI 8226 cells (Farrell 2008, Pupovac 2009, Gadeock 2010). To determine if P2X7 was confined to the surface of RPMI 8226 cells or was also present intracellularly, cell surface or total (surface and intracellular) P2X7 was examined in fresh cells, or fixed and permeabilised cells, respectively by immunofluorescent labelling. Expression of P2X7 was similar in both fresh cells, and fixed and permeabilised cells (22.6 ± 0.1 versus 20.2 ± 4.1 mean fluorescence intensity (MFI) of P2X7 expression respectively, $n = 3$, $P = 0.3499$; Figure 3.3).

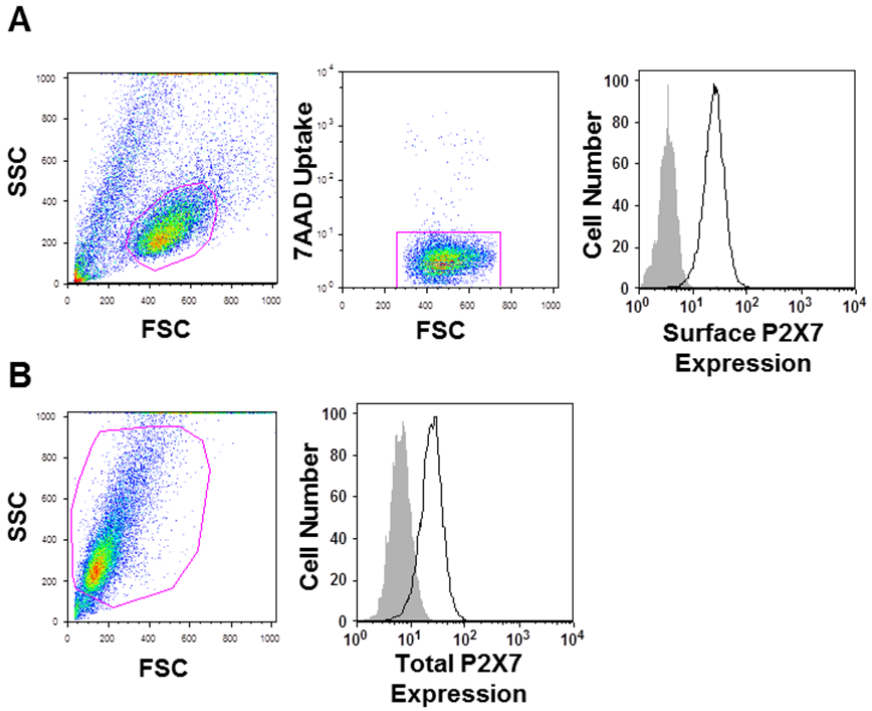

Figure 3.3: RPMI 8226 cells express cell surface but not intracellular P2X7. (A) Fresh cells or (B) fixed and permeabilised cells were labelled with Alexa Fluor® 647-conjugated anti-P2X7 (black line) or isotype control (grey fill) monoclonal antibody (mAb), and the relative P2X7 expression (MFI) determined by flow cytometry (right panels). (A) 7-aminoactinomycin D was included with fresh cells to exclude dead cells, and were gated first by forward scatter (FSC) and side scatter (SSC) (left panel), followed by 7-aminoactinomycin D negative cells as shown (centre panel). (B) Fixed and permeabilised cells were gated by FSC and SSC as shown (left panel). Representative results from three experiments are shown.

3.2.3 ATP induces ethidium$^+$ uptake into RPMI 8226 cells in a time-dependent manner

Previous data from our group demonstrates that 5 min incubation with ATP induces ethidium$^+$ uptake into RPMI 8226 cells (Farrell 2008, Pupovac 2009, Gadeock 2010).

To determine whether ATP induces ethidium$^+$ uptake in a time-dependent manner, cells were incubated with ATP for up to 9 min and ethidium$^+$ uptake measured by flow cytometry. ATP-induced ethidium$^+$ uptake into RPMI 8226 cells linearly, in a time-dependent fashion (Figure 3.4). Ethidium$^+$ uptake in the absence of ATP was minimal over 9 min (results not shown).

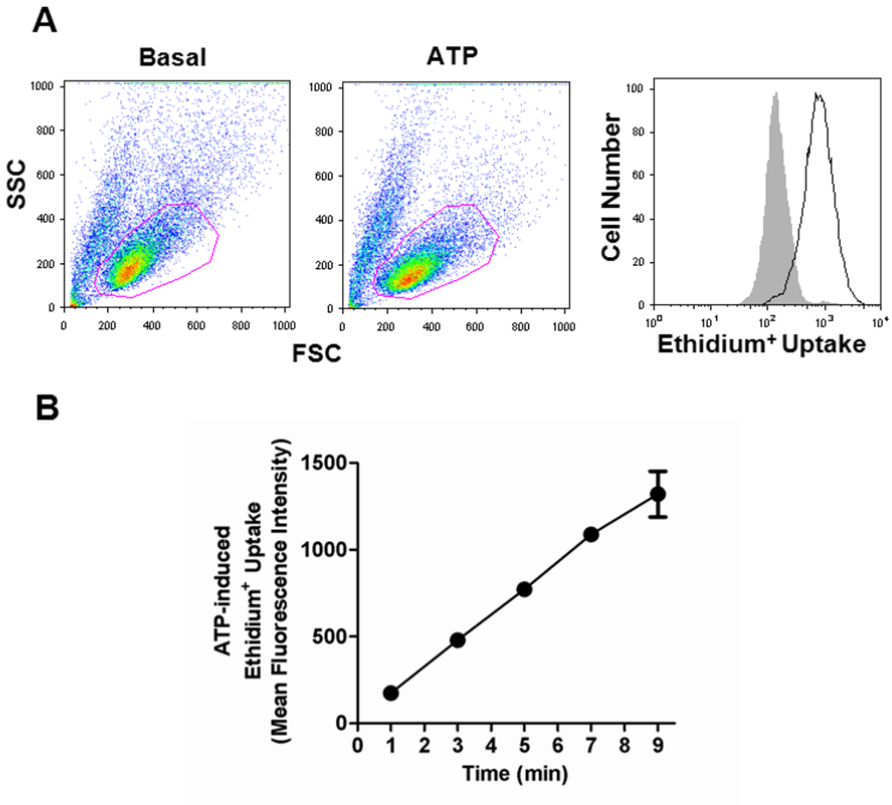

Figure 3.4: ATP induces ethidium$^+$ uptake into RPMI 8226 cells in a time-dependent manner. (A, B) RPMI 8226 cells in NaCl medium were incubated with 25 µM ethidium$^+$ in the absence (basal) or presence of 1 mM ATP at 37ºC for up to 9 min (as indicated). Incubations were stopped by addition of $MgCl_2$ medium and centrifugation, and the MFI of ethidium$^+$ uptake determined by flow cytometry. (A) Basal or ATP-treated cells were gated by the same gate against FSC and SSC as shown, and histograms represent basal (grey fill) and ATP-induced (black line) ethidium$^+$ uptake in RPMI 8226 cells at 5 min. (B) Results are mean ± standard deviation (SD) (n = 3).

3.2.4 Ca^{2+} and Mg^{2+} inhibit ATP-induced ethidium^{+} uptake into RPMI 8226 cells

The above data (Figure 3.4) and our preliminary data (Farrell 2008, Pupovac 2009, Gadeock 2010) were obtained in medium nominally free of Ca^{2+} and Mg^{2+}. To determine the effect of extracellular divalent cations on P2X7 function in RPMI 8226 cells, cells were incubated with increasing concentrations of ATP in the absence or presence of physiological concentrations of Ca^{2+} and Mg^{2+}, and ethidium^{+} uptake measured by flow cytometry. In the absence of extracellular Ca^{2+} and Mg^{2+}, ATP induced ethidium^{+} uptake in a concentration-dependent manner, with maximal uptake occurring at 0.5 mM ATP, and with an approximate half maximal effective concentration (EC_{50}) of 116 ± 15 μM (Figure 3.5). In the presence of extracellular Ca^{2+} and Mg^{2+}, ATP also induced ethidium^{+} uptake in a concentration-dependent manner, but the amount of uptake was lower with near-maximal uptake occurring at 5 mM ATP, and with an EC_{50} of 1 ± 0.4 mM (Figure 3.5).

3.2.5 ATP-induced ethidium^{+} uptake into RPMI 8226 cells is enhanced in sucrose and KCl medium compared to NaCl medium

Na^{+} in cell media is known to inhibit P2X7 function (Wiley et al. 1992, Michel et al. 1999). To assess whether the absence of Na^{+} alters the potency of ATP against P2X7 in RPMI 8226 cells, cells were incubated in sucrose, KCl or NaCl medium in the presence of increasing concentrations of ATP. Similar to above (Figure 3.5), ATP induced ethidium^{+} uptake into RPMI 8226 cells suspended in NaCl medium in a concentration-dependent manner and with an EC_{50} of 99 ± 20 μM (Figure 3.6). In

contrast, the EC_{50} values for ATP-induced ethidium$^+$ uptake into RPMI 8226 cells suspended in either sucrose or KCl medium, both nominally free of Na^+, were lower (3 ± 3 or 18 ± 8 μM, respectively) compared to the EC_{50} for ATP in NaCl medium (Figure 3.6).

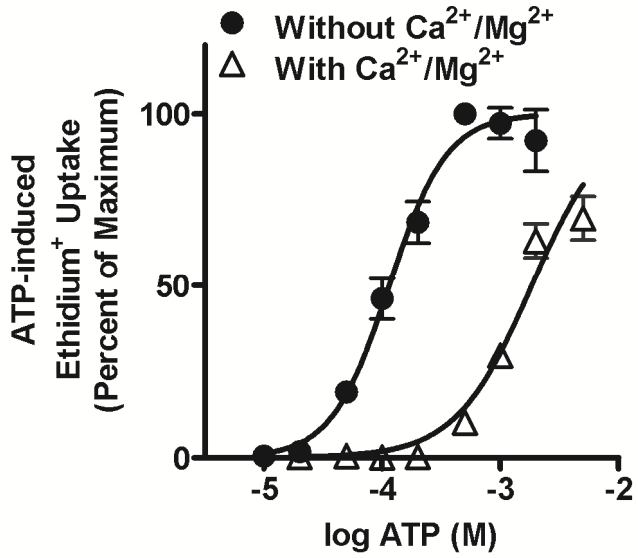

Figure 3.5: Ca^{2+} and Mg^{2+} impair ATP-induced ethidium$^+$ uptake into RPMI 8226 cells. RPMI 8226 cells in NaCl medium or NaCl medium containing 1.5 mM $CaCl_2$ and 1 mM $MgCl_2$ were incubated with 25 μM ethidium$^+$ in the absence (basal) or presence of varying ATP concentrations (as indicated) at 37°C for 5 min. Incubations were stopped by addition of $MgCl_2$ medium and centrifugation, and the MFI of ethidium$^+$ uptake determined by flow cytometry. Ethidium$^+$ uptake is expressed as percent maximum response compared to 0.5 mM ATP. Results are mean ± SD (*n* = 3).

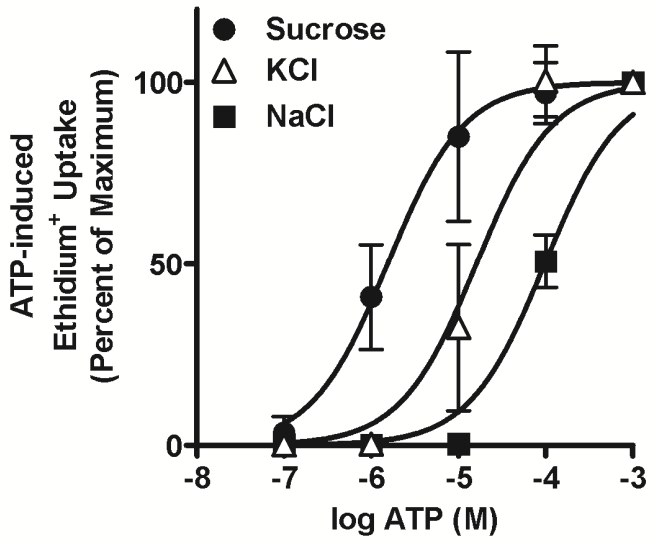

Figure 3.6: ATP-induced ethidium$^+$ uptake into RPMI 8226 cells is enhanced in sucrose and KCl medium compared to NaCl medium. RPMI 8226 cells in sucrose, KCl or NaCl medium were incubated with 25 μM ethidium$^+$ in the presence of varying amounts of ATP (as indicated) at 37°C for 5 min. Incubations were stopped by $MgCl_2$ solution and centrifugation, and the MFI of ethidium$^+$ uptake determined by flow cytometry. Ethidium$^+$ uptake is expressed as percent maximum response compared to 1 mM ATP for each corresponding medium. Results are mean ± SD (n = 9).

3.2.6 P2X7 antagonists impair ATP-induced ethidium$^+$ uptake into RPMI 8226 cells in a concentration-dependent manner

Specific P2X7 antagonists including AZ10606120 (Michel et al. 2008), AZ11645373 (Stokes et al. 2006) and A-438079 (Nelson et al. 2006) have been characterised using cells expressing recombinant P2X7. However these antagonists have been far less studied on cells expressing endogenous (or native) P2X7. Therefore, to test these specific P2X7 antagonists on endogenously expressed P2X7, RPMI 8226 cells were preincubated in the absence or presence of increasing concentrations of AZ10606120,

AZ11645373 or A-438079, and the ATP-induced ethidium$^+$ uptake was measured by flow cytometry. AZ10606120, AZ11645373 and A-438079 impaired ATP-induced ethidium$^+$ uptake in a concentration-dependent manner, with maximal inhibition occurring at 100 nM, 300 nM and 10 μM, and with a half maximal inhibitory concentrations (IC_{50s}) of 11 ± 1 nM, 27 ± 3 nM and 900 ± 100 nM, respectively (Figure 3.7).

3.2.7 Probenecid, but not colchicine impairs ATP-induced ethidium$^+$ uptake into RPMI 8226 cells

The pannexin-1 antagonist, probenecid and the microtubule destabiliser, colchicine impair P2X7-induced dye uptake into cells (Silverman et al. 2009, Marques-da-Silva et al. 2011). Therefore, to determine whether these compounds impair P2X7-induced ethidium$^+$ uptake in RPMI 8226 cells, cells were preincubated in the absence or presence of either compound at concentrations previously shown to block P2X7-induced dye uptake (Silverman et al. 2009, Marques-da-Silva et al. 2011), and ATP-induced ethidium$^+$ uptake was measured by flow cytometry. Probenecid impaired ATP-induced ethidium$^+$ uptake by 42 ± 5% (Figure 3.8), whereas colchicine did not affect ATP-induced ethidium$^+$ uptake (Figure 3.8). In the absence of ATP, neither compound altered basal ethidium$^+$ uptake (Figure 3.8).

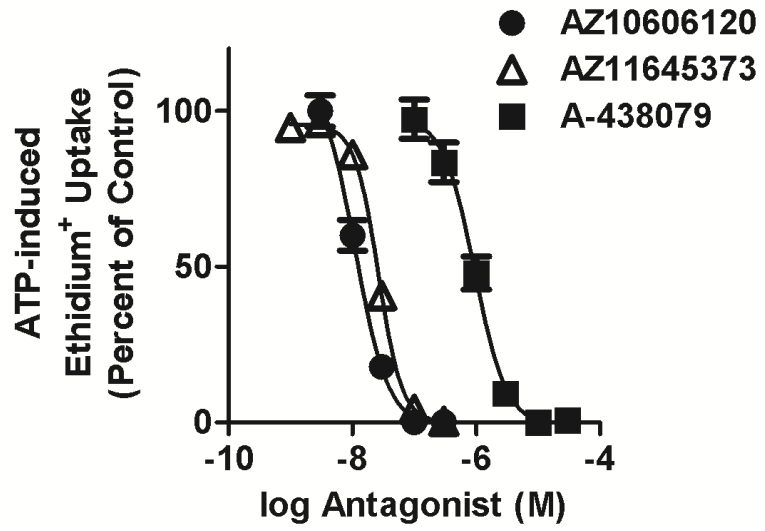

Figure 3.7: P2X7 antagonists impair ATP-induced ethidium$^+$ uptake into RPMI 8226 cells in a concentration-dependent manner. RPMI 8226 cells in NaCl medium were preincubated at 37°C for 15 min in the absence or presence of varying concentrations of antagonist (as indicated). Cells were then incubated with 25 μM ethidium$^+$ in the absence or presence of 1 mM ATP at 37°C for 5 min. Incubations were stopped by addition of $MgCl_2$ medium and centrifugation, and the MFI of ethidium$^+$ uptake determined by flow cytometry. Results are the mean percent of ATP-induced ethidium$^+$ uptake in the absence of antagonist ± SD (n = 3).

3.2.8 RPMI 8226 cells contain several single nucleotide polymorphisms in the *P2RX7* gene

Human *P2RX7* is highly polymorphic, with a number of single nucleotide polymorphisms (SNPs) coding for loss or gain of function (Sluyter and Stokes 2011). Therefore, to determine if RPMI 8226 cells encode *P2RX7* SNPs, full-length P2X7 cDNA was amplified by RT-PCR and sequenced. The *P2RX7* gene of RPMI 8226 cells was homozygous for three non-synonymous SNPs (Figure 3.9; Table 3.1), and two

synonymous SNPs (Table 3.1). Of note, these cells contained the A348T gain-of-function SNP (Cabrini et al. 2005, Roger et al. 2010, Stokes et al. 2010), and the H521Q SNP, which reduces the sensitivity of the receptor to inhibition by extracellular Ca^{2+} (Roger et al. 2010) (Figure 3.9; Table 3.1). RPMI 8226 were wild-type at other nucleotide positions in the *P2RX7* gene (results not shown).

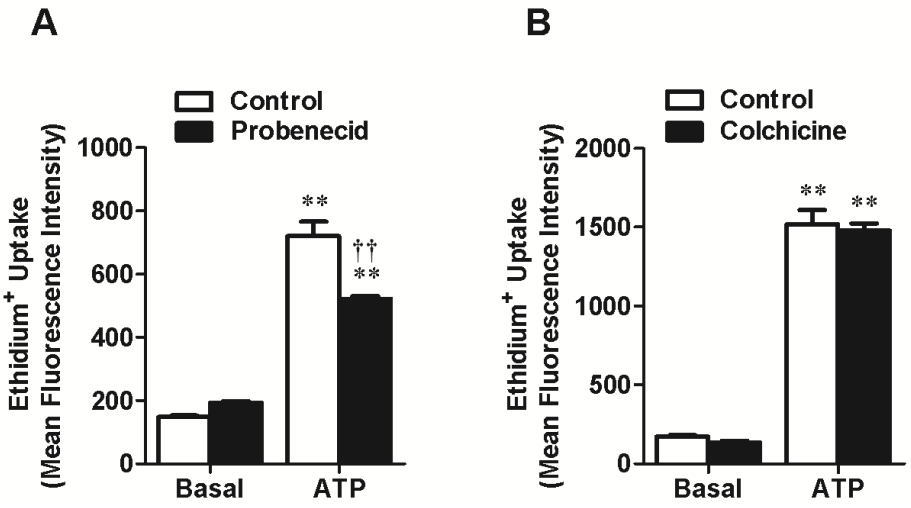

Figure 3.8: Probenecid, but not colchicine, impairs ATP-induced ethidium$^+$ uptake into RPMI 8226 cells. RPMI 8226 cells in NaCl were preincubated in the absence or presence of (A) 2.5 mM probenecid for 15 min or (B) 50 μM colchicine for 1 hour. Cells were then incubated with 25 μM ethidium$^+$ in the absence (basal) or presence of 1 mM ATP at 37°C for 5 min. Incubations were stopped by addition of $MgCl_2$ medium and centrifugation, and the MFI of ethidium$^+$ uptake determined by flow cytometry. Results are mean ± SD (n = 3). $^{**}P < 0.01$ compared to corresponding basal control, $^{††}P < 0.01$ compared to ATP alone.

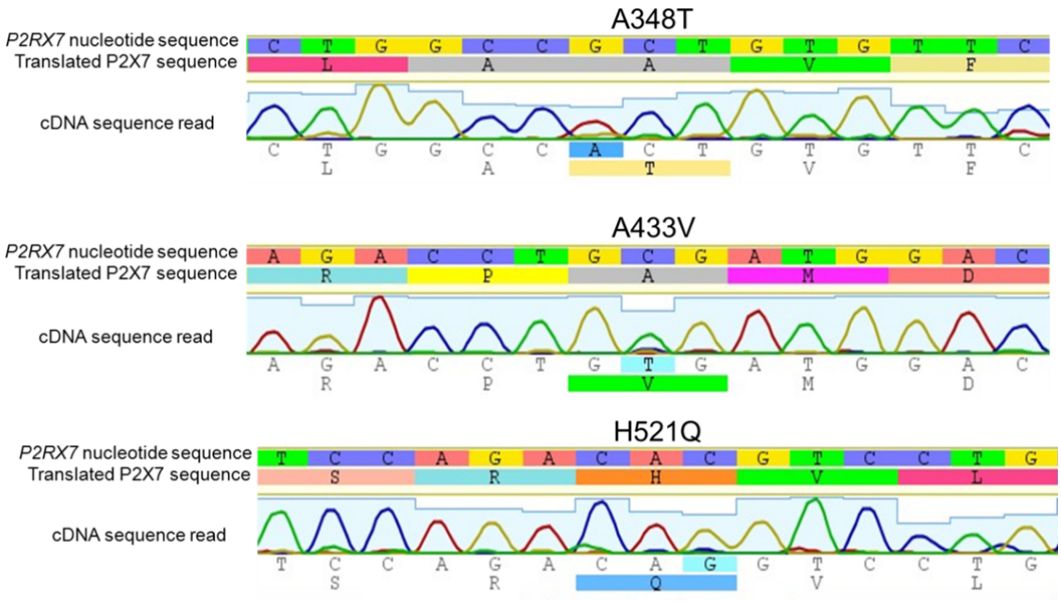

Figure 3.9: RPMI 8226 cells contain three non-synonymous SNPs in the *P2RX7* gene. Full-length P2X7 cDNA from RPMI 8226 cells was amplified by RT-PCR and sequenced using primers spanning full-length P2X7 cDNA to identify SNPs. Representative sequences from two separate reactions are shown.

3.2.9 ATP induces CD23 loss from RPMI 8226 cells in a time-dependent manner

Previous data from our group demonstrates that ATP induces CD23 loss from the cell surface of RPMI 8226 cells (Farrell 2008). To confirm that P2X7 activation induces CD23 loss from RPMI 8226 cells, cells were incubated with 1 mM ATP for up to 30 min and cell surface CD23 expression measured by flow cytometry. As expected, ATP induced the rapid loss of cell surface CD23 in a time-dependent manner with a $t_{1/2}$ of approximately 7 min (Figure 3.10).

Table 3.1: RPMI 8226 cells contain several SNPs in the *P2RX7* gene.

dbSNP rs# cluster ID[a]	Base change[b]	Amino acid change	Effect on function
rs28360448	GTG>GTA	V154V	Synonymous[c]
rs1718119	GCT>ACT	A348T	Gain
rs28360459	GCG>GTG	A433V	Unknown
rs2230913	CAC>CAG	H521Q	Neutral[d]
rs1621388	CCG>CCA	P582P	Synonymous

[a]http://www.ncbi.nlm.nih.gov/SNP/snp_ref.cgi?locusId=5027.

[b]Full length P2X7 cDNA from RPMI 8226 cells was amplified by RT-PCR and sequenced to identify SNPs. Representative sequences from two separate reactions are shown.

[c]Synonymous mutations are predicted to have neutral effect on function.

[d]Neutral effect; however the mutant receptor displays reduced sensitivity to inhibition by extracellular Ca^{2+} (Roger et al. 2010).

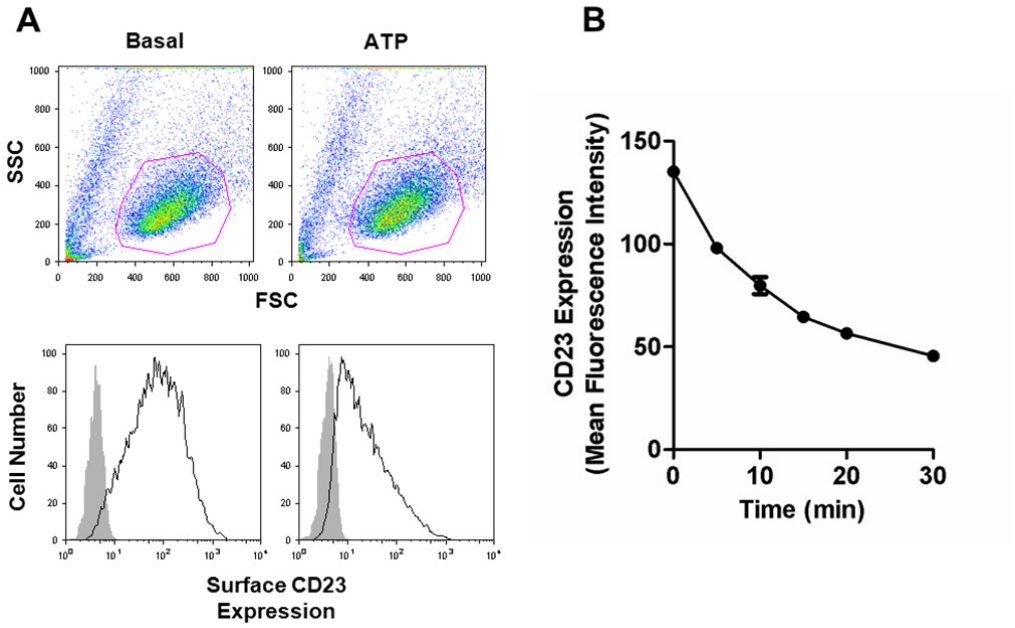

Figure 3.10: ATP induces CD23 loss from RPMI 8226 cells in a time-dependent manner. (A, B) RPMI 8226 cells in NaCl medium were incubated for up to 30 min (as indicated) at 37°C in the absence (basal) or presence of 1 mM ATP. Incubations were stopped by addition of $MgCl_2$ medium and centrifugation. Cells were then labelled with phycoerythrin (PE)-conjugated anti-CD23 or isotype control mAb, and the MFI of cell surface CD23 expression determined by flow cytometry. (A) Cells incubated in the absence (Basal) or presence of ATP were gated against FSC and SSC as shown (top panel). Representative histograms show CD23 (black line) or isotype control mAb binding (grey fill) on RPMI 8226 cells incubated in the absence (basal) or presence of 1 mM ATP for 30 min (bottom panel). (B) Results are mean ± SD (n = 3).

3.2.10 ATP induces CD23 loss from RPMI 8226 cells in a concentration-dependent manner

To further characterise ATP-induced CD23 loss from RPMI 8226 cells, cells were incubated in the presence of increasing concentrations of ATP and cell surface CD23 measured by flow cytometry. ATP induced a loss of CD23 in a concentration-dependent

manner, with maximal loss occurring at 1 mM ATP, and with an EC_{50} of 74 ± 12 μM (Figure 3.11).

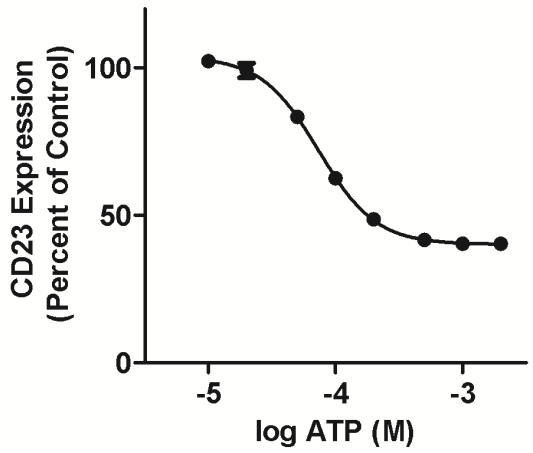

Figure 3.11: ATP induces CD23 loss from RPMI 8226 cells in a concentration-dependent manner. RPMI 8226 cells in NaCl medium were incubated with increasing concentrations of ATP (as indicated) at 37°C for 7 min. Incubations were stopped by addition of $MgCl_2$ medium and centrifugation. Cells were then labelled with PE-conjugated anti-CD23 or isotype control mAb, and the MFI of cell surface CD23 expression determined by flow cytometry. CD23 expression is expressed as percentage of CD23 expression in the absence of ATP. Results are mean ± SD (n = 3); where error bars are absent SD is too small to be seen.

3.2.11 AZ10606120 impairs ATP-induced CD23 loss from RPMI 8226 cells

To confirm that ATP-induced CD23 loss is mediated by P2X7, RPMI 8226 cells were preincubated in the absence or presence of 100 nM AZ10606120 and then with ATP and cell surface CD23 measured by flow cytometry. As above (Figure 3.10 and 3.11), ATP induced a loss of CD23 from the surface of RPMI 8226 cells (Figure 3.12). AZ10606120 impaired ATP-induced CD23 loss by 88 ± 9% compared to ATP-induced

CD23 loss in the absence of AZ10606120 (Figure 3.12). In the absence of ATP, AZ10606120 did not significantly alter cell surface CD23 expression (Figure 3.12).

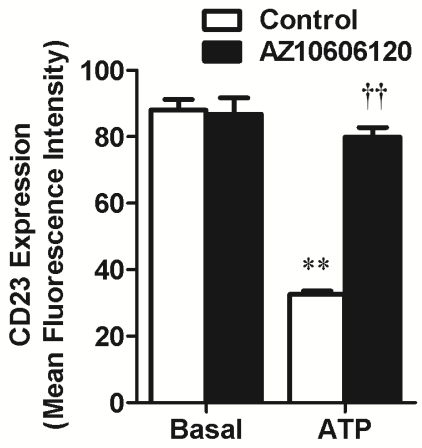

Figure 3.12: AZ10606120 impairs ATP-induced CD23 loss from RPMI 8226 cells. RPMI 8226 cells in NaCl medium were preincubated at 37°C for 15 min in the absence or presence of 100 nM AZ10606120, and then in the absence (basal) or presence of 1 mM ATP for 7 min at 37°C. Incubations were stopped by addition of $MgCl_2$ medium and centrifugation. Cells were then labelled with PE-conjugated anti-CD23 or isotype control mAb, and the MFI of cell surface CD23 expression determined by flow cytometry. Results are mean ± SD (n = 3); $^{**}P < 0.01$ compared to corresponding basal control, and $^{††}P < 0.01$ compared to ATP alone.

3.2.12 ATP induces CD23 shedding from RPMI 8226 cells

To confirm that the ATP-induced loss of cell surface CD23 was due to CD23 shedding, RPMI 8226 cells were incubated with ATP, and the amount of soluble CD23 in cell-free supernatants measured by enzyme-linked immunosorbent assay (ELISA). Incubation of

cells with 1 mM ATP resulted in a significantly higher release of soluble CD23 compared to cells incubated in the absence of ATP (Figure 3.13).

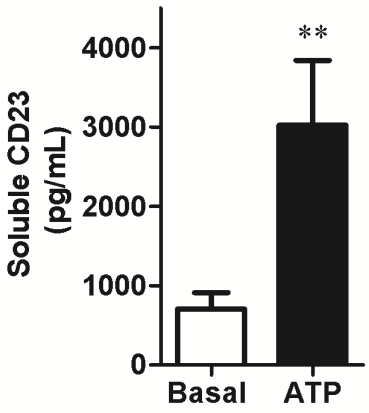

Figure 3.13: ATP induces CD23 shedding from RPMI 8226 cells. RPMI 8226 cells in NaCl medium (5 x 10^6 cells/ml) were incubated in the absence (basal) or presence of 1 mM ATP for 20 min, incubations were stopped by centrifugation and the amount of soluble CD23 in cell-free supernatants determined by ELISA. Results are mean ± SD (n = 3); $^{**}P < 0.01$ compared to basal control.

3.3 Discussion

Preliminary data in our laboratory indicated that the human RPMI 8226 multiple myeloma B cell line expresses functional P2X7. Using immunofluorescent labelling and immunoblotting our group has previously shown the presence of P2X7 in RPMI 8226 cells (Farrell 2008, Pupovac 2009, Gadeock 2010). Moreover, flow cytometric measurements have demonstrated that ATP and the most potent P2X7 antagonist BzATP, can induce ethidium$^+$ uptake into, and CD23 shedding from RPMI 8226 cells, and that these processes could be impaired by the P2X7 antagonists, KN-62 and

A-438079 (Farrell 2008, Pupovac 2009, Gadeock 2010). This chapter confirms that RPMI 8226 cells express functional P2X7 and makes a number of new observations. First, RT-PCR and immunolabelling confirmed that P2X7 was present in RPMI 8226 cells. Second, ATP induced ethidium^{+} uptake in a time-dependent and concentration-dependent fashion with an EC_{50} (~116 μM), similar to ATP-induced cation fluxes mediated by recombinant P2X7 (Rassendren et al. 1997). Third, ATP-induced ethidium^{+} uptake was reduced in the presence of extracellular Ca^{2+} and Mg^{2+}, and increased with removal of Na^{+} ions which is characteristic of P2X7 in other cell types (Wiley et al. 1992, Michel et al. 1999). Fourth, the P2X7 antagonists A-438079, AZ10606120 and AZ11645373 impaired ATP-induced ethidium^{+} in a concentration-dependent manner. The rank order of potency AZ10606120 > AZ11645373 > A-438079 obtained in this study corresponds to previous published values of heterologous P2X7 (IC_{50} of ~1.4 nM, 10-90 nM and ~300 nM respectively) (Nelson et al. 2006, Stokes et al. 2006, Michel et al. 2008).

Preliminary data in our laboratory indicated that P2X7 activation induces the shedding of CD23 from RPMI 8226 cells (Farrell 2008). This chapter also confirms that P2X7 activation induces CD23 shedding from these cells. First, ATP induced a loss of CD23 from RPMI 8226 cells in a time-dependent manner, with a $t_{1/2}$ (~7 min) similar to that obtained by Farrell (2008). Second, new observations showed that ATP induced a loss of CD23 in a concentration-dependent manner, with an EC_{50} (~74 μM) similar to ATP-induced ethidium^{+} uptake (Figure 3.5) and to ATP-induced CD23 shedding from CLL cells (Gu et al. 1998). Third, the new generation antagonist, AZ10606120, near-completely impaired ATP-induced CD23 loss from RPMI 8226 cells similar to that observed by Farrell (2008), who showed that A-438079 and KN-62 near-completely

prevented ATP-induced CD23 shedding from these cells. Finally, using a human CD23 ELISA, the ATP-induced CD23 loss from RPMI 8226 cells was demonstrated to be due to shedding; similar amounts of ATP-induced soluble CD23 were observed by Farrell (2008). Other studies have also showed the rapid shedding of CD23 (< 30 min) from CLL cells (Gu et al. 1998) and human monocyte-derived dendritic cells (Sluyter and Wiley 2002, Georgiou et al. 2005). Thus, combined this data reinforces a role for P2X7 activation in the rapid shedding of CD23 from human leukocytes and supports the use of RPMI 8226 cells to investigate this process further.

Probenecid, but not colchicine, impaired ATP-induced ethidium^{+} uptake into RPMI 8226 cells. Probenecid is commonly used as a pannexin-1 inhibitor (Silverman et al. 2009), however it has long been recognised that probenecid blocks other molecules (Di Virgilio et al. 1990). More recently, probenecid has been shown to impair P2X7 directly (Bhaskaracharya et al. 2014). Whether probenecid inhibits ATP-induced ethidium^{+} uptake in RPMI 8226 cells by blocking pannexin-1 or by blocking P2X7 directly remains unknown. Microarray studies show that pannexin-1 gene is overexpressed in some human multiple myeloma cell lines (Largo et al. 2006), however whether RPMI 8226 cells express pannexin-1 protein is unknown. The microtubule destabiliser, colchicine, impairs ATP-induced YO-PRO-1^{2+} uptake in *Xenopus* oocytes and human embryonic kidney 293 cells expressing human P2X7, and ethidium^{+} uptake in murine peritoneal macrophages (Marques-da-Silva et al. 2011). In contrast, colchicine, used at the same concentration (50 μM) does not impair ATP-induced ethidium^{+} uptake in RPMI 8226 cells. Colchicine used at concentrations below 50 μM impairs ATP-induced IL-1β release in murine microglial MG6 cells (Takenouchi et al. 2008) but not in human monocytic THP-1 cells (Martinon et al. 2006) suggesting that the effect of colchicine

may be cell specific. Marques-da-Silva and colleagues reported that colchicine concentrations used by Martinon and colleagues were ineffective at inhibiting ATP-induced cell permeabilisation in their experiments (Marques-da-Silva et al. 2011). Therefore it is possible that colchicine concentrations greater than 50 μM are required to impair ATP-induced ethidium^{+} uptake in RPMI 8226 cells.

In addition to P2X7 transcripts, RT-PCR revealed the strong expression of P2X4 and P2X5 transcripts, as well as the weak expression of P2X1 transcripts in RPMI 8226 cells. Prior to this study, the expression of P2X subtypes in RPMI 8226 cells was unknown. The pattern of P2X mRNA expression in RPMI 8226 cells is similar to that described for Epstein-Barr virus-infected human B cells, which express relatively high amounts of P2X4 and P2X5, and lower amounts of P2X1 and P2X7, but little or no P2X2, P2X3 or P2X6 (Lee et al. 2006). Whether P2X1, P2X4 and P2X5 mRNA are translated to protein or lead to functional P2X channels in these cells or in RPMI 8226 cells remains unknown. However, immunofluorescent labelling demonstrated the presence of P2X1 and P2X4, as well as P2X7, but not P2X5, in human CLL B cells (Sluyter et al. 2001) suggesting that other P2X subtypes, apart from P2X7, may also form functional P2X channels in RPMI 8226 cells and other cells of the B cell lineage. Data from this chapter also showed that the P2X5 cDNA transcript contained an extra 66 nucleotide bp suggesting the presence of a potential P2X5 variant in RPMI 8226 cells. This sequence is located between exon 9 and 10 in the *P2RX5* gene. Further experiments are required to determine whether this variant encodes a functional receptor. Future experiments will need to examine the size of P2X5 protein in RPMI 8226 cells by Western blotting and determine whether this receptor is functional using electrophysiology. This however, was beyond the scope of this thesis. It is well known

that the most prevalent P2X5 isoform (P2X5a) occurs in humans as a non-functional variant due to a SNP in the 3' splice site of exon 10 (Bo et al. 2003, Kotnis et al. 2010). Therefore, it would be of interest to determine if RPMI 8226 cells encode this SNP, however due to the partial sequence of exon 10 obtained in the current study this appears unlikely.

The results in this chapter revealed for the first time that RPMI 8226 cells are homozygous for the gain-of-function A348T SNP, as well as the A433V and H521Q SNPs (Figure 3.14). Although not formally demonstrated, A433V may also act as an additional gain-of-function SNP in these cells as the opposite amino acid exchange at position 76 of P2X7 (V76A) causes a loss of function (Roger et al. 2010, Stokes et al. 2010). Others have shown that H521Q impairs ATP-induced inward currents but not ethidium^{+} uptake (Roger et al. 2010). Moreover, this same group showed that H521Q reduced the sensitivity of P2X7 to inhibition by extracellular Ca^{2+} (Roger et al. 2010). In contrast, maximal ATP-induced ethidium^{+} uptake was only partly lower in RPMI 8226 cells suspended in NaCl medium containing Ca^{2+}/Mg^{2+} compared to cells in NaCl medium nominally free of Ca^{2+}/Mg^{2+} (Figure 3.5). However, this data is complicated by the presence of Mg^{2+} (in the medium used), which is known to impair P2X7 by binding to H130 and H201 (Acuna-Castillo et al. 2007) and by reducing the amount of extracellular ATP^{4-}, the presumed ligand of P2X7 (Jiang 2009).

This chapter confirms that RPMI 8226 cells express functional P2X7 and that its activation results in the rapid shedding of CD23, supporting the use of these cells as a model to study the mechanisms involved in P2X7-induced CD23 shedding. Moreover,

this chapter demonstrates new features regarding P2X7 in RPMI 8226 cells including its sensitivity to extracellular Ca^{2+}, Mg^{2+} and Na^{+}, to three more recently developed P2X7 antagonists, and to probenecid, as well as presence of the non-synonymous SNPs, A348T, A433V and H521Q in these cells.

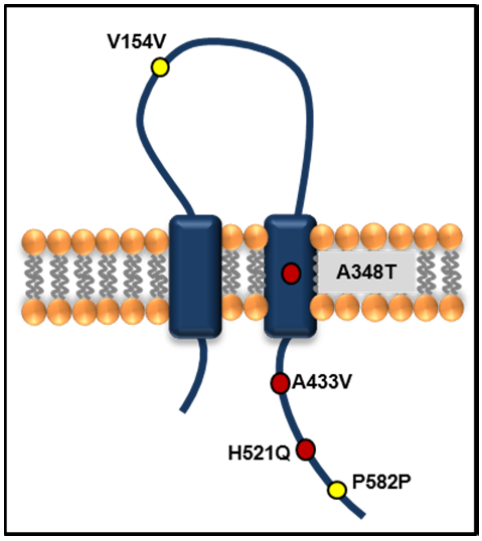

Figure 3.14: A schematic of the P2X7 subunit showing the SNPs identified in RPMI 8226 cells. The *P2RX7* gene in RPMI 8226 cells contains two synonymous SNPs, V154V and P582P, and three non-synonymous SNPs, A348T, A433V, and H521Q.

CHAPTER 4

CAY10593 (VU0155069) inhibits human P2X7 independently of phospholipase D1 stimulation

4.1 Introduction

Prolonged exposure of P2X7 to extracellular adenosine 5'-triphosphate (ATP) opens a second permeability state or pore that allows the uptake of organic cations including fluorescent dyes such as ethidium^{+} (Wiley et al. 1998, Cankurtaran-Sayar et al. 2009). Whether this second permeability state is attributed to intrinsic channel dilation (Yan et al. 2010), the pannexin-1 channel (Pelegrin and Surprenant 2006) or an alternate but unknown uptake pathway (Schachter et al. 2008, Cankurtaran-Sayar et al. 2009, Marques-da-Silva et al. 2011) remains controversial. Recently it has been shown that large organic dyes can directly permeate P2X7 (Browne et al. 2013). Moreover, our understanding of this permeability state is further complicated with some (Donnelly-Roberts et al. 2004, Faria et al. 2005, Bianco et al. 2009) but not other (da Cruz et al. 2006, Michel et al. 2006, Wang and Sluyter 2013) studies showing that P2X7-induced dye uptake involves the p38 mitogen-activated protein kinase (MAPK).

Regardless of the true identity of the P2X7 pore and the mechanism by which it opens, P2X7 activation stimulates multiple signalling pathways via molecules such as MAPK, protein kinase C (PKC), mitogen/extracellular regulated kinase 1/2 (MEK1/2), c-Jun N-terminal kinase (JNK), rho-kinase, phosphoinositide 3-kinase (PI3K), glycogen synthase kinase (GSK)-3 and phospholipase A2 (PLA2), C (PLC) and D (PLD). These signalling pathways induce various cellular events including inflammatory mediator release, reactive oxygen and nitrogen species formation, and cell proliferation or death (Lenertz et al. 2011, Wiley et al. 2011). P2X7 activation also induces the shedding of cell surface molecules including CD23 (Gu et al. 1998, Sluyter and Wiley 2002, Georgiou et al. 2005). Furthermore, data from our laboratory shows that P2X7

activation induces CD23 shedding from RPMI 8226 cells (Farrell 2008; Chapter 3). However, the intracellular signalling pathways that mediate this process are unknown.

PLD catalyses the hydrolysis of phosphatidylcholine to phosphatidic acid and choline, which subsequently participate in various cellular events (McDermott et al. 2004). Two isoforms of mammalian PLD have been described, PLD1 and PLD2 (McDermott et al. 2004). P2X7 activation can stimulate PLD in B cells (Gargett et al. 1996, Shemon et al. 2007) and macrophages (el-Moatassim and Dubyak 1993, Humphreys and Dubyak 1996). P2X7-induced PLD stimulation in macrophages plays a role in the killing of intracellular mycobacteria (Kusner and Adams 2000, Fairbairn et al. 2001) and the generation of microvesicles capable of further macrophage activation (Thomas and Salter 2010). In contrast, the role of P2X7-induced PLD stimulation in B cells remains unknown. This chapter aims to examine the signalling pathways involved in P2X7-induced CD23 shedding using RPMI 8226 cells as model.

4.2 Results

4.2.1 ATP-induced CD23 shedding from RPMI 8226 cells is not prevented by changes in intracellular cation concentrations

To assess a potential role for changes in intracellular cation concentrations in P2X7-induced CD23 shedding, ATP-induced CD23 shedding from RPMI 8226 cells was compared between cells suspended in NaCl medium (control) to cells suspended in

either choline Cl medium, KCl medium, or in NaCl medium containing ethylene glycol tetraacetic acid (EGTA) or 1,2-bis(o-aminophenoxy)ethane-N,N,N',N'-tetraacetic acid (BAPTA-AM), which prevent Na^+ influx, K^+ efflux, Ca^{2+} influx or intracellular Ca^{2+} increases, respectively. ATP-induced CD23 shedding was assessed using flow cytometry as described in Chapter 3. As observed in Chapter 3, ATP induced CD23 shedding from RPMI 8226 cells in NaCl medium (Figure 4.1A-D). ATP-induced CD23 shedding was potentiated from cells suspended in either choline Cl or KCl medium compared to cells in NaCl medium (Figure 4.1A, B). In contrast, ATP-induced CD23 shedding was similar from cells suspended in NaCl medium containing 100 μM EGTA or 50 μM BAPTA-AM compared to cells in NaCl medium (Figure 4.1C, D).

4.2.2 PLD antagonists but not other enzyme antagonists inhibit P2X7-induced CD23 shedding from RPMI 8226 cells

To determine the involvement of intracellular signalling pathways in P2X7-induced CD23 shedding, cells were preincubated in the presence of antagonists of various enzymes or their corresponding diluent control, and the ATP-induced CD23 shedding assessed using flow cytometry as above. Antagonist concentrations were based on previously published concentrations (Table 4.1). Most of the enzyme antagonists failed to significantly impair ATP-induced CD23 shedding (Table 4.1). Of note, the PLD1 antagonist CAY10593 (VU0155069), and to a lesser extent, the PLD2 antagonist CAY10594 and the non-selective PLD antagonist halopemide (all at 10 μM) significantly impaired ATP-induced CD23 shedding (Table 4.1; Figure 4.2). In the absence of ATP, the PLD antagonists did not significantly alter cell surface expression of CD23 compared to control treated cells (Figure 4.2).

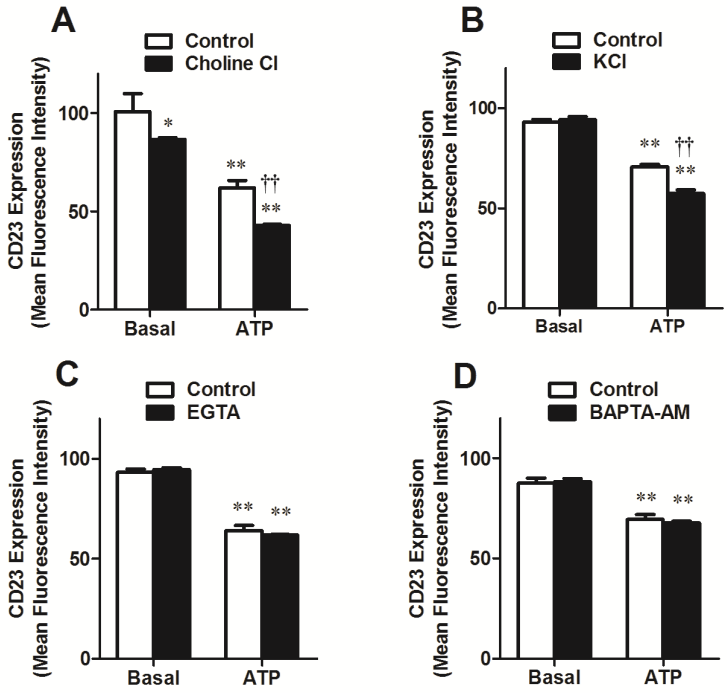

Figure 4.1: ATP-induced CD23 shedding from RPMI 8226 cells is not prevented by changes in intracellular cation concentrations. (A-D) RPMI 8226 cells in NaCl medium (control), in (A) choline Cl medium, (B) KCl medium, or in (C, D) NaCl medium containing (C) 0.1 mM EGTA or (D) 50 μM BAPTA-AM were preincubated at 37°C for (A-C) 5 min or (D) 30 min. (A-D) Cells were then incubated in the absence (basal) or presence of 1 mM ATP at 37°C for 7 min. Incubations were stopped by addition of $MgCl_2$ medium and centrifugation. Cells were labelled with phycoerythrin (PE)-conjugated anti-CD23 or isotype control monoclonal antibody (mAb), and the mean fluorescence intensity (MFI) of cell surface CD23 expression determined by flow cytometry. Results are mean ± standard deviation (SD) ($n = 3$); $^{*}P < 0.05$ and $^{**}P < 0.01$ compared to basal control, and $^{\dagger\dagger}P < 0.01$ compared to ATP control.

Table 4.1: PLD antagonists impair ATP-induced CD23 shedding from RPMI 8226 cells.

Compound (μM)	Target[a]	Percent inhibition of ATP-induced CD23 loss[b]	Reference
GF109203X (10)	PKC α, β	2 (3)	(Shemon et al. 2007)
Rottlerin (20)	PKC δ, θ	13 (6)	(Shemon et al. 2007)
SB202190 (20)	p38 MAPK	7 (7)	(Noguchi et al. 2008)
SB203580 (20)	p38 MAPK	10 (6)	(Noguchi et al. 2008)
AG126 (50)	p42 MAPK	0 (0)	(Verhoef et al. 2005)
U0126 (10)	MEK1/2	6 (7)	(Pfeiffer et al. 2004)
SP600125 (20)	JNK	2 (2)	(Noguchi et al. 2008)
Fasudil (10)	Rho-kinase	0 (0)	(Verhoef et al. 2003)
Y-27632 (10)	Rho-kinase	1 (2)	(Verhoef et al. 2003)
LY294002 (10)	PI3K	0 (1)	(Pfeiffer et al. 2004)
SB216763 (3)	GSK-3	3 (3)	(Ortega et al. 2009)
AACOCF3 (40)	iPLA2, cPLA2	0 (0)	(Andrei et al. 2004)
D609 (100)	PLC	0 (0)	(Andrei et al. 2004)
CAY10593 (10)	PLD1	43 (4)**	(Thomas and Salter 2010)
CAY10594 (10)	PLD2	19 (6) **	(Thomas and Salter 2010)
Halopemide (10)	PLD	6 (7)*	(Scott et al. 2009)
Imipramine (10)	aSmase	8 (5)	(Bianco et al. 2009)
Probenecid (2500)	Pannexin-1	3 (3)	(Silverman et al. 2009)
Carbenoxolone (50)	Pannexin-1	0 (0)	(Silverman et al. 2009)
NH_4Cl (10000)	Endosomes	8 (3)	(Mathews et al. 2010)

Abbreviations: aSmase, acid sphingomyelinase; JNK, c-Jun N-terminal kinase; MAPK, mitogen-activated protein kinase; MEK 1/2, mitogen-activated kinase/ERK kinase 1/2; NADPH, nicotinamide adenine dinucleotide phosphate; NH_4Cl, ammonium chloride; PKC, protein kinase C; PLA2, phospholipase A2; PLC, phospholipase C; PLD, phospholipase D.

[b]RPMI 8226 cells in NaCl medium were preincubated at 37°C in the presence of compound (as indicated) or corresponding diluents, for 15 min (or 30 min for LY294002 or NH_4Cl, or 1 h for SB216763 or Imipramine) and then in the absence or presence of 1 mM ATP at 37°C for 7 min. Incubations were stopped by addition of $MgCl_2$ medium and centrifugation. Cells were labelled with PE- or allophycocyanin (APC)-conjugated anti-CD23 or isotype control mAb, and the MFI of cell surface CD23 expression determined by flow cytometry. Results are the mean percent inhibition of ATP-induced CD23 loss ± SD (n = 3). $^{*}P < 0.05$ and $^{**}P < 0.01$ compared to ATP alone.

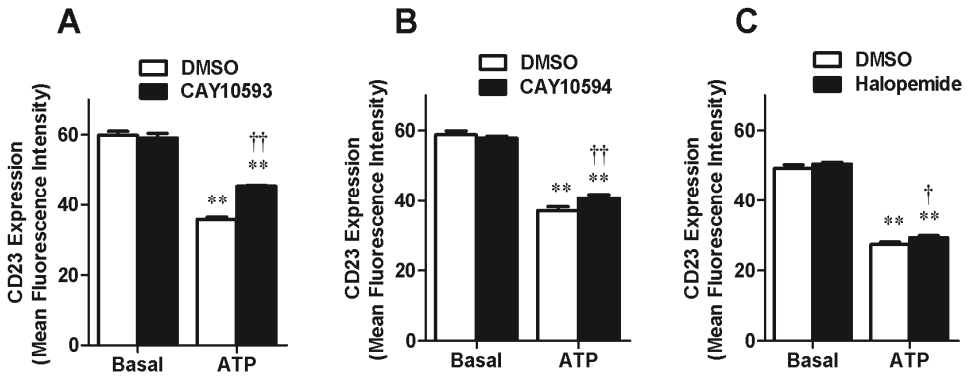

Figure 4.2: PLD antagonists impair ATP-induced CD23 shedding from RPMI 8226 cells. (A-C) RPMI 8226 cells in NaCl medium were preincubated at 37°C for 15 min in the presence of dimethyl sulphoxide (DMSO), or 10 μM (A) CAY10593, (B) CAY10594 or (C) halopemide. Cells were then incubated in the absence (basal) or presence of 1 mM ATP at 37°C for 7 min. Incubations were stopped by addition of $MgCl_2$ medium and centrifugation. Cells were then labelled with PE-conjugated anti-CD23 or isotype control mAb, and the MFI of cell surface CD23 expression determined by flow cytometry. Results are mean ± SD (n = 3); $^{**}P < 0.01$ compared to corresponding DMSO control, and $^{\dagger}P < 0.05$ and $^{\dagger\dagger}P < 0.01$ compared to ATP with DMSO.

4.2.3 PLD antagonists impair ATP-induced ethidium$^+$ uptake into RPMI 8226 cells

The above data (Table 4.1; Figure 4.2) indicates that the PLD antagonists can inhibit P2X7-induced CD23 shedding. Therefore, the mode of action by which these compounds impaired P2X7-induced CD23 shedding was investigated. Since previous studies have highlighted that some enzyme antagonists directly block P2X7 (Shemon et al. 2004, Shemon et al. 2008), the current study first investigated whether PLD antagonists impaired ATP-induced CD23 shedding by blocking P2X7 activation. Thus, RPMI 8226 cells were preincubated in the presence of DMSO, CAY10593, CAY10594

or halopemide (each at 10 μM), and the ATP-induced ethidium$^+$ uptake was measured by flow cytometry. The PLD antagonists significantly inhibited ATP-induced ethidium$^+$ uptake by 56 ± 4%, 20 ± 6% and 15 ± 5%, respectively compared to ATP-induced ethidium$^+$ uptake in cells preincubated with DMSO (Figure 4.3). In the absence of ATP, these antagonists did not significantly alter basal ethidium$^+$ uptake (Figure 4.3).

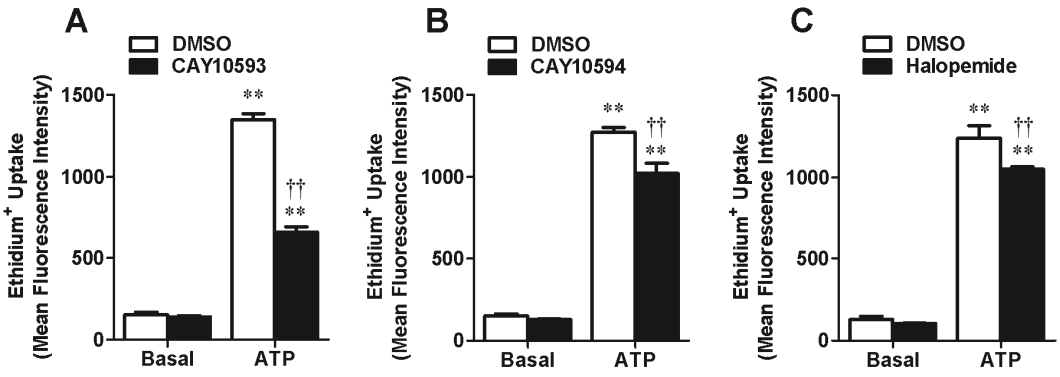

Figure 4.3: PLD antagonists impair ATP-induced ethidium$^+$ uptake into RPMI 8226 cells. RPMI 8226 cells in NaCl medium were preincubated at 37°C for 15 min in the presence of DMSO, or 10 μM CAY10593, CAY10594 or halopemide. Cells were then incubated with 25 μM ethidium$^+$ in the absence (basal) or presence of 1 mM ATP at 37°C for 5 min. Incubations were stopped by addition of $MgCl_2$ medium and centrifugation, and the MFI of ethidium$^+$ uptake determined by flow cytometry. Results are mean ± SD (n = 3); $^{**}P < 0.01$ compared to DMSO control, and $^{††}P < 0.01$ compared to ATP with DMSO.

4.2.4 PLD antagonists impair ATP-induced ethidium$^+$ uptake into RPMI 8226 cells in a concentration-dependent manner

The above data (Figure 4.3) suggests that the inhibitory action of the PLD antagonists on P2X7-induced CD23 shedding is due to impaired P2X7 activation. Therefore, to further characterise the effect of the above three PLD antagonists on P2X7 activation, cells were preincubated in the presence of increasing concentrations of each antagonist and the ATP-induced ethidium$^+$ uptake measured, using 120 μM ATP which is approximate to the half maximal effective concentration (EC_{50}) for ATP in this process (see Chapter 3). CAY10593 inhibited ATP-induced ethidium$^+$ uptake in a concentration-dependent manner, with maximal inhibition occurring near 10 μM and a half maximal inhibitory concentration (IC_{50}) of 2.0 ± 0.5 μM (Figure 4.4). At the highest concentration used (10 μM), CAY10594 and halopemide inhibited ATP-induced ethidium$^+$ uptake by less than 29% on average and the IC_{50} values for these antagonists could not be reliably determined due to this low amount of inhibition (Figure 4.4). Thus, the mode of action by which CAY10593 impairs P2X7 was studied further.

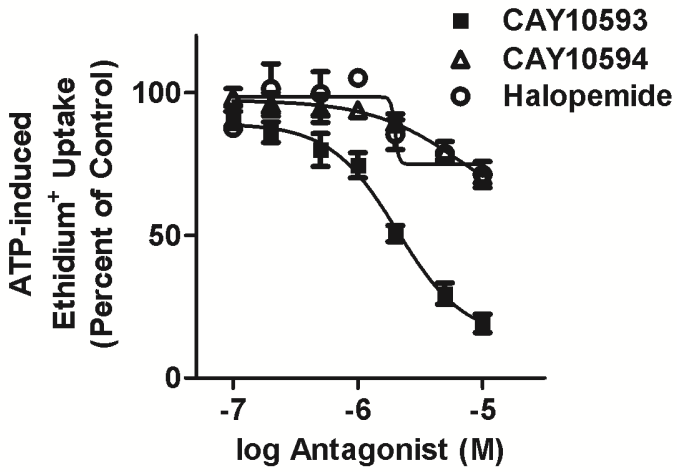

Figure 4.4: PLD antagonists impair ATP-induced ethidium$^+$ uptake into RPMI 8226 cells in a concentration-dependent manner. RPMI 8226 cells in NaCl medium were preincubated at 37°C for 15 min in the presence of DMSO or varying concentrations of antagonist (as indicated). Cells were then incubated with 25 μM ethidium$^+$ in the absence or presence of 120 μM ATP at 37°C for 5 min. Incubations were stopped by addition of $MgCl_2$ medium and centrifugation, and the MFI of ethidium$^+$ uptake determined by flow cytometry. Results are the mean percent of ATP-induced ethidium$^+$ uptake in the absence of antagonist ± SD (n = 3).

4.2.5 CAY10593 impairs ATP-induced ethidium$^+$ uptake into RPMI 8226 cells in a non-competitive-like manner

To determine whether CAY10593 inhibits P2X7-induced pore formation in a competitive or non-competitive manner, RPMI 8226 cells were preincubated in the presence of DMSO, or 2 or 10 μM CAY10593, and then the ethidium$^+$ uptake was measured in the presence of increasing concentrations of ATP. In the absence of CAY10593, ATP induced ethidium$^+$ uptake in a concentration-dependent manner with maximal uptake occurring at 0.5 mM ATP and with an EC_{50} of 116 ± 31 μM (Figure 4.5). In the presence of 2 μM CAY10593, the mean maximum ATP response was

reduced by 17% and with a slight increase in the EC_{50} to 154 ± 26 μM (Figure 4.5). In the presence of 10 μM CAY10593, the mean maximum ATP response was reduced by 60% and with a larger increase in the EC_{50} to 256 ± 22 μM (Figure 4.5).

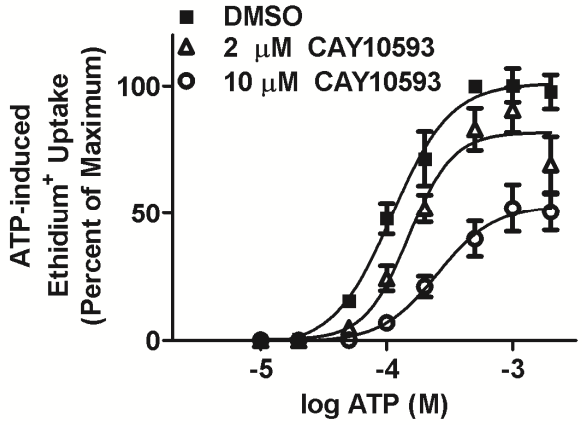

Figure 4.5: CAY10593 impairs ATP-induced ethidium$^+$ uptake into RPMI 8226 cells in a non-competitive-like manner. RPMI 8226 cells in NaCl medium were preincubated at 37°C for 15 min in the presence of DMSO, or 2 μM or 10 μM CAY10593. Cells were then incubated with 25 μM ethidium$^+$ in the absence or presence of varying concentrations of ATP at 37°C for 5 min. Incubations were stopped by addition of $MgCl_2$ medium and centrifugation, and the MFI of ethidium$^+$ uptake determined by flow cytometry. Results are the mean percent of maximum ATP (0.5 mM)-induced ethidium$^+$ uptake ± SD (n = 3).

4.2.6 PLD1 is not required for ATP-induced ethidium$^+$ uptake into RPMI 8226 cells

Collectively, the above results show that the PLD1 specific antagonist CAY10593 can impair P2X7-induced pore formation. Therefore, to determine whether this effect is due to inhibition of PLD1 or direct inhibition of P2X7 itself, a series of experiments were performed. First, the presence of PLD1 and PLD2 in RPMI 8226 cells was examined by RT-PCR. The human skin epithelial carcinoma cell line, A431, which expresses both PLD isoforms (Min et al. 2001), was used as a positive control. RT-PCR revealed the presence of PLD1 (666 bp) in A431 cells but not in RPMI 8226 cells, despite the presence of PLD2 (561 bp) in both cell lines (Fig. 4.6A). Next, choline Cl medium has previously been shown to prevent P2X7-induced PLD stimulation (el-Moatassim and Dubyak 1993, Fernando et al. 1999). Therefore, RPMI 8226 cells were suspended in either choline Cl or NaCl medium and the ATP-induced ethidium$^+$ uptake measured. ATP-induced ethidium$^+$ uptake was potentiated in cells incubated in choline Cl compared to NaCl medium (Figure 4.6B). Finally, in the presence of a primary alcohol, PLD catalyses a transphosphatidylation reaction to form a phosphatidyl alcohol product, which does not serve as a substrate for PLD-mediated signal transduction (Morris et al. 1997). Therefore, RPMI 8226 cells were preincubated in the presence of the primary alcohol, 0.27% (v/v) 1-butanol, or the secondary alcohol, 0.27% (v/v) 2-butanol as a negative control, and the ATP-induced ethidium$^+$ uptake measured. ATP-induced ethidium$^+$ uptake into cells treated with 1-butanol was also increased compared to cells treated with 2-butanol (Figure 4.6C). In the absence of ATP, ethidium$^+$ uptake into cells in choline Cl or NaCl media in the presence of either alcohol was similar (Figure 4.6B, C).

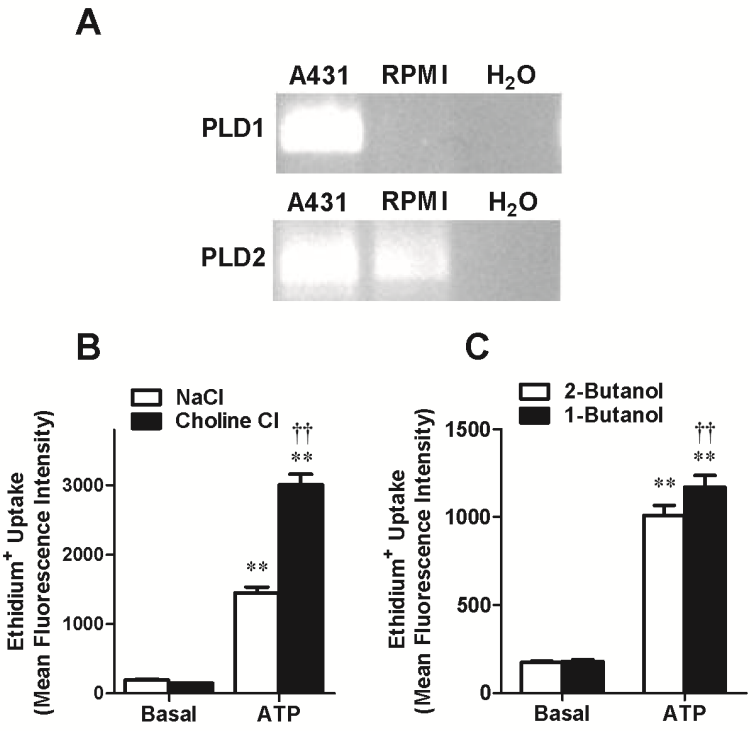

Figure 4.6: PLD1 is not required for ATP-induced ethidium$^+$ uptake into RPMI 8226 cells. (A) RNA was isolated from A431 (positive control) and RPMI 8226 cells, and then analysed by RT-PCR using primers for PLD1 and PLD2. RNA substituted with H_2O was used as a negative control. PCR products were visualised by agarose gel electrophoresis and ethidium bromide staining. A representative result from three experiments is shown. (B, C) RPMI 8226 cells were preincubated at 37°C for 5 min in (B) choline Cl or NaCl medium, or (C) NaCl medium in the presence of 0.27% (v/v) 2-butanol (negative control) or 1-butanol. (B, C) Cells were then incubated with 25 μM ethidium$^+$ in the absence (basal) or presence of 1 mM ATP at 37°C for 5 min. Incubations were stopped by addition of $MgCl_2$ medium and centrifugation, and the MFI of ethidium$^+$ uptake determined by flow cytometry. Results are the mean ± SD (n = 3); $^{*}P < 0.05$ and $^{**}P < 0.01$ compared to corresponding basal control, and $^{\dagger\dagger}P < 0.01$ compared to (B) ATP in NaCl medium or (C) ATP with 2-butanol.

4.2.7 CAY10593 impairs ATP-induced inward currents and pore formation in human P2X7-transfected human embryonic kidney 293 cells

The above results (Figure 4.6) indicate that PLD signalling is not required for P2X7-induced pore formation and that CAY10593 directly impairs P2X7. Therefore, the effect of CAY10593 on P2X7 channel activity in human P2X7-transfected human embryonic kidney (HEK) 293 cells was assessed by electrophysiology. In the absence of 10 μM CAY10593, ATP induced an inward current typical of P2X7 (Figure 4.7A). Removal of extracellular ATP, and subsequent 3-5 min incubation with 10 μM CAY10593 followed by ATP, reduced the ATP-induced inward current to 29.5 ± 2.6 % of control (Figure 4.7A). To confirm that CAY10593 impairs P2X7 pore formation in these cells, P2X7-transfected HEK 293 cells were preincubated with CAY10593 for 15 min at 37°C and ATP-induced ethidium$^+$ uptake was measured. CAY10593 impaired ATP-induced ethidium$^+$ uptake into P2X7-transfected HEK 293 cells by 72% (Figure 4.7B).

4.2.8 CAY10593 impairs ATP-induced ethidium$^+$ uptake into primary human peripheral blood mononuclear cells

To determine if CAY10593 inhibits P2X7-induced pore formation in primary cells, peripheral blood mononuclear cells (PBMCs) from a human donor were preincubated in the presence of DMSO or 10 μM CAY10593 and ethidium$^+$ uptake was measured in the absence or presence of ATP. CAY10593 inhibited ATP-induced ethidium$^+$ uptake into B cells, T cells and monocytes by 66 ± 5%, 76 ± 3% and 80 ± 4%, respectively (Figure

4.8). In the absence of ATP, CAY10593 did not significantly alter ethidium$^+$ uptake compared to DMSO treated cells (Figure 4.8). Similar amounts of inhibition (77 ± 15%, 91 ± 6% and 76 ± 12%) were observed in B cells, T cells and monocytes, respectively from a second donor (figure not shown).

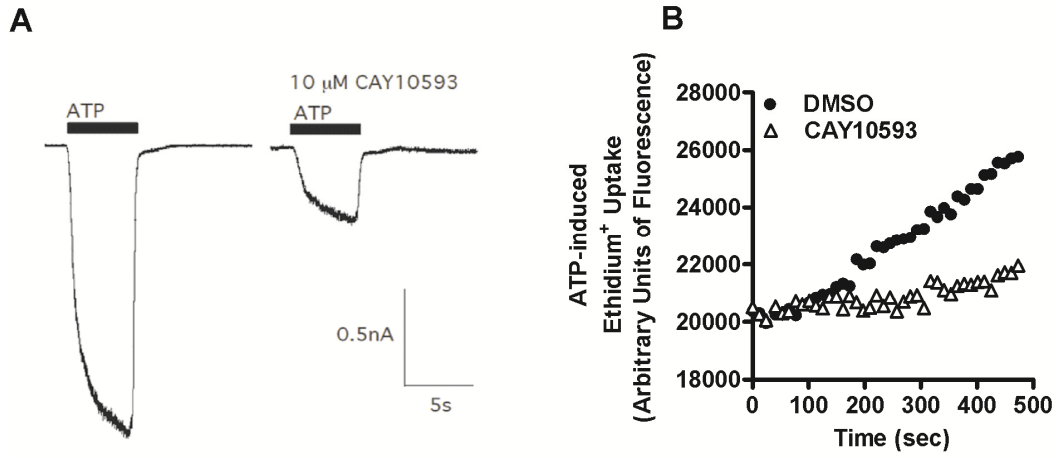

Figure 4.7: CAY10593 impairs ATP-induced inward currents and pore formation in human P2X7-transfected HEK 293 cells. (A) Inward currents were elicited using 1 mM ATP in low divalent NaCl solution. ATP was added for 5 seconds (black bar) before and after treatment with 10 μM CAY10593 (3-5 minutes). ATP was added in the continued presence of CAY10593 (single representative trace of 4 to 7 cells is shown). (B) P2X7-transfected HEK 293 cells in low divalent NaCl solution containing 25 μM ethidium$^+$ were preincubated in the presence of DMSO or CAY10593 for 15 min at 37°C. ATP (1 mM) was injected after 40 s. Fluorescence was measured every 10 s using a plate reader (representative result from three experiments shown).

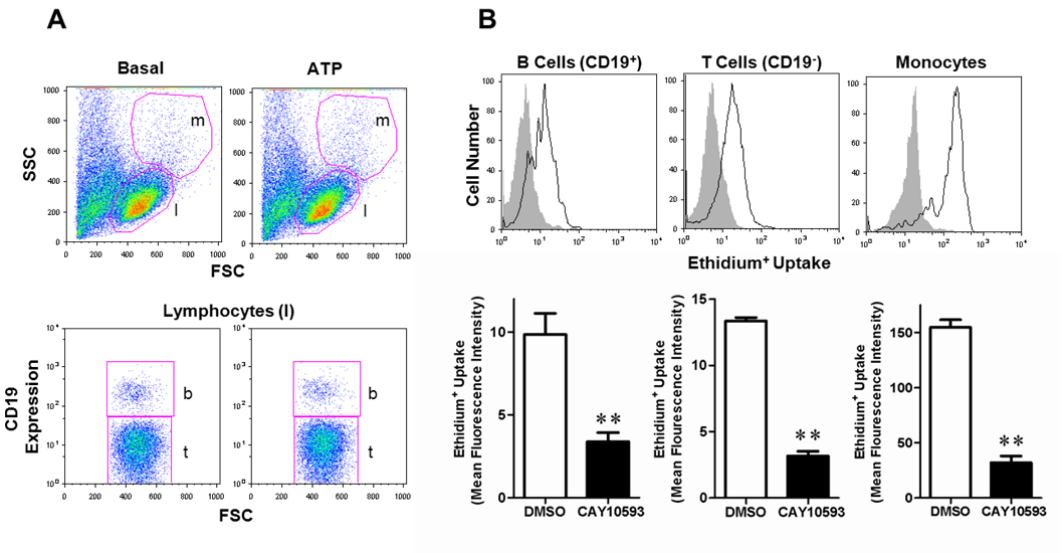

Figure 4.8: CAY10593 impairs ATP-induced ethidium$^+$ uptake into primary human PBMCs. (A, B) PBMCs in NaCl medium were preincubated for 15 min in the presence of DMSO or 10 µM CAY10593. Cells were then incubated with 25 µM ethidium$^+$ in the absence or presence of 1 mM ATP at 37°C for 5 min. Incubations were stopped by addition of $MgCl_2$ medium and centrifugation, and washed once with NaCl medium. Cells were then labelled with APC-conjugated anti-CD19 mAb. The MFI of ethidium$^+$ uptake into B cells, T cells and monocytes was determined by flow cytometry. (A) (top panel) Basal or ATP-treated lymphocytes (l) or monocytes (m) were gated by forward scatter (FSC) and side scatter (SSC). CD19$^+$ B cells (b) or CD19$^-$ T cells (t) were further gated as shown (bottom panel). (B) Representative histograms show basal (grey fill) and ATP-induced (solid line) ethidium$^+$ uptake (top panel). Results are the mean ATP-induced ethidium$^+$ uptake ± SD (n = 3); $^{**}P < 0.01$ compared to corresponding DMSO.

4.2.9 CAY10593 impairs human but not murine P2X7-induced pore formation

The murine erythroleukemia (MEL) cell line expresses P2X7 (Constantinescu et al. 2010, Wang and Sluyter 2013). Therefore, to test whether CAY10593 inhibits murine P2X7, MEL cells were preincubated with 10 μM CAY10593 and ATP-induced ethidium$^+$ uptake was measured by flow cytometry (Figure 4.9A). The RPMI 8226 cell line was used as a positive control. CAY10593 impaired ATP-induced ethidium$^+$ uptake into MEL cells by only 2 ± 3% (Figure 4.9B). Furthermore, in the absence of ATP, CAY10593 significantly impaired ethidium$^+$ uptake in DMSO treated MEL cells. Therefore, CAY10593 did not impair the net ATP-induced ethidium$^+$ uptake. As expected, CAY10593 significantly impaired ATP-induced ethidium$^+$ uptake by 62 ± 2% in RPMI 8226 cells (Figure 4.9B). In contrast, in the absence of ATP, CAY10593 did not significantly alter ethidium$^+$ uptake in DMSO treated RPMI 8226 cells (Figure 4.9B).

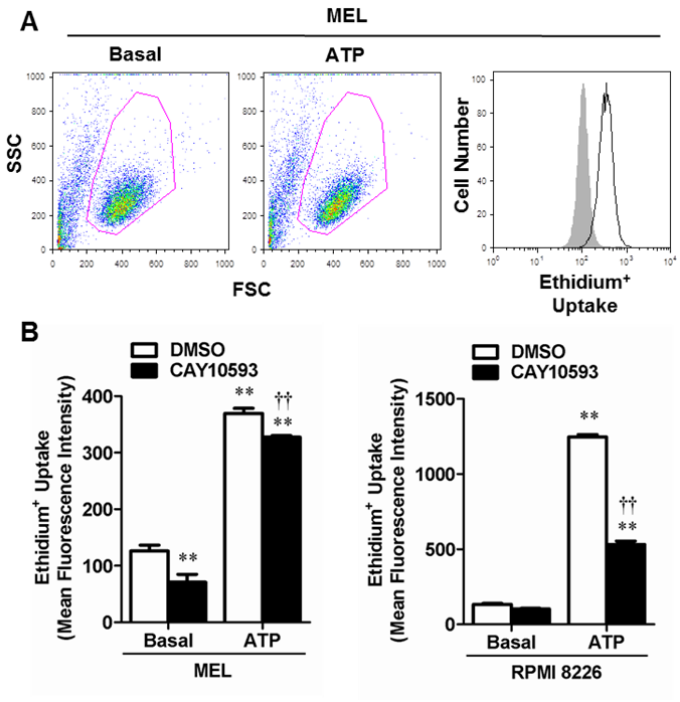

Figure 4.9: CAY10593 impairs human but not murine P2X7-induced pore formation. (A, B) MEL cells or (B) RPMI 8226 cells in NaCl medium were preincubated for 15 min in the presence of DMSO or 10 µM CAY10593. Cells were then incubated with 25 µM ethidium$^+$ in the absence or presence of 1 mM ATP at 37°C for 5 min. Incubations were stopped by addition of $MgCl_2$ medium and centrifugation and the MFI of ethidium$^+$ uptake measured by flow cytometry. (A) Basal or ATP-treated MEL cells were gated by FSC and SSC. Representative histograms show basal (grey fill) and ATP-induced (solid line) ethidium$^+$ uptake. (B) Results are mean ± SD (n = 3); $^{**}P < 0.01$ compared to DMSO control, and $^{††}P < 0.01$ compared to ATP with DMSO.

4.3 Discussion

This chapter demonstrates that the PLD1 antagonist, CAY10593 directly impairs human P2X7 activation. Preliminary investigations demonstrated that CAY10593 impaired ATP-induced CD23 shedding. However, CAY10593 also impaired ATP-induced ethidium$^+$ uptake into RPMI 8226 cells in a concentration-dependent manner, and with

an IC_{50} similar to that of the P2X7 antagonist, A-438079 as observed previously by Nelson et al. (2006) and in Chapter 3. Unlike A-438079, however, which blocks P2X7 in a competitive manner (Nelson et al. 2006), CAY10593 impaired P2X7 in a non-competitive-like manner. CAY10593 also impaired ATP-induced ethidium$^+$ uptake into P2X7-transfected HEK 293 cells, and primary human B cells, T cells and monocytes.

Data from this chapter also shows that CAY10593 impairs P2X7 activation independently of PLD1 stimulation. First, CAY10593 was far more effective at inhibiting P2X7-induced pore formation than halopemide, which both impair cellular PLD1 with similar efficacies (Scott et al. 2009). Second, the IC_{50} value of CAY10593 for inhibition of P2X7-induced pore formation was two logs greater than that observed for the inhibition of phorbol 12-myristate 13-acetate-induced PLD1 stimulation in the non-small-cell lung cancer cell line, Calu-1 (Scott et al. 2009) (2 μM vs. 11 nM, respectively). Third, PLD1 mRNA was absent in RPMI 8226 cells, indicating that these cells do not contain this PLD isoform. Fourth, the primary alcohol, 1-butanol, which prevents PLD-mediated signalling (Morris et al. 1997), did not impair P2X7-induced pore formation. In fact, 1-butanol potentiated this process, similar to a previous study in which incubation with 1-butanol increased P2X7-induced pore formation and cytolysis in murine macrophages compared to controls (Le Stunff and Raymond 2007). The authors of this previous study concluded that phosphatidic acid production, resulting from PLD stimulation, delays P2X7-induced pore formation and cytolysis. Thus, it is possible that PLD-induced phosphatidic acid production may also delay P2X7-induced pore formation in human cells. Fifth and similar to the effect of 1-butanol, P2X7-induced pore formation and CD23 shedding were not impaired in choline Cl

medium, which prevents P2X7-induced PLD stimulation in murine macrophages (el-Moatassim and Dubyak 1993) and human chronic lymphocytic leukemic lymphocytes (Fernando et al. 1999). Sixth, CAY10593 also impaired P2X7 channel activity, a function of P2X7 not directly linked to the activation of intracellular signalling molecules (Pelegrin 2011). Finally, it is unlikely that CAY10593 impairs P2X7 activity via a PLD2-dependent mechanism despite the presence of PLD2 mRNA in RPMI 8226 cells; the PLD2 inhibitor, CAY10594, was far less effective at impairing ATP-induced ethidium^{+} uptake and CD23 shedding compared to CAY10593. Combined this data highlights the importance of ensuring that antagonists used in intracellular signalling studies downstream of P2X7 activation do not directly affect P2X7 itself. In this regard, CAY10593 has been used at 50 μM to support a role for PLD in the generation of P2X7-induced microvesicles capable of activating macrophages (Thomas and Salter 2010). However, data from this chapter suggests that CAY10593 may have also acted on P2X7 itself in this previous study. Conversely, this data in combination with that of Scott and colleagues (Scott et al. 2009) indicates that the use of CAY10593 at nM concentrations is of potential value in determining if PLD1 is involved in signalling pathways downstream of P2X7 activation.

As noted above CAY10593 impaired P2X7-induced pore formation more efficaciously than CAY10594 or halopemide. Moreover, CAY10593 blocked P2X7-induced CD23 shedding to a greater extent than CAY10594 or halopemide. CAY10593 was originally synthesised via the modification of the 1-(piperidin-4-yl)-1*H*-benzo[*d*]imidazol-2(3*H*)-one analogue halopemide, but unlike halopemide, CAY10593 contains a chiral (*S*)-methyl group which prompts PLD1 preferring pharmacology (Scott et al. 2009), CAY10594, which has a 1-phenyl-1,3,8-triazaspiro[4,5]decan-4-one scaffold instead of

a 1-(piperidin-4-yl)-1*H*-benzo[*d*]imidazol-2(3*H*)-one scaffold, also lacks a chiral (*S*)-methyl group (Scott et al. 2009). Therefore, this structural group may be of importance in the interaction of CAY10593 with P2X7. The scaffold or structural groups of CAY10593 may provide useful leads in the development of new P2X7 antagonists. In this regard, the study of analogues of the P2X7 antagonist KN-62, which is also an inhibitor of Ca^{2+}/calmodulin-dependent protein kinase II, has provided valuable insight into moieties which interact with P2X7 and the design of new P2X7 antagonists (Romagnoli et al. 2005).

CAY10593 failed to impair ATP-induced ethidium^{+} uptake into MEL cells, indicating that this antagonist does not act on murine P2X7. In this regard, P2X7 antagonists also show species selectivity, for example KN-62 impairs human and murine P2X7 but not rat P2X7 (Humphreys et al. 1998). However, CAY10593 reduced basal ethidium^{+} uptake into MEL cells but not into RPMI 8226 cells, suggesting that this compound affects the membrane permeability of MEL cells to ethidium^{+}. In human umbilical vein endothelial cells, siRNA silencing of PLD2 decreases basal permeability of these cells to horseradish peroxidase flux (Zeiller et al. 2009). Further, this same study also found that PLD2 regulates permeability through cytoskeleton reorganisation (Zeiller et al. 2009). Therefore it is possible that basal ethidium^{+} permeability in MEL cells may be dependent on PLD1 activity. It would be valuable to determine if the PLD2 antagonist, CAY10594 or the broad spectrum PLD antagonist, halopemide, also modify basal ethidium^{+} uptake into these cells.

It is unknown if P2X7-induced CD23 shedding results from changes in intracellular cation concentrations, stimulation of signalling pathways downstream of P2X7 activation or by a direct physical interaction of P2X7 itself. The current chapter reports data exploring the first two of these three potential mechanisms. In this study, we show that P2X7-induced CD23 shedding does not require changes in intracellular Na^+, K^+ or Ca^{2+} concentrations. Changes in intracellular cation concentrations are crucial for some P2X7-mediated downstream processes. For example, P2X7-induced interleukin (IL)-1β processing and release is dependent on K^+ efflux from human monocytes (Andrei et al. 2004, Sluyter et al. 2004), murine and human macrophages (Perregaux and Gabel 1994, Ferrari et al. 1997a, Kahlenberg and Dubyak 2004) and murine microglia (Sanz and Di Virgilio 2000). Moreover, P2X7-induced secretion of IL-1β is dependent on the influx of extracellular Ca^{2+} and a sustained increase in intracellular Ca^{2+} in human monocytes (Gudipaty et al. 2003, Andrei et al. 2004), murine macrophages and P2X7-transfected HEK 293 cells (Gudipaty et al. 2003). Finally, P2X7-induced rapid phosphatidylserine exposure on murine thymocytes is dependent on Na^+ influx (Courageot et al. 2004). In contrast to these studies, we found that neither K^+ efflux, Na^+ influx, Ca^{2+} influx nor an increase in intracellular Ca^{2+} is essential for P2X7-induced CD23 shedding from RPMI 8226 cells. Of note, choline Cl and KCl medium potentiated ATP-induced CD23 shedding compared to NaCl medium, which is likely due to the omission of extracellular Na^+, a cation known to inhibit P2X7 activity (Wiley et al. 1992, Michel et al. 1999), as well as the possible inhibition of phosphatidic acid production by choline as discussed above.

The data in this chapter also shows that several signalling pathways downstream of P2X7 activation, including PKC, MAPK, MEK1/2, JNK, Rho kinase, PI3K, GSK-3,

PLA, PLC and aSmase (Table 4.1) are unlikely to be involved in P2X7-induced CD23 shedding. Furthermore, pannexin-1, as well as cell membrane-related structures including endosomes are also unlikely to be involved (Table 4.1). However, it should be noted that the compounds used to target these enzymes and molecules were only used at a single concentration, and thus the involvement of these or other signalling pathways in P2X7-induced CD23 shedding cannot be excluded.

In conclusion, this chapter demonstrates the PLD1 antagonist, CAY10593, impairs human P2X7 independently of PLD1 stimulation. This chapter highlights the importance of ensuring that antagonists used in intracellular signalling studies downstream of P2X7 activation do not directly affect P2X7 itself. Moreover, this study suggests that CAY10593 may serve in studies of P2X7-induced PLD1 stimulation when used at nM concentrations, as well as a future lead compound in the development of P2X7 antagonists.

CHAPTER 5

The effect of reactive oxygen species on P2X7-induced CD23 shedding from RPMI 8226 cells

5.1 Introduction

It is well established that P2X7 activation induces reactive oxygen species (ROS) generation via the activation of nicotinamide adenine dinucleotide phosphate (NADPH) oxidase in several cell types (Noguchi et al. 2008, Seil et al. 2008, Lenertz et al. 2009, Bartlett et al. 2013, Wang and Sluyter 2013), however little is known about the role of P2X7 and ROS in B cells. Furthermore, ROS generation is involved in nucleotide-induced shedding of cell membrane molecules such as transforming growth factor-α (Boots et al. 2009, Myers et al. 2009), but whether ROS is involved in P2X7-induced CD23 shedding also remains unknown. Several molecules that are involved in P2X7-induced downstream events were not implicated in P2X7-induced CD23 shedding from RPMI 8226 cells (Chapter 4). During the course of these investigations, Foster and colleagues published a study showing mitochondrial superoxide, generated via the pharmacological modulation of mitochondrial enzymes, enhanced P2X7-mediated loss of CD62L from human T cells (Foster et al. 2013). Furthermore, this study (Foster et al. 2013) and a previous study (Wang et al. 2009) show that hydrogen peroxide (H_2O_2), a form of ROS, downregulates cell surface CD62L. The aim of this chapter was to investigate the effect of the ROS H_2O_2, and rotenone (which uncouples mitochondrial complex I and leads to the enhancement of mitochondrial superoxide) (Foster et al. 2013) and diphenyleneiodonium (DPI) (an inhibitor of flavone containing enzymes) (Foster et al. 2013) on P2X7-induced CD23 shedding from RPMI 8226 cells.

5.2 Results

5.2.1 H_2O_2 but not DPI or rotenone enhance ATP-induced CD23 loss from RPMI 8226 cells

To determine whether H_2O_2, DPI or rotenone affect P2X7-induced CD23 shedding, RPMI 8226 cells were preincubated in the absence or presence of 100 μM H_2O_2, or in the presence of dimethyl sulphoxide (DMSO), 100 μM DPI or 5 μM rotenone and then with 1 mM adenosine 5'-triphosphate (ATP), and cell surface CD23 expression measured by flow cytometry as described in Chapter 3. As observed in Chapters 3 and 4, ATP induced a loss of CD23 from the cell surface of RPMI 8226 cells (Figure 5.1A-C). H_2O_2 significantly enhanced ATP-induced CD23 loss approximately 2-fold compared to ATP-induced CD23 shedding alone (Figure 5.1A). In contrast, DPI and rotenone did not affect ATP-induced CD23 loss (Figure 5.1B, C). In the absence of ATP, H_2O_2 and rotenone but not DPI caused a small but significant amount of basal CD23 loss (Figure 5.1A-C).

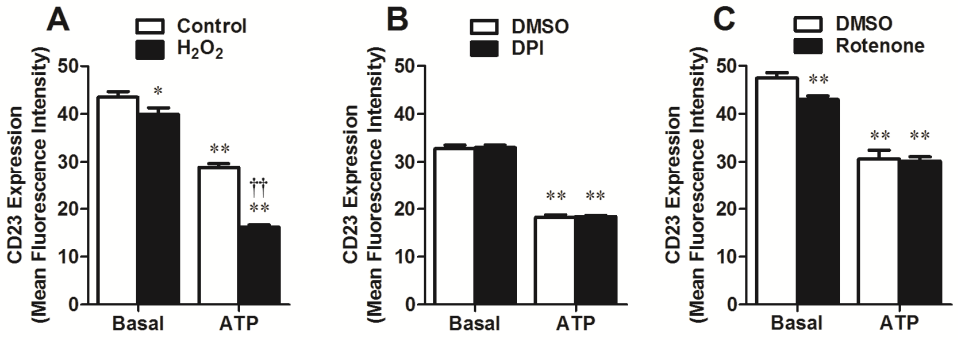

Figure 5.1: H_2O_2 but not DPI or rotenone enhance ATP-induced CD23 loss from RPMI 8226 cells. RPMI 8226 cells in NaCl medium were preincubated at 37°C in the absence or presence of (A) 100 μM H_2O_2 for 15 min, or in the presence of (B,C) DMSO, (B) 100 μM DPI for 1 h, or (C) 5 μM rotenone for 30 min. Cells were then incubated in the absence (basal) or presence of 1 mM ATP at 37°C for 7 min. Incubations were stopped by addition of $MgCl_2$ medium and centrifugation. Cells were labelled with phycoerythrin (PE)-conjugated anti-CD23 or isotype control monoclonal antibody (mAb), and the mean fluorescence intensity (MFI) of cell surface CD23 expression determined by flow cytometry. Results are mean ± standard deviation (SD) (n = 3); $^{*}P < 0.05$ and $^{**}P < 0.01$ compared to corresponding basal or DMSO control, and $^{††}P < 0.01$ compared to ATP alone.

5.2.2 ATP, DPI and rotenone induce ROS formation in RPMI 8226 cells

To determine if DPI and rotenone could induce ROS formation in RPMI 8226 cells, cells were loaded with the broad spectrum ROS indicator 5 μM dichlorodihydrofluorescein diacetate (H_2DCFDA) or the superoxide indicator 2.5 μM mitoSOX Red. Cells were then incubated in the absence or presence of 100 μM DPI or 5 μM rotenone and ROS formation was detected by measuring dichlorodihydrofluorescein (DCF) or mitoSOX Red fluorescence using flow cytometry.

Since ATP can induce ROS formation in several cell types (Seil et al. 2008, Lenertz et al. 2009, Bartlett et al. 2013, Wang and Sluyter 2013), 1 mM ATP was used as a comparison. ATP induced approximately a 7-fold increase in DCF fluorescence compared to cells incubated without ATP (Figure 5.2A). DPI and rotenone induced approximately a 2-fold and 6-fold increase in DCF fluorescence respectively compared to cells incubated with DMSO (Figure 5.2B, C). In contrast to DCF fluorescence, ATP did not induce mitoSOX Red fluorescence compared to cells incubated without ATP (Figure 5.2D). However, DPI induced approximately a 2-fold increase compared to DMSO, while rotenone induced a small, but significant increase in mitoSOX Red fluorescence compared to DMSO (Figure 5.2E, F). Collectively, these results show that DPI and rotenone can induce ROS formation in RPMI 8226 cells (Figure 5.2), but only H_2O_2 can increase ATP-induced CD23 loss (Figure 5.1). Therefore the effects of H_2O_2 on CD23 loss were assessed further.

5.2.3 H_2O_2 enhances ATP-induced CD23 loss from RPMI 8226 cells in a time-dependent manner

H_2O_2 induces the rapid shedding (<15 min) of CD62L from human T cells in a time-dependent manner (Foster et al. 2013). Therefore to determine whether H_2O_2 enhances ATP-induced CD23 loss in a time-dependent manner, RPMI 8226 cells were preincubated with 100 μM H_2O_2 and then with ATP for up to 7 min and cell surface CD23 measured by flow cytometry. H_2O_2 enhanced ATP-induced CD23 loss compared to cells incubated with ATP alone at each time point measured from 1-7 min (Figure 5.3). In contrast, preincubation with H_2O_2 had no significant effect on CD23 expression at 0 min (Figure 5.3).

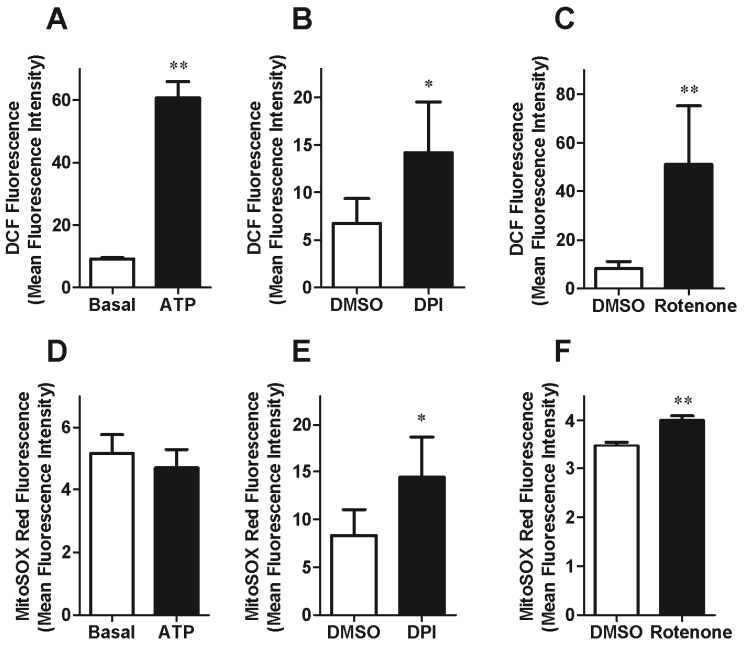

Figure 5.2: ATP, DPI and rotenone induce ROS formation in RPMI 8226 cells. (A-F) RPMI 8226 cells in NaCl medium were loaded with (A-C) 5 µM H_2DCFDA for 5 min or (D-F) 2.5 µM mitoSOX Red for 30 min at 37°C and washed once with NaCl medium. (A-F) Cells were then incubated at 37°C in the absence (basal) or presence of (A, D) 1 mM ATP for 20 min, or in the presence of (B, C, E, F) DMSO, (B, E) 100 µM DPI for 1 h or (C, F) 5 µM rotenone for 30 min. Incubations were stopped by addition of $MgCl_2$ medium and centrifugation. The MFI of DCF or mitoSOX Red fluorescence was measured by flow cytometry. Results are mean ± SD; (A, F, n = 3; B-E, n = 6); $^{*}P < 0.05$ and $^{**}P < 0.01$ compared to corresponding basal or DMSO control.

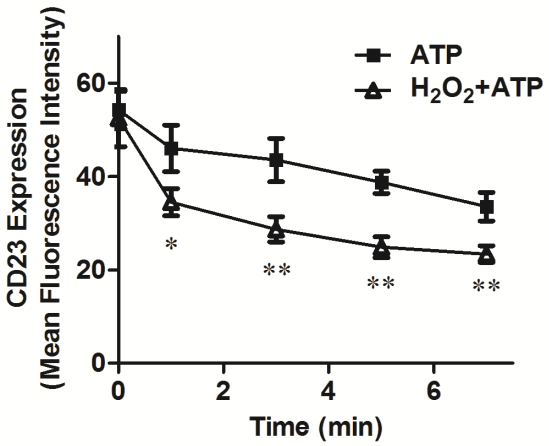

Figure 5.3: H_2O_2 enhances ATP-induced CD23 loss from RPMI 8226 cells in a time-dependent manner. RPMI 8226 cells were preincubated at 37°C for 15 min in the absence or presence of 100 μM H_2O_2 and then with 1 mM ATP at 37°C for up to 7 min (as indicated). Incubations were stopped by addition of $MgCl_2$ medium and centrifugation. Cells were labelled with PE-conjugated anti-CD23 or isotype control mAb, and the MFI of cell surface CD23 expression determined by flow cytometry. Results are mean ± SD (n = 3); $^{*}P < 0.05$ and $^{**}P < 0.01$ compared to corresponding ATP alone.

5.2.4 P2X7 activation is not involved in H_2O_2-induced enhancement of ATP-induced CD23 loss from RPMI 8226 cells

To determine if P2X7 activation is involved in H_2O_2-induced enhancement of ATP-induced CD23 loss, RPMI 8226 cells were preincubated in the absence or presence of 100 nM AZ10606120, or in the absence or presence of 100 nM AZ10606120 with 100 μM H_2O_2. Cells were then incubated in the absence or presence of ATP, and cell surface CD23 measured by flow cytometry. As observed above (Figure 5.1 and 5.3), ATP induced a loss of CD23 compared to basal control, which was enhanced by H_2O_2 (Figure 5.4). Also as expected, the P2X7 antagonist, AZ10606120

impaired ATP-induced CD23 loss by 97 ± 5% compared to ATP-induced CD23 loss in the absence of AZ10606120 (Figure 5.4). However, in the presence of H_2O_2, AZ10606120 impaired ATP-induced CD23 loss by only 69 ± 9% compared to ATP-induced CD23 loss in the absence of AZ10606120 (Figure 5.4). In the absence of ATP, AZ106016120 did not significantly alter cell surface CD23 expression in the absence or presence of H_2O_2 (Figure 5.4). Thus, the incomplete inhibition of ATP-induced CD23 loss in the presence of H_2O_2 by AZ10606120 suggests that P2X7 activation is not involved in the enhanced ATP-induced CD23 loss by H_2O_2.

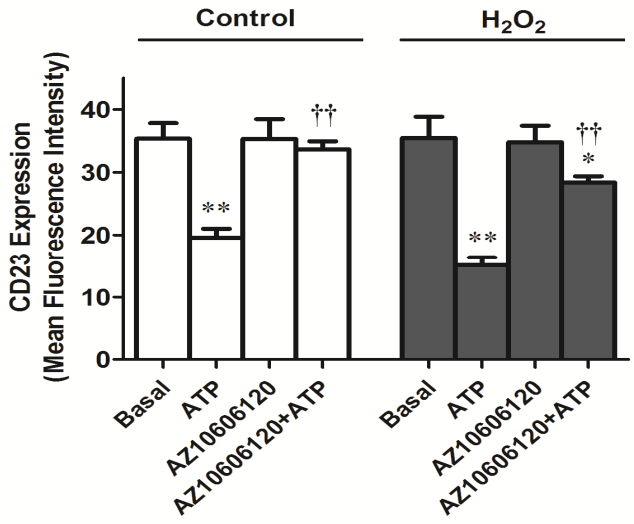

Figure 5.4: P2X7 activation is not involved in H_2O_2-induced enhancement of ATP-induced CD23 loss from RPMI 8226 cells. RPMI 8226 cells were preincubated at 37°C in the absence or presence of 100 nM AZ10606120 for 15 min (control), or in the absence or presence of 100 nM AZ10606120 for 15 min, followed by absence (left) or presence (right) of 100 μM H_2O_2 for 15 min. Cells were then incubated in the absence (basal) or presence of ATP at 37°C for 7 min. Incubations were stopped by addition of $MgCl_2$ medium and centrifugation. Cells were labelled with PE-conjugated anti-CD23 or isotype control mAb, and the MFI of cell surface CD23 expression determined by flow cytometry. Results are mean ± SD (n = 3); $^{*}P < 0.05$ and $^{**}P < 0.01$ compared to corresponding basal control, and $^{\dagger\dagger}P < 0.01$ compared to corresponding ATP in the absence of AZ10606120.

5.2.5 H_2O_2 does not affect ATP-induced ethidium$^+$ uptake nor AZ10606120 inhibition of ATP-induced ethidium$^+$ uptake into RPMI 8226 cells.

To examine if H_2O_2 affects P2X7 activation, RPMI 8226 cells were preincubated in the absence or presence of 100 nM AZ10606120 alone, or with 100 μM H_2O_2 in the absence or presence of 100 nM AZ10606120. Cells were then incubated with ATP, and ethidium$^+$ uptake measured by flow cytometry. As previously observed (Chapters 3 and 4), ATP-induced significant ethidium$^+$ uptake compared to basal control (Figure 5.5). AZ10606120 impaired ATP-induced ethidium$^+$ uptake by 100 ± 0% compared to ATP-induced ethidium$^+$ uptake in the absence of AZ10606120 (Figure 5.5). In the presence of H_2O_2, ATP induced similar amounts of ethidium$^+$ uptake compared to basal control, and this was impaired by AZ10606120 with the same efficacy as the AZ10606120-mediated inhibition of ATP-induced ethidium$^+$ uptake in the absence of H_2O_2 (Figure 5.5). AZ106016120 did not significantly alter basal ethidium$^+$ uptake in the absence or presence of H_2O_2 (Figure 5.5).

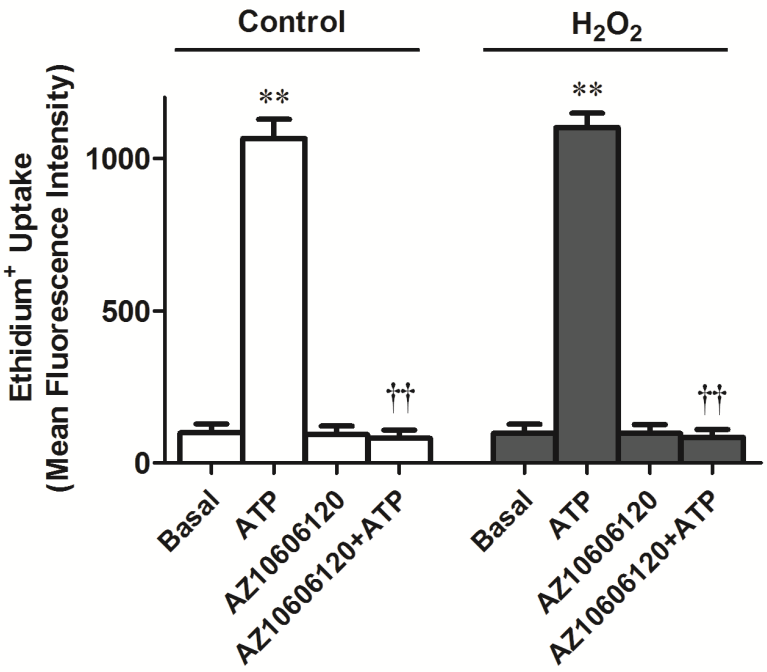

Figure 5.5: H_2O_2 does not affect ATP-induced ethidium$^+$ uptake nor AZ10606120 inhibition of ATP-induced ethidium$^+$ uptake into RPMI 8226 cells. RPMI 8226 cells were preincubated at 37°C in the absence or presence of 100 nM AZ10606120 for 15 min (control), or in the absence or presence of 100 nM AZ10606120 for 15 min followed by the absence (left) or presence (right) of 100 μM H_2O_2 for 15 min. Cells were then incubated in the absence (basal) or presence of ATP at 37°C for 5 min. Incubations were stopped by addition of $MgCl_2$ medium and centrifugation and the MFI of ethidium$^+$ uptake determined by flow cytometry. Results are mean ± SD (n = 3); $^{**}P < 0.01$ compared to corresponding basal control, and $^{††}P < 0.01$ compared to corresponding ATP in the absence of AZ10606120.

5.2.6 H_2O_2 does not enhance basal or ATP-induced soluble CD23 shedding from RPMI 8226 cells.

To determine whether H_2O_2 enhances ATP-induced soluble CD23 shedding, RPMI 8226 cells were preincubated in the absence or presence 100 μM H_2O_2 and then

with ATP, and the amount of soluble CD23 in cell-free supernatants measured by an enzyme-linked immunosorbent assay (ELISA). As observed previously (Chapter 3), incubation of cells with ATP resulted in significantly higher release of soluble CD23 compared to basal control cells (Figure 5.6). However, in the presence of H_2O_2, ATP induced similar amounts of soluble CD23 release compared to cells incubated with ATP in the absence of H_2O_2 (Figure 5.6). Basal soluble CD23 release was similar in the absence or presence of H_2O_2 (Figure 5.6). This suggests that H_2O_2 does not enhance ATP-induced soluble CD23 shedding from RPMI 8226 cells, but alters cell surface CD23 by another mechanism.

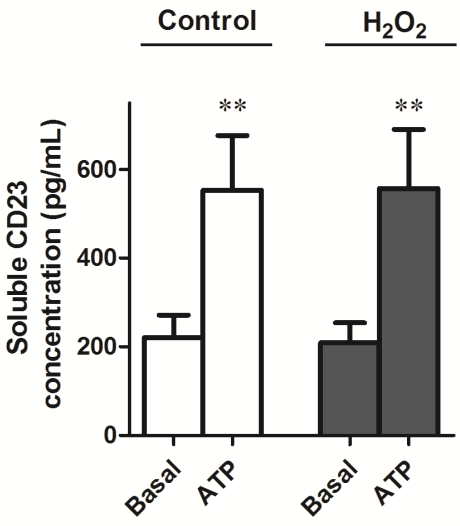

Figure 5.6: H_2O_2 does not enhance basal or ATP-induced soluble CD23 shedding from RPMI 8226 cells. RPMI 8226 cells in NaCl medium (1 x 10^6 cells/ml) were preincubated in the absence (left) or presence (right) of 100 μM H_2O_2, and then in the absence (basal) or presence of 1 mM ATP for 20 min. Incubations were stopped by centrifugation and the amount of soluble CD23 in cell-free supernatants determined by ELISA. Results are mean ± SD (n = 6); $^{**}P < 0.01$ compared to corresponding basal control.

5.3 Discussion

This chapter demonstrates that H_2O_2 enhances ATP-induced cell surface loss of CD23 from RPMI 8226 cells in a rapid and time-dependent manner. However, H_2O_2 did not enhance ATP-induced soluble CD23 release from RPMI 8226 cells. Therefore it is possible the H_2O_2-induced enhancement of ATP-induced CD23 loss, from RPMI 8226 cells is an artefact due to H_2O_2 altering the binding of the CD23 mAb to cell surface CD23. In this regard, it has been shown that H_2O_2 treatment reduces binding of some mAb to their ligands (Ibsen 1996). However, if this explanation is true it is curious that H_2O_2 generally reduces mAb binding to CD23 in the presence but not in the absence of ATP. An alternate explanation is that H_2O_2 enhances internalisation of CD23 leading to an increased loss of CD23 from the cell surface. H_2O_2 has been shown to induce the internalisation of the keratinocyte growth factor receptor (Belleudi et al. 2006). However, given that AZ10606120 did not completely impair the ATP-induced loss of CD23 in the presence of H_2O_2, the potential internalisation of CD23 by H_2O_2 was not examined further. The inability of AZ10606120 to completely prevent the ATP-induced loss of cell surface CD23 in the presence of H_2O_2 was not due to an effect of H_2O_2 on AZ10606120, as the P2X7 antagonist completely impaired ATP-induced ethidium$^+$ uptake in the presence of H_2O_2. Furthermore, H_2O_2 did not increase ATP-induced ethidium$^+$ uptake excluding a direct effect of the ROS on P2X7 function. However, ATP induced significant ROS formation in RPMI 8226 cells which was almost completely impaired by AZ10606120 (results not shown). This suggests P2X7 activation plays a role in ROS formation in RPMI 8226 cells. It would be of interest to determine the significance of P2X7-induced ROS formation in these cells, however it was beyond the scope of this thesis.

Foster and colleagues showed that DPI and rotenone enhanced ATP-induced CD62L shedding from human T cells, and that this enhancement is due to P2X7 activation (Foster et al. 2013). In contrast, DPI and rotenone did not significantly affect ATP-induced CD23 loss, despite both compounds being able to induce ROS formation in RPMI 8226 cells. The effect of DPI and rotenone on ATP-induced CD62L loss from human T cells was not examined in the present study, but such a study would have also served as a suitable positive control. Nevertheless, the reason for the difference between the current study and that of Foster and colleagues, with DPI and rotenone on ATP-induced shedding of cell surface molecules remains unknown. Foster and colleagues treated human T cells with 3 mM ATP for an hour, whereas RPMI 8226 cells were treated with 1 mM ATP for 7 min, therefore it is possible that in the presence of these compounds, treatment of RPMI 8226 cells with ATP for longer or at higher concentrations may enhance ATP-induced CD23 loss. An alternate, but not mutually exclusive reason for the differences between the two studies may relate to the ADAMs mediating CD23 and CD62L shedding. ADAM17 is implicated in nucleotide-induced CD62L shedding from murine B cells and T cells (Le Gall et al. 2009, Le Gall et al. 2010). Therefore it is likely that superoxide-enhancement of P2X7-induced CD62L loss from human T cells involves ADAM17 (Foster et al. 2013). In contrast, ATP-induced CD23 shedding from RPMI 8226 cells involves ADAM10 (Chapter 6). Finally, it should be noted that it was not determined if the superoxide-induced enhancement of P2X7-induced CD62L loss from T cells (Foster et al. 2013) was a result of CD62L shedding or internalisation. Thus, further studies are also required in this model to better understand the mechanisms involved.

This chapter demonstrates that H_2O_2 does not enhance ATP-induced CD23 shedding from RPMI 8226 cells but the possibility remains that H_2O_2 alters CD23 mAb binding to CD23 or induces CD23 internalisation. However, given that this effect appeared to be independent of P2X7 this was not investigated further. Furthermore, neither rotenone nor DPI affected ATP-induced CD23 shedding from RPMI 8226 cells indicating that ROS, along with several other signalling pathways (Chapter 4), do not play a significant role in P2X7-induced CD23 shedding from these cells.

CHAPTER 6

ADAM10 is involved in P2X7-induced CD23 and CXCL16 shedding from RPMI 8226 cells

6.1 Introduction

P2X7 activation induces the shedding of cell surface molecules including CD23 from chronic lymphocytic leukaemia B cells (Gu et al. 1998), RPMI 8226 multiple myeloma B cells (Farrell 2008; Chapters 3-5) and normal dendritic cells (Sluyter and Wiley 2002, Georgiou et al. 2005), and the interleukin-6 receptor (IL-6R) from murine splenic T cells, and P2X7/IL-6R co-transfected human embryonic kidney (HEK 293) cells and murine NIH3T3 fibroblasts (Garbers et al. 2011). P2X7-induced IL-6R shedding is mediated by a disintegrin and metalloprotease (ADAM) 10 (Garbers et al. 2011). ADAM10 is also responsible for the constitutive, and ionomycin-induced shedding of CD23 (Weskamp et al. 2006, Le Gall et al. 2009), and other molecules such as the CXCR6 ligand and chemokine CXCL16 (Abel et al. 2004, Gough et al. 2004). Broad spectrum metalloprotease inhibitors have implicated a role for metalloproteases in P2X7-induced CD23 shedding from leukemic B cells (Gu et al. 1998) and RPMI 8226 cells (Sluyter and Wang, *personal communication*), but the identity of the metalloprotease remains unknown. Given the role of ADAM10 in constitutive and inducible CD23 shedding, it is a likely candidate in P2X7-induced CD23 shedding. Therefore, using RPMI 8226 cells the aim of this chapter was to determine whether ADAM10 is involved in P2X7-induced CD23 shedding.

6.2 Results

6.2.1 ADAM10 is expressed in RPMI 8226 cells

To determine if RPMI 8226 cells express ADAM10, RNA was isolated from RPMI 8226 cells and examined by reverse transcriptase-polymerase chain reaction

(RT-PCR). RT-PCR showed the expression of ADAM10 messenger RNA (509 base pairs) in these cells (Figure 6.1). No PCR products were observed in the H_2O controls (Figure 6.1).

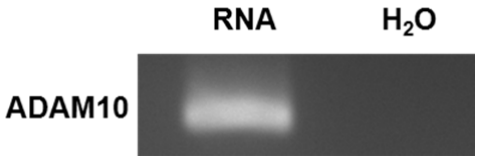

Figure 6.1: ADAM10 is expressed in RPMI 8226 cells. RNA was isolated from RPMI 8226 cells, and then analysed by RT-PCR using primers for ADAM10. RNA substituted with H_2O was used as a negative control. PCR products were visualised using ethidium bromide. A representative result from three experiments is shown.

6.2.2 The ADAM10 antagonist, GI254023X impairs P2X7-induced CD23 shedding but not ethidium$^+$ uptake into RPMI 8226 cells

To determine whether ADAM10 is involved in P2X7-induced CD23 shedding, RPMI 8226 cells were preincubated in the absence or presence of the ADAM10 antagonist 3 μM GI254023X (Ludwig et al. 2005a), and then with adenosine 5'-triphosphate (ATP), and cell surface CD23 expression measured by flow cytometry. As previously observed (Chapters 3-5), ATP induced the rapid shedding of CD23 from RPMI 8226 cells (Figure 6.2A). GI254023X impaired P2X7-induced CD23 shedding by 57 ± 11% (Figure 6.2A). To exclude a direct inhibitory role of GI254023X on P2X7 itself, cells were preincubated in the absence or presence of GI254023X for 15 min and ATP-induced ethidium$^+$ uptake was measured by flow cytometry. GI254023X (3 μM) did not affect ATP-induced ethidium$^+$ uptake into cells (Figure 6.2B). In the absence of ATP,

GI254023X did not significantly alter CD23 shedding or ethidium$^+$ uptake compared with cells incubated in dimethyl sulphoxide (DMSO) alone (Figure 6.2A, B).

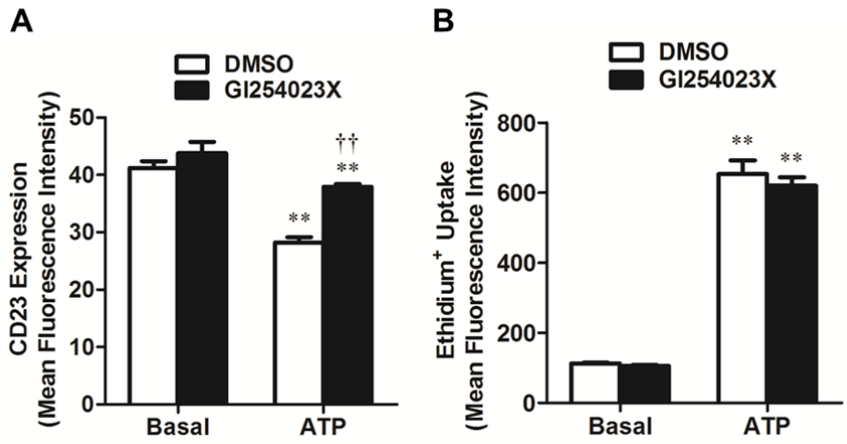

Figure 6.2: The ADAM10 antagonist, GI254023X impairs P2X7-induced CD23 shedding but not ethidium$^+$ uptake into RPMI 8226 cells. (A, B) RPMI 8226 cells in NaCl medium were preincubated at 37°C for 15 min in the presence of DMSO or 3 μM GI254023X, and then in the absence (basal) or presence of (A) 1 mM ATP at 37°C for 7 min or (B) 25 μM ethidium$^+$ in the absence or presence of 1 mM ATP for 5 min at 37°C. Incubations were stopped by addition of $MgCl_2$ medium and centrifugation. (A) Cells were then labelled with phycoerythrin (PE)-conjugated anti-CD23 or isotype control monoclonal antibody (mAb). The mean fluorescence intensity (MFI) of (A) cell surface CD23 expression or (B) ethidium$^+$ uptake was determined by flow cytometry. Results are mean ± standard deviation (SD) (n = 3); $^{**}P < 0.01$ compared to corresponding basal control, and $^{††}P < 0.01$ compared to corresponding ATP with DMSO.

6.2.3 CXCL16 is expressed on RPMI 8226 cells

To confirm a role for ADAM10 in P2X7-induced CD23 shedding, several attempts were made to knockdown ADAM10 in RPMI 8226 cells using short inhibitory RNA. However, this approach was unsuccessful due to poor transfection efficiency (results not shown). Therefore to confirm that P2X7 activates ADAM10, the effect of P2X7 activation was examined on a second ADAM10 substrate, CXCL16. First, to determine whether RPMI 8226 cells express CXCL16, cells were labelled with an anti-CXCL16 or control IgG antibody (Ab) and fluorescence measured by flow cytometry. CXCL16 was present on RPMI 8226 cells (MFI of 14 ± 1, Figure 6.3).

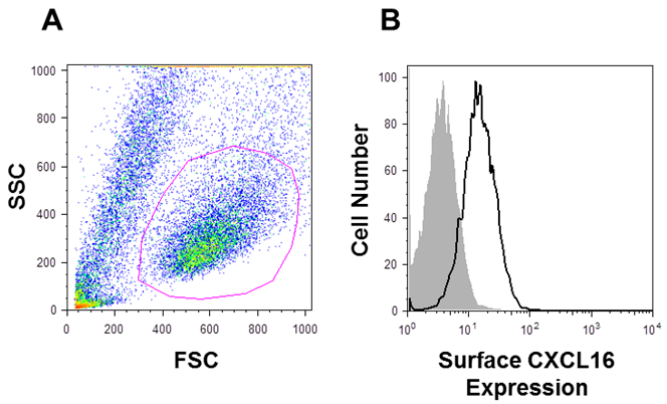

Figure 6.3: CXCL16 is expressed on RPMI 8226 cells. (A, B) RPMI 8226 cells in NaCl medium were labelled with anti-CXCL16 (solid line) or isotype IgG control (shaded) Ab, and then with a fluorescein isothiocyanate (FITC)-conjugated secondary Ab. The MFI of CXCL16 cell surface expression was determined by flow cytometry. (A) RPMI 8226 cells were gated by forward scatter (FSC) and side scatter (SSC) as shown. (B) A representative result from three experiments is shown.

6.2.4 ATP induces CXCL16 loss from RPMI 8226 cells in a time-dependent manner

To determine if ATP induces CXCL16 shedding, cells were incubated with 1 mM ATP which resulted in an 83 ± 8% (n = 3) loss of cell surface CXCL16 at 30 min, with a similar loss of CXCL16 observed at 10 and 20 min (results not shown). ATP-induced cell surface CXCL16 loss was then determined over shorter time points. ATP induced the rapid loss of cell surface CXCL16 in a time-dependent fashion, with a $t_{1/2}$ of approximately 1 min (Figure 6.4).

6.2.5 ATP induces CXCL16 shedding from RPMI 8226 cells

To determine if ATP-induced loss of cell surface CXCL16 was due to CXCL16 shedding, RPMI 8226 cells were incubated in the absence or presence of 1 mM ATP, and the amount of soluble CXCL16 in cell-free supernatants quantified by enzyme-linked immunosorbent assay (ELISA). Incubation of cells with ATP resulted in a significantly higher release of soluble CXCL16 compared with cells incubated in the absence of ATP (Figure 6.5).

6.2.6 ATP and BzATP induce CXCL16 shedding from RPMI 8226 cells

To determine if the ATP-induced CXCL16 shedding was mediated by P2X7, cells were incubated for 1 min (the $t_{1/2}$) in the absence or presence of ATP, the most potent P2X7 agonist 2'(3')-O-(4-benzoylbenzoyl)adenosine-5'-triphosphate (BzATP), or the non-P2X7 agonists adenosine 5’-diphosphate (ADP) and uridine 5’-triphosphate (UTP)

(all at 100 μM) and cell surface CXCL16 expression measured by flow cytometry. ATP and BzATP induced a 62 ± 8% and 64 ± 1% loss of cell surface CXCL16 respectively, while ADP and UTP had no effect compared to cells incubated in the absence of nucleotide (Figure 6.6).

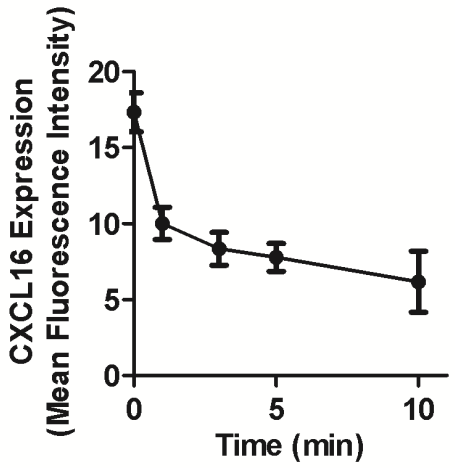

Figure 6.4: ATP induces CXCL16 loss from RPMI 8226 cells in a time-dependent manner. RPMI 8226 cells in NaCl medium were incubated for up to 10 min (as indicated) at 37°C in the absence or presence of 1 mM ATP. Incubations were stopped by addition of $MgCl_2$ medium and centrifugation. Cells were then labelled with anti-CXCL16 or IgG control Ab, and then with a FITC-conjugated anti-rabbit IgG Ab. The MFI of cell surface CXCL16 expression was determined by flow cytometry. Results are mean ± SD (n = 3).

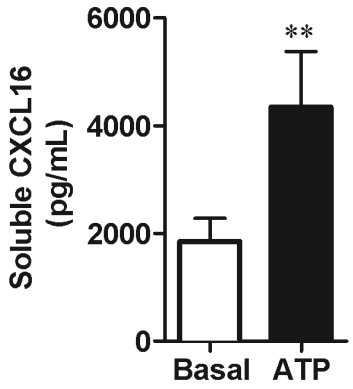

Figure 6.5: ATP induces CXCL16 shedding from RPMI 8226 cells. RPMI 8226 cells in NaCl medium were incubated in the absence (basal) or presence of 1 mM ATP at 37°C for 10 min. Incubations were stopped by centrifugation and amount of soluble CXCL16 in cell-free supernatants determined by ELISA. Results are mean ± SD (n = 3); $^{**}P < 0.01$ compared to basal.

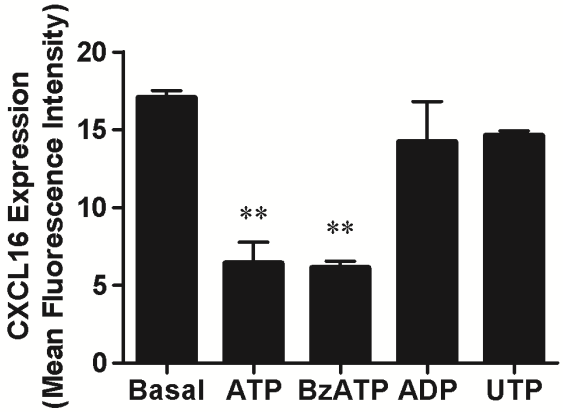

Figure 6.6: ATP and BzATP induce CXCL16 shedding from RPMI 8226 cells. RPMI 8226 cells in NaCl medium were incubated in the absence (basal) or presence of 1 mM ATP, BzATP, ADP or UTP (all 100 μM) at 37°C for 1 min. Incubations were stopped by addition of $MgCl_2$ medium and centrifugation. Cells were then labelled with anti-CXCL16 or IgG control Ab, and then with a FITC-conjugated anti-rabbit IgG Ab. The MFI of cell surface CXCL16 expression was determined by flow cytometry. Results are mean ± SD (n = 3); $^{**}P < 0.01$ compared to basal.

6.2.7 P2X7 antagonists impair ATP-induced CXCL16 shedding from RPMI 8226 cells

To confirm that ATP-induced shedding of CXCL16 was mediated by P2X7, cells were preincubated in the absence or presence of the P2X7 antagonists, AZ10606120 and KN-62, and then with ATP, and cell surface CXCL16 expression measured by flow cytometry. Both 100 nM AZ10606120 and 1 μM KN-62 impaired ATP-induced CXCL16 shedding by 86 ± 24 % and 90 ± 9% respectively, compared to ATP-induced CXCL16 shedding in the absence of P2X7 antagonists (Figure 6.7). In the absence of ATP, neither antagonist significantly altered CXCL16 shedding (Figure 6.7).

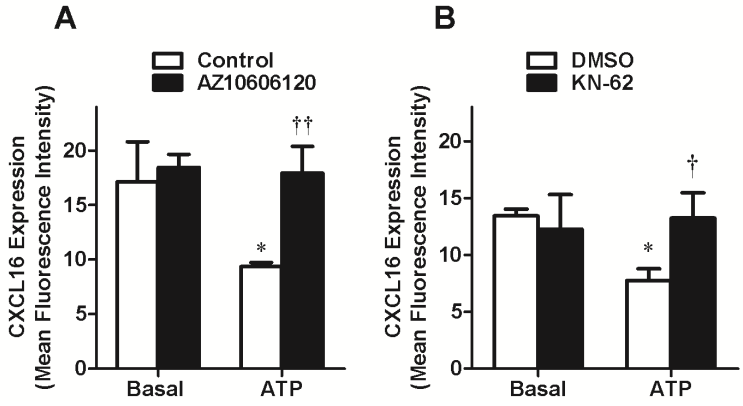

Figure 6.7: P2X7 antagonists impair ATP-induced CXCL16 shedding from RPMI 8226 cells. (A, B) RPMI 8226 cells in NaCl medium were preincubated at 37°C for 15 min (A) in the absence (control) or presence of 100 nM AZ10606120, or (B) in the presence of DMSO or 1 μM KN-62, and then in the absence (basal) or presence of 1 mM ATP for 1 min at 37°C. Incubations were stopped by addition of $MgCl_2$ medium and centrifugation. Cells were then labelled with anti-CXCL16 or IgG control Ab, and then with a FITC-conjugated anti-rabbit IgG Ab. The MFI of cell surface CXCL16 expression was determined by flow cytometry. Results are mean ± SD (n = 3); $^{*}P < 0.05$ compared with corresponding basal; $^{\dagger}P < 0.05$ or $^{\dagger\dagger}P < 0.01$ compared with corresponding ATP without antagonist.

6.2.8 Metalloprotease antagonists impair P2X7-induced CXCL16 shedding from RPMI 8226 cells

To determine a role for metalloproteases in P2X7-induced CXCL16 shedding, cells were preincubated in the absence or presence of broad spectrum metalloprotease antagonists BB-94 (Davies et al. 1993) and GM6001 (Grobelny et al. 1992), and then in the absence or presence of ATP and cell surface CXCL16 expression measured by flow cytometry. Both 1 μM BB-94 and 1 μM GM6001 impaired P2X7-induced CXCL16 shedding by 77 ± 20% and 52 ± 30 % respectively (Figure 6.8). In the absence of ATP, neither antagonist significantly altered CXCL16 shedding (Figure 6.8).

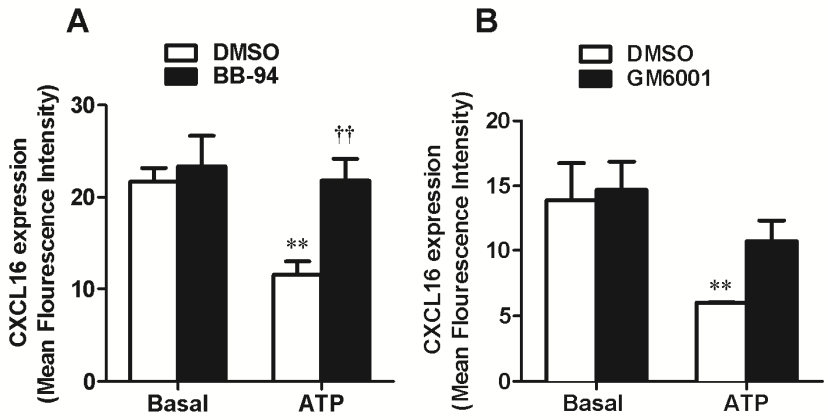

Figure 6.8: Metalloprotease antagonists impair P2X7-induced CXCL16 shedding from RPMI 8226 cells. (A, B) RPMI 8226 cells in NaCl medium were preincubated at 37°C for 15 min in the presence of (A, B,) DMSO, (A) 1 μM BB-94 or (B) 1 μM GM6001, and then in the absence (basal) or presence of 1 mM ATP for 1 min at 37°C. Incubations were stopped by addition of $MgCl_2$ medium and centrifugation. Cells were then labelled with anti-CXCL16 or IgG control Ab, and then with a FITC-conjugated anti-rabbit IgG Ab. The MFI of cell surface CXCL16 expression was determined by flow cytometry. Results are mean ± SD (n = 3); $^{**}P < 0.01$ compared with corresponding basal DMSO; $^{††}P$ < 0.01 compared with corresponding ATP with DMSO.

6.2.9 GI254023X impairs P2X7-induced CXCL16 shedding from RPMI 8226 cells

To determine a role for ADAM10 in P2X7-induced CXCL16 shedding, cells were preincubated in the absence or presence of the ADAM10 antagonist GI254023X, and then with ATP and cell surface CXCL16 expression determined as above. GI254023X (3 μM) impaired P2X7-induced CXCL16 shedding by 87 ± 15% (Figure 6.9). In the absence of ATP, GI254023X did not significantly alter CXCL16 shedding compared with cells incubated with DMSO alone (Figure 6.9).

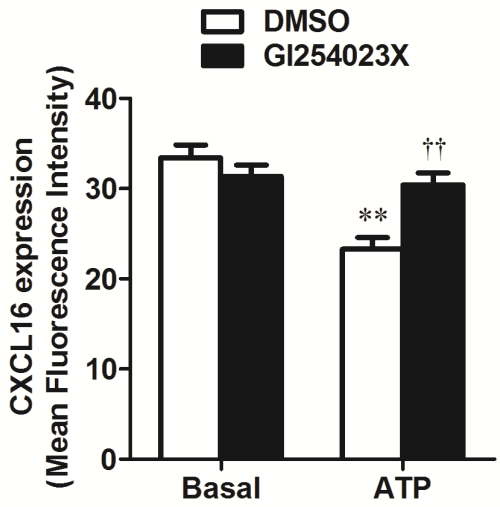

Figure 6.9: GI254023X impairs P2X7-induced CXCL16 shedding from RPMI 8226 cells. RPMI 8226 cells in NaCl medium were preincubated at 37°C for 15 min in the presence of DMSO or 3 μM GI254023X, and then in the absence (basal) or presence of 1 mM ATP for 1 min at 37°C. Incubations were stopped by addition of $MgCl_2$ medium and centrifugation. Cells were then labelled with anti-CXCL16 or IgG control Ab, and then with a FITC-conjugated anti-rabbit IgG Ab. The MFI of cell surface CXCL16 expression was determined by flow cytometry. Results are mean ± SD (n = 3); $^{**}P < 0.01$ compared with corresponding basal DMSO; $^{††}P < 0.01$ compared with corresponding ATP with DMSO.

6.3 Discussion

Activation of P2X7 induces the shedding of CD23 from leukemic B cells (Gu et al. 1998) and normal dendritic cells (Sluyter and Wiley 2002, Georgiou et al. 2005). Data from this chapter and previous chapters (Chapters 3-5) confirms that P2X7 activation induces the rapid shedding of CD23 from RPMI 8226 cells. Broad spectrum metalloprotease antagonists have implicated a role for metalloproteases in P2X7-induced CD23 shedding from leukemic B cells (Gu et al. 1998) and RPMI 8226 (Wang and Sluyter, *personal communication*), but the identity of the metalloprotease involved has remained inconclusive. Using the specific ADAM10 antagonist GI254023X and RPMI 8226 cells, data from this chapter shows for the first time that ADAM10 mediates P2X7-induced CD23 shedding. A role for ADAM10 in nucleotide-induced CD23 shedding was described for human leukaemic monocytic U937 cells using an inhibitory prodomain construct of ADAM10, A10-(23-213) (Lemieux et al. 2007), and for CD23-transfected Chinese hamster ovary cells or murine B cells using GI254023X (Le Gall et al. 2009, Le Gall et al. 2010). However, a direct role for P2X7 in this process was not established in any of these studies.

Data from this chapter also shows for the first time that P2X7 activation induces the rapid shedding of CXCL16, and that this process is mediated by ADAM10. The P2X7 agonists ATP and BzATP induced the rapid cell surface loss of CXCL16 from RPMI 8226 cells and measurements of soluble CXCL16 indicated that the ATP-induced loss was a result of shedding. Specific P2X7 antagonists AZ10606120 (Michel et al. 2008) and KN-62 (Gargett and Wiley 1997) almost completely impaired ATP-induced

CXCL16 shedding, while the non P2X7 agonists ADP and UTP had no effect on CXCL16 expression. Moreover, P2X7-induced CXCL16 shedding could be impaired by broad spectrum metalloprotease antagonists, BB-94 (Davies et al. 1993) and GM6001 (Grobelny et al. 1992), outlining a role for metalloproteases in this process. The inhibition of these two metalloprotease inhibitors was not due to direct inhibition of P2X7, as previous work in our laboratory has shown that neither BB-94 nor GM6001 impair ATP-induced ethidium^{+} uptake into RPMI 8226 cells (Wang and Sluyter, *personal communication*). The specific involvement of ADAM10 in this process was established by the ADAM10 antagonist GI254023X (Ludwig et al. 2005a), which like BB-94 and GM6001 did not affect P2X7-induced ethidium^{+} uptake. Thus, the P2X7-induced shedding of CXCL16 indicates that P2X7 activation stimulates ADAM10. Of note, GI254023X impaired P2X7-induced CXCL16 and CD23 shedding by ~87% and ~57%, respectively. This reduced capacity for GI254023X to block P2X7-induced CD23 shedding may reflect differences in cell surface expression and/or rates of shedding between CXCL16 and CD23.

P2X7 activation induces ADAM10-mediated CD23 and CXCL16 shedding from human RPMI 8226 cells. The role of ADAM10 in this process is consistent with ADAM10 mediating P2X7-induced shedding of the interleukin-6 receptor from murine splenic T cells, and from P2X7/interleukin-6 receptor co-transfected HEK 293 and NIH323 cells (Garbers et al. 2011). The possibility remains however, that other ADAMs may be partly involved in P2X7-induced CD23 and CXCL16 shedding. ADAM8, 15, 28 and 33 (Fourie et al. 2003, Weskamp et al. 2006) have been associated with CD23 shedding from CD23-transfected HEK 293 cells (Fourie et al. 2003) and primary murine embryonic fibroblasts (Weskamp et al. 2006). Further, ADAM17 can mediate phorbol

ester-induced CXCL16 shedding in CXCL16-transfected COS-7 cells (Abel et al. 2004, Ludwig et al. 2005a, Hundhausen et al. 2007).

Chemokines and their receptors are important in human multiple myeloma plasma cell migration and compartmentalisation in the bone marrow (Moller et al. 2003). CXCL16 induces chemotactic responses in human bone marrow plasma cells and directly adheres to plasma cells expressing its receptor CXCR6 (Nakayama et al. 2003), suggesting these molecules play a role in plasma cell tissue migration and localisation. A more recent study showed that an anti-tumour molecule, comprised of snake venom and nanoparticles, decreases the expression of CXCL16, and its receptor CXCR6 on murine multiple myeloma cells (Al-Sadoon et al. 2013), suggesting that these molecules are important in multiple myeloma survival. Despite these studies, there is a lack of knowledge outlining a mechanistic role for CXCL16 in multiple myeloma. Therefore, data from this chapter suggests P2X7-induced CXCL16 shedding is a novel pathway that may be involved in multiple myeloma migration, localisation and survival.

In conclusion, data from this chapter demonstrates for the first time that human P2X7-induced CD23 shedding is mediated by ADAM10 in RPMI 8226 cells. Also for the first time, data from this chapter shows that P2X7 activation induces the rapid shedding of CXCL16 from RPMI 8226 cells, and that this process is also mediated by ADAM10.

CHAPTER 7

P2X7 activation induces rapid CD23 shedding from primary human and murine B cells

7.1 Introduction

CD23 is a 'low affinity', transmembrane receptor for IgE that is expressed on B cells and other leukocytes (Sarfati et al. 1992). Transmembrane CD23 can be released from the cell surface to form soluble CD23, which also binds IgE, and exerts cytokine-like activities on B cells and other leukocytes (Sarfati et al. 1992). Soluble CD23 sustains growth of B cell precursors (Borland et al. 2007), promotes B and T cell differentiation (Mossalayi et al. 1990a, Liu et al. 1991), and drives cytokine release from monocytes (Hermann et al. 1999). The release of CD23 is mediated by membrane metalloproteases of the ADAM (a disintegrin and metalloprotease) family. ADAM10 is principally responsible for the constitutive and calcium-induced shedding of CD23 (Weskamp et al. 2006, Lemieux et al. 2007).

Activation of P2X7 by extracellular adenosine 5'-triphosphate (ATP) causes the uptake of organic cations such as ethidium^{+} and YO-PRO-1^{2+} (Cankurtaran-Sayar et al. 2009). P2X7 activation induces a number of downstream effects including the shedding of CD23 from chronic lymphocytic leukaemia B cells (Gu et al. 1998), RPMI 8226 human multiple myeloma cells (chapters 3-6) and human monocyte-derived dendritic cells (Sluyter and Wiley 2002, Georgiou et al. 2005). Data from chapter 6 demonstrates that P2X7-induced CD23 shedding from RPMI 8226 cells is mediated by ADAM10. 2' (3')-O-(4-benzoylbenzoyl) ATP (BzATP)-induced CD23 shedding from murine B cells is also mediated by ADAM10 (Le Gall et al. 2009, Le Gall et al. 2010), but a direct role for P2X7 in this process was not established in these studies. Therefore, it remains unknown if P2X7 activation induces CD23 shedding from primary murine B cells or from primary human B cells. The aim of this chapter was to determine

whether P2X7 activation induces the rapid shedding from primary human and murine cells, and if so whether this process involves ADAM10.

7.2 Results

7.2.1 ATP induces CD23 loss from human B cells in a time-dependent manner

To first determine if ATP induces CD23 loss from human B cells, peripheral blood mononuclear cells (PBMCs) were incubated with ATP for up to 30 min and cell surface CD23 expression measured by flow cytometry. ATP induced a rapid loss of cell surface CD23 from B cells with a $t_{1/2}$ of approximately 6 min (Figure 7.1).

7.2.2 ATP induces CD23 shedding from human B cells

To determine if the P2X7-induced loss of cell surface CD23 was due to CD23 shedding, PBMCs were incubated in the absence or presence of 1 mM ATP, and the relative amount of soluble CD23 in cell-free supernatants quantified by enzyme-linked immunosorbent assay (ELISA). Incubation of PBMCs with ATP resulted in a significantly higher release of soluble CD23 compared with cells incubated in the absence of ATP (Figure 7.2).

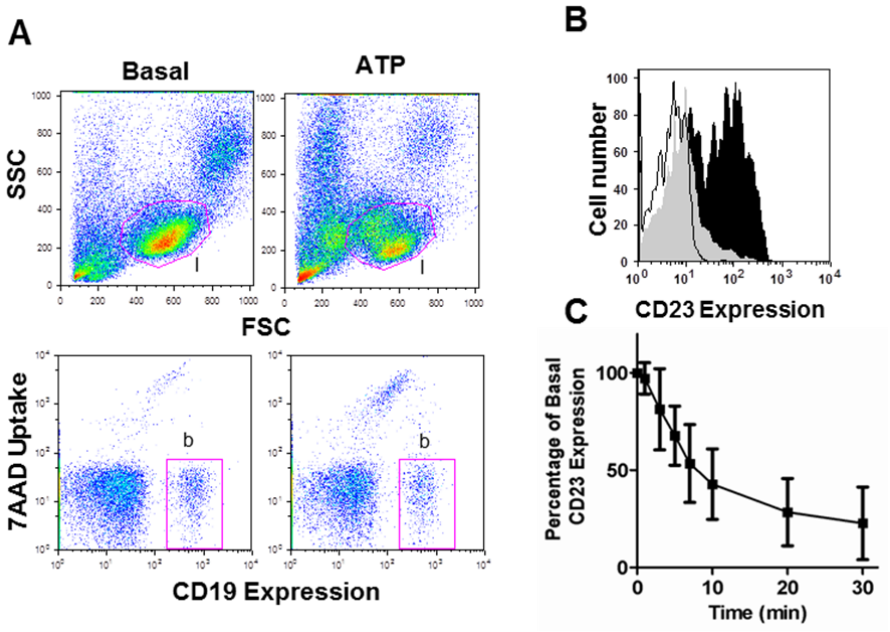

Figure 7.1: ATP induces CD23 loss from human B cells in a time-dependent manner. (A-C) PBMCs in NaCl medium were incubated for up to 30 min at 37°C in the absence (control) or presence of 1 mM ATP as indicated. Incubations were stopped by addition of $MgCl_2$ medium and centrifugation. PBMCs were labelled with allophycocyanin (APC)-conjugated anti-CD19, phycoerythrin (PE)-conjugated anti-CD23 or isotype control monoclonal antibody (mAb) and 7-aminoactinomycin D (7AAD). The mean fluorescence intensity (MFI) of cell surface CD23 expression on $CD19^+7AAD^-$ B cells was determined by flow cytometry. (A) Basal or ATP-treated lymphocytes (l) were gated by forward scatter (FSC) and side scatter (SSC) as shown (top panel). $CD19^+7AAD^-$ B cells (b) were gated as shown (bottom panel). (B) Histograms (from one representative individual) show CD23 expression on (black or grey fill) or isotype control mAb binding (black line) to $CD19^+7AAD^-$ PBMCs incubated in the absence (black fill or black line) or presence (grey fill) of 1 mM ATP for 30 min; isotype control mAb binding to $CD19^+7AAD^-$ PBMCs incubated in the presence of ATP was similar to that of cells incubated in the absence of ATP (not shown). (C) Results are mean ± standard deviation (SD) (n = 3 individuals).

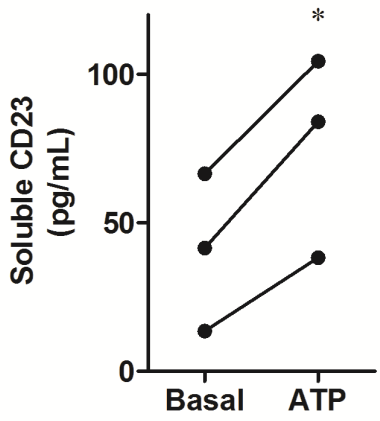

Figure 7.2: ATP induces CD23 shedding from human B cells. PBMCs in NaCl medium were incubated in the absence (basal) or presence of 1 mM ATP at 37°C for 20 min, incubations were stopped by centrifugation and the amount of soluble CD23 in cell-free supernatants determined by ELISA. Results are mean ± SD (n = 3 individuals); $^{*}P < 0.05$ and $^{**}P < 0.01$ compared to basal.

7.2.3 ATP and BzATP induce CD23 shedding from human B cells

To determine whether ATP-induced CD23 loss was mediated by P2X7, PBMCs were incubated for 6 min (the $t_{1/2}$) in the absence or presence of 1 mM ATP, the most potent P2X7 agonist 0.3 mM BzATP, or the non-P2X7 agonists 1 mM adenosine diphosphate (ADP) and uridine 5'-triphosphate (UTP), and cell surface CD23 expression measured by flow cytometry. ATP and BzATP induced a 49 ± 9% and 60 ± 9% loss of cell surface CD23, respectively, while ADP and UTP had no effect on CD23 expression compared to cells incubated without nucleotide (Figure 7.3).

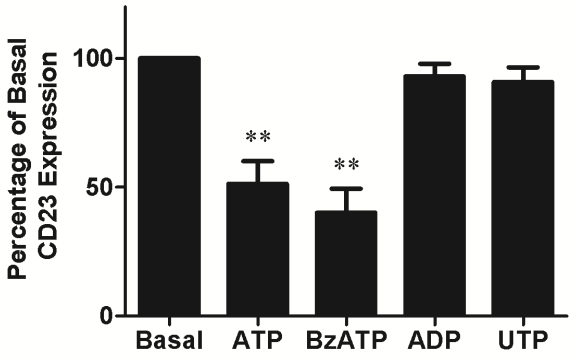

Figure 7.3: ATP and BzATP induce CD23 shedding from human B cells. PBMCs in NaCl medium were incubated in the absence (basal) or presence of 1 mM ATP, 0.3 mM BzATP, 1 mM ADP or 1 mM UTP at 37°C for 6 min. Incubations were stopped by addition of $MgCl_2$ medium and centrifugation. PBMCs were labelled with APC-conjugated anti-CD19, PE-conjugated anti-CD23 or isotype control mAb, and 7AAD. The MFI of cell surface CD23 expression on $CD19^+7AAD^-$ B cells was determined by flow cytometry. Results are mean ± SD (n = 3 individuals); $^{**}P < 0.01$ compared to basal.

7.2.4 The P2X7 antagonist, AZ10606120 impairs ATP-induced CD23 shedding from human B cells

To confirm that ATP-induced loss of CD23 was mediated by P2X7, PBMCs were preincubated in the absence or presence of 100 nM AZ10606120, and then with ATP, and cell surface CD23 expression measured by flow cytometry. AZ10606120 impaired ATP-induced CD23 loss by 89 ± 12% compare to ATP-induced loss of CD23 in the absence of AZ10606120 (Figure 7.4). In the absence of ATP, AZ10606120 did not alter CD23 expression (Figure 7.4).

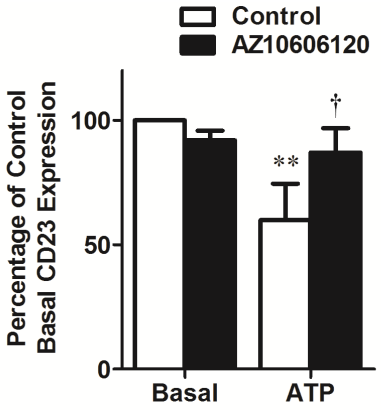

Figure 7.4: The P2X7 antagonist, AZ10606120 impairs ATP-induced CD23 shedding from human B cells. PBMCs in NaCl medium were preincubated at 37°C for 15 min in the absence or presence of 100 nM AZ10606120 and then in the absence (basal) or presence of 1 mM ATP for 6 min at 37°C. Incubations were stopped by addition of $MgCl_2$ medium and centrifugation. PBMCs were labelled with APC-conjugated anti-CD19, PE-conjugated anti-CD23 or isotype control mAb, and 7AAD. The MFI of cell surface CD23 expression on $CD19^+7AAD^-$ B cells was determined by flow cytometry. Results are mean ± SD (n = 3 individuals); $^{**}P < 0.01$ compared to corresponding control basal and $^{\dagger}P < 0.05$ compared to corresponding ATP alone.

7.2.5 AZ10606120 impairs ATP-induced YO-PRO-1^{2+} uptake into murine B cells

The presence of functional P2X7 on primary human B cells is well-established (Gu et al. 2000, Gu et al. 2001, Sluyter et al. 2001), but less well known for murine B cells. Therefore, to first test whether functional P2X7 was present on murine B cells from C57BL/6 and DBA/1 mice, splenic cells from these two strains were preincubated in the absence or presence of 10 μM AZ10606120, and ATP-induced YO-PRO-1^{2+} uptake into B cells determined by flow cytometry. C57BL/6 mice were studied because of the availability of the Pfizer P2X7 knockout mice (Solle et al. 2001), which had been

backcrossed onto a C57BL/6 background (Tran et al. 2010). DBA/1 mice were also studied, as this strain has been used to demonstrate a role for CD23 in rheumatoid arthritis (Plater-Zyberk and Bonnefoy 1995), a disease in which P2X7 is also thought to be involved (Labasi et al. 2002, Portales-Cervantes et al. 2012). ATP induced significant YO-PRO-1^{2+} uptake into murine B cells, from either C57BL/6 or DBA/1 mice, compared to YO-PRO-1^{2+} uptake in the absence of ATP (Figure 7.5). Moreover, 10 μM AZ10606120 significantly impaired ATP-induced YO-PRO-1^{2+} uptake in B cells from C57BL/6 or DBA/1 mice, by 88 ± 14% or 95 ± 8%, respectively, compared to ATP-induced YO-PRO-1^{2+} uptake in the absence of AZ10606120 (Figure 7.5). In the absence of ATP, AZ10606120 did not alter YO-PRO-1^{2+} uptake in B cells from either mouse strain (Figure 7.5).

7.2.6 ATP induces CD23 loss from murine B cells in a time-dependent manner

To determine if ATP induces CD23 loss from murine B cells, splenic cells were incubated with ATP for up to 30 min and cell surface CD23 expression measured by flow cytometry. ATP induced a rapid loss of cell surface CD23 from B cells of C57BL/6 and DBA/1 mice with a $t_{1/2}$ of approximately 7 min (Figure 7.6).

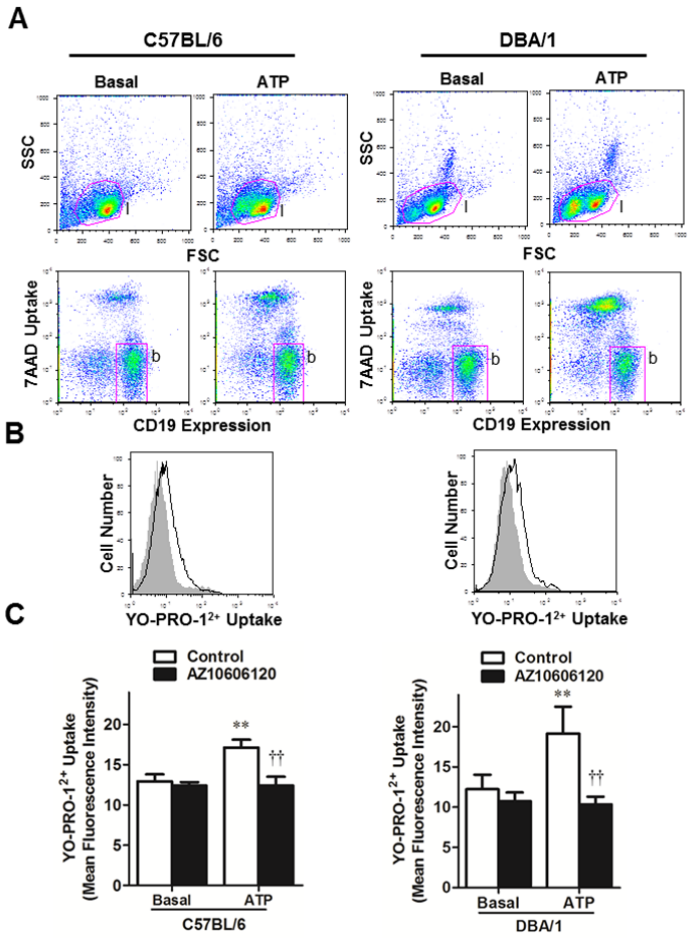

Figure 7.5: AZ10606120 impairs ATP-induced YO-PRO-1^{2+} uptake into murine B cells. (A-C) Splenic cells in NaCl medium were preincubated in the absence or presence of 10 µM AZ10606120 at 37°C for 15 min. Cells were then incubated with 1 µM YO-PRO-1^{2+} in the absence (basal) or presence of 1 mM ATP at 37°C for 15 min. Incubations were stopped by the addition of $MgCl_2$ medium and centrifugation. Cells were labelled with APC-conjugated anti-CD19 mAb and 7AAD, and the MFI of YO-PRO-1^{2+} uptake in $CD19^{+}7AAD^{-}$ B cells was determined by flow cytometry. (A) Lymphocytes (l) were gated by FSC and SSC as shown. B cells (b) were gated as shown (bottom panel). (B) Representative histograms show basal (grey fill) and ATP-induced (solid line) YO-PRO-1^{2+} uptake. (C) Results are mean ± SD (n = 3 mice (C57BL/6), or duplicate values from 2 mice (DBA/1)); $^{**}P < 0.01$ compared to corresponding control basal and $^{††}P < 0.01$ compared to corresponding ATP alone.

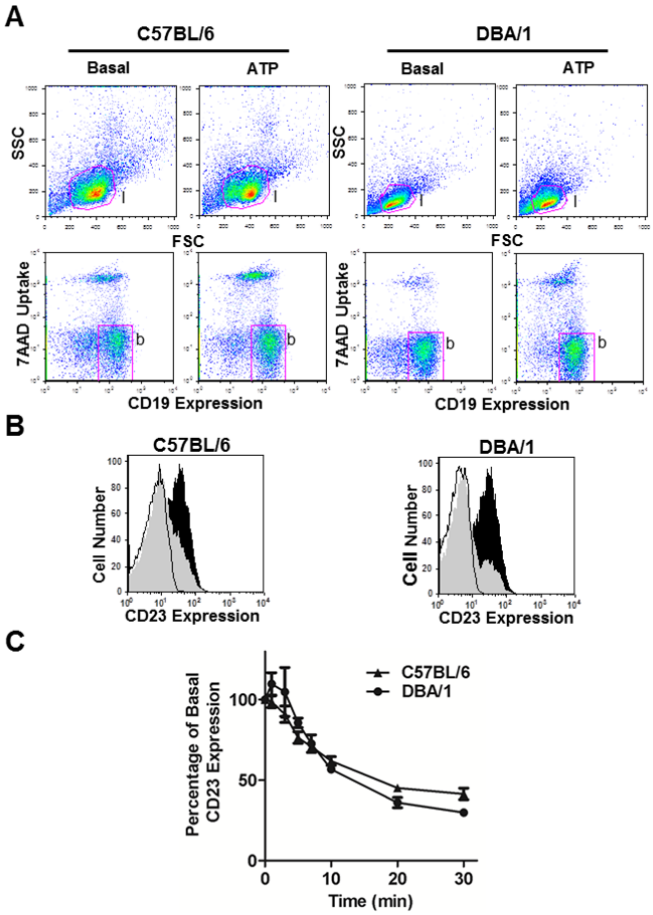

Figure 7.6: ATP induces CD23 loss from murine B cells in a time-dependent manner. (A-C) Splenic cells in NaCl medium were incubated for up to 30 min at 37°C in the absence or presence of 1 mM ATP as indicated. Incubations were stopped by addition of $MgCl_2$ medium and centrifugation. Cells were labelled with APC-conjugated anti-CD19, FITC-conjugated anti-CD23, or isotype control mAb, and 7AAD. The MFI of cell surface CD23 expression on $CD19^+7AAD^-$ B cells was determined by flow cytometry. (A) Lymphocytes (l) were gated by FSC and SSC as shown (top panel). B cells (b) were gated as shown (bottom panel). (B) Representative histograms show CD23 expression on (black or grey fill) or isotype control mAb binding (black line) to $CD19^+7AAD^-$ PBMCs incubated in the absence (black fill or black line) or presence (grey fill) of 1 mM ATP for 30 min; isotype control mAb binding to $CD19^+7AAD^-$ splenic cells incubated in the presence of ATP was similar to that of cells incubated in the absence of ATP (not shown). (C) Results are mean ± SD (*n* = triplicate values from 1 mouse).

7.2.7 ATP and BzATP induce CD23 loss from murine B cells

To determine if ATP-induced CD23 loss was mediated by P2X7, cells from both mouse strains were incubated for 7 min (the $t_{1/2}$) in the absence or presence of 1 mM ATP, 0.3 mM BzATP, 1 mM ADP or 1 mM UTP, and cell surface CD23 expression measured by flow cytometry. Similar to above (Figure 7.6), ATP induced a 37 ± 4% and 57 ± 4% loss of cell surface CD23 from B cells of C57BL/6 and DBA/1 mice, respectively (Figure 7.7). BzATP induced a 33 ± 8% and 58 ± 5% loss of cell surface CD23 from B cells of C57BL/6 and DBA/1 mice, respectively, while ADP and UTP had no effect compared to cells incubated without nucleotide in either mouse strain (Figure 7.7).

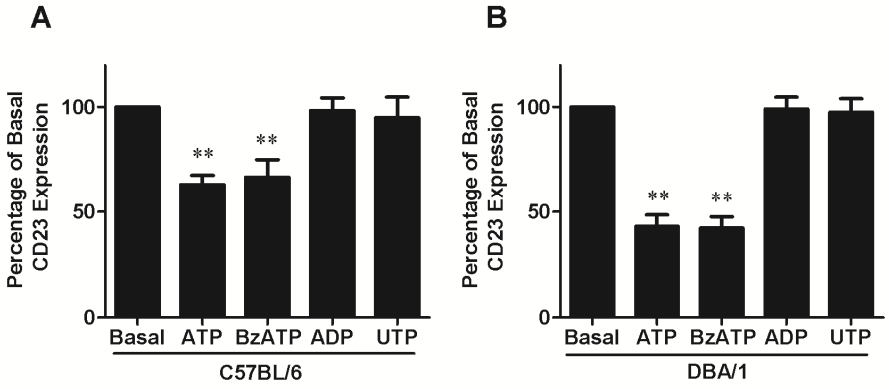

Figure 7.7: ATP and BzATP induce CD23 loss from murine B cells. (A, B) Splenic cells in NaCl medium were incubated in the absence (basal) or presence of 1 mM ATP, 0.3 mM BzATP, 1 mM ADP or 1 mM UTP at 37°C for 7 min. Incubations were stopped by addition of $MgCl_2$ medium and centrifugation. Cells were labelled with APC-conjugated anti-CD19, FITC-conjugated anti-CD23 or isotype control mAb, and 7AAD. The MFI of cell surface CD23 expression on $CD19^+7AAD^-$ B cells was determined by flow cytometry. Results are mean ± SD (n = 3 mice); $^{**}P < 0.01$ compared to basal.

7.2.8 AZ160606120 impairs ATP-induced CD23 loss from murine B cells

To confirm that ATP-induced loss of CD23 was mediated by P2X7, cells were preincubated in the absence or presence of 10 μM AZ10606120, and then with ATP, and cell surface CD23 expression measured by flow cytometry. AZ10606120 impaired ATP-induced CD23 loss by 95 ± 8% and 97 ± 6% from B cells of C57BL/6 and DBA/1, mice respectively compared to ATP-induced CD23 shedding in the absence of AZ10606120 (Figure 7.8). In the absence of ATP, AZ10606120 did not alter CD23 expression in B cells from either mouse strain (Figure 7.8).

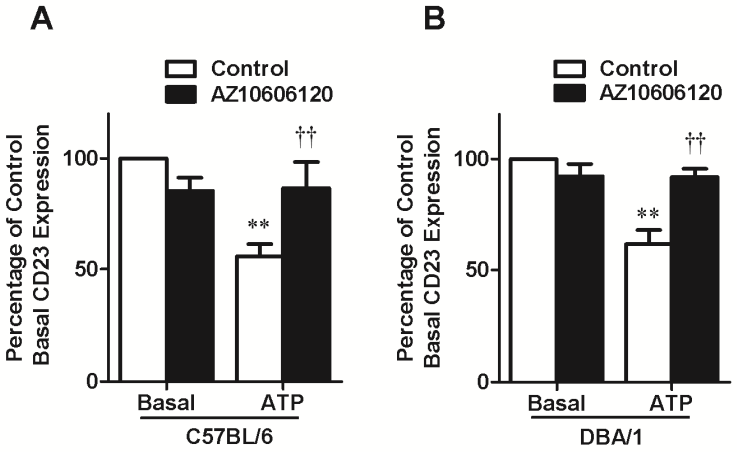

Figure 7.8: AZ160606120 impairs ATP-induced CD23 loss from murine B cells. (A, B) Splenic cells in NaCl medium were preincubated at 37°C for 15 min in the absence or presence of 10 μM AZ10606120 and then in the absence (basal) or presence of 1 mM ATP for 7 min at 37°C. Incubations were stopped by addition of $MgCl_2$ medium and centrifugation. Cells were labelled with APC-conjugated anti-CD19, FITC-conjugated anti-CD23 or isotype control mAb, and 7AAD. The MFI of cell surface CD23 expression on $CD19^{+}7AAD^{-}$ B cells was determined by flow cytometry. Results are mean ± SD (n = (A) triplicate values from 1 mouse or (B) 3 mice). $^{**}P < 0.01$ compared to corresponding control basal and $^{††}P < 0.01$ compared to corresponding ATP alone.

7.2.9 ATP-induced CD23 loss does not occur in P2X7 knockout mice

Finally, to further confirm a role for P2X7 in ATP-induced CD23 loss, P2X7 knockout mice were used. Flow cytometric measurements demonstrated that the amount of CD23 expression between control-treated B cells from wild-type and P2X7 knockout mice was similar (Figure 7.9). In contrast, incubation with 1 mM ATP induced a loss of cell surface CD23 in B cells from wild-type mice (34 ± 10% loss), but ATP-induced CD23 loss from B cells from P2X7 knockout mice was minimal (8 ± 7% loss) (Figure 7.9).

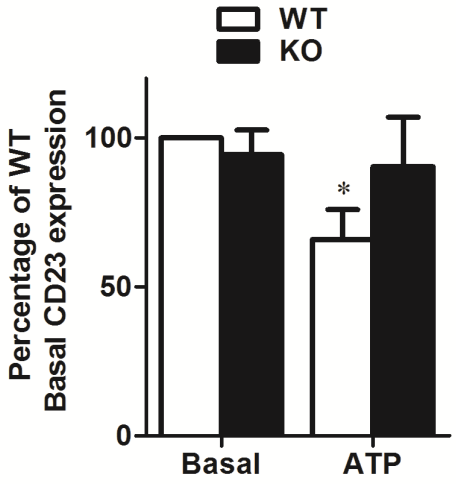

Figure 7.9: ATP-induced CD23 loss does not occur in P2X7 knockout mice. Splenic cells from wild-type (WT) or P2X7 knockout (KO) C57BL/6 mice in NaCl medium were incubated in the absence (basal) or presence of 1 mM ATP for 20 min at 37°C. Incubations were stopped by addition of $MgCl_2$ medium and centrifugation. Cells were labelled with APC-conjugated anti-CD19, FITC-conjugated anti-CD23 or isotype control mAb, and 7AAD. The MFI of cell surface CD23 expression on $CD19^{+}7AAD^{-}$ B cells was determined by flow cytometry. Results are mean ± SD (n = 3 mice); $^{*}P <$ 0.05 compared to basal control.

7.2.10 P2X7 activation induces CD23 shedding from B cells of C57BL/6 mice

Staining of fixed and permeabilised cells can be used to assess internalisation of cell surface receptors (Schmid et al. 1991, Turac et al. 2013). Therefore, to assess if cells are permeabilised using the method of Schmid and colleagues (Schmid et al. 1991), the presence of the intracellular molecule Toll-like receptor 9 (TLR-9) was examined in RPMI 8226 cells. Fixed RPMI 8226 cells, or fixed and permeabilised RPMI 8226 cells were labelled with an anti-TLR-9 or IgG control mAb and the fluorescence measured by flow cytometry. TLR-9 was expressed in fixed and permeabilised RPMI 8226 cells but was minimal on fixed RPMI 8226 cells (Figure 7.10).

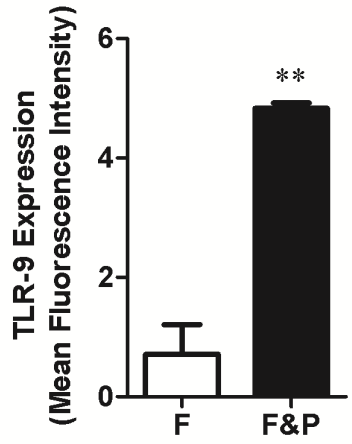

Figure 7.10: TLR-9 is expressed in fixed and permeabilised RPMI 8226 cells. RPMI 8226 cells were fixed with paraformaldehyde and labelled with PE-conjugated anti-TLR-9 or isotype control mAb in the absence (fixed, F) or presence (fixed and permeabilised, F&P) of Tween-20. The MFI of TLR-9 expression was determined by flow cytometry. Results are mean ± SD (n = 3); $^{**}P < 0.01$ compared to control.

Next, to indirectly assess if the ATP-induced loss of CD23 from murine B cells was a result of CD23 shedding or internalisation, splenic cells from C57BL/6 mice were incubated in the absence or presence of 1 mM ATP for 20 min and the expression of cell surface CD23 on fixed cells, or total CD23 in fixed and permeabilised cells was measured by flow cytometry. CD23 expression was similar in fixed cells compared to fixed and permeabilised cells (Figure 7.11A) suggesting that the P2X7-induced loss of CD23 was due to CD23 shedding rather than internalisation. To directly determine if the P2X7-induced loss of cell surface CD23 was due to CD23 shedding, splenic cells from C57BL/6 wild-type and P2X7 knockout mice were incubated in the absence or presence of 1 mM ATP for 20 min, and the relative amount of soluble CD23 in cell-free supernatants quantified by ELISA. Incubation of wild-type cells with ATP resulted in a significantly higher release of soluble CD23 compared with P2X7 knockout cells incubated with ATP, or cells of either strain incubated in the absence of ATP (Figure 7.11B). Moreover, the amount of soluble CD23 release from P2X7 knockout cells incubated in the absence or presence of ATP was similar to that of wild-type cells incubated in the absence of ATP (Figure 7.11B).

7.2.11 The broad spectrum metalloprotease antagonist, BB-94 impairs P2X7-induced CD23 shedding from human and murine B cells

To determine a role for metalloproteases in P2X7-induced CD23 shedding, human PBMCs or murine splenic cells were preincubated in the absence or presence of the broad spectrum metalloprotease antagonist, 1 μM BB-94 (Davies et al. 1993) and then with ATP, and cell surface CD23 expression measured by flow cytomtery. BB-94 impaired P2X7-induced CD23 shedding from B cells by 66 ± 10%, 100 ± 0% and

96 ± 6% from human, C57BL/6 and DBA/1 mice, respectively (Figure 7.12). In the absence of ATP, BB-94 did not alter basal CD23 expression in human and murine B cells (Figure 7.12).

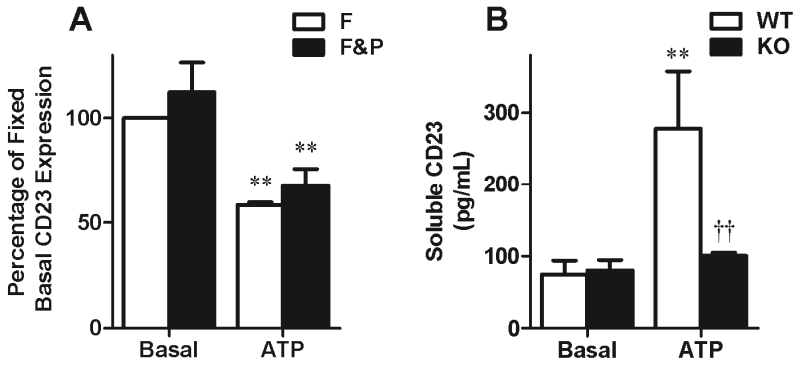

Figure 7.11: P2X7 activation induces CD23 shedding from B cells of C57BL/6 mice. Splenic cells from (A, B) wild-type (WT) or (B) P2X7 knockout (KO) C57BL/6 mice in NaCl medium were incubated for 20 min at 37°C in the absence (basal) or presence of 1 mM ATP. (A) Incubations were stopped by addition of $MgCl_2$ medium and centrifugation. Cells were labelled with APC-conjugated anti-CD19 mAb and 7AAD, and fixed with paraformaldehyde. Fixed cells were then labelled with FITC-conjugated anti-CD23 or isotype control mAb in the absence (fixed, F) or presence (fixed and permeabilised, F & P) of Tween-20. The MFI of CD23 expression in $CD19^{+}7AAD^{-}$ B cells was determined by flow cytometry. (B) Incubations were stopped by centrifugation and the amount of soluble CD23 in cell-free supernatants determined by ELISA. Results are mean ± SD (n = (A) 3 or (B) 4 mice); $^{**}P < 0.01$ compared to basal control and $^{††}P < 0.01$ compared to ATP.

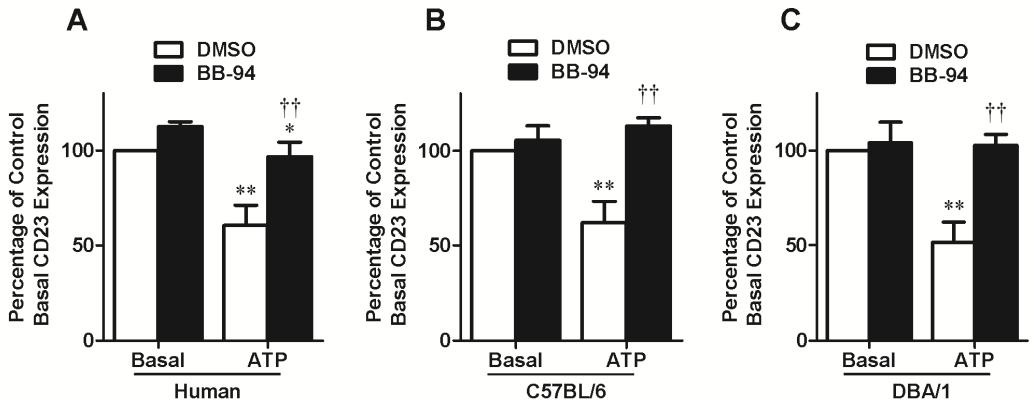

Figure 7.12: The broad spectrum metalloprotease antagonist, BB-94 impairs P2X7-induced CD23 shedding from human and murine B cells. (A) Human PBMCs and (B) C57BL/6 or (C) DBA/1 murine splenic cells were preincubated in the presence of (A-C) dimethyl sulphoxide (DMSO) or 1 μM BB-94 and then in the absence (basal) or presence of 1 mM ATP at 37°C for (A) 6 min or (B, C) 7 min. Incubations were stopped by addition of $MgCl_2$ medium and centrifugation. Cells were labelled with APC-conjugated anti-CD19 mAb, PE- or FITC-conjugated anti-CD23 or isotype control mAb, and 7AAD. The MFI of cell surface CD23 expression on $CD19^+7AAD^-$ B cells was determined by flow cytometry. Results are mean ± SD (n = (A) 4 individuals, or (B, C) 3 mice); $^*P < 0.05$ and $^{**}P < 0.01$ compared to corresponding basal DMSO, and $^{††}P < 0.01$ compared to corresponding ATP in the presence of DMSO.

7.2.12 The ADAM10 antagonist, GI254023X impairs P2X7-induced CD23 shedding from human and murine B cells

To determine a role for ADAM10 in P2X7-induced CD23 shedding, human PBMCs or murine splenic cells were preincubated in the absence or presence of ADAM10 antagonist, 3 μM GI254023X (Ludwig et al. 2005a), and then with ATP, and CD23 expression measured by flow cytometry. GI254023X impaired P2X7-induced CD23 shedding from B cells by 77 ± 20%, 83 ± 29% and 100 ± 0% from human, C57BL/6 and DBA/1 mice, respectively (Figure 7.13). GI254023X did not alter basal CD23

expression in human or DBA/1 B cells (Figure 7.13A, C). In contrast, GI254023X significantly increased basal CD23 expression on C57BL/6 B cells (Figure 7.13B).

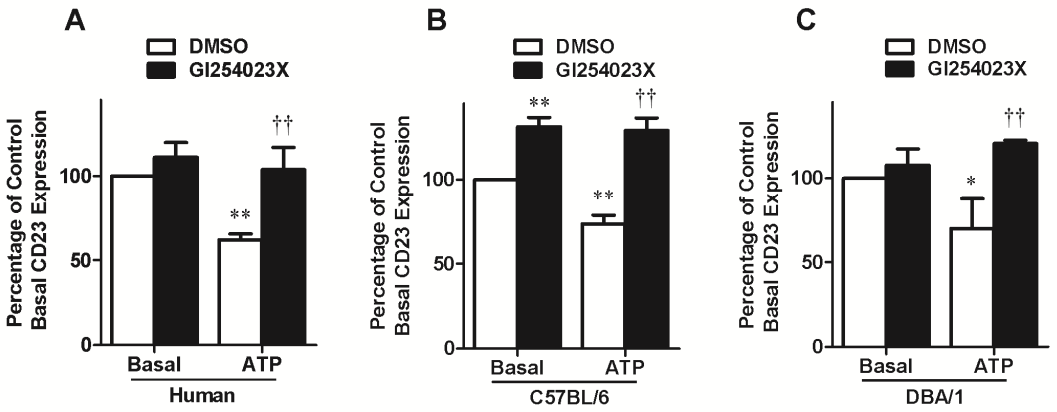

Figure 7.13: The ADAM10 antagonist, GI254023X impairs P2X7-induced CD23 shedding from human and murine B cells. (A) Human PBMCs, and (B) C57BL/6 or (C) DBA/1 murine splenic cells were preincubated in the presence of (A-C) DMSO or 3 μM GI254023X and then in the absence (basal) or presence of 1 mM ATP at 37°C for (A) 6 min or (B, C) 7 min. Incubations were stopped by addition of $MgCl_2$ medium and centrifugation. Cells were labelled with APC-conjugated anti-CD19 mAb, PE- or FITC-conjugated anti-CD23 or isotype control mAb, and 7AAD. The MFI of cell surface CD23 expression on $CD19^+7AAD^-$ B cells was determined by flow cytometry. Results are mean ± SD (n = (A) 3 individuals, or (B, C) 3 mice); $^*P < 0.05$ and $^{**}P < 0.01$ compared to corresponding basal DMSO, and $^{††}P < 0.01$ compared to corresponding ATP in the presence of DMSO.

7.3 Discussion

Data from this chapter shows for the first time that P2X7 activation induces the rapid shedding of CD23 from primary human and murine B cells. This was confirmed by a series of experiments. First, ATP induced the rapid loss of cell surface CD23 shedding

with a $t_{1/2}$ of approximately 6 and 7 min from human and murine B cells, respectively. Second, the most potent P2X7 agonist BzATP also induced the rapid loss of cell surface CD23, whereas the non-agonists ADP and UTP had no effect. Third, a specific P2X7 antagonist, AZ10606120 (Michel et al. 2008), almost completely impaired the ATP-induced cell surface CD23 loss from both human and murine B cells. Fourth, ATP failed to induce CD23 loss from B cells from C57BL/6 P2X7 knockout mice. Finally, measurements of soluble CD23 (as well as total CD23 expression for murine B cells) indicated that cell surface loss of CD23 was due to shedding from both human and murine B cells.

Using the ADAM10 inhibitor, GI254023X (Ludwig et al. 2005a), data from this chapter shows that P2X7-induced CD23 shedding from human and murine B cells is mediated by ADAM10. This finding is consistent with a role for ADAM10 in P2X7-induced CD23 shedding from RPMI 8226 cells (Chapter 6). A potential role for ADAM10 in P2X7-induced CD23 shedding from primary B cells is indirectly supported by other studies. ATP-induced CD23 shedding from human leukaemic monocytic U937 cells (Lemieux et al. 2007), and BzATP-induced CD23 shedding from Chinese hamster ovary cells (Le Gall et al. 2009) and murine B cells (Le Gall et al. 2010), are also mediated by ADAM10. Like with P2X7-induced CD23 shedding from RPMI 8226 cells (Chapter 6), the possibility remains that other metalloproteases may also be involved in P2X7-induced CD23 shedding from human and murine B cells. ADAM 8, 15, 28 and 33 have been associated with constitutive CD23 shedding from CD23-transfected HEK 293 cells (Fourie et al. 2003) and primary murine embryonic fibroblasts (Weskamp et al. 2006), although ADAM10 was identified as the principal sheddase of CD23 (Weskamp et al. 2006).

The current chapter also demonstrates the presence of functional P2X7 on murine B cells from both C57BL/6 and DBA/1 mice. Although the presence of functional P2X7 on human B cells is well established (Gu et al. 2000, Gu et al. 2001, Sluyter et al. 2001), reports of functional P2X7 on murine B cells are limited, with some studies indicating murine B cells do not respond to ATP (Chused et al. 1996, Tsukimoto et al. 2006) nor express P2X7 (Chused et al. 1996, Taylor et al. 2009a). In the current chapter, P2X7 activation induced CD23 shedding from murine B cells. Moreover, ATP was shown to induce YO-PRO-1^{2+} uptake into murine B cells, and that the process was impaired by AZ10606120. Consistent with this result, ATP fails to induce YO-PRO-1^{2+} uptake into B cells from P2X7 knockout mice (Geraghty and Sluyter, *personal communication*). Of note, the relative amounts of P2X7-mediated YO-PRO-1^{2+} uptake and rates of P2X7-mediated CD23 shedding were similar between C57BL/6 and DBA/1 mice. This similar amount of relative P2X7 function most likely reflects the presence of the partial loss-of-function mutation P451L in both of these strains (Adriouch et al. 2002, Syberg et al. 2012).

Fixation and permeabilisation of murine splenic cells was used to show that P2X7-induced CD23 loss from murine B cells was due to shedding rather than internalisation. This was assessed using the method published by Schmid and colleagues (Schmid et al. 1991), due to the initial unavailability of an ELISA for murine soluble CD23. TLR-9 is expressed intracellularly in RPMI 8226 cells (Takeshita et al. 2004) and was used to validate this method. This method showed that P2X7 activation induces the shedding, rather than internalisation of CD23 from splenic murine B cells. During the course of this investigation, a murine CD23 ELISA became available and

was used to confirm that P2X7 activation induces the shedding of CD23 from splenic cells.

In conclusion, data from this chapter demonstrates human and murine P2X7 activation induces the rapid shedding of CD23 from B cells. Moreover, the data indicates a role for ADAM10 in this process.

CHAPTER 8

Conclusions and significance

8.1 Conclusions and significance

Purinergic signalling induces an array of cellular processes and physiological responses, including inflammation and other pathological conditions (Lazarowski et al. 2003, Burnstock 2007). Purinergic signalling is mediated by extracellular nucleotides and nucleosides that activate P2 receptors (Lazarowski et al. 2003, Burnstock 2007). The P2X7 receptor is a ligand-gated cation channel, which is expressed on a variety of cell types, including B cells (Lenertz et al. 2011, Wiley et al. 2011). Adenosine 5'-triphosphate (ATP) activation of P2X7 allows a flux of cations across the cell membrane (Surprenant et al. 1996, Rassendren et al. 1997, Chessell et al. 1998b). Prolonged ATP activation induces cell permeabilisation or pore formation, which allows the uptake of large cations including ethidium^{+} and YO-PRO-1^{2+} (Jiang et al. 2005, Cankurtaran-Sayar et al. 2009). P2X7 activation also induces a variety of downstream events including interleukin (IL)-1 secretion (section 1.4.5.1), cell death and proliferation (section 1.4.5.2), transcription factor activation (section 1.4.5.3), reactive oxygen species (ROS) formation (section 1.4.5.4) and membrane-related changes (section 1.4.5.5), including the shedding of cell surface molecule, CD23 (section 1.5). Prior to the commencement of this thesis it was known that a disintegrin and metalloprotease (ADAM) 10 constitutively sheds CD23 from the surface of cells (Weskamp et al. 2006, Lemieux et al. 2007), however it was unknown if P2X7-induced CD23 shedding involved ADAM10. Also, prior to this thesis, P2X7 was recognised to play a role in ATP-induced CD23 shedding from malignant B cells (Gu et al. 1998) and cultured dendritic cells (Sluyter and Wiley 2002), but whether this process occurred in primary B cells was unknown.

Previous preliminary data from our laboratory indicated that the RPMI 8226 multiple myeloma B cell line express P2X7 and CD23, and that P2X7 activation induced CD23 shedding from these cells (Farrell 2008). Data from Chapter 3 of this thesis confirmed the presence of functional P2X7 on RPMI 8226 cells and also confirmed that P2X7 activation induces CD23 shedding from these cells. Moreover, data from this chapter revealed that P2X7 function in RPMI 8226 cells is sensitive to extracellular cations, and is increased in both KCl and sucrose medium. This modulation of P2X7 function corresponds with published studies, which showed that extracellular cations impair P2X7 function (Wiley et al. 1992, Michel et al. 1999), while KCl and sucrose medium (due to an absence of Na^+) increases P2X7 function (Michel et al. 1999). This chapter also showed that the new generation P2X7 antagonists A-438079 (Nelson et al. 2006), AZ10606120 (Michel et al. 2008) and AZ11645373 (Stokes et al. 2006), which were well-characterised using recombinant P2X7, are also potent antagonists of endogenous P2X7 in RPMI 8226 cells. In particular, AZ10606120 near-completely impaired both ATP-induced ethidium$^+$ uptake (pore formation) and CD23 shedding (Chapter 3). In summary, results from this chapter validated the use of the RPMI 8226 cell line as a suitable model to study the molecules and processes involved in P2X7-induced CD23 shedding.

Using a candidate approach (Chapter 4), it was shown that several signalling pathways involved in P2X7-induced responses, as well as changes in intracellular cation concentrations, which affect P2X7-induced responses, were not involved in P2X7-induced CD23 shedding from RPMI 8226 cells. Future studies, using large antagonist libraries and a high throughput assay may prove a more useful approach to identify potential signalling pathways in P2X7-induced CD23 shedding. During this

thesis, the ROS, mitochondrial superoxide, was shown to enhance P2X7-induced CD62L shedding from T cells (Foster et al. 2013), suggesting that ROS may also play a role in P2X7-induced CD23 shedding. However, ROS-inducing compounds did not affect P2X7-induced CD23 shedding from RPMI 8226 cells (Chapter 5). Although ROS produced as a result of these compounds did not seem to play a role in P2X7-induced CD23 shedding, P2X7 activation induced significant ROS formation in RPMI 8226 cells (Chapter 5). ROS formation after ATP treatment is involved in the ATP-induced shedding of transforming growth factor-α (Myers et al. 2009), and therefore it is possible that ROS formation after P2X7 activation influences CD23 shedding. However, in this case, it is unlikely, as the ROS inducing compounds diphenyleneiodonium and rotenone (Foster et al. 2013), which have also been used as ROS inhibitors (Seil et al. 2008, Wang and Sluyter 2013) did not alter P2X7-induced CD23 shedding from RPMI 8226 cells (Chapter 5). Thus neither this line of investigation nor the source of ROS formed downstream of P2X7 activation was examined further. There is also a lack of data showing a role for P2X7-induced ROS formation in primary B cells, thus it would be of interest to determine whether P2X7 activation induces ROS formation in primary B cells, and if so to determine the origins and biological significance of P2X7-induced ROS formation in these cells.

The phospholipase D (PLD) antagonists halopemide, CAY10593 (VU0155069) and CAY10594 significantly impaired CD23 shedding from RPMI 8226 cells by blocking P2X7 directly (Chapter 4). CAY10593 and CAY10594 impaired P2X7 at concentrations higher than previously used to directly target PLD (Scott et al. 2009). The PLD1 antagonist CAY10593, was particularly potent, impairing P2X7 independently of PLD1, with a half maximal inhibitory concentration (IC_{50}) of

approximately 2 μM (Chapter 4), which is similar, or lower to the IC_{50} values of the non-selective P2 receptor antagonists pyridoxal phosphate-6-azophenyl-2-4-disulphonic acid (PPADs) and suramin, respectively (Chessell et al. 1998a). This suggests that the CAY10593 scaffold may be useful in the future design of new P2X7 antagonists. Several potent P2X7 compounds have been created in this manner, including MRS 2540 which was based on the KN-62 scaffold (Lee et al. 2008, Hu et al. 2010). Furthermore, this data also indicates that it is becoming increasingly important to ensure that antagonists used in signalling studies do not directly affect P2X7. A growing list of compounds that target signalling molecules downstream of P2X7 have been shown to impair P2X7, including the protein kinase C antagonists, chelerythrine (Shemon et al. 2004) and Ro 31-8220 (Shemon et al. 2007), and the mitogen activated protein kinase antagonists, SB203580 and SB202190 (Michel et al. 2006).

Data from this thesis also showed that the pannexin-1 antagonist, probenecid (Silverman et al. 2009), impaired ATP-induced ethidium$^+$ uptake (Chapter 3), but not ATP-induced CD23 shedding from RPMI 8226 cells (Chapter 4). The reason for this remains unknown, however probenecid impaired ATP-induced ethidium$^+$ uptake by less than 50% (Chapter 3) and may be less effective at impairing events downstream of P2X7 activation such as ATP-induced CD23 shedding. Consistent with this, CAY10593 is a more potent blocker of ATP-induced ethidium$^+$ uptake than ATP-induced CD23 shedding (Chapter 4). However, CAY10594 and halopemide, which weakly impaired ATP-induced ethidium$^+$ uptake, also weakly impaired ATP-induced CD23 shedding (Chapter 4). An alternate explanation for the observations with probenecid, is that this compound may impair P2X7-mediated events dependent on ion fluxes but not those independent of ion fluxes, such as ATP-induced CD23 shedding. Recent data indicates

that probenecid impairs both P2X7-induced channel activity and dye uptake independently of pannexin-1 in P2X7-transfected HEK 293 cells (Bhaskaracharya et al. 2014). Further, probenecid also impairs P2X7-mediated IL-1β release (Bhaskaracharya et al. 2014), a process dependent on K^+ efflux (Perregaux and Gabel 1994). If this is the case, probenecid may be a useful tool to segregate P2X7-mediated events dependent on ion fluxes from those not dependent on ion fluxes.

For the first time, data from this thesis showed that ADAM10 mediates P2X7-induced CD23 shedding from RPMI 8226 cells (Chapter 6), and from primary murine and human B cells (Chapter 7). Remarkably, the rate of P2X7-induced CD23 shedding from human and murine B cells was similar to that observed for RPMI 8226 cells ($t_{1/2}$ of ~7 min) (Chapters 3 and 7). This indirectly supports the involvement of a common mechanism. Also for the first time, data from this thesis showed that P2X7 activation induces the shedding of CXCL16 (Chapter 6), another ADAM10 substrate (Abel et al. 2004, Gough et al. 2004, Ludwig et al. 2005b, Hundhausen et al. 2007), confirming that P2X7 activates ADAM10. To further confirm a role for ADAM10 in P2X7-induced CD23 shedding, several attempts were made to knockdown ADAM10 using short inhibitory RNA (siRNA) in RPMI 8226 cells. These however, were unsuccessful due to the difficulty of transient transfection of these cells (results not shown). A recent study outlines a more efficient way of transiently transfecting siRNA into multiple myeloma cells using electroporation (Steinbrunn et al. 2014), which will be of use for future experiments.

The possibility remains that other metalloproteases may also be involved in P2X7-induced CD23 shedding from human and murine B cells. ADAM 8, 15, 28 and 33 have been associated with constitutive CD23 shedding from CD23-transfected HEK 293 cells (Fourie et al. 2003) and primary murine embryonic fibroblasts (Weskamp et al. 2006), although ADAM10 was identified as the principal sheddase of CD23 (Weskamp et al. 2006). To assess whether any of these metalloproteases affect P2X7-induced CD23 shedding, future experiments should determine whether these are expressed in RPMI 8226 cells, and using siRNA knockdown (with electroporation), assess the effects of these ADAMs on P2X7-induced CD23 shedding. The involvement of these metalloproteases downstream of P2X7 activation is also further complicated by their ability to induce the shedding of ADAM10 from cells (Tousseyn et al. 2009). Currently, there is no indication that P2X7 activation induces the shedding of ADAM10, however, an enzyme-linked immunosorbent assay or immunoblotting could be used to examine this.

As noted above, the candidate approach used in Chapter 4 failed to identify potential intracellular signalling molecules involved in P2X7-induced CD23 shedding. Thus, the possibility remains that P2X7 activation induces cell surface CD23 shedding through the colocalisation of ADAM10 and CD23, rather than by directly stimulating ADAM10. ADAM10 has been shown to colocalise with CD44, the hyaluronic acid receptor (Anderegg et al. 2009), a molecule that is also shed after P2X7 activation (Lin et al. 2012). Confocal microscopy could be used in future studies to determine whether ADAM10 colocalises with CD23 following P2X7 activation.

Data from this thesis also showed for the first time the presence of three non-synonymous P2X7 single nucleotide polymorphisms (SNPs) in RPMI 8226 cells; the A348T gain-of-function SNP (Cabrini et al. 2005, Roger et al. 2010, Stokes et al. 2010), the A433V SNP, which may be an additional gain-of-function SNP (Roger et al. 2010, Stokes et al. 2010) and the H521Q SNP, which partly impairs P2X7 channel activity (Roger et al. 2010). The presence of these gain-of-function SNPs may account for the large amount of ATP-induced ethidium^{+} uptake in RPMI 8226 cells relative to other cell lines (Farrell 2008, Pupovac 2009, Gadeock 2010). It would be of interest to assess whether P2X7 SNPs affect P2X7-induced CD23 or CXCL16 shedding. Studies have shown that the P2X7 loss-of-function SNP, G496A is associated with a slower ATP-induced loss of CD23 from human monocyte-derived dendritic cells (Sluyter and Wiley 2002), and CD62L from human CD4^{+} and CD8^{+} T cells (Sluyter and Wiley 2014), while the gain-of-function SNP A348T, is associated with increased IL-1β secretion from lipopolysaccharide (LPS)-primed human monocytes (Stokes et al. 2010). Furthermore, it would also be of future interest to determine if P2X7 splice variants (Cheewatrakoolpong et al. 2005, Adinolfi et al. 2010) mediate ATP-induced CD23 or CXCL16 shedding.

A previous study has shown that LPS can induce CD23 shedding from human and murine B cells, and that this process is mediated by Toll-like receptor 4 (TLR4) and matrix metalloprotease 9 (Jackson et al. 2009). However it remains unlikely that LPS, potentially present in the reagents used, was responsible for the ATP-induced CD23 shedding observed in the current study. First, ATP induced the rapid (< 30 min) shedding of CD23 (Chapters 3 and 7); in contrast LPS induces the slow (24 h) shedding of CD23 (Jackson et al. 2009). Second, ADP and UTP (prepared in the same solution as

those for ATP) failed to induce CD23 shedding (Chapter 7). Third, ATP-induced CD23 shedding was impaired by P2X7 antagonists from both RPMI 8226 cells (Chapter 3) and primary B cells (Chapter 7), as well as in B cells from P2X7 knockout mice (Chapter 7). Nevertheless, future studies using B cells from either C3H/HeJ mice, which are hyporesponsive to LPS due to single point mutation in the *TLR4* gene (Hoshino et al. 1999), or TLR4 knockout mice will be of value to address this potential issue further.

There is a possibility that ATP-induced CD23 shedding is an early event of P2X7-mediated apoptosis. In the current study, 30 min incubation with ATP caused a small but significant amount of apoptosis, determined by forward scatter (cell shrinkage) and 7AAD uptake (loss of membrane integrity) (Philpott et al. 1996), in primary murine but not primary human B cells compared to respective B cells incubated in the absence of ATP (results not shown). In contrast, human and murine B cell apoptosis was not increased following 6-7 min treatment with either ATP or BzATP compared to control treatment, nor was B cell apoptosis increased following incubation with AZ10606120 in the absence or presence of ATP (results not shown). Furthermore, control and ATP-treated RPMI 8226 cells showed similar gated percentages continuously throughout experiments. Nevertheless, given that P2X7 activation can induce apoptosis at 24h in human peripheral blood mononuclear cells (Gu et al. 2001), murine splenic cells (Tsukimoto et al. 2006) and RPMI 8226 cells (Farrell 2008), the possibility remains that ATP-induced CD23 shedding is an early upstream event in P2X7-mediated apoptosis of B cells.

Human genetic (Portales-Cervantes et al. 2012, Lester et al. 2013) and murine model studies (Labasi et al. 2002, Woods et al. 2012) suggest a role for P2X7 in rheumatoid arthritis and Sjogren's syndrome. The role of P2X7 in these disorders has largely been attributed to the release of the proinflammatory cytokines, IL-1β and IL-18 (Labasi et al. 2002, Baldini et al. 2013). However, synovial soluble CD23 (Huissoon et al. 2000, Ribbens et al. 2000) and CXCL16 (Ribbens et al. 2000, Nanki et al. 2005) are elevated in patients with rheumatoid arthritis, and circulating soluble CD23 is elevated in Sjogren's syndrome (Bansal et al. 1992). Moreover, B cells also play major roles in the pathogenesis of these disorders (Bendaoud et al. 1991, Schellekens et al. 1998). Thus, the possibility remains that P2X7-induced shedding of proinflammatory soluble CD23 and CXCL16 from B cells may also be involved in rheumatoid arthritis, Sjogren's syndrome or other disorders. However, evidence directly linking B cells, P2X7, CD23 and CXCL16 in inflammatory and autoimmune disease is lacking.

Overall, this study shows, for the first time that ADAM10 mediates P2X7-induced CD23 and CXCL16 shedding from RPMI 8226 cells, as well as CD23 from primary human and murine B cells (Figure 8.1). Moreover, this study excludes a potential role for various signalling molecules including ROS and the flux of various cations in P2X7-induced CD23 shedding. Finally, this study shows that the PLD1 antagonist, CAY10593 (VU0155069), impairs P2X7 independently of PLD1 (Figure 8.1).

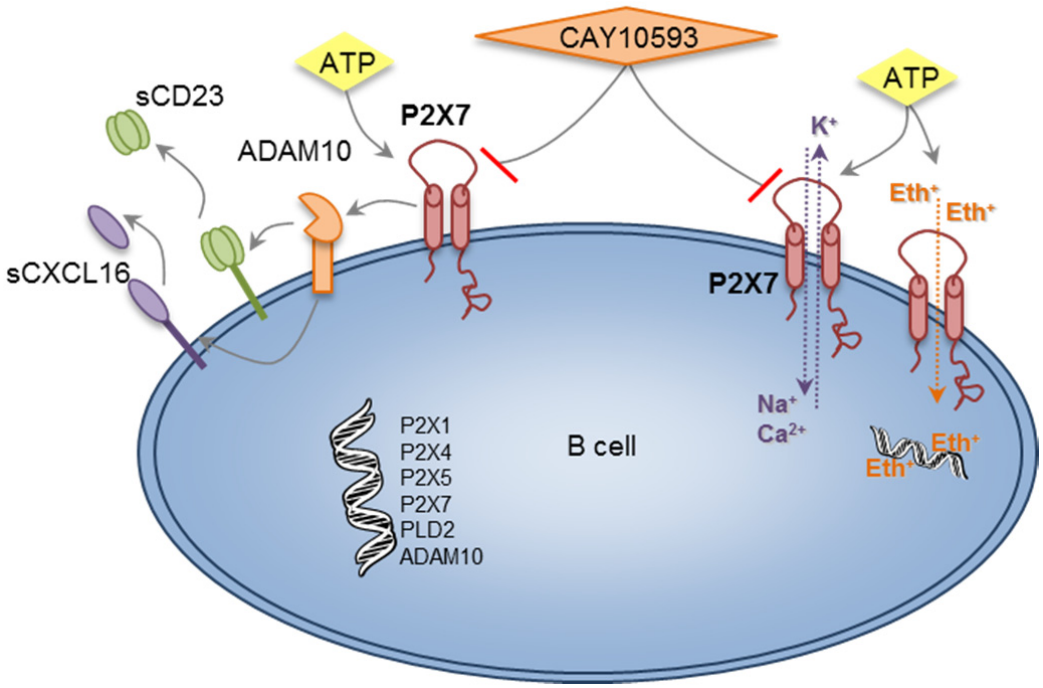

Figure 8.1: Summary schematic of the main findings in this thesis. ADAM10 mediates P2X7-induced CD23 and CXCL16 shedding from RPMI 8226 B cells, as well as CD23 from primary human and murine B cells. RPMI 8226 cells express P2X1, P2X4, P2X5, PLD2 and ADAM10 mRNA. The PLD1 antagonist, CAY10593 (VU0155069), impairs P2X7-induced CD23 shedding, P2X7 channel and pore formation independently of PLD1. **Abbreviations:** ATP, adenosine 5'-triphosphate; ADAM, a disintegrin and metalloprotease, Eth^+, $Ethidium^+$, PLD, phospholipase D; sCD23, soluble CD23; sCXCL16, soluble CXCL16.

REFERENCES

Abel, S., Hundhausen, C., Mentlein, R., Schulte, A., Berkhout, T. A., Broadway, N., Hartmann, D., Sedlacek, R., Dietrich, S., Muetze, B., Schuster, B., Kallen, K. J., Saftig, P., Rose-John, S. and Ludwig, A. (2004). "The transmembrane CXC-chemokine ligand 16 is induced by IFN-γ and TNF-α and shed by the activity of the disintegrin-like metalloproteinase ADAM10". J Immunol **172**(10): 6362-6372.

Acharya, M., Borland, G., Edkins, A. L., Maclellan, L. M., Matheson, J., Ozanne, B. W. and Cushley, W. (2010). "CD23/FcεRII: molecular multi-tasking". Clin Exp Immunol **162**(1): 12-23.

Acuna-Castillo, C., Coddou, C., Bull, P., Brito, J. and Huidobro-Toro, J. P. (2007). "Differential role of extracellular histidines in copper, zinc, magnesium and proton modulation of the P2X7 purinergic receptor". J Neurochem **101**(1): 17-26.

Adinolfi, E., Amoroso, F. and Giuliani, A. L. (2012). "P2X7 receptor function in bone-related cancer". J Osteoporos **2012**: 637863.

Adinolfi, E., Cirillo, M., Woltersdorf, R., Falzoni, S., Chiozzi, P., Pellegatti, P., Callegari, M. G., Sandona, D., Markwardt, F., Schmalzing, G. and Di Virgilio, F. (2010). "Trophic activity of a naturally occurring truncated isoform of the P2X7 receptor". FASEB J **24**(9): 3393-3404.

Adriouch, S., Dox, C., Welge, V., Seman, M., Koch-Nolte, F. and Haag, F. (2002). "Cutting edge: a natural P451L mutation in the cytoplasmic domain impairs the function of the mouse P2X7 receptor". J Immunol **169**(8): 4108-4112.

Agematsu, K., Kobata, T., Sugita, K., Freeman, G. J., Beckmann, M. P., Schlossman, S. F. and Morimoto, C. (1994). "Role of CD27 in T cell immune response. Analysis by recombinant soluble CD27". J Immunol **153**(4): 1421-1429.

Aichem, A., Masilamani, M. and Illges, H. (2006). "Redox regulation of CD21 shedding involves signaling via PKC and indicates the formation of a juxtamembrane stalk". J Cell Sci **119**(Pt 14): 2892-2902.

Al-Sadoon, M. K., Rabah, D. M. and Badr, G. (2013). "Enhanced anticancer efficacy of snake venom combined with silica nanoparticles in a murine model of human multiple myeloma: molecular targets for cell cycle arrest and apoptosis induction". Cell Immunol **284**(1-2): 129-138.

Al-Shukaili, A., Al-Kaabi, J., Hassan, B., Al-Araimi, T., Al-Tobi, M., Al-Kindi, M., Al-Maniri, A., Al-Gheilani, A. and Al-Ansari, A. (2011). "P2X7 receptor gene polymorphism analysis in rheumatoid arthritis". Int J Immunogenet **38**(5): 389-396.

Alberto, A. V., Faria, R. X., Couto, C. G., Ferreira, L. G., Souza, C. A., Teixeira, P. C., Froes, M. M. and Alves, L. A. (2013). "Is pannexin the pore associated with the P2X7 receptor?". Naunyn Schmiedebergs Arch Pharmacol **386**(9): 775-787.

Anderegg, U., Eichenberg, T., Parthaune, T., Haiduk, C., Saalbach, A., Milkova, L., Ludwig, A., Grosche, J., Averbeck, M., Gebhardt, C., Voelcker, V., Sleeman, J. P. and Simon, J. C. (2009). "ADAM10 is the constitutive functional sheddase of CD44 in human melanoma cells". J Invest Dermatol **129**(6): 1471-1482.

Andrei, C., Margiocco, P., Poggi, A., Lotti, L. V., Torrisi, M. R. and Rubartelli, A. (2004). "Phospholipases C and A_2 control lysosome-mediated IL-1β secretion: Implications for inflammatory processes". Proc Natl Acad Sci U S A **101**(26): 9745-9750.

Armant, M., Rubio, M., Delespesse, G. and Sarfati, M. (1995). "Soluble CD23 directly activates monocytes to contribute to the antigen-independent stimulation of resting T cells". J Immunol **155**(10): 4868-4875.

Armitage, R. J., Goff, L. K. and Beverley, P. C. (1989). "Expression and functional role of CD23 on T cells". Eur J Immunol **19**(1): 31-35.

Arribas, J., Coodly, L., Vollmer, P., Kishimoto, T. K., Rose-John, S. and Massague, J. (1996). "Diverse cell surface protein ectodomains are shed by a system sensitive to metalloprotease inhibitors". J Biol Chem **271**(19): 11376-11382.

Aswad, F. and Dennert, G. (2006). "$P2X_7$ receptor expression levels determine lethal effects of a purine based danger signal in T lymphocytes". Cell Immunol **243**(1): 58-65.

Baldini, C., Rossi, C., Ferro, F., Santini, E., Seccia, V., Donati, V. and Solini, A. (2013). "The P2X7 receptor-inflammasome complex has a role in modulating the inflammatory response in primary Sjogren's syndrome". J Intern Med **274**(5): 480-489.

Bansal, A., Roberts, T., Hay, E. M., Kay, R., Pumphrey, R. S. and Wilson, P. B. (1992). "Soluble CD23 levels are elevated in the serum of patients with primary Sjogren's syndrome and systemic lupus erythematosus". Clin Exp Immunol **89**(3): 452-455.

Bansal, A. S., Haeney, M. R., Cochrane, S., Pumphrey, R. S., Green, L. M., Bhavnani, M. and Wilson, P. B. (1994). "Serum soluble CD23 in patients with hypogammaglobulinaemia". Clin Exp Immunol **97**(2): 239-241.

Barbera-Cremades, M., Baroja-Mazo, A., Gomez, A. I., Machado, F., Di Virgilio, F. and Pelegrin, P. (2012). "P2X7 receptor-stimulation causes fever via PGE2 and IL-1β release". FASEB J **26**(7): 2951-2962.

Barden, N., Harvey, M., Gagne, B., Shink, E., Tremblay, M., Raymond, C., Labbe, M., Villeneuve, A., Rochette, D., Bordeleau, L., Stadler, H., Holsboer, F. and Muller-Myhsok, B. (2006). "Analysis of single nucleotide polymorphisms in genes in the chromosome 12Q24.31 region points to P2RX7 as a susceptibility gene to bipolar affective disorder". Am J Med Genet B Neuropsychiatr Genet **141B**(4): 374-382.

Baroja-Mazo, A., Barbera-Cremades, M. and Pelegrin, P. (2013). "P2X7 receptor activation impairs exogenous MHC class I oligopeptides presentation in antigen presenting cells". PLoS One **8**(8): e70577.

Bartlett, R., Stokes, L. and Sluyter, R. (2014). "The P2X7 receptor channel: recent developments and the use of P2X7 antagonists in models of disease". Pharmacol Rev **66**(3): 638-675.

Bartlett, R., Yerbury, J. J. and Sluyter, R. (2013). "P2X7 receptor activation induces reactive oxygen species formation and cell death in murine EOC13 microglia". Mediators Inflamm **2013**: 271813.

Bazan, J. F., Bacon, K. B., Hardiman, G., Wang, W., Soo, K., Rossi, D., Greaves, D. R., Zlotnik, A. and Schall, T. J. (1997). "A new class of membrane-bound chemokine with a CX3C motif". Nature **385**(6617): 640-644.

Beaucage, K. L., Xiao, A., Pollmann, S. I., Grol, M. W., Beach, R. J., Holdsworth, D. W., Sims, S. M., Darling, M. R. and Dixon, S. J. (2014). "Loss of P2X7 nucleotide receptor function leads to abnormal fat distribution in mice". Purinergic Signal **10**(2): 291-304.

Becherel, P. A., LeGoff, L., Frances, C., Chosidow, O., Guillosson, J. J., Debre, P., Mossalayi, M. D. and Arock, M. (1997). "Induction of IL-10 synthesis by human keratinocytes through CD23 ligation: a cyclic adenosine 3',5'-monophosphate-dependent mechanism". J Immunol **159**(12): 5761-5765.

Belleudi, F., Leone, L., Aimati, L., Stirparo, M. G., Cardinali, G., Marchese, C., Frati, L., Picardo, M. and Torrisi, M. R. (2006). "Endocytic pathways and biological effects induced by UVB-dependent or ligand-dependent activation of the keratinocyte growth factor receptor". FASEB J **20**(2): 395-397.

Bendaoud, B., Pennec, Y. L., Lelong, A., Le Noac'h, J. F., Magadur, G., Jouquan, J. and Youinou, P. (1991). "IgA-containing immune complexes in the circulation of patients with primary Sjogren's syndrome". J Autoimmun **4**(1): 177-184.

Bertho, J. M., Fourcade, C., Dalloul, A. H., Debre, P. and Mossalayi, M. D. (1991). "Synergistic effect of interleukin 1 and soluble CD23 on the growth of human $CD4^+$ bone marrow-derived T cells". Eur J Immunol **21**(4): 1073-1076.

Bhaskaracharya, A., Dao-Ung, P., Jalilian, I., Spildrejorde, M., Skarratt, K. K., Fuller, S. J., Sluyter, R. and Stokes, L. (2014). "Probenecid blocks human P2X7 receptor-induced dye uptake via a pannexin-1 independent mechanism". PLoS One **9**(3): e93058.

Bianchi, B. R., Lynch, K. J., Touma, E., Niforatos, W., Burgard, E. C., Alexander, K. M., Park, H. S., Yu, H., Metzger, R., Kowaluk, E., Jarvis, M. F. and van Biesen, T. (1999). "Pharmacological characterization of recombinant human and rat P2X receptor subtypes". Eur J Pharmacol **376**(1-2): 127-138.

Bianco, F., Ceruti, S., Colombo, A., Fumagalli, M., Ferrari, D., Pizzirani, C., Matteoli, M., Di Virgilio, F., Abbracchio, M. P. and Verderio, C. (2006). "A role for $P2X_7$ in microglial proliferation". J Neurochem **99**(3): 745-758.

Bianco, F., Perrotta, C., Novellino, L., Francolini, M., Riganti, L., Menna, E., Saglietti, L., Schuchman, E. H., Furlan, R., Clementi, E., Matteoli, M. and Verderio, C. (2009). "Acid sphingomyelinase activity triggers microparticle release from glial cells". EMBO J **28**(8): 1043-1054.

Bieber, T., Rieger, A., Neuchrist, C., Prinz, J. C., Rieber, E. P., Boltz-Nitulescu, G., Scheiner, O., Kraft, D., Ring, J. and Stingl, G. (1989). "Induction of FcεR2/CD23 on human epidermal Langerhans cells by human recombinant interleukin 4 and γ interferon". J Exp Med **170**(1): 309-314.

Bjorck, P., Elenstrom-Magnusson, C., Rosen, A., Severinson, E. and Paulie, S. (1993). "CD23 and CD21 function as adhesion molecules in homotypic aggregation of human B lymphocytes". Eur J Immunol **23**(8): 1771-1775.

Bles, N., Di Pietrantonio, L., Boeynaems, J. M. and Communi, D. (2010). "ATP confers tumorigenic properties to dendritic cells by inducing amphiregulin secretion". Blood **116**(17): 3219-3226.

Bo, X., Jiang, L. H., Wilson, H. L., Kim, M., Burnstock, G., Surprenant, A. and North, R. A. (2003). "Pharmacological and biophysical properties of the human P2X5 receptor". Mol Pharmacol **63**(6): 1407-1416.

Boots, A. W., Hristova, M., Kasahara, D. I., Haenen, G. R., Bast, A. and van der Vliet, A. (2009). "ATP-mediated activation of the NADPH oxidase DUOX1 mediates airway epithelial responses to bacterial stimuli". J Biol Chem **284**(26): 17858-17867.

Borland, G., Edkins, A. L., Acharya, M., Matheson, J., White, L. J., Allen, J. M., Bonnefoy, J. Y., Ozanne, B. W. and Cushley, W. (2007). "αvβ5 integrin sustains growth of human pre-B cells through an RGD-independent interaction with a basic domain of the CD23 protein". J Biol Chem **282**(37): 27315-27326.

Bradley, H. J., Baldwin, J. M., Goli, G. R., Johnson, B., Zou, J., Sivaprasadarao, A., Baldwin, S. A. and Jiang, L. H. (2011a). "Residues 155 and 348 contribute to the determination of $P2X_7$ receptor function via distinct mechanisms revealed by single-nucleotide polymorphisms". J Biol Chem **286**(10): 8176-8187.

Bradley, H. J., Browne, L. E., Yang, W. and Jiang, L. H. (2011b). "Pharmacological properties of the rhesus macaque monkey P2X7 receptor". Br J Pharmacol **164**(2b): 743-754.

Brough, D., Le Feuvre, R. A., Wheeler, R. D., Solovyova, N., Hilfiker, S., Rothwell, N. J. and Verkhratsky, A. (2003). "Ca^{2+} stores and Ca^{2+} entry differentially contribute to the release of IL-1β and IL-1α from murine macrophages". J Immunol **170**(6): 3029-3036.

Browne, L. E., Compan, V., Bragg, L. and North, R. A. (2013). "P2X7 receptor channels allow direct permeation of nanometer-sized dyes". J Neurosci **33**(8): 3557-3566.

Browne, L. E., Jiang, L. H. and North, R. A. (2010). "New structure enlivens interest in P2X receptors". Trends Pharmacol Sci **31**(5): 229-237.

Burnstock, G. (2007). "Physiology and pathophysiology of purinergic neurotransmission". Physiol Rev **87**(2): 659-797.

Burnstock, G. and Knight, G. E. (2004). "Cellular distribution and functions of P2 receptor subtypes in different systems". Int Rev Cytol **240**: 31-304.

Cabrini, G., Falzoni, S., Forchap, S. L., Pellegatti, P., Balboni, A., Agostini, P., Cuneo, A., Castoldi, G., Baricordi, O. R. and Di Virgilio, F. (2005). "A His-155 to Tyr polymorphism confers gain-of-function to the human $P2X_7$ receptor of human leukemic lymphocytes". J Immunol **175**(1): 82-89.

Cairns, J. A. and Gordon, J. (1990). "Intact, 45-kDa (membrane) form of CD23 is consistently mitogenic for normal and transformed B lymphoblasts". Eur J Immunol **20**(3): 539-543.

Camden, J. M., Schrader, A. M., Camden, R. E., Gonzalez, F. A., Erb, L., Seye, C. I. and Weisman, G. A. (2005). "$P2Y_2$ nucleotide receptors enhance α-secretase-dependent amyloid precursor protein processing". J Biol Chem **280**(19): 18696-18702.

Camerini, D., Walz, G., Loenen, W. A., Borst, J. and Seed, B. (1991). "The T cell activation antigen CD27 is a member of the nerve growth factor/tumor necrosis factor receptor gene family". J Immunol **147**(9): 3165-3169.

Canel, M., Serrels, A., Frame, M. C. and Brunton, V. G. (2013). "E-cadherin-integrin crosstalk in cancer invasion and metastasis". J Cell Sci **126**(Pt 2): 393-401.

Cankurtaran-Sayar, S., Sayar, K. and Ugur, M. (2009). "P2X7 receptor activates multiple selective dye-permeation pathways in RAW 264.7 and human embryonic kidney 293 cells". Mol Pharmacol **76**(6): 1323-1332.

Cascabulho, C. M., Bani Correa, C., Cotta-de-Almeida, V. and Henriques-Pons, A. (2012). "Defective T-lymphocyte migration to muscles in dystrophin-deficient mice". Am J Pathol **181**(2): 593-604.

Chalaris, A., Garbers, C., Rabe, B., Rose-John, S. and Scheller, J. (2011). "The soluble Interleukin 6 receptor: generation and role in inflammation and cancer". Eur J Cell Biol **90**(6-7): 484-494.

Chandrasekar, B., Bysani, S. and Mummidi, S. (2004). "CXCL16 signals via Gi, phosphatidylinositol 3-kinase, Akt, IκB kinase, and nuclear factor-κB and induces cell-cell adhesion and aortic smooth muscle cell proliferation". J Biol Chem **279**(5): 3188-3196.

Chandrasekar, B., Mummidi, S., Valente, A. J., Patel, D. N., Bailey, S. R., Freeman, G. L., Hatano, M., Tokuhisa, T. and Jensen, L. E. (2005). "The pro-atherogenic cytokine

interleukin-18 induces CXCL16 expression in rat aortic smooth muscle cells via MyD88, interleukin-1 receptor-associated kinase, tumor necrosis factor receptor-associated factor 6, c-Src, phosphatidylinositol 3-kinase, Akt, c-Jun N-terminal kinase, and activator protein-1 signaling". J Biol Chem **280**(28): 26263-26277.

Chaumont, S. and Khakh, B. S. (2008). "Patch-clamp coordinated spectroscopy shows $P2X_2$ receptor permeability dynamics require cytosolic domain rearrangements but not Panx-1 channels". Proc Natl Acad Sci U S A **105**(33): 12063-12068.

Cheewatrakoolpong, B., Gilchrest, H., Anthes, J. C. and Greenfeder, S. (2005). "Identification and characterization of splice variants of the human $P2X_7$ ATP channel". Biochem Biophys Res Commun **332**(1): 17-27.

Chen, J. R., Gu, B. J., Dao, L. P., Bradley, C. J., Mulligan, S. P. and Wiley, J. S. (1999). "Transendothelial migration of lymphocytes in chronic lymphocytic leukaemia is impaired and involved down-regulation of both L-selectin and CD23". Br J Haematol **105**(1): 181-189.

Chen, Z., Koralov, S. B. and Kelsoe, G. (2000). "Regulation of humoral immune responses by CD21/CD35". Immunol Rev **176**: 194-204.

Chessell, I. P., Hatcher, J. P., Bountra, C., Michel, A. D., Hughes, J. P., Green, P., Egerton, J., Murfin, M., Richardson, J., Peck, W. L., Grahames, C. B., Casula, M. A., Yiangou, Y., Birch, R., Anand, P. and Buell, G. N. (2005). "Disruption of the $P2X_7$ purinoceptor gene abolishes chronic inflammatory and neuropathic pain". Pain **114**(3): 386-396.

Chessell, I. P., Michel, A. D. and Humphrey, P. P. (1998a). "Effects of antagonists at the human recombinant P2X7 receptor". Br J Pharmacol **124**(6): 1314-1320.

Chessell, I. P., Simon, J., Hibell, A. D., Michel, A. D., Barnard, E. A. and Humphrey, P. P. (1998b). "Cloning and functional characterisation of the mouse $P2X_7$ receptor". FEBS Lett **439**(1-2): 26-30.

Chetty, C., Vanamala, S. K., Gondi, C. S., Dinh, D. H., Gujrati, M. and Rao, J. S. (2012). "MMP-9 induces CD44 cleavage and CD44 mediated cell migration in glioblastoma xenograft cells". Cell Signal **24**(2): 549-559.

Chihara, J., Gruart, V., Plumas, J., Tavernier, J., Kusnierz, J. P., Prin, L., Capron, A. and Capron, M. (1992). "Induction of CD23, CD25 and CD4 expression on an eosinophilic cell line (EoL-3) by interleukin-3 (IL-3), granulocyte-macrophage colony-stimulating factor (GM-CSF) and interleukin-5 (IL-5)". Eur Cytokine Netw **3**(1): 53-61.

Chused, T. M., Apasov, S. and Sitkovsky, M. (1996). "Murine T lymphocytes modulate activity of an ATP-activated P_{2Z}-type purinoceptor during differentiation". J Immunol **157**(4): 1371-1380.

Communi, D., Robaye, B. and Boeynaems, J. M. (1999). "Pharmacological characterization of the human P2Y11 receptor". Br J Pharmacol **128**(6): 1199-1206.

Compan, V., Ulmann, L., Stelmashenko, O., Chemin, J., Chaumont, S. and Rassendren, F. (2012). "P2X2 and P2X5 subunits define a new heteromeric receptor with P2X7-like properties". J Neurosci **32**(12): 4284-4296.

Constantinescu, P., Wang, B., Kovacevic, K., Jalilian, I., Bosman, G. J., Wiley, J. S. and Sluyter, R. (2010). "P2X7 receptor activation induces cell death and microparticle release in murine erythroleukemia cells". Biochim Biophys Acta **1798**(9): 1797-1804.

Cooper, A. M., Hobson, P. S., Jutton, M. R., Kao, M. W., Drung, B., Schmidt, B., Fear, D. J., Beavil, A. J., McDonnell, J. M., Sutton, B. J. and Gould, H. J. (2012). "Soluble

CD23 controls IgE synthesis and homeostasis in human B cells". J Immunol **188**(7): 3199-3207.

Courageot, M. P., Lepine, S., Hours, M., Giraud, F. and Sulpice, J. C. (2004). "Involvement of sodium in early phosphatidylserine exposure and phospholipid scrambling induced by P2X7 purinoceptor activation in thymocytes". J Biol Chem **279**(21): 21815-21823.

da Cruz, C. M., Ventura, A. L., Schachter, J., Costa-Junior, H. M., da Silva Souza, H. A., Gomes, F. R., Coutinho-Silva, R., Ojcius, D. M. and Persechini, P. M. (2006). "Activation of ERK1/2 by extracellular nucleotides in macrophages is mediated by multiple P2 receptors independently of $P2X_7$-associated pore or channel formation". Br J Pharmacol **147**(3): 324-334.

Dallerac, G., Rampon, C. and Doyere, V. (2013). "NCAM function in the adult brain: lessons from mimetic peptides and therapeutic potential". Neurochem Res **38**(6): 1163-1173.

Darmellah, A., Rayah, A., Auger, R., Cuif, M. H., Prigent, M., Arpin, M., Alcover, A., Delarasse, C. and Kanellopoulos, J. M. (2012). "Ezrin/radixin/moesin are required for the purinergic P2X7 receptor (P2X7R)-dependent processing of the amyloid precursor protein". J Biol Chem **287**(41): 34583-34595.

Davey, E. J., Bartlett, W. C., Kikutani, H., Fujiwara, H., Kishimoto, T., Conrad, D. H. and Severinson, E. (1995). "Homotypic aggregation of murine B lymphocytes is independent of CD23". Eur J Immunol **25**(5): 1224-1229.

Davies, B., Brown, P. D., East, N., Crimmin, M. J. and Balkwill, F. R. (1993). "A synthetic matrix metalloproteinase inhibitor decreases tumor burden and prolongs survival of mice bearing human ovarian carcinoma xenografts". Cancer Res **53**(9): 2087-2091.

Defrance, T., Aubry, J. P., Rousset, F., Vanbervliet, B., Bonnefoy, J. Y., Arai, N., Takebe, Y., Yokota, T., Lee, F., Arai, K. and et al. (1987). "Human recombinant interleukin 4 induces Fcε receptors (CD23) on normal human B lymphocytes". J Exp Med **165**(6): 1459-1467.

Delarasse, C., Auger, R., Gonnord, P., Fontaine, B. and Kanellopoulos, J. M. (2011). "The purinergic receptor P2X7 triggers α-secretase-dependent processing of the amyloid precursor protein". J Biol Chem **286**(4): 2596-2606.

Denault, J. B., D'Orleans-Juste, P., Masaki, T. and Leduc, R. (1995). "Inhibition of convertase-related processing of proendothelin-1". J Cardiovasc Pharmacol **26 Suppl 3**: S47-50.

Dewitz, C., Moller-Hackbarth, K., Schweigert, O., Reiss, K., Chalaris, A., Scheller, J. and Rose-John, S. (2014). "T-cell immunoglobulin and mucin domain 2 (TIM-2) is a target of ADAM10-mediated ectodomain shedding". FEBS J **281**(1): 157-174.

Di Virgilio, F. (2003). "Novel data point to a broader mechanism of action of oxidized ATP: the $P2X_7$ receptor is not the only target". Br J Pharmacol **140**(3): 441-443.

Di Virgilio, F., Steinberg, T. H. and Silverstein, S. C. (1990). "Inhibition of Fura-2 sequestration and secretion with organic anion transport blockers". Cell Calcium **11**(2-3): 57-62.

Diaz-Hernandez, J. I., Gomez-Villafuertes, R., Leon-Otegui, M., Hontecillas-Prieto, L., Del Puerto, A., Trejo, J. L., Lucas, J. J., Garrido, J. J., Gualix, J., Miras-Portugal, M. T. and Diaz-Hernandez, M. (2012). "In vivo P2X7 inhibition reduces amyloid plaques in Alzheimer's disease through GSK3β and secretases". Neurobiol Aging **33**(8): 1816-1828.

Diaz-Hernandez, M., Diez-Zaera, M., Sanchez-Nogueiro, J., Gomez-Villafuertes, R., Canals, J. M., Alberch, J., Miras-Portugal, M. T. and Lucas, J. J. (2009). "Altered P2X7-receptor level and function in mouse models of Huntington's disease and therapeutic efficacy of antagonist administration". FASEB J **23**(6): 1893-1906.

Diegelmann, J., Seiderer, J., Niess, J. H., Haller, D., Goke, B., Reinecker, H. C. and Brand, S. (2010). "Expression and regulation of the chemokine CXCL16 in Crohn's disease and models of intestinal inflammation". Inflamm Bowel Dis **16**(11): 1871-1881.

Donnelly-Roberts, D. L., Namovic, M. T., Faltynek, C. R. and Jarvis, M. F. (2004). "Mitogen-activated protein kinase and caspase signaling pathways are required for $P2X_7$ receptor ($P2X_7R$)-induced pore formation in human THP-1 cells". J Pharmacol Exp Ther **308**(3): 1053-1061.

Donnelly-Roberts, D. L., Namovic, M. T., Han, P. and Jarvis, M. F. (2009). "Mammalian P2X7 receptor pharmacology: comparison of recombinant mouse, rat and human P2X7 receptors". Br J Pharmacol **157**(7): 1203-1214.

el-Moatassim, C. and Dubyak, G. R. (1993). "Dissociation of the pore-forming and phospholipase D activities stimulated via P_{2z} purinergic receptors in BAC1.2F5 macrophages. Product inhibition of phospholipase D enzyme activity". J Biol Chem **268**(21): 15571-15578.

Elliott, J. I. and Higgins, C. F. (2004). "Major histocompatibility complex class I shedding and programmed cell death stimulated through the proinflammatory $P2X_7$ receptor: a candidate susceptibility gene for NOD diabetes". Diabetes **53**(8): 2012-2017.

Elliott, J. I., Surprenant, A., Marelli-Berg, F. M., Cooper, J. C., Cassady-Cain, R. L., Wooding, C., Linton, K., Alexander, D. R. and Higgins, C. F. (2005). "Membrane phosphatidylserine distribution as a non-apoptotic signalling mechanism in lymphocytes". Nat Cell Biol **7**(8): 808-816.

Evans, R. J., Lewis, C., Buell, G., Valera, S., North, R. A. and Surprenant, A. (1995). "Pharmacological characterization of heterologously expressed ATP-gated cation channels (P2x purinoceptors)". Mol Pharmacol **48**(2): 178-183.

Fairbairn, I. P., Stober, C. B., Kumararatne, D. S. and Lammas, D. A. (2001). "ATP-mediated killing of intracellular mycobacteria by macrophages is a $P2X_7$-dependent process inducing bacterial death by phagosome-lysosome fusion". J Immunol **167**(6): 3300-3307.

Faria, R. X., Defarias, F. P. and Alves, L. A. (2005). "Are second messengers crucial for opening the pore associated with $P2X_7$ receptor?". Am J Physiol Cell Physiol **288**(2): C260-271.

Farrell, A. W. (2008). The multiple myeloma RPMI-8226 cell line expresses functional $P2X_7$ receptors. BSc (Honours) Thesis, University of Wollongong.

Feng, Y. H., Li, X., Wang, L., Zhou, L. and Gorodeski, G. I. (2006). "A truncated P2X7 receptor variant ($P2X_{7-j}$) endogenously expressed in cervical cancer cells antagonizes the full-length $P2X_7$ receptor through hetero-oligomerization". J Biol Chem **281**(25): 17228-17237.

Fernando, K. C., Gargett, C. E. and Wiley, J. S. (1999). "Activation of the $P2Z/P2X_7$ receptor in human lymphocytes produces a delayed permeability lesion: involvement of phospholipase D". Arch Biochem Biophys **362**(2): 197-202.

Ferrari, D., Chiozzi, P., Falzoni, S., Dal Susino, M., Melchiorri, L., Baricordi, O. R. and Di Virgilio, F. (1997a). "Extracellular ATP triggers IL-1β release by activating the purinergic P2Z receptor of human macrophages". J Immunol **159**(3): 1451-1458.

Ferrari, D., Stroh, C. and Schulze-Osthoff, K. (1999). "$P2X_7$/P2Z purinoreceptor-mediated activation of transcription factor NFAT in microglial cells". J Biol Chem **274**(19): 13205-13210.

Ferrari, D., Wesselborg, S., Bauer, M. K. and Schulze-Osthoff, K. (1997b). "Extracellular ATP activates transcription factor NF-κB through the P2Z purinoreceptor by selectively targeting NF-κB p65 (RelA)". J Cell Biol **139**(7): 1635-1643.

Flores-Romo, L., Johnson, G. D., Ghaderi, A. A., Stanworth, D. R., Veronesi, A. and Gordon, J. (1990). "Functional implication for the topographical relationship between MHC class II and the low-affinity IgE receptor: occupancy of CD23 prevents B lymphocytes from stimulating allogeneic mixed lymphocyte responses". Eur J Immunol **20**(11): 2465-2469.

Fonfria, E., Clay, W. C., Levy, D. S., Goodwin, J. A., Roman, S., Smith, G. D., Condreay, J. P. and Michel, A. D. (2008). "Cloning and pharmacological characterization of the guinea pig P2X7 receptor orthologue". Br J Pharmacol **153**(3): 544-556.

Foster, J. G., Carter, E., Kilty, I., MacKenzie, A. B. and Ward, S. G. (2013). "Mitochondrial superoxide generation enhances P2X7R-mediated loss of cell surface CD62L on naive human $CD4^+$ T lymphocytes". J Immunol **190**(4): 1551-1559.

Fourcade, C., Arock, M., Ktorza, S., Ouaaz, F., Merle-Beral, H., Mentz, F., Kilchherr, E., Debre, P. and Mossalayi, M. D. (1992). "Expression of CD23 by human bone marrow stromal cells". Eur Cytokine Netw **3**(6): 539-543.

Fourie, A. M., Coles, F., Moreno, V. and Karlsson, L. (2003). "Catalytic activity of ADAM8, ADAM15, and MDC-L (ADAM28) on synthetic peptide substrates and in ectodomain cleavage of CD23". J Biol Chem **278**(33): 30469-30477.

Freeman, G. J., Casasnovas, J. M., Umetsu, D. T. and DeKruyff, R. H. (2010). "TIM genes: a family of cell surface phosphatidylserine receptors that regulate innate and adaptive immunity". Immunol Rev **235**(1): 172-189.

Fremeaux-Bacchi, V., Aubry, J. P., Bonnefoy, J. Y., Kazatchkine, M. D., Kolb, J. P. and Fischer, E. M. (1998a). "Soluble CD21 induces activation and differentiation of human monocytes through binding to membrane CD23". Eur J Immunol **28**(12): 4268-4274.

Fremeaux-Bacchi, V., Fischer, E., Lecoanet-Henchoz, S., Mani, J. C., Bonnefoy, J. Y. and Kazatchkine, M. D. (1998b). "Soluble CD21 (sCD21) forms biologically active complexes with CD23: sCD21 is present in normal plasma as a complex with trimeric CD23 and inhibits soluble CD23-induced IgE synthesis by B cells". Int Immunol **10**(10): 1459-1466.

Gadeock, S. (2010). Expression and function of the P2X7 receptor on human malignant cell lines. MSc Thesis, University of Wollongong.

Garbers, C., Janner, N., Chalaris, A., Moss, M. L., Floss, D. M., Meyer, D., Koch-Nolte, F., Rose-John, S. and Scheller, J. (2011). "Species specificity of ADAM10 and ADAM17 proteins in interleukin-6 (IL-6) trans-signaling and novel role of ADAM10 in inducible IL-6 receptor shedding". J Biol Chem **286**(17): 14804-14811.

Gargett, C. E., Cornish, E. J. and Wiley, J. S. (1996). "Phospholipase D activation by P2Z-purinoceptor agonists in human lymphocytes is dependent on bivalent cation influx". Biochem J **313 (Pt 2)**: 529-535.

Gargett, C. E. and Wiley, J. S. (1997). "The isoquinoline derivative KN-62 a potent antagonist of the P2Z-receptor of human lymphocytes". Br J Pharmacol **120**(8): 1483-1490.

Gartland, A., Skarratt, K. K., Hocking, L. J., Parsons, C., Stokes, L., Jorgensen, N. R., Fraser, W. D., Reid, D. M., Gallagher, J. A. and Wiley, J. S. (2012). "Polymorphisms in the P2X7 receptor gene are associated with low lumbar spine bone mineral density and accelerated bone loss in post-menopausal women". Eur J Hum Genet **20**(5): 559-564.

Gavala, M. L., Hill, L. M., Lenertz, L. Y., Karta, M. R. and Bertics, P. J. (2010). "Activation of the transcription factor FosB/activating protein-1 (AP-1) is a prominent downstream signal of the extracellular nucleotide receptor P2RX7 in monocytic and osteoblastic cells". J Biol Chem **285**(44): 34288-34298.

Gavala, M. L., Pfeiffer, Z. A. and Bertics, P. J. (2008). "The nucleotide receptor P2RX7 mediates ATP-induced CREB activation in human and murine monocytic cells". J Leukoc Biol **84**(4): 1159-1171.

Genty, V., Dine, G. and Dufer, J. (2004). "Phenotypical alterations induced by glucocorticoids resistance in RPMI 8226 human myeloma cells". Leuk Res **28**(3): 307-313.

Georgiou, J. G., Skarratt, K. K., Fuller, S. J., Martin, C. J., Christopherson, R. I., Wiley, J. S. and Sluyter, R. (2005). "Human epidermal and monocyte-derived langerhans cells express functional P2X receptors". J Invest Dermatol **125**(3): 482-490.

Germain, R. N. (1994). "MHC-dependent antigen processing and peptide presentation: providing ligands for T lymphocyte activation". Cell **76**(2): 287-299.

Germain, R. N. (2002). "T-cell development and the CD4-CD8 lineage decision". Nat Rev Immunol **2**(5): 309-322.

Gibb, D. R., El Shikh, M., Kang, D. J., Rowe, W. J., El Sayed, R., Cichy, J., Yagita, H., Tew, J. G., Dempsey, P. J., Crawford, H. C. and Conrad, D. H. (2010). "ADAM10 is

essential for Notch2-dependent marginal zone B cell development and CD23 cleavage in vivo". J Exp Med **207**(3): 623-635.

Gordon, J., Katira, A., Strain, A. J. and Gillis, S. (1991). "Inhibition of interleukin 4-promoted CD23 production in human B lymphocytes by transforming growth factor-β, interferons or anti-CD19 antibody is overriden on engaging CD40". Eur J Immunol **21**(8): 1917-1922.

Gough, P. J., Garton, K. J., Wille, P. T., Rychlewski, M., Dempsey, P. J. and Raines, E. W. (2004). "A disintegrin and metalloproteinase 10-mediated cleavage and shedding regulates the cell surface expression of CXC chemokine ligand 16". J Immunol **172**(6): 3678-3685.

Gould, H. J. and Sutton, B. J. (2008). "IgE in allergy and asthma today". Nat Rev Immunol **8**(3): 205-217.

Grenier-Brossette, N., Bourget, I., Akoundi, C., Bonnefoy, J. Y. and Cousin, J. L. (1992). "Spontaneous and ligand-induced endocytosis of CD23 (Fcε receptor II) from the surface of B lymphocytes generates a 16-kDa intracellular fragment". Eur J Immunol **22**(6): 1573-1577.

Grobelny, D., Poncz, L. and Galardy, R. E. (1992). "Inhibition of human skin fibroblast collagenase, thermolysin, and *Pseudomonas aeruginosa* elastase by peptide hydroxamic acids". Biochemistry **31**(31): 7152-7154.

Gu, B., Bendall, L. J. and Wiley, J. S. (1998). "Adenosine triphosphate-induced shedding of CD23 and L-selectin (CD62L) from lymphocytes is mediated by the same receptor but different metalloproteases". Blood **92**(3): 946-951.

Gu, B. J., Saunders, B. M., Jursik, C. and Wiley, J. S. (2010). "The $P2X_7$-nonmuscle myosin membrane complex regulates phagocytosis of nonopsonized particles and bacteria by a pathway attenuated by extracellular ATP". Blood **115**(8): 1621-1631.

Gu, B. J., Sluyter, R., Skarratt, K. K., Shemon, A. N., Dao-Ung, L. P., Fuller, S. J., Barden, J. A., Clarke, A. L., Petrou, S. and Wiley, J. S. (2004). "An Arg^{307} to Gln polymorphism within the ATP-binding site causes loss of function of the human $P2X_7$ receptor". J Biol Chem **279**(30): 31287-31295.

Gu, B. J., Zhang, W., Worthington, R. A., Sluyter, R., Dao-Ung, P., Petrou, S., Barden, J. A. and Wiley, J. S. (2001). "A Glu-496 to Ala polymorphism leads to loss of function of the human $P2X_7$ receptor". J Biol Chem **276**(14): 11135-11142.

Gu, B. J., Zhang, W. Y., Bendall, L. J., Chessell, I. P., Buell, G. N. and Wiley, J. S. (2000). "Expression of $P2X_7$ purinoceptors on human lymphocytes and monocytes: evidence for nonfunctional $P2X_7$ receptors". Am J Physiol Cell Physiol **279**(4): C1189-1197.

Gudipaty, L., Munetz, J., Verhoef, P. A. and Dubyak, G. R. (2003). "Essential role for Ca^{2+} in regulation of IL-1β secretion by $P2X_7$ nucleotide receptor in monocytes, macrophages, and HEK-293 cells". Am J Physiol Cell Physiol **285**(2): C286-299.

Gursel, M., Gursel, I., Mostowski, H. S. and Klinman, D. M. (2006). "CXCL16 influences the nature and specificity of CpG-induced immune activation". J Immunol **177**(3): 1575-1580.

Haag, F., Koch-Nolte, F., Kuhl, M., Lorenzen, S. and Thiele, H. G. (1994). "Premature stop codons inactivate the RT6 genes of the human and chimpanzee species". J Mol Biol **243**(3): 537-546.

Haass, C., Kaether, C., Thinakaran, G. and Sisodia, S. (2012). "Trafficking and proteolytic processing of APP". Cold Spring Harb Perspect Med **2**(5): a006270.

Hakonarson, H., Carter, C., Kim, C. and Grunstein, M. M. (1999). "Altered expression and action of the low-affinity IgE receptor FcεRII (CD23) in asthmatic airway smooth muscle". J Allergy Clin Immunol **104**(3 Pt 1): 575-584.

Hayashida, K., Bartlett, A. H., Chen, Y. and Park, P. W. (2010). "Molecular and cellular mechanisms of ectodomain shedding". Anat Rec (Hoboken) **293**(6): 925-937.

Hermann, P., Armant, M., Brown, E., Rubio, M., Ishihara, H., Ulrich, D., Caspary, R. G., Lindberg, F. P., Armitage, R., Maliszewski, C., Delespesse, G. and Sarfati, M. (1999). "The vitronectin receptor and its associated CD47 molecule mediates proinflammatory cytokine synthesis in human monocytes by interaction with soluble CD23". J Cell Biol **144**(4): 767-775.

Holmoy, T., Loken-Amsrud, K. I., Bakke, S. J., Beiske, A. G., Bjerve, K. S., Hovdal, H., Lilleas, F., Midgard, R., Pedersen, T., Saltyte Benth, J., Torkildsen, O., Wergeland, S., Myhr, K. M., Michelsen, A. E., Aukrust, P. and Ueland, T. (2013). "Inflammation markers in multiple sclerosis: CXCL16 reflects and may also predict disease activity". PLoS One **8**(9): e75021.

Horiuchi, T., Mitoma, H., Harashima, S., Tsukamoto, H. and Shimoda, T. (2010). "Transmembrane TNF-α: structure, function and interaction with anti-TNF agents". Rheumatology (Oxford) **49**(7): 1215-1228.

Hoshino, K., Takeuchi, O., Kawai, T., Sanjo, H., Ogawa, T., Takeda, Y., Takeda, K. and Akira, S. (1999). "Cutting edge: Toll-like receptor 4 (TLR4)-deficient mice are hyporesponsive to lipopolysaccharide: evidence for TLR4 as the Lps gene product". J Immunol **162**(7): 3749-3752.

Hu, H., Lu, W., Zhang, M., Zhang, X., Argall, A. J., Patel, S., Lee, G. E., Kim, Y. C., Jacobson, K. A., Laties, A. M. and Mitchell, C. H. (2010). "Stimulation of the P2X7 receptor kills rat retinal ganglion cells in vivo". Exp Eye Res **91**(3): 425-432.

Hua, S. (2013). "Targeting sites of inflammation: intercellular adhesion molecule-1 as a target for novel inflammatory therapies". Front Pharmacol **4**: 127.

Hubschmann, M. V., Skladchikova, G., Bock, E. and Berezin, V. (2005). "Neural cell adhesion molecule function is regulated by metalloproteinase-mediated ectodomain release". J Neurosci Res **80**(6): 826-837.

Huissoon, A. P., Emery, P., Bacon, P. A., Gordon, J. and Salmon, M. (2000). "Increased expression of CD23 in rheumatoid synovitis". Scand J Rheumatol **29**(3): 154-159.

Humphreys, B. D. and Dubyak, G. R. (1996). "Induction of the P2z/$P2X_7$ nucleotide receptor and associated phospholipase D activity by lipopolysaccharide and IFN-gamma in the human THP-1 monocytic cell line". J Immunol **157**(12): 5627-5637.

Humphreys, B. D. and Dubyak, G. R. (1998). "Modulation of $P2X_7$ nucleotide receptor expression by pro- and anti-inflammatory stimuli in THP-1 monocytes". J Leukoc Biol **64**(2): 265-273.

Humphreys, B. D., Rice, J., Kertesy, S. B. and Dubyak, G. R. (2000). "Stress-activated protein kinase/JNK activation and apoptotic induction by the macrophage P2X7 nucleotide receptor". J Biol Chem **275**(35): 26792-26798.

Humphreys, B. D., Virginio, C., Surprenant, A., Rice, J. and Dubyak, G. R. (1998). "Isoquinolines as antagonists of the $P2X_7$ nucleotide receptor: high selectivity for the human versus rat receptor homologues". Mol Pharmacol **54**(1): 22-32.

Hundhausen, C., Schulte, A., Schulz, B., Andrzejewski, M. G., Schwarz, N., von Hundelshausen, P., Winter, U., Paliga, K., Reiss, K., Saftig, P., Weber, C. and Ludwig, A. (2007). "Regulated shedding of transmembrane chemokines by the disintegrin and metalloproteinase 10 facilitates detachment of adherent leukocytes". J Immunol **178**(12): 8064-8072.

Ibsen, P. H. (1996). "The effect of formaldehyde, hydrogen peroxide and genetic detoxification of pertussis toxin on epitope recognition by murine monoclonal antibodies". Vaccine **14**(5): 359-368.

Jackson, L., Cady, C. T. and Cambier, J. C. (2009). "TLR4-mediated signaling induces MMP9-dependent cleavage of B cell surface CD23". J Immunol **183**(4): 2585-2592.

Jacobson, K. A. and Boeynaems, J. M. (2010). "P2Y nucleotide receptors: promise of therapeutic applications". Drug Discov Today **15**(13-14): 570-578.

Jacobson, K. A., Jayasekara, M. P. and Costanzi, S. (2012). "Molecular Structure of P2Y Receptors: Mutagenesis, Modeling, and Chemical Probes". Wiley Interdiscip Rev Membr Transp Signal **1**(6).

Jalilian, I., Peranec, M., Curtis, B. L., Seavers, A., Spildrejorde, M., Sluyter, V. and Sluyter, R. (2012). "Activation of the damage-associated molecular pattern receptor P2X7 induces interleukin-1beta release from canine monocytes". Vet Immunol Immunopathol **149**(1-2): 86-91.

Jamieson, G. P., Snook, M. B., Thurlow, P. J. and Wiley, J. S. (1996). "Extracellular ATP causes of loss of L-selectin from human lymphocytes via occupancy of P2Z purinocepters". J Cell Physiol **166**(3): 637-642.

Jansson, A. M., Aukrust, P., Ueland, T., Smith, C., Omland, T., Hartford, M. and Caidahl, K. (2009). "Soluble CXCL16 predicts long-term mortality in acute coronary syndromes". Circulation **119**(25): 3181-3188.

Jarvis, M. F. and Khakh, B. S. (2009). "ATP-gated P2X cation-channels". Neuropharmacology **56**(1): 208-215.

Jiang, L.-H. (2012). "P2X receptor-mediated ATP purinergic signaling in health and disease". Cell health and cytoskeleton **4**: 83-101.

Jiang, L. H. (2009). "Inhibition of $P2X_7$ receptors by divalent cations: old action and new insight". Eur Biophys J **38**(3): 339-346.

Jiang, L. H., Mackenzie, A. B., North, R. A. and Surprenant, A. (2000). "Brilliant blue G selectively blocks ATP-gated rat $P2X_7$ receptors". Mol Pharmacol **58**(1): 82-88.

Jiang, L. H., Rassendren, F., Mackenzie, A., Zhang, Y. H., Surprenant, A. and North, R. A. (2005). "N-methyl-D-glucamine and propidium dyes utilize different permeation pathways at rat $P2X_7$ receptors". Am J Physiol Cell Physiol **289**(5): C1295-1302.

Jiang, R., Taly, A. and Grutter, T. (2013). "Moving through the gate in ATP-activated P2X receptors". Trends Biochem Sci **38**(1): 20-29.

Jorgensen, N. R., Husted, L. B., Skarratt, K. K., Stokes, L., Tofteng, C. L., Kvist, T., Jensen, J. E., Eiken, P., Brixen, K., Fuller, S., Clifton-Bligh, R., Gartland, A., Schwarz, P., Langdahl, B. L. and Wiley, J. S. (2012). "Single-nucleotide polymorphisms in the P2X7 receptor gene are associated with post-menopausal bone loss and vertebral fractures". Eur J Hum Genet **20**(6): 675-681.

Kaczmarek-Hajek, K., Lorinczi, E., Hausmann, R. and Nicke, A. (2012). "Molecular and functional properties of P2X receptors--recent progress and persisting challenges". Purinergic Signal **8**(3): 375-417.

Kahlenberg, J. M. and Dubyak, G. R. (2004). "Mechanisms of caspase-1 activation by $P2X_7$ receptor-mediated K^+ release". Am J Physiol Cell Physiol **286**(5): C1100-1108.

Kajita, M., Itoh, Y., Chiba, T., Mori, H., Okada, A., Kinoh, H. and Seiki, M. (2001). "Membrane-type 1 matrix metalloproteinase cleaves CD44 and promotes cell migration". J Cell Biol **153**(5): 893-904.

Kawate, T., Michel, J. C., Birdsong, W. T. and Gouaux, E. (2009). "Crystal structure of the ATP-gated $P2X_4$ ion channel in the closed state". Nature **460**(7255): 592-598.

Ke, H. Z., Qi, H., Weidema, A. F., Zhang, Q., Panupinthu, N., Crawford, D. T., Grasser, W. A., Paralkar, V. M., Li, M., Audoly, L. P., Gabel, C. A., Jee, W. S., Dixon, S. J., Sims, S. M. and Thompson, D. D. (2003). "Deletion of the P2X7 nucleotide receptor reveals its regulatory roles in bone formation and resorption". Mol Endocrinol **17**(7): 1356-1367.

Khakh, B. S. and North, R. A. (2006). "P2X receptors as cell-surface ATP sensors in health and disease". Nature **442**(7102): 527-532.

Kijimoto-Ochiai, S. and Noguchi, A. (2000). "Two peptides from CD23, including the inverse RGD sequence and its related peptide, interact with the MHC class II molecule". Biochem Biophys Res Commun **267**(3): 686-691.

Kikutani, H., Yokota, A., Uchibayashi, N., Yukawa, K., Tanaka, T., Sugiyama, K., Barsumian, E. L., Suemura, M. and Kishimoto, T. (1989). "Structure and function of

Fcε receptor II (FcεRII/CD23): a point of contact between the effector phase of allergy and B cell differentiation". Ciba Found Symp **147**: 23-31; discussion 31-25.

Kilmon, M. A., Shelburne, A. E., Chan-Li, Y., Holmes, K. L. and Conrad, D. H. (2004). "CD23 trimers are preassociated on the cell surface even in the absence of its ligand, IgE". J Immunol **172**(2): 1065-1073.

Klouche, M., Klinger, M. H., Kuhnel, W. and Wilhelm, D. (1997). "Endocytosis, storage, and release of IgE by human platelets: differences in patients with type I allergy and nonatopic subjects". J Allergy Clin Immunol **100**(2): 235-241.

Kong, Q., Peterson, T. S., Baker, O., Stanley, E., Camden, J., Seye, C. I., Erb, L., Simonyi, A., Wood, W. G., Sun, G. Y. and Weisman, G. A. (2009). "Interleukin-1β enhances nucleotide-induced and α-secretase-dependent amyloid precursor protein processing in rat primary cortical neurons via up-regulation of the $P2Y_2$ receptor". J Neurochem **109**(5): 1300-1310.

Korcok, J., Raimundo, L. N., Ke, H. Z., Sims, S. M. and Dixon, S. J. (2004). "Extracellular nucleotides act through P2X7 receptors to activate NF-κB in osteoclasts". J Bone Miner Res **19**(4): 642-651.

Kotnis, S., Bingham, B., Vasilyev, D. V., Miller, S. W., Bai, Y., Yeola, S., Chanda, P. K., Bowlby, M. R., Kaftan, E. J., Samad, T. A. and Whiteside, G. T. (2010). "Genetic and functional analysis of human P2X5 reveals a distinct pattern of exon 10 polymorphism with predominant expression of the nonfunctional receptor isoform". Mol Pharmacol **77**(6): 953-960.

Krebs, C., Adriouch, S., Braasch, F., Koestner, W., Leiter, E. H., Seman, M., Lund, F. E., Oppenheimer, N., Haag, F. and Koch-Nolte, F. (2005). "CD38 controls ADP-ribosyltransferase-2-catalyzed ADP-ribosylation of T cell surface proteins". J Immunol **174**(6): 3298-3305.

Kusner, D. J. and Adams, J. (2000). "ATP-induced killing of virulent *Mycobacterium tuberculosis* within human macrophages requires phospholipase D". J Immunol **164**(1): 379-388.

Labasi, J. M., Petrushova, N., Donovan, C., McCurdy, S., Lira, P., Payette, M. M., Brissette, W., Wicks, J. R., Audoly, L. and Gabel, C. A. (2002). "Absence of the $P2X_7$ receptor alters leukocyte function and attenuates an inflammatory response". J Immunol **168**(12): 6436-6445.

Largo, C., Alvarez, S., Saez, B., Blesa, D., Martin-Subero, J. I., Gonzalez-Garcia, I., Brieva, J. A., Dopazo, J., Siebert, R., Calasanz, M. J. and Cigudosa, J. C. (2006). "Identification of overexpressed genes in frequently gained/amplified chromosome regions in multiple myeloma". Haematologica **91**(2): 184-191.

Larkin, M. A., Blackshields, G., Brown, N. P., Chenna, R., McGettigan, P. A., McWilliam, H., Valentin, F., Wallace, I. M., Wilm, A., Lopez, R., Thompson, J. D., Gibson, T. J. and Higgins, D. G. (2007). "Clustal W and Clustal X version 2.0". Bioinformatics **23**(21): 2947-2948.

Lazarowski, E. R., Boucher, R. C. and Harden, T. K. (2003). "Mechanisms of release of nucleotides and integration of their action as P2X- and P2Y-receptor activating molecules". Mol Pharmacol **64**(4): 785-795.

le Blanc, L. M., van Lieshout, A. W., Adema, G. J., van Riel, P. L., Verbeek, M. M. and Radstake, T. R. (2006). "CXCL16 is elevated in the cerebrospinal fluid versus serum and in inflammatory conditions with suspected and proved central nervous system involvement". Neurosci Lett **397**(1-2): 145-148.

Le Gall, S. M., Bobe, P., Reiss, K., Horiuchi, K., Niu, X. D., Lundell, D., Gibb, D. R., Conrad, D., Saftig, P. and Blobel, C. P. (2009). "ADAMs 10 and 17 represent differentially regulated components of a general shedding machinery for membrane

proteins such as transforming growth factor α, L-selectin, and tumor necrosis factor α". Mol Biol Cell **20**(6): 1785-1794.

Le Gall, S. M., Maretzky, T., Issuree, P. D., Niu, X. D., Reiss, K., Saftig, P., Khokha, R., Lundell, D. and Blobel, C. P. (2010). "ADAM17 is regulated by a rapid and reversible mechanism that controls access to its catalytic site". J Cell Sci **123**(Pt 22): 3913-3922.

Le Stunff, H., Auger, R., Kanellopoulos, J. and Raymond, M. N. (2004). "The Pro-451 to Leu polymorphism within the C-terminal tail of P2X7 receptor impairs cell death but not phospholipase D activation in murine thymocytes". J Biol Chem **279**(17): 16918-16926.

Le Stunff, H. and Raymond, M. N. (2007). "P2X7 receptor-mediated phosphatidic acid production delays ATP-induced pore opening and cytolysis of RAW 264.7 macrophages". Cell Signal **19**(9): 1909-1918.

Le, Y., Zhou, Y., Iribarren, P. and Wang, J. (2004). "Chemokines and chemokine receptors: their manifold roles in homeostasis and disease". Cell Mol Immunol **1**(2): 95-104.

Lecoanet-Henchoz, S., Gauchat, J. F., Aubry, J. P., Graber, P., Life, P., Paul-Eugene, N., Ferrua, B., Corbi, A. L., Dugas, B., Plater-Zyberk, C. and et al. (1995). "CD23 regulates monocyte activation through a novel interaction with the adhesion molecules CD11b-CD18 and CD11c-CD18". Immunity **3**(1): 119-125.

Lecoanet-Henchoz, S., Plater-Zyberk, C., Graber, P., Gretener, D., Aubry, J. P., Conrad, D. H. and Bonnefoy, J. Y. (1997). "Mouse CD23 regulates monocyte activation through an interaction with the adhesion molecule CD11b/CD18". Eur J Immunol **27**(9): 2290-2294.

Lee, D. H., Park, K. S., Kong, I. D., Kim, J. W. and Han, B. G. (2006). "Expression of P2 receptors in human B cells and Epstein-Barr virus-transformed lymphoblastoid cell lines". BMC Immunol **7**: 22.

Lee, G. E., Joshi, B. V., Chen, W., Jeong, L. S., Moon, H. R., Jacobson, K. A. and Kim, Y. C. (2008). "Synthesis and structure-activity relationship studies of tyrosine-based antagonists at the human P2X7 receptor". Bioorg Med Chem Lett **18**(2): 571-575.

Lehrke, M., Konrad, A., Schachinger, V., Tillack, C., Seibold, F., Stark, R., Parhofer, I. G. and Broedl, U. C. (2008). "CXCL16 is a surrogate marker of inflammatory bowel disease". Scand J Gastroenterol **43**(3): 283-288.

Lehrke, M., Millington, S. C., Lefterova, M., Cumaranatunge, R. G., Szapary, P., Wilensky, R., Rader, D. J., Lazar, M. A. and Reilly, M. P. (2007). "CXCL16 is a marker of inflammation, atherosclerosis, and acute coronary syndromes in humans". J Am Coll Cardiol **49**(4): 442-449.

Lemieux, G. A., Blumenkron, F., Yeung, N., Zhou, P., Williams, J., Grammer, A. C., Petrovich, R., Lipsky, P. E., Moss, M. L. and Werb, Z. (2007). "The low affinity IgE receptor (CD23) is cleaved by the metalloproteinase ADAM10". J Biol Chem **282**(20): 14836-14844.

Lenertz, L. Y., Gavala, M. L., Hill, L. M. and Bertics, P. J. (2009). "Cell signaling via the $P2X_7$ nucleotide receptor: linkage to ROS production, gene transcription, and receptor trafficking". Purinergic Signal **5**(2): 175-187.

Lenertz, L. Y., Gavala, M. L., Zhu, Y. and Bertics, P. J. (2011). "Transcriptional control mechanisms associated with the nucleotide receptor P2X7, a critical regulator of immunologic, osteogenic, and neurologic functions". Immunol Res **50**(1): 22-38.

Leon-Otegui, M., Gomez-Villafuertes, R., Diaz-Hernandez, J. I., Diaz-Hernandez, M., Miras-Portugal, M. T. and Gualix, J. (2011). "Opposite effects of P2X7 and $P2Y_2$ nucleotide receptors on α-secretase-dependent APP processing in Neuro-2a cells". FEBS Lett **585**(14): 2255-2262.

Lester, S., Stokes, L., Skarratt, K. K., Gu, B. J., Sivils, K. L., Lessard, C. J., Wiley, J. S. and Rischmueller, M. (2013). "Epistasis with HLA DR3 implicates the P2X7 receptor in the pathogenesis of primary Sjogren's syndrome". Arthritis Res Ther **15**(4): R71.

Letellier, M., Nakajima, T., Pulido-Cejudo, G., Hofstetter, H. and Delespesse, G. (1990). "Mechanism of formation of human IgE-binding factors (soluble CD23): III. Evidence for a receptor (FcεRII)-associated proteolytic activity". J Exp Med **172**(3): 693-700.

Lin, C., Ren, S., Zhang, L., Jin, H., Sun, J. and Zuo, Y. (2012). "Extracellular ATP induces CD44 shedding from macrophage-like P388D1 cells via the P2X7 receptor". Hematol Oncol **30**(2): 70-75.

Liu, Y. J., Cairns, J. A., Holder, M. J., Abbot, S. D., Jansen, K. U., Bonnefoy, J. Y., Gordon, J. and MacLennan, I. C. (1991). "Recombinant 25-kDa CD23 and interleukin 1α promote the survival of germinal center B cells: evidence for bifurcation in the development of centrocytes rescued from apoptosis". Eur J Immunol **21**(5): 1107-1114.

Locovei, S., Scemes, E., Qiu, F., Spray, D. C. and Dahl, G. (2007). "Pannexin1 is part of the pore forming unit of the $P2X_7$ receptor death complex". FEBS Lett **581**(3): 483-488.

Lopez-Castejon, G., Theaker, J., Pelegrin, P., Clifton, A. D., Braddock, M. and Surprenant, A. (2010). "$P2X_7$ receptor-mediated release of cathepsins from macrophages is a cytokine-independent mechanism potentially involved in joint diseases". J Immunol **185**(4): 2611-2619.

Lucae, S., Salyakina, D., Barden, N., Harvey, M., Gagne, B., Labbe, M., Binder, E. B., Uhr, M., Paez-Pereda, M., Sillaber, I., Ising, M., Bruckl, T., Lieb, R., Holsboer, F. and Muller-Myhsok, B. (2006). "*P2RX7*, a gene coding for a purinergic ligand-gated ion channel, is associated with major depressive disorder". Hum Mol Genet **15**(16): 2438-2445.

Ludin, C., Hofstetter, H., Sarfati, M., Levy, C. A., Suter, U., Alaimo, D., Kilchherr, E., Frost, H. and Delespesse, G. (1987). "Cloning and expression of the cDNA coding for a human lymphocyte IgE receptor". EMBO J **6**(1): 109-114.

Ludwig, A., Hundhausen, C., Lambert, M. H., Broadway, N., Andrews, R. C., Bickett, D. M., Leesnitzer, M. A. and Becherer, J. D. (2005a). "Metalloproteinase inhibitors for the disintegrin-like metalloproteinases ADAM10 and ADAM17 that differentially block constitutive and phorbol ester-inducible shedding of cell surface molecules". Comb Chem High Throughput Screen **8**(2): 161-171.

Ludwig, A., Schulte, A., Schnack, C., Hundhausen, C., Reiss, K., Brodway, N., Held-Feindt, J. and Mentlein, R. (2005b). "Enhanced expression and shedding of the transmembrane chemokine CXCL16 by reactive astrocytes and glioma cells". J Neurochem **93**(5): 1293-1303.

Lynch, K. J., Touma, E., Niforatos, W., Kage, K. L., Burgard, E. C., van Biesen, T., Kowaluk, E. A. and Jarvis, M. F. (1999). "Molecular and functional characterization of human $P2X_2$ receptors". Mol Pharmacol **56**(6): 1171-1181.

Maenaka, K. and Jones, E. Y. (1999). "MHC superfamily structure and the immune system". Curr Opin Struct Biol **9**(6): 745-753.

Marques-da-Silva, C., Chaves, M. M., Castro, N. G., Coutinho-Silva, R. and Guimaraes, M. Z. (2011). "Colchicine inhibits cationic dye uptake induced by ATP in P2X2 and

P2X7 receptor-expressing cells: implications for its therapeutic action". Br J Pharmacol **163**(5): 912-926.

Martin, U., Scholler, J., Gurgel, J., Renshaw, B., Sims, J. E. and Gabel, C. A. (2009). "Externalization of the leaderless cytokine IL-1F6 occurs in response to lipopolysaccharide/ATP activation of transduced bone marrow macrophages". J Immunol **183**(6): 4021-4030.

Martinon, F., Petrilli, V., Mayor, A., Tardivel, A. and Tschopp, J. (2006). "Gout-associated uric acid crystals activate the NALP3 inflammasome". Nature **440**(7081): 237-241.

Masin, M., Young, C., Lim, K., Barnes, S. J., Xu, X. J., Marschall, V., Brutkowski, W., Mooney, E. R., Gorecki, D. C. and Murrell-Lagnado, R. (2012). "Expression, assembly and function of novel C-terminal truncated variants of the mouse P2X7 receptor: re-evaluation of P2X7 knockouts". Br J Pharmacol **165**(4): 978-993.

Massa, M., Pignatti, P., Oliveri, M., De Amici, M., De Benedetti, F. and Martini, A. (1998). "Serum soluble CD23 levels and CD23 expression on peripheral blood mononuclear cells in juvenile chronic arthritis". Clin Exp Rheumatol **16**(5): 611-616.

Mathews, J. A., Gibb, D. R., Chen, B. H., Scherle, P. and Conrad, D. H. (2010). "CD23 Sheddase A disintegrin and metalloproteinase 10 (ADAM10) is also required for CD23 sorting into B cell-derived exosomes". J Biol Chem **285**(48): 37531-37541.

Matloubian, M., David, A., Engel, S., Ryan, J. E. and Cyster, J. G. (2000). "A transmembrane CXC chemokine is a ligand for HIV-coreceptor Bonzo". Nat Immunol **1**(4): 298-304.

Matsushita, K., Toiyama, Y., Tanaka, K., Saigusa, S., Hiro, J., Uchida, K., Inoue, Y. and Kusunoki, M. (2012). "Soluble CXCL16 in preoperative serum is a novel prognostic marker and predicts recurrence of liver metastases in colorectal cancer patients". Ann Surg Oncol **19 Suppl 3**: S518-527.

Maurer, D., Holter, W., Majdic, O., Fischer, G. F. and Knapp, W. (1990). "CD27 expression by a distinct subpopulation of human B lymphocytes". Eur J Immunol **20**(12): 2679-2684.

McDermott, M., Wakelam, M. J. and Morris, A. J. (2004). "Phospholipase D". Biochem Cell Biol **82**(1): 225-253.

Mehta, V. B., Hart, J. and Wewers, M. D. (2001). "ATP-stimulated release of interleukin (IL)-1β and IL-18 requires priming by lipopolysaccharide and is independent of caspase-1 cleavage". J Biol Chem **276**(6): 3820-3826.

Meuleman, N., Stamatopoulos, B., Dejeneffe, M., El Housni, H., Lagneaux, L. and Bron, D. (2008). "Doubling time of soluble CD23: a powerful prognostic factor for newly diagnosed and untreated stage A chronic lymphocytic leukemia patients". Leukemia **22**(10): 1882-1890.

Michel, A. D., Chambers, L. J. and Walter, D. S. (2008). "Negative and positive allosteric modulators of the $P2X_7$ receptor". Br J Pharmacol **153**(4): 737-750.

Michel, A. D., Chessell, I. P. and Humphrey, P. P. (1999). "Ionic effects on human recombinant $P2X_7$ receptor function". Naunyn Schmiedebergs Arch Pharmacol **359**(2): 102-109.

Michel, A. D., Thompson, K. M., Simon, J., Boyfield, I., Fonfria, E. and Humphrey, P. P. (2006). "Species and response dependent differences in the effects of MAPK inhibitors on $P2X_7$ receptor function". Br J Pharmacol **149**(7): 948-957.

Milenkovic, I., Weick, M., Wiedemann, P., Reichenbach, A. and Bringmann, A. (2003). "P2Y receptor-mediated stimulation of Muller glial cell DNA synthesis: dependence on EGF and PDGF receptor transactivation". Invest Ophthalmol Vis Sci **44**(3): 1211-1220.

Miller, C. M., Boulter, N. R., Fuller, S. J., Zakrzewski, A. M., Lees, M. P., Saunders, B. M., Wiley, J. S. and Smith, N. C. (2011a). "The role of the $P2X_7$ receptor in infectious diseases". PLoS Pathog **7**(11): e1002212.

Miller, C. M., Zakrzewski, A. M., Ikin, R. J., Boulter, N. R., Katrib, M., Lees, M. P., Fuller, S. J., Wiley, J. S. and Smith, N. C. (2011b). "Dysregulation of the inflammatory response to the parasite, *Toxoplasma gondii*, in $P2X_7$ receptor-deficient mice". Int J Parasitol **41**(3-4): 301-308.

Min, D. S., Ahn, B. H. and Jo, Y. H. (2001). "Differential tyrosine phosphorylation of phospholipase D isozymes by hydrogen peroxide and the epidermal growth factor in A431 epidermoid carcinoma cells". Mol Cells **11**(3): 369-378.

Mirastschijski, U., Impola, U., Karsdal, M. A., Saarialho-Kere, U. and Agren, M. S. (2002). "Matrix metalloproteinase inhibitor BB-3103 unlike the serine proteinase inhibitor aprotinin abrogates epidermal healing of human skin wounds ex vivo". J Invest Dermatol **118**(1): 55-64.

Moller, C., Stromberg, T., Juremalm, M., Nilsson, K. and Nilsson, G. (2003). "Expression and function of chemokine receptors in human multiple myeloma". Leukemia **17**(1): 203-210.

Monif, M., Reid, C. A., Powell, K. L., Smart, M. L. and Williams, D. A. (2009). "The $P2X_7$ receptor drives microglial activation and proliferation: a trophic role for $P2X_7R$ pore". J Neurosci **29**(12): 3781-3791.

Moon, H., Na, H. Y., Chong, K. H. and Kim, T. J. (2006). "$P2X_7$ receptor-dependent ATP-induced shedding of CD27 in mouse lymphocytes". Immunol Lett **102**(1): 98-105.

Morris, A. J., Frohman, M. A. and Engebrecht, J. (1997). "Measurement of phospholipase D activity". Anal Biochem **252**(1): 1-9.

Mossalayi, M. D., Arock, M., Bertho, J. M., Blanc, C., Dalloul, A. H., Hofstetter, H., Sarfati, M., Delespesse, G. and Debre, P. (1990a). "Proliferation of early human myeloid precursors induced by interleukin-1 and recombinant soluble CD23". Blood **75**(10): 1924-1927.

Mossalayi, M. D., Lecron, J. C., Dalloul, A. H., Sarfati, M., Bertho, J. M., Hofstetter, H., Delespesse, G. and Debre, P. (1990b). "Soluble CD23 (FcεRII) and interleukin 1 synergistically induce early human thymocyte maturation". J Exp Med **171**(3): 959-964.

Mullberg, J., Durie, F. H., Otten-Evans, C., Alderson, M. R., Rose-John, S., Cosman, D., Black, R. A. and Mohler, K. M. (1995). "A metalloprotease inhibitor blocks shedding of the IL-6 receptor and the p60 TNF receptor". J Immunol **155**(11): 5198-5205.

Munoz-Planillo, R., Kuffa, P., Martinez-Colon, G., Smith, B. L., Rajendiran, T. M. and Nunez, G. (2013). "K^+ efflux is the common trigger of NLRP3 inflammasome activation by bacterial toxins and particulate matter". Immunity **38**(6): 1142-1153.

Myers, T. J., Brennaman, L. H., Stevenson, M., Higashiyama, S., Russell, W. E., Lee, D. C. and Sunnarborg, S. W. (2009). "Mitochondrial reactive oxygen species mediate

GPCR-induced TACE/ADAM17-dependent transforming growth factor-α shedding". Mol Biol Cell **20**(24): 5236-5249.

Nakayama, T., Hieshima, K., Izawa, D., Tatsumi, Y., Kanamaru, A. and Yoshie, O. (2003). "Cutting edge: profile of chemokine receptor expression on human plasma cells accounts for their efficient recruitment to target tissues". J Immunol **170**(3): 1136-1140.

Nanki, T., Shimaoka, T., Hayashida, K., Taniguchi, K., Yonehara, S. and Miyasaka, N. (2005). "Pathogenic role of the CXCL16-CXCR6 pathway in rheumatoid arthritis". Arthritis Rheum **52**(10): 3004-3014.

Nelson, D. W., Gregg, R. J., Kort, M. E., Perez-Medrano, A., Voight, E. A., Wang, Y., Grayson, G., Namovic, M. T., Donnelly-Roberts, D. L., Niforatos, W., Honore, P., Jarvis, M. F., Faltynek, C. R. and Carroll, W. A. (2006). "Structure-activity relationship studies on a series of novel, substituted 1-benzyl-5-phenyltetrazole $P2X_7$ antagonists". J Med Chem **49**(12): 3659-3666.

Nicke, A., Kuan, Y. H., Masin, M., Rettinger, J., Marquez-Klaka, B., Bender, O., Gorecki, D. C., Murrell-Lagnado, R. D. and Soto, F. (2009). "A functional P2X7 splice variant with an alternative transmembrane domain 1 escapes gene inactivation in P2X7 knock-out mice". J Biol Chem **284**(38): 25813-25822.

Noguchi, T., Ishii, K., Fukutomi, H., Naguro, I., Matsuzawa, A., Takeda, K. and Ichijo, H. (2008). "Requirement of reactive oxygen species-dependent activation of ASK1-p38 MAPK pathway for extracellular ATP-induced apoptosis in macrophage". J Biol Chem **283**(12): 7657-7665.

North, R. A. (2002). "Molecular physiology of P2X receptors". Physiol Rev **82**(4): 1013-1067.

Ortega, F., Perez-Sen, R., Delicado, E. G. and Miras-Portugal, M. T. (2009). "$P2X_7$ nucleotide receptor is coupled to GSK-3 inhibition and neuroprotection in cerebellar granule neurons". Neurotox Res **15**(3): 193-204.

Ortega, F., Perez-Sen, R., Morente, V., Delicado, E. G. and Miras-Portugal, M. T. (2010). "P2X7, NMDA and BDNF receptors converge on GSK3 phosphorylation and cooperate to promote survival in cerebellar granule neurons". Cell Mol Life Sci **67**(10): 1723-1733.

Padro, C. J., Shawler, T. M., Gormley, M. G. and Sanders, V. M. (2013). "Adrenergic regulation of IgE involves modulation of CD23 and ADAM10 expression on exosomes". J Immunol **191**(11): 5383-5397.

Palombella, V. J., Rando, O. J., Goldberg, A. L. and Maniatis, T. (1994). "The ubiquitin-proteasome pathway is required for processing the NF-κB1 precursor protein and the activation of NF-κB". Cell **78**(5): 773-785.

Pearce, E. L., Shedlock, D. J. and Shen, H. (2004). "Functional characterization of MHC class II-restricted $CD8^+CD4^-$ and $CD8^-CD4^-$ T cell responses to infection in $CD4^{-/-}$ mice". J Immunol **173**(4): 2494-2499.

Pelegrin, P. (2011). "Many ways to dilate the P2X7 receptor pore". Br J Pharmacol **163**(5): 908-911.

Pelegrin, P. and Surprenant, A. (2006). "Pannexin-1 mediates large pore formation and interleukin-1β release by the ATP-gated $P2X_7$ receptor". EMBO J **25**(21): 5071-5082.

Pelegrin, P. and Surprenant, A. (2007). "Pannexin-1 couples to maitotoxin- and nigericin-induced interleukin-1β release through a dye uptake-independent pathway". J Biol Chem **282**(4): 2386-2394.

Perregaux, D. and Gabel, C. A. (1994). "Interleukin-1β maturation and release in response to ATP and nigericin. Evidence that potassium depletion mediated by these agents is a necessary and common feature of their activity". J Biol Chem **269**(21): 15195-15203.

Petrey, A. C. and de la Motte, C. A. (2014). "Hyaluronan, a crucial regulator of inflammation". Front Immunol **5**: 101.

Pfeiffer, Z. A., Aga, M., Prabhu, U., Watters, J. J., Hall, D. J. and Bertics, P. J. (2004). "The nucleotide receptor P2X7 mediates actin reorganization and membrane blebbing in RAW 264.7 macrophages via p38 MAP kinase and Rho". J Leukoc Biol **75**(6): 1173-1182.

Philpott, N. J., Turner, A. J., Scopes, J., Westby, M., Marsh, J. C., Gordon-Smith, E. C., Dalgleish, A. G. and Gibson, F. M. (1996). "The use of 7-amino actinomycin D in identifying apoptosis: simplicity of use and broad spectrum of application compared with other techniques". Blood **87**(6): 2244-2251.

Plater-Zyberk, C. and Bonnefoy, J. Y. (1995). "Marked amelioration of established collagen-induced arthritis by treatment with antibodies to CD23 in vivo". Nat Med **1**(8): 781-785.

Portales-Cervantes, L., Nino-Moreno, P., Doniz-Padilla, L., Baranda-Candido, L., Garcia-Hernandez, M., Salgado-Bustamante, M., Gonzalez-Amaro, R. and Portales-Perez, D. (2010). "Expression and function of the $P2X_7$ purinergic receptor in patients with systemic lupus erythematosus and rheumatoid arthritis". Hum Immunol **71**(8): 818-825.

Portales-Cervantes, L., Nino-Moreno, P., Salgado-Bustamante, M., Garcia-Hernandez, M. H., Baranda-Candido, L., Reynaga-Hernandez, E., Barajas-Lopez, C., Gonzalez-Amaro, R. and Portales-Perez, D. P. (2012). "The His155Tyr (489C>T) single

nucleotide polymorphism of *P2RX7* gene confers an enhanced function of P2X7 receptor in immune cells from patients with rheumatoid arthritis". Cell Immunol **276**(1-2): 168-175.

Pupovac, A. (2009). The presence of $P2X_7$ on epidermal cell populations. BBiotech (Adv) (Honours) Thesis, University of Wollongong.

Qiu, F. and Dahl, G. (2009). "A permeant regulating its permeation pore: inhibition of pannexin 1 channels by ATP". Am J Physiol Cell Physiol **296**(2): C250-255.

Qu, Y. and Dubyak, G. R. (2009). "P2X7 receptors regulate multiple types of membrane trafficking responses and non-classical secretion pathways". Purinergic Signal **5**(2): 163-173.

Qu, Y., Misaghi, S., Newton, K., Gilmour, L. L., Louie, S., Cupp, J. E., Dubyak, G. R., Hackos, D. and Dixit, V. M. (2011). "Pannexin-1 is required for ATP release during apoptosis but not for inflammasome activation". J Immunol **186**(11): 6553-6561.

Ralevic, V. and Burnstock, G. (1998). "Receptors for purines and pyrimidines". Pharmacol Rev **50**(3): 413-492.

Rassendren, F., Buell, G. N., Virginio, C., Collo, G., North, R. A. and Surprenant, A. (1997). "The permeabilizing ATP receptor, $P2X_7$. Cloning and expression of a human cDNA". J Biol Chem **272**(9): 5482-5486.

Rezzonico, R., Imbert, V., Chicheportiche, R. and Dayer, J. M. (2001). "Ligation of CD11b and CD11c β_2 integrins by antibodies or soluble CD23 induces macrophage inflammatory protein 1α (MIP-1α) and MIP-1β production in primary human monocytes through a pathway dependent on nuclear factor-κB". Blood **97**(10): 2932-2940.

Ribbens, C., Bonnet, V., Kaiser, M. J., Andre, B., Kaye, O., Franchimont, N., de Groote, D., Beguin, Y. and Malaise, M. G. (2000). "Increased synovial fluid levels of soluble CD23 are associated with an erosive status in rheumatoid arthritis (RA)". Clin Exp Immunol **120**(1): 194-199.

Rieber, E. P., Rank, G., Kohler, I. and Krauss, S. (1993). "Membrane expression of FcεRII/CD23 and release of soluble CD23 by follicular dendritic cells". Adv Exp Med Biol **329**: 393-398.

Rizzo, R., Ferrari, D., Melchiorri, L., Stignani, M., Gulinelli, S., Baricordi, O. R. and Di Virgilio, F. (2009). "Extracellular ATP acting at the $P2X_7$ receptor inhibits secretion of soluble HLA-G from human monocytes". J Immunol **183**(7): 4302-4311.

Roger, S., Mei, Z. Z., Baldwin, J. M., Dong, L., Bradley, H., Baldwin, S. A., Surprenant, A. and Jiang, L. H. (2010). "Single nucleotide polymorphisms that were identified in affective mood disorders affect ATP-activated $P2X_7$ receptor functions". J Psychiatr Res **44**(6): 347-355.

Romagnoli, R., Baraldi, P. G. and Di Virgilio, F. (2005). "Recent progress in the discovery of antagonists acting at $P2X_7$ receptor". Expert Opin. Ther. Patents **15**(3): 271-287.

Roman, S., Cusdin, F. S., Fonfria, E., Goodwin, J. A., Reeves, J., Lappin, S. C., Chambers, L., Walter, D. S., Clay, W. C. and Michel, A. D. (2009). "Cloning and pharmacological characterization of the dog P2X7 receptor". Br J Pharmacol **158**(6): 1513-1526.

Rosenwasser, L. J. and Meng, J. (2005). "Anti-CD23". Clin Rev Allergy Immunol **29**(1): 61-72.

Rosito, M., Deflorio, C., Limatola, C. and Trettel, F. (2012). "CXCL16 orchestrates adenosine A_3 receptor and MCP-1/CCL2 activity to protect neurons from excitotoxic cell death in the CNS". J Neurosci **32**(9): 3154-3163.

Rowlands, D. J., Islam, M. N., Das, S. R., Huertas, A., Quadri, S. K., Horiuchi, K., Inamdar, N., Emin, M. T., Lindert, J., Ten, V. S., Bhattacharya, S. and Bhattacharya, J. (2011). "Activation of TNFR1 ectodomain shedding by mitochondrial Ca^{2+} determines the severity of inflammation in mouse lung microvessels". J Clin Invest **121**(5): 1986-1999.

Sakimoto, T., Ohnishi, T. and Ishimori, A. (2014). "Significance of ectodomain shedding of TNF receptor 1 in ocular surface". Invest Ophthalmol Vis Sci **55**(4): 2419-2423.

Sanz, J. M. and Di Virgilio, F. (2000). "Kinetics and mechanism of ATP-dependent IL-1β release from microglial cells". J Immunol **164**(9): 4893-4898.

Sarfati, M., Bron, D., Lagneaux, L., Fonteyn, C., Frost, H. and Delespesse, G. (1988). "Elevation of IgE-binding factors in serum of patients with B cell-derived chronic lymphocytic leukemia". Blood **71**(1): 94-98.

Sarfati, M., Fournier, S., Wu, C. Y. and Delespesse, G. (1992). "Expression, regulation and function of human Fc epsilon RII (CD23) antigen". Immunol Res **11**(3-4): 260-272.

Schachter, J., Motta, A. P., de Souza Zamorano, A., da Silva-Souza, H. A., Guimaraes, M. Z. and Persechini, P. M. (2008). "ATP-induced $P2X_7$-associated uptake of large molecules involves distinct mechanisms for cations and anions in macrophages". J Cell Sci **121**(Pt 19): 3261-3270.

Schellekens, G. A., de Jong, B. A., van den Hoogen, F. H., van de Putte, L. B. and van Venrooij, W. J. (1998). "Citrulline is an essential constituent of antigenic determinants recognized by rheumatoid arthritis-specific autoantibodies". J Clin Invest **101**(1): 273-281.

Schmid, I., Uittenbogaart, C. H. and Giorgi, J. V. (1991). "A gentle fixation and permeabilization method for combined cell surface and intracellular staining with improved precision in DNA quantification". Cytometry **12**(3): 279-285.

Schneider, M. R. and Wolf, E. (2008). "The epidermal growth factor receptor and its ligands in female reproduction: insights from rodent models". Cytokine Growth Factor Rev **19**(2): 173-181.

Schramme, A., Abdel-Bakky, M. S., Kampfer-Kolb, N., Pfeilschifter, J. and Gutwein, P. (2008). "The role of CXCL16 and its processing metalloproteinases ADAM10 and ADAM17 in the proliferation and migration of human mesangial cells". Biochem Biophys Res Commun **370**(2): 311-316.

Schwarz, N., Drouot, L., Nicke, A., Fliegert, R., Boyer, O., Guse, A. H., Haag, F., Adriouch, S. and Koch-Nolte, F. (2012). "Alternative splicing of the N-terminal cytosolic and transmembrane domains of P2X7 controls gating of the ion channel by ADP-ribosylation". PLoS One **7**(7): e41269.

Scott, S. A., Selvy, P. E., Buck, J. R., Cho, H. P., Criswell, T. L., Thomas, A. L., Armstrong, M. D., Arteaga, C. L., Lindsley, C. W. and Brown, H. A. (2009). "Design of isoform-selective phospholipase D inhibitors that modulate cancer cell invasiveness". Nat Chem Biol **5**(2): 108-117.

Seil, M., El Ouaaliti, M., Fontanils, U., Etxebarria, I. G., Pochet, S., Dal Moro, G., Marino, A. and Dehaye, J. P. (2010). "Ivermectin-dependent release of IL-1β in

response to ATP by peritoneal macrophages from $P2X_7$-KO mice". Purinergic Signal **6**(4): 405-416.

Seil, M., Fontanils, U., Etxebarria, I. G., Pochet, S., Garcia-Marcos, M., Marino, A. and Dehaye, J. P. (2008). "Pharmacological evidence for the stimulation of NADPH oxidase by $P2X_7$ receptors in mouse submandibular glands". Purinergic Signal **4**(4): 347-355.

Sellers, A. and Woessner, J. F., Jr. (1980). "The extraction of a neutral metalloproteinase from the involuting rat uterus, and its action on cartilage proteoglycan". Biochem J **189**(3): 521-531.

Seman, M., Adriouch, S., Scheuplein, F., Krebs, C., Freese, D., Glowacki, G., Deterre, P., Haag, F. and Koch-Nolte, F. (2003). "NAD-induced T cell death: ADP-ribosylation of cell surface proteins by ART2 activates the cytolytic P2X7 purinoceptor". Immunity **19**(4): 571-582.

Sengstake, S., Boneberg, E. M. and Illges, H. (2006). "CD21 and CD62L shedding are both inducible via P2X7Rs". Int Immunol **18**(7): 1171-1178.

Shemon, A. N., Sluyter, R., Conigrave, A. D. and Wiley, J. S. (2004). "Chelerythrine and other benzophenanthridine alkaloids block the human P2X7 receptor". Br J Pharmacol **142**(6): 1015-1019.

Shemon, A. N., Sluyter, R., Stokes, L., Manley, P. W. and Wiley, J. S. (2008). "Inhibition of the human $P2X_7$ receptor by a novel protein tyrosine kinase antagonist". Biochem Biophys Res Commun **365**(3): 515-520.

Shemon, A. N., Sluyter, R. and Wiley, J. S. (2007). "Rottlerin inhibits $P2X_7$ receptor-stimulated phospholipase D activity in chronic lymphocytic leukaemia B-lymphocytes". Immunol Cell Biol **85**(1): 68-72.

Shimaoka, T., Kume, N., Minami, M., Hayashida, K., Kataoka, H., Kita, T. and Yonehara, S. (2000). "Molecular cloning of a novel scavenger receptor for oxidized low density lipoprotein, SR-PSOX, on macrophages". J Biol Chem **275**(52): 40663-40666.

Shimaoka, T., Nakayama, T., Fukumoto, N., Kume, N., Takahashi, S., Yamaguchi, J., Minami, M., Hayashida, K., Kita, T., Ohsumi, J., Yoshie, O. and Yonehara, S. (2004). "Cell surface-anchored SR-PSOX/CXC chemokine ligand 16 mediates firm adhesion of CXC chemokine receptor 6-expressing cells". J Leukoc Biol **75**(2): 267-274.

Shimaoka, T., Nakayama, T., Kume, N., Takahashi, S., Yamaguchi, J., Minami, M., Hayashida, K., Kita, T., Ohsumi, J., Yoshie, O. and Yonehara, S. (2003). "Cutting edge: SR-PSOX/CXC chemokine ligand 16 mediates bacterial phagocytosis by APCs through its chemokine domain". J Immunol **171**(4): 1647-1651.

Silverman, W. R., de Rivero Vaccari, J. P., Locovei, S., Qiu, F., Carlsson, S. K., Scemes, E., Keane, R. W. and Dahl, G. (2009). "The pannexin 1 channel activates the inflammasome in neurons and astrocytes". J Biol Chem **284**(27): 18143-18151.

Skarratt, K. K., Fuller, S. J., Sluyter, R., Dao-Ung, L. P., Gu, B. J. and Wiley, J. S. (2005). "A 5' intronic splice site polymorphism leads to a null allele of the $P2X_7$ gene in 1-2% of the Caucasian population". FEBS Lett **579**(12): 2675-2678.

Sluyter, R., Barden, J. A. and Wiley, J. S. (2001). "Detection of P2X purinergic receptors on human B lymphocytes". Cell Tissue Res **304**(2): 231-236.

Sluyter, R., Shemon, A. N. and Wiley, J. S. (2004). "Glu^{496} to Ala polymorphism in the $P2X_7$ receptor impairs ATP-induced IL-1β release from human monocytes". J Immunol **172**(6): 3399-3405.

Sluyter, R. and Stokes, L. (2011). "Significance of P2X7 receptor variants to human health and disease". Recent Pat DNA Gene Seq **5**(1): 41-54.

Sluyter, R. and Wiley, J. S. (2002). "Extracellular adenosine 5'-triphosphate induces a loss of CD23 from human dendritic cells via activation of $P2X_7$ receptors". Int Immunol **14**(12): 1415-1421.

Sluyter, R. and Wiley, J. S. (2014). "P2X7 receptor activation induces CD62L shedding from human $CD4^+$ and $CD8^+$ T cells". Inflammation and Cell Signaling **1**(3): 44-49.

Smalley, D. M. and Ley, K. (2005). "L-selectin: mechanisms and physiological significance of ectodomain cleavage". J Cell Mol Med **9**(2): 255-266.

So, T., Lee, S. W. and Croft, M. (2006). "Tumor necrosis factor/tumor necrosis factor receptor family members that positively regulate immunity". Int J Hematol **83**(1): 1-11.

Solle, M., Labasi, J., Perregaux, D. G., Stam, E., Petrushova, N., Koller, B. H., Griffiths, R. J. and Gabel, C. A. (2001). "Altered cytokine production in mice lacking $P2X_7$ receptors". J Biol Chem **276**(1): 125-132.

Sommer, A., Fries, A., Cornelsen, I., Speck, N., Koch-Nolte, F., Gimpl, G., Andra, J., Bhakdi, S. and Reiss, K. (2012). "Melittin modulates keratinocyte function through P2 receptor-dependent ADAM activation". J Biol Chem **287**(28): 23678-23689.

Stefano, L., Rossler, O. G., Griesemer, D., Hoth, M. and Thiel, G. (2007). "$P2X^7$ receptor stimulation upregulates Egr-1 biosynthesis involving a cytosolic Ca^{2+} rise, transactivation of the EGF receptor and phosphorylation of ERK and Elk-1". J Cell Physiol **213**(1): 36-44.

Steinbrunn, T., Chatterjee, M., Bargou, R. C. and Stuhmer, T. (2014). "Efficient transient transfection of human multiple myeloma cells by electroporation--an appraisal". PLoS One **9**(6): e97443.

Steinmann-Niggli, K., Lukes, M. and Marti, H. P. (1997). "Rat mesangial cells and matrix metalloproteinase inhibitor: inhibition of 72-kD type IV collagenase (MMP-2) and of cell proliferation". J Am Soc Nephrol **8**(3): 395-405.

Stokes, L., Fuller, S. J., Sluyter, R., Skarratt, K. K., Gu, B. J. and Wiley, J. S. (2010). "Two haplotypes of the $P2X_7$ receptor containing the Ala-348 to Thr polymorphism exhibit a gain-of-function effect and enhanced interleukin-1β secretion". FASEB J **24**(8): 2916-2927.

Stokes, L., Jiang, L. H., Alcaraz, L., Bent, J., Bowers, K., Fagura, M., Furber, M., Mortimore, M., Lawson, M., Theaker, J., Laurent, C., Braddock, M. and Surprenant, A. (2006). "Characterization of a selective and potent antagonist of human $P2X_7$ receptors, AZ11645373". Br J Pharmacol **149**(7): 880-887.

Suadicani, S. O., Iglesias, R., Spray, D. C. and Scemes, E. (2009). "Point mutation in the mouse $P2X_7$ receptor affects intercellular calcium waves in astrocytes". ASN Neuro **1**(1).

Sun, H., Chung, W. C., Ryu, S. H., Ju, Z., Tran, H. T., Kim, E., Kurie, J. M. and Koo, J. S. (2008). "Cyclic AMP-responsive element binding protein- and nuclear factor-κB-regulated CXC chemokine gene expression in lung carcinogenesis". Cancer Prev Res (Phila) **1**(5): 316-328.

Surprenant, A., Rassendren, F., Kawashima, E., North, R. A. and Buell, G. (1996). "The cytolytic P_{2Z} receptor for extracellular ATP identified as a P_{2X} receptor ($P2X_7$)". Science **272**(5262): 735-738.

Susa, M., Luong-Nguyen, N. H., Cappellen, D., Zamurovic, N. and Gamse, R. (2004). "Human primary osteoclasts: in vitro generation and applications as pharmacological and clinical assay". J Transl Med **2**(1): 6.

Suter, U., Bastos, R. and Hofstetter, H. (1987). "Molecular structure of the gene and the 5'-flanking region of the human lymphocyte immunoglobulin E receptor". Nucleic Acids Res **15**(18): 7295-7308.

Syberg, S., Schwarz, P., Petersen, S., Steinberg, T. H., Jensen, J. E., Teilmann, J. and Jorgensen, N. R. (2012). "Association between P2X7 Receptor Polymorphisms and Bone Status in Mice". J Osteoporos **2012**: 637986.

Tabata, S., Kadowaki, N., Kitawaki, T., Shimaoka, T., Yonehara, S., Yoshie, O. and Uchiyama, T. (2005). "Distribution and kinetics of SR-PSOX/CXCL16 and CXCR6 expression on human dendritic cell subsets and $CD4^+$ T cells". J Leukoc Biol **77**(5): 777-786.

Takamune, Y., Ikebe, T., Nagano, O., Nakayama, H., Ota, K., Obayashi, T., Saya, H. and Shinohara, M. (2007). "ADAM-17 associated with CD44 cleavage and metastasis in oral squamous cell carcinoma". Virchows Arch **450**(2): 169-177.

Takei, M., Azuhata, T., Yoshimatu, T., Shigihara, S., Hashimoto, S., Horie, T., Horikoshi, A. and Sawada, S. (1995). "Increased soluble CD23 molecules in serum/saliva and correlation with the stage of sialoectasis in patients with primary Sjogren's syndrome". Clin Exp Rheumatol **13**(6): 711-715.

Takenouchi, T., Iwamaru, Y., Sugama, S., Sato, M., Hashimoto, M. and Kitani, H. (2008). "Lysophospholipids and ATP mutually suppress maturation and release of IL-1β in mouse microglial cells using a Rho-dependent pathway". J Immunol **180**(12): 7827-7839.

Takeshita, F., Suzuki, K., Sasaki, S., Ishii, N., Klinman, D. M. and Ishii, K. J. (2004). "Transcriptional regulation of the human TLR9 gene". J Immunol **173**(4): 2552-2561.

Taylor, S. R., Gonzalez-Begne, M., Sojka, D. K., Richardson, J. C., Sheardown, S. A., Harrison, S. M., Pusey, C. D., Tam, F. W. and Elliott, J. I. (2009a). "Lymphocytes from P2X7-deficient mice exhibit enhanced P2X7 responses". J Leukoc Biol **85**(6): 978-986.

Taylor, S. R., Turner, C. M., Elliott, J. I., McDaid, J., Hewitt, R., Smith, J., Pickering, M. C., Whitehouse, D. L., Cook, H. T., Burnstock, G., Pusey, C. D., Unwin, R. J. and Tam, F. W. (2009b). "$P2X_7$ deficiency attenuates renal injury in experimental glomerulonephritis". J Am Soc Nephrol **20**(6): 1275-1281.

Thomas, L. M. and Salter, R. D. (2010). "Activation of macrophages by $P2X_7$-induced microvesicles from myeloid cells is mediated by phospholipids and is partially dependent on TLR4". J Immunol **185**(6): 3740-3749.

Tousseyn, T., Thathiah, A., Jorissen, E., Raemaekers, T., Konietzko, U., Reiss, K., Maes, E., Snellinx, A., Serneels, L., Nyabi, O., Annaert, W., Saftig, P., Hartmann, D. and De Strooper, B. (2009). "ADAM10, the rate-limiting protease of regulated intramembrane proteolysis of Notch and other proteins, is processed by ADAMS-9, ADAMS-15, and the γ-secretase". J Biol Chem **284**(17): 11738-11747.

Tran, J. N., Pupovac, A., Taylor, R. M., Wiley, J. S., Byrne, S. N. and Sluyter, R. (2010). "Murine epidermal Langerhans cells and keratinocytes express functional P2X7 receptors". Exp Dermatol **19**(8): e151-157.

Tran, M. D. (2011). "P2 receptor stimulation induces amyloid precursor protein production and secretion in rat cortical astrocytes". Neurosci Lett **492**(3): 155-159.

Tsukimoto, M., Maehata, M., Harada, H., Ikari, A., Takagi, K. and Degawa, M. (2006). "P2X7 receptor-dependent cell death is modulated during murine T cell maturation and mediated by dual signaling pathways". J Immunol **177**(5): 2842-2850.

Turac, G., Hindley, C. J., Thomas, R., Davis, J. A., Deleidi, M., Gasser, T., Karaoz, E. and Pruszak, J. (2013). "Combined flow cytometric analysis of surface and intracellular antigens reveals surface molecule markers of human neuropoiesis". PLoS One **8**(6): e68519.

van der Voort, R., van Lieshout, A. W., Toonen, L. W., Sloetjes, A. W., van den Berg, W. B., Figdor, C. G., Radstake, T. R. and Adema, G. J. (2005). "Elevated CXCL16 expression by synovial macrophages recruits memory T cells into rheumatoid joints". Arthritis Rheum **52**(5): 1381-1391.

Varma, R., Chai, Y., Troncoso, J., Gu, J., Xing, H., Stojilkovic, S. S., Mattson, M. P. and Haughey, N. J. (2009). "Amyloid-β induces a caspase-mediated cleavage of P2X4 to promote purinotoxicity". Neuromolecular Med **11**(2): 63-75.

Vercelli, D., Jabara, H. H., Lee, B. W., Woodland, N., Geha, R. S. and Leung, D. Y. (1988). "Human recombinant interleukin 4 induces FcεR2/CD23 on normal human monocytes". J Exp Med **167**(4): 1406-1416.

Verhoef, P. A., Estacion, M., Schilling, W. and Dubyak, G. R. (2003). "P2X7 receptor-dependent blebbing and the activation of Rho-effector kinases, caspases, and IL-1β release". J Immunol **170**(11): 5728-5738.

Verhoef, P. A., Kertesy, S. B., Lundberg, K., Kahlenberg, J. M. and Dubyak, G. R. (2005). "Inhibitory effects of chloride on the activation of caspase-1, IL-1β secretion, and cytolysis by the P2X7 receptor". J Immunol **175**(11): 7623-7634.

Verrier, S., Hogan, A., McKie, N. and Horton, M. (2004). "ADAM gene expression and regulation during human osteoclast formation". Bone **35**(1): 34-46.

Virginio, C., Church, D., North, R. A. and Surprenant, A. (1997). "Effects of divalent cations, protons and calmidazolium at the rat $P2X_7$ receptor". Neuropharmacology **36**(9): 1285-1294.

Virginio, C., MacKenzie, A., North, R. A. and Surprenant, A. (1999). "Kinetics of cell lysis, dye uptake and permeability changes in cells expressing the rat $P2X_7$ receptor". J Physiol **519 Pt 2**: 335-346.

Wada, N., Otani, Y., Kubota, T., Kimata, M., Minagawa, A., Yoshimizu, N., Kameyama, K., Saikawa, Y., Yoshida, M., Furukawa, T., Fujii, M., Kumai, K., Okada, Y. and Kitajima, M. (2003). "Reduced angiogenesis in peritoneal dissemination of gastric cancer through gelatinase inhibition". Clin Exp Metastasis **20**(5): 431-435.

Wang, B. and Sluyter, R. (2013). "P2X7 receptor activation induces reactive oxygen species formation in erythroid cells". Purinergic Signal **9**(1): 101-112.

Wang, F., Kikutani, H., Tsang, S. F., Kishimoto, T. and Kieff, E. (1991). "Epstein-Barr virus nuclear protein 2 transactivates a cis-acting CD23 DNA element". J Virol **65**(8): 4101-4106.

Wang, Y., Herrera, A. H., Li, Y., Belani, K. K. and Walcheck, B. (2009). "Regulation of mature ADAM17 by redox agents for L-selectin shedding". J Immunol **182**(4): 2449-2457.

Wareham, K., Vial, C., Wykes, R. C., Bradding, P. and Seward, E. P. (2009). "Functional evidence for the expression of P2X1, P2X4 and P2X7 receptors in human lung mast cells". Br J Pharmacol **157**(7): 1215-1224.

Weskamp, G., Ford, J. W., Sturgill, J., Martin, S., Docherty, A. J., Swendeman, S., Broadway, N., Hartmann, D., Saftig, P., Umland, S., Sehara-Fujisawa, A., Black, R. A., Ludwig, A., Becherer, J. D., Conrad, D. H. and Blobel, C. P. (2006). "ADAM10 is a principal 'sheddase' of the low-affinity immunoglobulin E receptor CD23". Nat Immunol **7**(12): 1293-1298.

White, G. E. and Greaves, D. R. (2012). "Fractalkine: a survivor's guide: chemokines as antiapoptotic mediators". Arterioscler Thromb Vasc Biol **32**(3): 589-594.

White, L. J., Ozanne, B. W., Graber, P., Aubry, J. P., Bonnefoy, J. Y. and Cushley, W. (1997). "Inhibition of apoptosis in a human pre-B-cell line by CD23 is mediated via a novel receptor". Blood **90**(1): 234-243.

Wilbanks, A., Zondlo, S. C., Murphy, K., Mak, S., Soler, D., Langdon, P., Andrew, D. P., Wu, L. and Briskin, M. (2001). "Expression cloning of the STRL33/BONZO/TYMSTRligand reveals elements of CC, CXC, and CX3C chemokines". J Immunol **166**(8): 5145-5154.

Wildman, S. S., Unwin, R. J. and King, B. F. (2003). "Extended pharmacological profiles of rat P2Y2 and rat P2Y4 receptors and their sensitivity to extracellular H^+ and Zn^{2+} ions". Br J Pharmacol **140**(7): 1177-1186.

Wiley, J. S., Chen, R., Wiley, M. J. and Jamieson, G. P. (1992). "The ATP^{4-} receptor-operated ion channel of human lymphocytes: inhibition of ion fluxes by amiloride analogs and by extracellular sodium ions". Arch Biochem Biophys **292**(2): 411-418.

Wiley, J. S., Dao-Ung, L. P., Li, C., Shemon, A. N., Gu, B. J., Smart, M. L., Fuller, S. J., Barden, J. A., Petrou, S. and Sluyter, R. (2003). "An Ile-568 to Asn polymorphism prevents normal trafficking and function of the human $P2X_7$ receptor". J Biol Chem **278**(19): 17108-17113.

Wiley, J. S., Gargett, C. E., Zhang, W., Snook, M. B. and Jamieson, G. P. (1998). "Partial agonists and antagonists reveal a second permeability state of human lymphocyte P2Z/P2X$_7$ channel". Am J Physiol **275**(5 Pt 1): C1224-1231.

Wiley, J. S. and Gu, B. J. (2012). "A new role for the P2X7 receptor: a scavenger receptor for bacteria and apoptotic cells in the absence of serum and extracellular ATP". Purinergic Signal **8**(3): 579-586.

Wiley, J. S., Sluyter, R., Gu, B. J., Stokes, L. and Fuller, S. J. (2011). "The human P2X7 receptor and its role in innate immunity". Tissue Antigens **78**(5): 321-332.

Wilhelm, K., Ganesan, J., Muller, T., Durr, C., Grimm, M., Beilhack, A., Krempl, C. D., Sorichter, S., Gerlach, U. V., Juttner, E., Zerweck, A., Gartner, F., Pellegatti, P., Di Virgilio, F., Ferrari, D., Kambham, N., Fisch, P., Finke, J., Idzko, M. and Zeiser, R. (2010). "Graft-versus-host disease is enhanced by extracellular ATP activating P2X$_7$R". Nat Med **16**(12): 1434-1438.

Wilson, H. L., Francis, S. E., Dower, S. K. and Crossman, D. C. (2004). "Secretion of intracellular IL-1 receptor antagonist (type 1) is dependent on P2X$_7$ receptor activation". J Immunol **173**(2): 1202-1208.

Woods, L. T., Camden, J. M., Batek, J. M., Petris, M. J., Erb, L. and Weisman, G. A. (2012). "P2X7 receptor activation induces inflammatory responses in salivary gland epithelium". Am J Physiol Cell Physiol **303**(7): C790-801.

Yamaoka, K. A., Arock, M., Issaly, F., Dugas, N., Le Goff, L. and Kolb, J. P. (1996). "Granulocyte macrophage colony stimulating factor induces FcεRII/CD23 expression on normal human polymorphonuclear neutrophils". Int Immunol **8**(4): 479-490.

Yan, Z., Khadra, A., Li, S., Tomic, M., Sherman, A. and Stojilkovic, S. S. (2010). "Experimental characterization and mathematical modeling of P2X7 receptor channel gating". J Neurosci **30**(42): 14213-14224.

Yegutkin, G. G. (2008). "Nucleotide- and nucleoside-converting ectoenzymes: Important modulators of purinergic signalling cascade". Biochim Biophys Acta **1783**(5): 673-694.

Yiangou, Y., Facer, P., Durrenberger, P., Chessell, I. P., Naylor, A., Bountra, C., Banati, R. R. and Anand, P. (2006). "COX-2, CB2 and P2X7-immunoreactivities are increased in activated microglial cells/macrophages of multiple sclerosis and amyotrophic lateral sclerosis spinal cord". BMC Neurol **6**: 12.

Yin, J., Xu, K., Zhang, J., Kumar, A. and Yu, F. S. (2007). "Wound-induced ATP release and EGF receptor activation in epithelial cells". J Cell Sci **120**(Pt 5): 815-825.

Yin, J. and Yu, F. S. (2009). "ERK1/2 mediate wounding- and G-protein-coupled receptor ligands-induced EGFR activation via regulating ADAM17 and HB-EGF shedding". Invest Ophthalmol Vis Sci **50**(1): 132-139.

Yip, L., Woehrle, T., Corriden, R., Hirsh, M., Chen, Y., Inoue, Y., Ferrari, V., Insel, P. A. and Junger, W. G. (2009). "Autocrine regulation of T-cell activation by ATP release and $P2X_7$ receptors". FASEB J **23**(6): 1685-1693.

Yokota, A., Kikutani, H., Tanaka, T., Sato, R., Barsumian, E. L., Suemura, M. and Kishimoto, T. (1988). "Two species of human Fcε receptor II (FcεRII/CD23): tissue-specific and IL-4-specific regulation of gene expression". Cell **55**(4): 611-618.

Young, M. T. (2010). "P2X receptors: dawn of the post-structure era". Trends Biochem Sci **35**(2): 83-90.

Young, M. T., Pelegrin, P. and Surprenant, A. (2006). "Identification of Thr^{283} as a key determinant of $P2X_7$ receptor function". Br J Pharmacol **149**(3): 261-268.

Yu, L. C., Montagnac, G., Yang, P. C., Conrad, D. H., Benmerah, A. and Perdue, M. H. (2003). "Intestinal epithelial CD23 mediates enhanced antigen transport in allergy: evidence for novel splice forms". Am J Physiol Gastrointest Liver Physiol **285**(1): G223-234.

Yu, P., Kosco-Vilbois, M., Richards, M., Kohler, G. and Lamers, M. C. (1994). "Negative feedback regulation of IgE synthesis by murine CD23". Nature **369**(6483): 753-756.

Zeiller, C., Mebarek, S., Jaafar, R., Pirola, L., Lagarde, M., Prigent, A. F. and Nemoz, G. (2009). "Phospholipase D2 regulates endothelial permeability through cytoskeleton reorganization and occludin downregulation". Biochim Biophys Acta **1793**(7): 1236-1249.

Zhang, J., Zhang, K., Gao, Z. G., Paoletta, S., Zhang, D., Han, G. W., Li, T., Ma, L., Zhang, W., Muller, C. E., Yang, H., Jiang, H., Cherezov, V., Katritch, V., Jacobson, K. A., Stevens, R. C., Wu, B. and Zhao, Q. (2014a). "Agonist-bound structure of the human P2Y12 receptor". Nature **509**(7498): 119-122.

Zhang, K., Zhang, J., Gao, Z. G., Zhang, D., Zhu, L., Han, G. W., Moss, S. M., Paoletta, S., Kiselev, E., Lu, W., Fenalti, G., Zhang, W., Muller, C. E., Yang, H., Jiang, H., Cherezov, V., Katritch, V., Jacobson, K. A., Stevens, R. C., Wu, B. and Zhao, Q. (2014b). "Structure of the human P2Y12 receptor in complex with an antithrombotic drug". Nature **509**(7498): 115-118.

Zhang, Z., Oliver, P., Lancaster, J. R., Jr., Schwarzenberger, P. O., Joshi, M. S., Cork, J. and Kolls, J. K. (2001). "Reactive oxygen species mediate tumor necrosis factor α-

converting, enzyme-dependent ectodomain shedding induced by phorbol myristate acetate". FASEB J **15**(2): 303-305.

Zhao, L., Wu, F., Jin, L., Lu, T., Yang, L., Pan, X., Shao, C., Li, X. and Lin, Z. (2014). "Serum CXCL16 as a novel marker of renal injury in type 2 diabetes mellitus". PLoS One **9**(1): e87786.

Zhuge, X., Murayama, T., Arai, H., Yamauchi, R., Tanaka, M., Shimaoka, T., Yonehara, S., Kume, N., Yokode, M. and Kita, T. (2005). "CXCL16 is a novel angiogenic factor for human umbilical vein endothelial cells". Biochem Biophys Res Commun **331**(4): 1295-1300.